Assessing the bioavailability of the radionuclides technetium-99, selenium-79 and uranium-238 in contaminated soils using the diffusive gradients in thin-films (DGT) technique

Alexander Chapman BSc, MSc

Lancaster University

Submitted for the degree of Doctor of Philosophy (PhD)

November 2018

ABSTRACT

"*Assessing the bioavailability of the radionuclides technetium-99, selenium-79 and uranium-238 in contaminated soils using the diffusive gradients in thin-films (DGT) technique*".

Alexander Chapman BSc, MSc

Submitted for the degree of Doctor of Philosophy (PhD), November 2018

The increasing global inventory of ^{99}Tc, ^{79}Se and ^{238}U as components of nuclear waste, coupled with the legacy of contaminated sites, means that increasing attention has been centred on understanding the environmental behaviour of these radionuclides. Over the last 15 years, the technique of diffusive gradients in thin-films (DGT) has emerged as a promising tool for assessing bioavailability based on its demonstrated ability to successfully predict plant uptake for a range of metals and metalloids in soil (Zhang and Davison, 2015). It is therefore utilised in this thesis to address a substantial knowledge gap regarding the bioavailability and aging of Tc, Se and U in soils.

Initially, the performance of a Chelex-ferrihydrite mixed binding layer (MBL) DGT for the novel simultaneous measurement of Se and U was investigated to validate its suitability for subsequent use. An assessment of the availability and aging of all three elements was centred on an 18-month laboratory incubation of a suite of spiked soils, throughout which time a series of DGT deployments were made. Lastly, the ability of DGT to predict ryegrass uptake of Tc across a range of soil types was investigated.

The experimental work presented in this thesis reveals that the MBL DGT is an acceptable method for determining labile Se and U in soil, although at higher pH (> 7) and with increasing concentrations of HCO_3^-, uptake of both elements was impaired. The availability and aging of Se and Tc within soil is governed by soil organic carbon, in addition to the Al and Fe oxide content for Se. Quantitatively, the aging of Tc could be best described by a pseudo-second-order model, yet a natural exponential function provided the best fit for Se. U was found to be particularly resilient to aging within soils exposed to a fluctuating wet-dry moisture regime, where changes in pH were hypothesised to alter the solubility of key U binding phases, namely Fe and Al oxides and dissolved carbonate ligands. DGT was unable to reliably predict the extent of uptake of Tc within ryegrass across a range of soil types, although in situ deployments whilst the ryegrass was actively growing did yield encouraging results.

Remedial efforts to reduce the soil-to-plant radionuclide transfer following a contamination event should look to utilise the complexing capacity of C_{org} in the case of Tc and Se, or prevent the exposure of the soil to wetting/drying events in the case of U. Where possible, DGT measurements of bioavailability within Tc-contaminated soils should be made in situ, although in a field setting this is logistically challenging and introduces significant uncertainties to the data. In practice, to reliably ascertain the bioavailability of Tc, it would seem that the best approach is to directly measure the accumulated activity within the plant.

ACKNOWLEDGEMENTS

I wish to acknowledge the guidance and support of my academic supervisors, Dr Jackie Pates and Professor Hao Zhang. In addition, I am extremely grateful to Professor Neil Willey and Alison Halliday for granting me use of the nuclear laboratory facilities at the University of the West of England, Bristol, to facilitate an important component of the experimental work presented in this thesis. For provision of soil samples and analytical support, I am indebted to colleagues at Nottingham University, namely Dr Maria Izquierdo, Dr Scott Young, Dr Liz Bailey and Professor George Shaw. Furthermore, I would like to thank several members of current and former staff at the Lancaster Environment Centre for their technical and laboratory assistance, particularly Dr Mohammed Al-Kasbi, Debbie Hurst and Dr Daniel Blackburn.

This page intentionally left blank

DECLARATION

I declare that the work in this thesis is my own and has not been submitted, in part or in full, to any alternative institution for any other degree of qualification.

Declared word count = 68,232 (excluding references)

STATEMENT OF AUTHORSHIP

Alex Chapman Jackie Pates Hao Zhang

This page intentionally left blank

CONTENTS

This page intentionally left blank

TABLE OF FIGURES

This page intentionally left blank

Chapter 1: Introduction and literature review

1.1 Context

Since the pioneering discovery of nuclear fission in 1938, the subsequent development of the nuclear industry has left a significant legacy of waste and radionuclide contamination throughout the environment, predominantly through nuclear power generation and nuclear weapons testing. Nuclear power is increasingly being recognised as an important source of energy given the pressing need to diverge from fossil fuel-driven economies to ensure future energy security and mitigate against anthropogenic global climate change. Conflicting societal attitudes and perceptions towards the nuclear industry exist however. Growing public concern stems from the secrecy surrounding nuclear technology and its military applications (Rosa and Clark, 1999), major reactor accidents such as at Chernobyl, as well as the environmental implications of nuclear waste disposal (van der Pligt, 1992). Global political instability means that nuclear proliferation remains a cause for concern. India, Israel and Pakistan are all non-signatories of the Non-Proliferation of Nuclear Weapons Treaty (NPT) enforced in 1970, and all four have developed nuclear weapons (Horovitz, 2015).

1.1.1 Nuclear power generation

As of February 2017, the total number of operational nuclear power plants worldwide stood at 449 across 30 different countries, with a further 60 reactors under construction (IAEA, 2017). In terms of the relative share for electricity generation, the nuclear power contribution was greater than 50% in four countries in 2015. These included France (76.3%), Ukraine (56.5%), Slovakia (55.9%) and Hungary (52.7%) (IAEA, 2017).

Several notable accidents at various nuclear installations have resulted in the substantial release of radioactivity into the environment. The most significant of these occurred at the Chernobyl Nuclear Power Plant in Ukraine (formerly the Soviet Union) on 26th April 1986 when an estimated 14 EBq (1 EBq = 10^{18} Bq) of radioactive fission products were released, in part as a result of human error during a test routine (IAEA, 2006). Two explosions destroyed the reactor core and radionuclides were dispersed in several directions during a fire which lasted for 10 days, leading to the contamination of more than 200,000 km^2 of land across Europe with ^{137}Cs concentrations in excess of 37 kBq m^{-2} (Balonov, 2007). Other notable accidents include a fire at the Windscale establishment in Cumbria in 1957 (Crick and Linsley, 1984), reactor meltdown at Three Mile Island, Pennsylvania, in 1979, and more recently the meltdown of three reactors at the Fukushima Daiichi Power Plant in Japan following a devastating tsunami on March 11th 2011, which incapacitated the cooling system (IAEA, 2015).

The routine and accidental release of radioactivity into the terrestrial and marine environment occurs as part of the nuclear fuel cycle. Primary sources include the mining and milling of uranium (U), enrichment and reprocessing plants, as well as the reactors themselves during power production (Cooper et al., 2003). The US Department of Energy has identified nearly 10,000 individual contaminated sites across 37 locations throughout the US that require remediation following 50 years of the development of nuclear technology and the manufacture and testing of nuclear weapons (US DOE, 1995). An estimated 25.3-36.7 TBq of fission product nuclides were accidentally released on the 6th April 1993 during the reprocessing of spent nuclear fuel at a plutonium extraction facility near Tomsk, in the Russian Federation, after overpressure built up in a reaction vessel (IAEA, 1998). Widespread and heterogeneous deposition occurred to the surrounding land up to a distance of 28 km from the site, and in the village of Georgievka decontamination was achieved through the removal of ~380 tonnes of snow and soil with subsequent burial at an undisclosed site.

1.1.2 Radioactive waste management

Radioactive waste is generated at all stages of the nuclear fuel cycle, as well as through use of radioactive materials in industrial materials in industrial, medical, research and defence-related applications. The most hazardous and long-lived radioactive wastes comprise spent nuclear fuel and high-level wastes derived from the reprocessing of spent nuclear fuel. Nuclear reactor fuel is considered 'spent' when it can no longer sustain a chain reaction at economic power levels because of the depletion of fissile isotopes and build-up of fission products which 'poison' the reaction by absorbing neutrons. The Nuclear Energy Agency (NEA, 2016) reported that in 2015, the total quantity of spent nuclear reactor fuel arising from nuclear power generation across member states was 7310 tonnes, in excess of the total annual fuel reprocessing capacity of 4200 tonnes. At the end of 2015, the total accumulated quantity of spent fuel in storage was 228,947 tonnes.

Geological disposal of nuclear waste in highly-engineered, subsurface (~1000 m) repositories is internationally recognised as the most feasible and safest long term management solution for the accumulating volume of the most hazardous high-level and long-lived radioactive wastes (NEA & OECD, 2008). Finland recently became the first country to approve construction of a geological disposal facility, which is expected to become operational in 2023 (Gibney, 2015). Interim surface storage is adopted in the meantime at sites such as Sellafield in Cumbria, where high-level wastes are vitrified and intermediate-level wastes encapsulated within purpose-built concrete, stainless steel or iron containers (DECC, 2014).

A GDF will be designed to isolate radionuclides from the biosphere for sufficient time so as to allow the majority of the radioactive material to undergo decay. However, it is anticipated that over geological time scales (> 10^5 years), releases of radioactivity from a geological disposal facility (GDF) are inevitable as the engineered barriers that contain the wasteforms

within the repository are eventually expected to corrode and degrade under repository conditions (Miller, 1994; Grambow, 2008). Cementitious materials feature prominently in the designs for all current concepts for geological disposal of higher activity wastes worldwide; applications include waste encapsulation grout, buffers and backfills, fracture grouts and tunnel/vault linings (Bamforth et al., 2012). Upon re-saturation of the GDF by intruding groundwater, dissolution of such cementitious material will yield a plume of hyperalkaline (pH 10-12) leachate. The cementitious environment is expected to remain hyperalkaline over extended periods, and under saturated conditions is intended to reduce the mobility of radionuclides such as uranium through the formation of insoluble hydrolysis products increased adsorption of cations to negatively-charged mineral surfaces (Braney et al., 1993).

The prevailing redox conditions will also be fundamental in influencing the speciation of radionuclides within the repository and subsequently the extent of such mobilisation (Toulhoat, 2002). The radiolysis and corrosion of metallic components under anoxic conditions will generate significant quantities of H_2 gas and therefore promote further reducing conditions. Deep geological environments are often devoid of organic compounds to support microbial life, but some authors have indicated that H_2 will serve as an efficient source of energy to replace organic matter (Libert et al., 2011). Dissolution or immobilisation of radionuclides can occur through the direct enzymatic or indirect non-enzymatic actions of microorganisms. These actions include: redox reactions; changes in pH and Eh; chelation or production of specific sequestering agents; bio-colloidal formation; bio-precipitation; and bioaccumulation by biomass (Francis, 1990).

Upward migration of radionuclides in solution through the host rock is expected to occur via fractures. Only a handful of long-lived radionuclides, including mainly anionic species such as

^{79}Se and ^{99}Tc, two of the three radionuclides specifically considered in this thesis, are expected to be mobile enough to reach the biosphere however (Abdelouas and Grambow, 2012). The long half-lives of ^{79}Se and ^{99}Tc mean that they are expected to make a significant contribution to radiation exposure in the long-term (>100,000 years), and are therefore integral components in long-term safety assessments for the management of nuclear waste disposal sites and determining the long-term radiological impact of a repository on the environment (Olyslaegers et al., 2005).

The Nuclear Decommissioning Authority's Generic Post-Closure Safety Assessment (NDA RWMD, 2010) calculated that beyond 200,000 years, the flux and inherent activity of radionuclides still emerging from a reference case engineered disposal system is dominated by ^{238}U and its daughters. A further isotope of U, ^{233}U (half-life = 159,200 years), produced from the decay of transuranic ^{237}Np in spent fuel, is also computed to make a significant contribution to the calculated risk from HLW (NDA RWMD, 2010).

The greatest radiological impact to humans associated with ^{238}U arises from its decay products, in particular ^{230}Th (half-life 77,000 years), ^{210}Pb (22 years), ^{226}Ra (1600 years) and ^{222}Rn (3.82 days). The radionuclides listed represent an elevated radiological risk for a variety of reasons, including their abundance, half-life, environmental behaviour and mobility, human exposure pathway, and finally their behaviour and retention within the body. Radon-222, a colourless and odourless gas produced from the decay of ^{226}Ra, accounts for approximately half of the effective annual radiation dose from natural sources received by the global population (WHO, 2016). Exposure occurs predominantly through inhalation; cellular damage within the lungs and respiratory tract occur through exposure to ionising alpha particles emitted through decay. In contrast, human exposure to ^{226}Ra, an alkaline earth metal, occurs through ingestion of contaminated food or drinking water. The radiological risk associated with radium is elevated owing to its high mobility under frequently-encountered

environmental conditions and tendency to accumulate within bone following uptake into the body, thereby delivering a prolonged dose.

1.1.3 Nuclear weapons

The human and environmental radiological impact of nuclear power generation is dwarfed by that of nuclear weapons, which has caused significant environmental contamination at testing sites and in areas where weapons materials were processed (Choppin, 2003). Prior to the implementation of the Limited Nuclear Testing Ban Treaty in 1963, over 2400 detonations of nuclear weapons had been documented, of which ~540 were atmospheric (UNSCEAR, 2000). The majority of such atmospheric tests were conducted on the Arctic island of Novaya Zemlya (by the Soviet Union) and the Bikini and Eniwetok Islands in the Pacific Ocean (by the US), whilst further test sites included Lopnor in Western China, Christmas Island, the Nevada Desert and the Australian Desert (Cooper et al., 2003). Despite the remoteness of these locations with respect to human habitation, distribution of the fallout from these tests is reported to be predominantly global (78% relative contribution), with the remainder being deposited locally (12%) and in a more regional latitude band around the test sites (10%) (Aarkrog, 1996).

1.2 Technetium, selenium and uranium in the environment

1.2.1 Technetium

Technetium-99 is a long-lived (half-life 2.1 x 10^5 years) pure beta-emitting (E_{max} = 294 keV) radionuclide that is produced with a relatively high yield during fission induced by thermal neutrons in nuclear reactors and nuclear weapons (Poinssot and Geckeis, 2012). At approximately 6%, the yield of ^{99}Tc in nuclear reactors is comparable in magnitude to ^{90}Sr and ^{137}Cs, and therefore forms a major component of spent fuel (Till, 1984). The natural

occurrence of ^{99}Tc produced by the spontaneous fission ^{238}U and neutron-induced fission of ^{235}U in U ores within the Earth's crust is negligible (Schwochau, 2000).

The nuclear fuel cycle represents the predominant anthropogenic source of ^{99}Tc in the environment, in comparison to stratospheric fallout from nuclear weapons and accidental releases from nuclear power plants (Schwochau, 2000). Poor waste management practice at nuclear facilities, in part driven by an absence of legislation surrounding waste treatment and disposal, means that a legacy of contaminated sites prevails. A notable example is the Hanford nuclear reservation in southeast Washington State, USA, now largely decommissioned. The United States Department of Energy (DOE) estimated that 67 of the 149 underground storage tanks used for isolating ^{99}Tc-bearing high-level waste between 1943 and 1987 have leaked, releasing on the order of one million gallons (~4500 L) of waste into the surrounding sediments (Butherus et al., 1995). Further major production sites across the USA exhibiting extensive contamination on a comparable scale include Savannah River (South Carolina), Rocky Flats (Colorado) and Oak Ridge (Tennessee) (Eisenbud and Gesell, 1997).

Significant quantities of ^{99}Tc have accumulated in the sub-tidal sediments of the Irish Sea (Jenkinson et al., 2014). The effluent routinely discharged from the Sellafield nuclear reprocessing plant in Cumbria, UK, became enhanced in ^{99}Tc between 1994 and 2004 (Leonard et al., 1997) following the commissioning of the Enhanced Actinide Removal Plant (EARP), which was inefficient at removing ^{99}Tc during the waste treatment process. At its peak, approximately 200 TBq ^{99}Tc were released in 1995 alone (CEC, 1990). Although discharged activities have since returned to acceptable (very low) levels, concern has arisen surrounding the potential for remobilisation of ^{99}Tc from contaminated sediments leading to secondary contamination of marine biota.

An Eh-pH diagram summarising the speciation of Tc in soil is shown in Figure 1.1. In an Eh-pH diagram, redox potential (Eh) (V) is plotted against acidity (pH) for an aqueous system, and the stability fields for various Tc species are shown. The solid lines represent conditions under which species on either side are present in equal concentrations. Superimposed on the diagram are dashed lines which indicate typical pH and redox conditions for normal, wet and waterlogged soils.

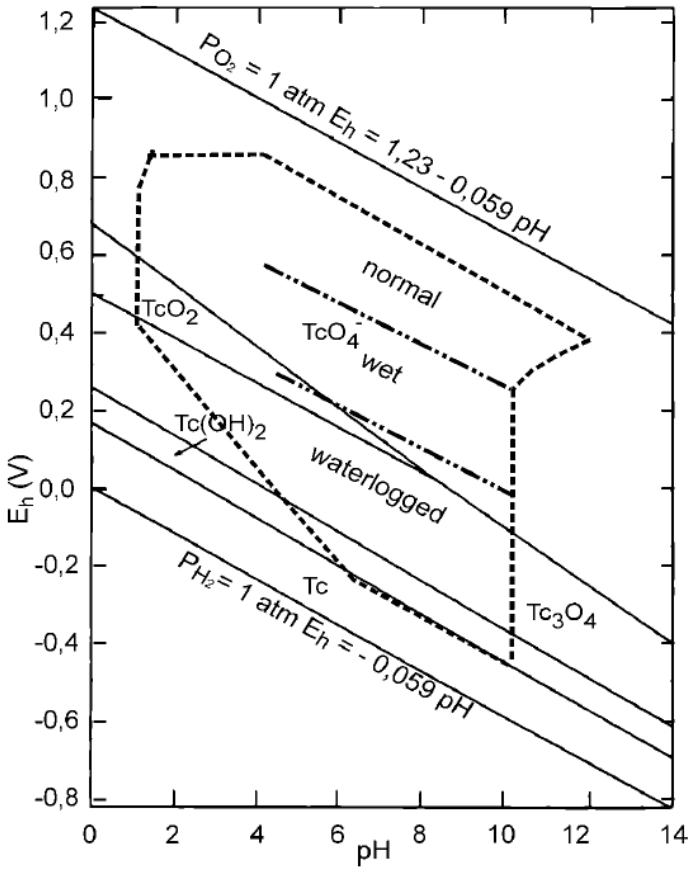

Figure 1.1. *Eh-pH diagram for technetium. Dotted lines delineate the redox limits for soil and microorganisms. From Tan (1998).*

The Eh-pH diagram for Tc shows that under oxidising conditions, Tc occurs predominantly in the +7 valence state as the pertechnetate ion, TcO_4^-. Pertechnetate demonstrates very limited sorption to a range of naturally-occurring minerals (Palmer and Meyer, 1981) and soil types (Sheppard et al., 1990), and is therefore highly mobile and available for plant uptake (Bennett

and Willey, 2003). At lower redox potentials and under reducing conditions relevant to soils, TcO_4^- is reduced to hydrous Tc(IV)O_2 species, which demonstrate greatly enhanced sorption to the soil solid phase, especially in the presence of organic carbon, as well as at higher pH and clay contents (Sheppard et al., 1990; Rossler et al., 2000). Mobility and availability in anaerobic soils is consequently much lower than for aerobic soils (Yanagisawa and Muramatsu, 1995; Tagami and Uchida, 1996).

Re-oxidation of reduced Tc species to TcO_4^- was reported in earlier studies to be very slow (Sheppard and Evenden, 1991; Tagami and Uchida, 1999), but more recently the rapid re-oxidation of Tc(IV) under oxic conditions has been observed (Ashworth and Shaw, 2005), which is enhanced in the presence of synthetic organic ligands, such as EDTA (Boggs et al., 2013), and naturally-occurring humic substances (Gu et al., 2011).

Limited structural information is available in the published literature concerning the nature of the interaction between Tc and humic substances (HS). The formation of soluble Tc(IV)-HS was investigated at low Tc(IV) concentrations by Boggs et al. (2011), who reported binding (stability) constants for the individual species $TcO(OH)^+$ and $TcO(OH)_2^0$ with humic substances of 6.8 and between 3.9 and 4.3 respectively. Similar values were measured for fulvic acid (FA). Maes et al. (2004) used X-ray absorption spectroscopy to investigate the association of Tc with humic acids and observed only Tc(IV)-Tc(IV) bonds, which implied a Tc colloid layer on the surface of the humics as opposed to Tc complexed with humic carboxylic acid functional groups.

1.2.2 Selenium

Selenium (atomic number 34) is a metalloid with six naturally-occurring stable isotopes. A number of short-lived and metastable radioactive isotopes spanning the mass range 64-95 are

known, of which ^{79}Se is the sole isotope with a half-life in excess of a year (NNDC, 2017). Selenium-79 is a pure beta-emitting (E_{max} = 149 keV) radionuclide derived mainly from nuclear reactors by the spontaneous fission of ^{235}U. It is only found at significant levels in spent nuclear fuel and in waste materials resulting from fuel reprocessing (Bienvenu et al., 2007). Estimates for the half-life of ^{79}Se are continuously being refined; recent studies by Bienvenu et al. (2007) and Jörg et al. (2010) report values of 3.77 (± 0.19) x 10^5 and 3.27 (± 0.08) x 10^5 years respectively.

An Eh-pH diagram for Se is given in Figure 1.2. The speciation of Se in soils under oxidising conditions (> 0.2 V) is dominated by the oxyanions selenate (SeO_4^{2-}) and selenite (SeO_3^{2-}), which have oxidation states of +6 and +4 respectively. Selenate is stable under oxidising conditions at near-neutral pH, whereas selenite is more stable at lower pH and redox potentials (reducing conditions). Reduction to scarcely-soluble metal-selenide (Se^2) precipitates (e.g. FeSe and $FeSe_2$) and elemental Se (Se^0) occurs at lower redox potentials (Elrashidi et al., 1987), with the reduction commonly being microbially-mediated (Stolz and Oremland, 1999). All the inorganic Se species may co-exist simultaneously owing to the reported slow transformation rates between species (Zawislanski and Zavarin, 1996).

The organic matter fraction of soil is reported to have a greater sorption capacity for Se than the mineral fraction (Coppin et al., 2009). This difference is reflected in the soil/solution partition coefficient (K_D) describing the distribution between the two phases; the IAEA (1994) recommend a K_D value of 1800 L kg^{-1} for organic soils, over twice the value for clay soils (740 L/kg). The inorganic soil components reported to be most important in the adsorption of Se are Fe oxides (Duc et al., 2003) and Fe oxyhydroxides, such as goethite (Parida et al., 1997; Rashid et al., 2002), Mn oxides (Saeki et al., 1995), and Al oxides, including gibbsite and allophane (Rajan, 1979; Neal et al., 1987). Selenite exhibits greater adsorption affinity for the soil matrix than selenate (Goh and Lim, 2004), which is likely due to differences in the nature

of the surface complexes formed (Rashid et al., 2002; Fernandez-Martinez and Charlet, 2009). Selenate is consequently more bioavailable for plant uptake (Balistrieri and Chao, 1987; Elrashidi et al., 1987). Selenium is predominantly taken up by plants as selenate, but uptake in the form of selenite and organic Se compounds is not insignificant (White et al., 2004; Sors et al., 2005; Nakamaru and Altansuvd, 2014).

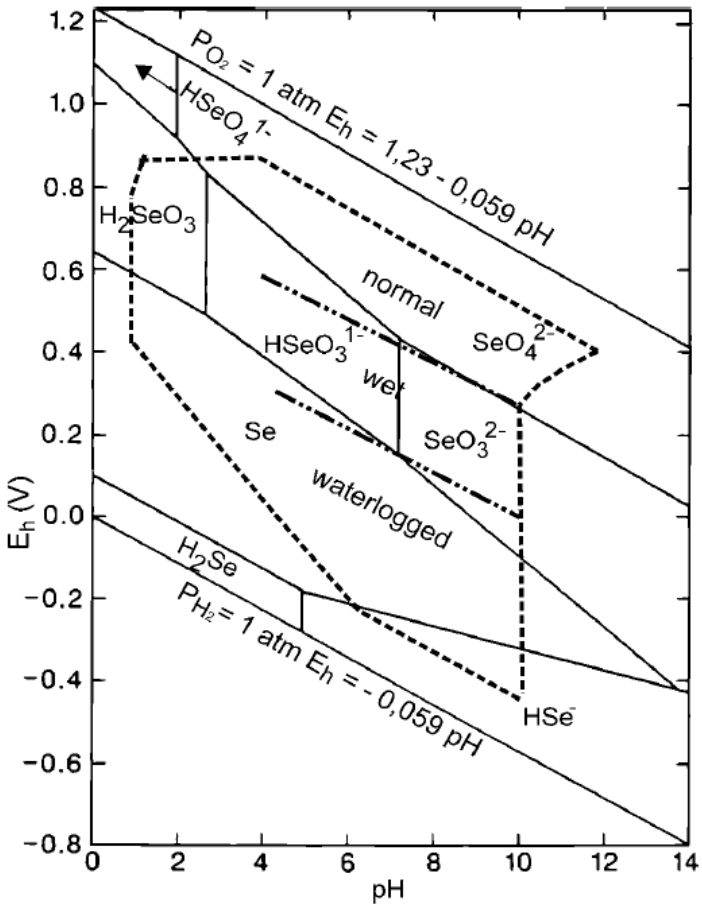

Figure 1.2. *Eh-pH diagram for selenium. Dotted lines delineate the redox limits for soil and microorganisms. From Tan (1998).*

Soil organic matter (OM) is reported to play a fundamental role in controlling availability of Se through complexation and adsorption processes, with decreasing availability generally reported at higher OM contents (Johnsson, 1991; Wang et al., 1996; Dhillon et al., 2010). Binding to the fulvic acid fraction is generally reported to be more prevalent than for humic

acid (Kang et al., 1991; Qin et al., 2012). The mechanisms of interaction between OM and Se are not fully understood however. Some studies suggest that Se undergoes direct complexation with OM (Cai, 2000; Bruggeman et al., 2007; Darcheville et al., 2008), whilst others speculate that Se is adsorbed indirectly by OM-cation (e.g. Fe, Al) complexes to form a Se-OM-metal ternary system (Gustafsson and Johnsson, 1994; Coppin et al., 2009; Jordan et al., 2009). A third hypothesis proposes that selenide produced through microbial reduction or plants is incorporated into carboxyl-, hydroxyl- or amino- groups present within OM (van Dorst and Peterson, 1984; Gustafsson and Johnsson, 1994; Darcheville et al., 2008).

Microorganisms are widely-reported to play a fundamental role in mediating Se transformations within soils (Neal, 1995). Under aerobic conditions, dissimilatory reduction of selenate and selenite to insoluble nanoparticles of elemental selenium (Se^0) is a key process, whereby microbes are able to utilise electron donors such as alcohols, sugar, organic acids and humic substances (Kashiwa et al., 2000; Nancharaiah and Lens, 2015). At the same time, biomethylation of Se oxyanions, Se^0, seleno-cysteine and seleno-methionine is demonstrated to produce a range of volatile compounds such as dimethyl selenide or dimethyl diselenide (Francis et al., 1974; Reamer and Zoller, 1980).

1.2.3 Uranium

Uranium has 23 isotopes, all of which are radioactive, but only three (^{234}U, half-life 2.455×10^5 years; ^{235}U, 7.04×10^8 years; ^{238}U, 4.47×10^9 years) occur naturally (Haynes and Lide, 2011). These three naturally-occurring radionuclides are primordial, their relative abundance dominated by ^{238}U (99.27% by mass) and ^{235}U (0.72%). All three emit alpha particles in the energy range 4.15-4.775 MeV (Cooper et al., 2003). Fissile ^{235}U is widely used as fuel in nuclear reactors, either in the same proportion as found in natural uranium (0.72% by mass), or more commonly following enrichment to around 3% by mass. Uranium-238 is not readily

fissionable, but does undergo transmutation by neutron capture to form the fissile isotope ^{239}Pu (Eisenbud and Gesell, 1997). Highly-enriched U suitable for use in nuclear weapons contains in excess of 20% ^{235}U (IAEA, 2005).

Uranium is ubiquitous throughout the environment. Worldwide soil concentrations are reported in the range from 0.3 to 11.7 mg kg^{-1} (UNSCEAR, 1993). However, an enormous legacy of sites contaminated with U can be found globally, primarily associated with the mining, milling and processing of U as part of the nuclear fuel cycle, but also through the manufacture and testing of nuclear weapons (Eisenbud and Gesell, 1997). Relatively high levels of U in sedimentary phosphorites means that elevated concentrations of U can be found in soil in the vicinity of phosphate mines as a result of crushing, milling, washing and storage of mined phosphate (Poinssot and Geckeis, 2012). Furthermore, intensive application of phosphate fertilisers to agricultural land has led to significant accumulations of U in the soil (Guzman et al., 2006; Stojanovic et al., 2006; Takeda et al., 2006).

The mining, milling and enrichment of U has been and is currently conducted at numerous sites worldwide, including Argentina, Brazil, China, France, Germany, India, Iran, Japan, North Korea, Russia, South Africa, the UK and the US (Poinssot and Geckeis, 2012). Over two-thirds of the world's production of U from mines is from Kazakhstan, Canada and Australia (World Nuclear Association). Across the US alone, the US Department of Energy (DOE) recognises 10,000 individual sites covering an area of 3,300 square miles (8,547 km^2) that require remediation following 50 years of the development of nuclear technology associated with power generation and weapons (US DOE, 1995). An estimated 450,000 kg of U was released during the operational lifetime of the DOE Fernald site in Ohio, which was used for the processing and storage of U metals and compounds between 1951 and 1989 (Janke et al., 1992; Fernald Citizen's Task Force, 1995). The total waste volume is estimated at 2.4 x 10^6 m^3, more than half of which is contaminated soil.

During the U enrichment process uranium hexafluoride (UF_6) gas is produced, which upon accidental release to the atmosphere will react with water vapour to form hydrogen fluoride and uranyl fluoride (Poinssot and Geckeis, 2012). Depending on meteorological conditions, the uranyl fluoride will eventually be deposited to the soil. The largest documented accidental UF_6 release of 1,184 kg to the environment occurred in 1958 at the Oak Ridge Reservation in Tennessee (ATSDR, 2010). During operation of this research and enrichment plant, huge quantities of U amongst other actinides, fission products and transuranics were dumped into unlined landfills, settling ponds and discharged to streams, the full extent of which is unknown (Alliance for Nuclear Accountability, 2011).

Uranium can exist in the +2, +3, +4, +5 and +6 oxidation states, but in soils the most stable valences are tetravalent (+4) and hexavalent (+6) forms (Mitchell et al., 2013). Figure 1.3 shows an Eh-pH diagram for U which summaries the key U species likely to be encountered in soils. Under oxidising conditions at low pH (<4), U exists in the +6 valence predominantly as the soluble UO_2^{2+} (uranyl) cation, but with increasing pH the uranyl cation undergoes hydrolysis to form various hydroxide complexes. In reducing environments, the +4 valence state is stable where it forms sparingly soluble minerals such as uraninite (UO_2) (Gavrilescu et al., 2009). A number of microorganisms have demonstrated the capacity to reduce U(VI) enzymatically (Wall and Krumholz, 2006), whilst various dissimilatory metal and sulphate-reducing bacteria, including *Shewanella*, *Geobacter* and *Desulfovibrio* species, act as oxido-reduction agents by coupling the oxidation of organic matter and H_2 to the reduction of U(VI) (Fredrickson et al., 2000; Luo et al., 2007).

Complexation reactions with inorganic ligands in the soil solution play a major role in determining the fate of U(VI) in the soil system. At higher pH (6-10) in the presence of carbonate ligands, U forms highly soluble bicarbonate [e.g. $UO_2(CO_3)^{2-}_2$] (Dementeyev and Syromyatnikov, 1968) and tricarbonate [e.g. $UO_2(CO_3)^{4-}_3$] (Giblin et al., 1981) complexes,

whilst phosphate complexes [e.g. $UO_2PO_4^-$] can also be prevalent (Brendler et al., 1995). Numerous studies have demonstrated that such anionic complexes have a substantially reduced adsorption affinity for soil minerals, including haematite (Ho and Miller, 1986), or even the complete soil matrix (Mason et al., 1997) compared to uranyl anions and hydroxy-complexes.

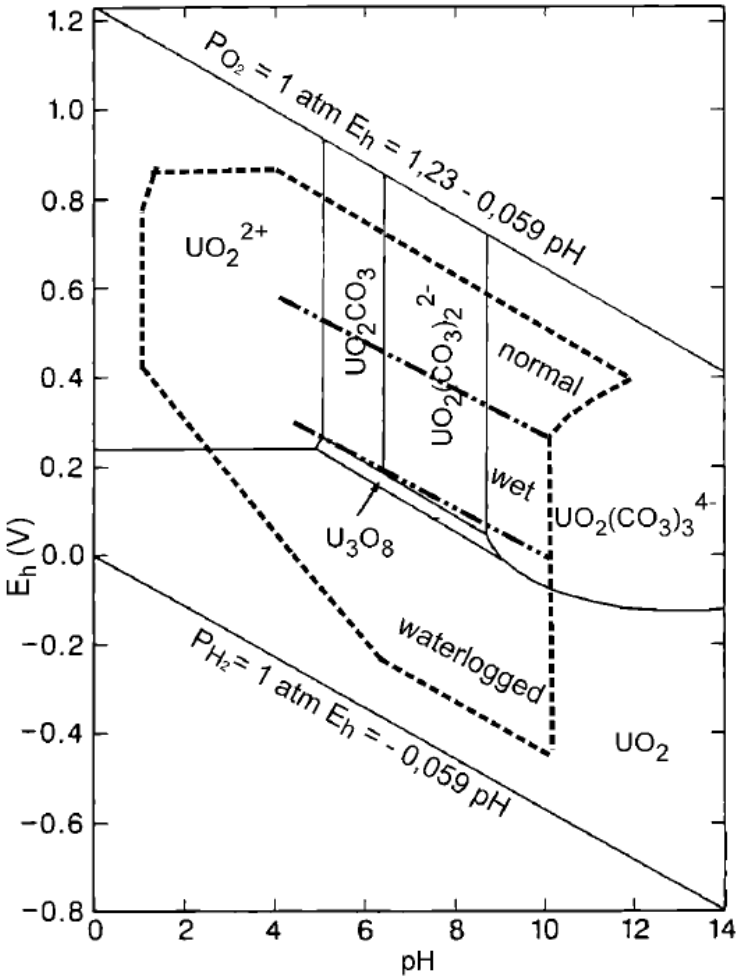

Figure 1.3. *Eh-pH diagram for uranium. Dotted lines delineate the redox limits for soil and microorganisms. From Tan (1998).*

Soil/solution distribution coefficients (K_D) for U are reported to range multiple orders of magnitude from 0.03 in sandy soils to 20,000 in clayey soils (Sheppard and Thibault, 1990; Willet and Bond, 1995). Hydroxyl functional groups on oxide mineral surfaces (-SOH) are

expected to be the dominant sorption sites (Manceau et al., 1992), but hydroxylated groups (-SiOH and -AlOH) situated along the edges of clay minerals can also have a significant contribution to sorption (Zachara and McKinley, 1993).

Vandenhove et al. (2007) and Duquene et al. (2010) reported that ryegrass uptake of U was best correlated with the summed soil solution concentration of the uranyl cation, uranyl carbonate and uranyl phosphate complexes. The high bioavailability of U carbonate complexes is corroborated by Shahandeh and Hossner (2002), who found that U uptake by sunflower (*Helianthus annuus*) and Indian mustard (*Brassica juncea*) was greatest in calcareous soils. The lowest plant tissue concentrations meanwhile were found in soils with high contents of Fe and Mn oxides and organic carbon (C_{org}). Several other studies report diminished plant uptake of U in the presence of C_{org} (Sheppard et al., 1983; Ramaswami et al., 2001) as well as clayey soils (Sheppard and Evenden, 1988; Mortvedt, 1994). Finally, Viehweger and Giepel (2010) observed substantially increased U accumulation in the roots and shoots of *Arabidopsis halleri* grown in Fe-deficient nutrient solution.

1.3 Speciation and bioavailability of metals in soil

This literature review considers metals in general as opposed to the radionuclides upon which this thesis is focussed. Both U and Tc, as well as many other radionuclides, are metals, and the body of literature surrounding the principles governing metal bioavailability in soil is more extensive than for radionuclides. Although strictly a metalloid – elements which share characteristics of metals and non-metals – Se is considered under the term 'metal' used throughout this literature review. In soil, both Se and Tc are commonly encountered as oxyanions of selenate/selenite and pertechnetate, respectively, although the behaviour of these species will be different to some extent. Many of the processes pertinent to metals described here are applicable to metalloids such as Se and As. Specifically, the processes

considered here encompass the soil physico-chemical and biological processes governing the speciation, bioavailability and plant uptake of elements, for example adsorption and complexation, as well as the physical and chemical methods used to determine the bioavailable fraction of an element in soil.

Within the soil system, metals can be present in multiple chemical forms, with the total pool being distributed between various solid phase components and the soil solution (Tamponnet et al., 2008). This distribution is conventionally expressed in terms of the partition coefficient (K_D), which empirically describes the ratio of the concentration of a metal associated with the solid phase divided by the equilibrium concentration in the solution phase (Sheppard et al., 2011). The term 'speciation' describes the distribution of an element between the various defined chemical species in a system (Templeton et al., 2000). Chemical species are the specific form of an element as defined by isotopic composition, electronic or oxidation state, and/or complex or molecular structure.

It is increasingly recognised that the total concentration of a metal in soil does not provide an accurate or reliable indication of its bioavailability for uptake by plants (Rieuwerts et al., 1998; Nolan et al., 2003). A significant fraction of a metal may be strongly bound to the soil solid phase components, such that it is inaccessible or unavailable for uptake by plants. Consequently, the concept of 'bioavailability' has been developed, which in general terms is understood to refer to the fraction of a metal or compound that is biologically available or can be made available for uptake by plants and biota (Desmet et al., 1991; Peijnenburg, 2004). A significant degree of ambiguity surrounds the term, however, since it has evolved to encompass a complex range of definitions due to its use in numerous scientific fields (Semple et al., 2004). The term 'phytoavailability' is also sometimes used to refer specifically to the availability of metals in soil for uptake and their subsequent accumulation in plant tissue (Song et al., 2004; Meers et al., 2007). Throughout this literature review and thesis, the more general

term ‘availability’ is favoured, which reflects availability for uptake by a biological sink, such as a plant, or a non-biological sink such as DGT (diffusive gradient in thin films), a device for measuring labile metals in soil (Sections 1.7 and 1.8).

Following deposition within soil, the bioavailability of a metal is influenced by its initial physico-chemical form (e.g. particulate, colloidal, simple ionic species), but over time its speciation will change as a result of interaction with other soil components, such that the distribution between the solution and solid phases gradually approaches a pseudo-equilibrium (McLaren and Crawford, 1973; Oughton et al., 1992). A variety of dynamic biological and biochemical soil processes are involved in the establishment of this equilibrium, including organic and mineral cation exchange, organic complex formation (Valcke and Cremers, 1994), adsorption to mineral or organic particles (Evans et al., 1983), and incorporation into microorganisms (Francis, 1982). The key soil solid phase components providing permanent or variable surface charge responsible for the binding (adsorption) of metals in soil include organic matter, layered silicate clay minerals, and oxides and hydroxides of Al, Fe and Mn (McLaughlin et al., 2000). A complex interplay of factors including changes in soil pH, temperature, redox potential, decomposition of soil organic matter, leaching, ion exchange processes and microbial activity are all responsible for the modification of the metal equilibrium, which can lead to the solubilisation of metal species or incorporation into the solid phase, and in turn influence availability (Kennedy et al., 1997).

Different solid phase components exhibit varying capacity to bind the metal in the soil, which in turn influences the availability. Metal that is non-specifically adsorbed to cation exchange sites on mineral surfaces through less-selective outer sphere complexes is considered relatively available. The stability of inorganic and organic-metal complexes greatly influences metal availability, where labile complexes that dissociate rapidly to release the free metal ion are considered to be more available than complexes of greater stability (Lehto et al., 2006).

Metal species which have been more strongly bound to the soil matrix to the extent where they are kinetically unreactive or physically occluded are largely unavailable for uptake by plants. This strong binding can occur through specific adsorption involving formation of inner sphere complexes, incorporation into insoluble organic species, or occlusion into the lattice structure of secondary and primary minerals including precipitated oxides of iron and manganese (Thornton, 1995).

1.4 Approaches for the assessment of bioavailability

Numerous studies have shown that the total concentration of metal in the soil solution can be a reliable indicator of the plant-available fraction for various metals (Smolders et al., 1997; Zhang et al., 2001; Nolan et al., 2005; Wang et al., 2014), since uptake by plant roots occurs directly from the solution phase. The solution phase is commonly separated from the soil solid phase by centrifuging the soil, and the resulting supernatant is filtered to 0.45 µm or less to exclude particulate material (Meers et al., 2006). Zhang and Davison (2006) describe how good correlation between the total metal in soil solution and the concentration in the plant implies fast uptake, such that the concentration of the species being taken up is depleted in the soil solution at the plant-root interface. In order for the correlation to be maintained, dissociation must not be accompanied by release of the element from the solid phase since this would vary with soil pH and other soil characteristics (Zhang and Davison, 2006).

Multiple different inorganic and organic metal species of varying lability may exist simultaneously in the soil solution, in addition to the free ion form, and there is considerable evidence that plant uptake is highly dependent on metal speciation in solution (Parker et al., 1995). The free ion activity model (FIAM) is an equilibrium model initially developed to describe metal toxicity and bioavailability to aquatic organisms in terms of the free ion activity in solution (Campbell, 1995). It has since been applied to explain plant uptake from soil

solution (Sauve et al., 1998; Vulkan et al., 2000; Hough et al., 2005). The model assumes that diffusional transport in the soil solution towards the site of uptake is not rate-limiting, and is therefore used to predict plant uptake where uptake is slow relative to the transport (Degryse et al., 2009). Under this scenario, depletion of the element at the root surface becomes negligible and its concentration in plant tissue can be expected to be proportional to the free ion activity in solution (Sauve et al., 1996). Methods used to determine the free ion activity in soil solution include ion-selective electrodes (Taboada-Castro et al., 2000), the Donnan Membrane technique (Fitch and Helmke, 1989) and resin-exchange methods (Holm et al., 1995), whilst anodic stripping voltammetry has been used extensively to measure free metal ions in addition to labile complexes that can rapidly dissociate (Buffle and Tercier-Waeber, 2000).

Several studies concerning uptake by higher plants do not conform to the FIAM however (Parker et al., 2001; Berkelaar and Hale, 2003), in which it is suggested that chemical species other than the free metal ion may be taken up by plants as intact complexes (Smolders and McLaughlin, 1996; McLaughlin et al., 1998). Furthermore, the FIAM is parameterised on bulk soil solution measurements and may therefore be compromised by rhizospheric effects where local depletion of ions in the vicinity of plant roots can occur (Zhang et al., 2001).

It has long been recognised that the bioavailable pool of metal in soil is not confined to the solution phase, as metal associated with the solid phase is identified as making an important contribution to the plant-available fraction (Beckett, 1964; Barber, 1995). The soil solution concentration does not account for the kinetic resupply of metal from the solid phase, and consequently may provide an inadequate prediction of the plant-available fraction in soils where diffusional supply processes from the solid phase are significant (Nolan et al., 2005). On this basis, chemical extraction methods utilising buffered and unbuffered salt solutions, weak mineral acids and chelating agents have been developed, which aim to quantitatively

determine the solid phase capacity of exchangeable and weakly-adsorbed metal retained on the solid surface through relatively weak electrostatic interactions, in addition to labile complexes and species in solution (Kennedy et al., 1997; Gleyzes et al., 2002).

Most extraction methods involve shaking a known mass of soil with an extraction solution, typically in a soil mass to extractant volume ratio of 1:10, for a predefined quantity of time at ambient temperature. Common extractants include solutions of the salts $MgCl_2$ (Tessier et al., 1979) and $CaCl_2$ (Novozamsky et al., 1993; Houba et al., 2000), which combine the strong ion-exchange capacity of divalent Mg^{2+} and Ca^{2+} cations with the weak complexing ability of Cl^-. The ionic strength of the salt solution is a key consideration, with generally weaker (~0.01 M) solutions comparable to the typical ionic strength of the soil solution favoured (Houba et al., 2000). Further examples of frequently-used extractions include acetate salts, in particular ammonium acetate (Adriano et al., 1977), as well as nitrate salts such as KNO_3, $NaNO_3$ and NH_4NO_3 (Gupta and Aten, 1993). The organic chelating agents diethylene triamine penta-acetic acid (DTPA) and ethylene diamine tetra-acetic acid (EDTA) have been widely adopted due to their ability to form highly stable and water-soluble metal-cation complexes (Haq et al., 1980; Norvell, 1984; Brun et al., 2001; Hammer and Keller, 2002). Weak solutions (≤ 0.1 M) of strong acids, including nitric and hydrochloric acid, have also been used (Ponnamperuma et al., 1981; Koster et al., 2005).

The plethora of extraction methods reported in the literature is an inherent complication of their use however, since no single method is recognised as a universal approach for assessing bioavailability. Redistribution and re-adsorption of the metal during the extraction process can occur if the correct soil mass to extractant volume ratio is not used (Chomchoei et al., 2002), whilst induced changes in pH can result in changes in speciation during sampling and extraction (Hooda et al., 1999). The comparability and reproducibility of the extractions has also been debated owing to methodological artefacts associated with temperature,

equilibration time and the soil:extractant ratio (Nirel and Morel, 1990; Clark et al., 1996; Tack et al., 2002). Further confounding factors that hinder the ability of chemical extractions to successfully assess bioavailability to plants include the presence of competing ions in the soil solution and variation between plant species with respect to root uptake processes (Kennedy et al., 1997).

Extraction procedures relate to the chemistry of the metal in the bulk soil and may therefore overlook rhizosphere effects on availability for plant uptake (Ehlken and Kirchner, 2002). Plant roots excrete a variety of substances and chelating agents including organic acids, sugars, amino acids, H^+ and HCO_3^- ions (Russell and Russell, 1973), which in combination with a dense population of microorganisms create micro-environments where bioavailability may be considerably different to that in the bulk soil (Courchesne and Gobran, 1997). Low molecular weight organic acids are reported to play an important role in enhancing metal uptake by roots (Naidu and Harter, 1998; Shan et al., 2003). More complex extraction solutions aimed at mimicking rhizosphere effects have consequently been developed. For example, Lakanen and Ervio (1971) developed a mixed EDTA-acetic acid procedure in which complexation by EDTA and acetic acid was postulated to simulate the complexing behaviour of root exudates, whilst the low pH simulates the acidic environment of the rhizosphere.

The proportion of metal in equilibrium with the soil solution can be determined using the isotopic dilution exchange method (ID), whereby an isotope of the analyte of interest is added to the soil (McAuliffe et al., 1947; Young et al., 2005). The isotopically exchangeable fraction of an element in soil is that which exchanges rapidly with the fraction in the soil solution. Isotopic dilution techniques can be applied using radioactive or enriched stable isotopes.

Where radioisotopes are used for isotopic dilution, measurement of the specific activity in the soil solution is used to derive an ‘E value’. Since the radioisotope will be identical to the stable

isotope in terms of its geochemical behaviour, the concentration of the isotopically-exchangeable stable element (labile pool or E value) can be derived through measuring the partitioning of the radioisotope between the solid and solution phases (K_D) and the concentration of the stable element in solution (M) after a period of equilibration (typically two to three days), as shown in Equation (1.1):

$$\mathrm{E\ (mg\ kg^{-1})} = \mathrm{M\ (mg\ L^{-1})} \times \mathrm{K_D\ (L\ kg^{-1}\ soil)} \quad (1.1)$$

Examples of radioisotopes used in ID studies include: ^{54}Mn, ^{59}Fe, ^{60}Co, ^{64}Cu and ^{65}Zn (Lopez and Graham, 1972); ^{27}Mg, ^{42}K and ^{45}Ca (Graham and Silva, 1979); ^{63}Ni (Echevarria et al., 1998) and ^{109}Cd (Smolders et al., 1999). Whereas chemical extraction methods rely on the assumption that the entirety of the isotopically-exchangeable fraction of an element is extracted from the soil into solution and participates in the sorption equilibrium, the advantage of the ID technique is that this isotopically-exchangeable fraction need not be transferred completely from the solid phase into solution by a strong extractant (Gabler et al., 2006). A review of the literature by Young et al. (2005) concluded that the ID technique appears reasonably robust, with limited variation in E values reported for variations in solid:solution ratio, suspension separation method, electrolyte composition, suspension pre-equilibration time and isotope equilibration time.

Similarly, plants may be grown on isotopically-equilibrated soils with the concentrations of the radioactive and stable isotope measured in the plant tissue to derive an L value that is conceptually identical to the E value (Larsen, 1952). Values for E and L should in theory be identical for a given element in a given soil, unless the plant modifies the soil rhizosphere in such a way that the non-isotopically-exchangeable element fraction becomes mobilised (Hedley et al., 1982). Values of E and L have often been found to be comparable (Hamon et al., 1997; Smolders et al., 1999; Stanhope et al., 2000). However, E values for Zn in alkaline

soils are typically found to be statistically higher than L values, possibly due to irreversible fixation of the added tracer and/or increased isotopic exchange in batch techniques compared to pot trials (Sinaj et al., 2004). In some cases, the presence of colloidal non-exchangeable metal in the soil solution may be the cause of reported differences in E and L values, since E value measurements of Zn will be affected by the presence of colloids unlike L value measurements (Lombi et al., 2003)

The short half-lives of certain radioisotopes constrains their use in deriving L values. This is the case for the most accessible radioisotope of Cu, ^{64}Cu, with a half-life of just 12.4 hours. As a result, the E value technique has been relied upon in isotopic investigations of soil Cu availability/lability. Recent advances in ICP-MS technology have meant that ID methods utilising stable isotopes have been developed (Hamon et al., 2002). In principle, mass-spectrometric-based ID techniques can be applied to all elements that have at least two stable or long-lived isotopes. For example, Nolan et al. (2004) developed a procedure for determining E values for Cu using the stable isotope ratio ^{65}Cu/^{63}Cu. Excellent agreement with values derived using the radioisotope ^{64}Cu was reported. Furthermore, Oliver et al. (2006) successfully developed a procedure for determining Cu L values where tomato plants and ryegrass were used to obtain a direct measure of available Cu. The L value was calculated according to Equation (1.2), and the E value according to Equation (1.3):

$$L = R \times \frac{AW(Cu_{nat})}{AW(^{65}Cu)} \times \frac{IR_{sp}\text{-}IR_{meas}}{IR_{meas}\text{-}IR_{nat}} \times (IR_{nat} + 1) \quad (1.2)$$

$$L = R \times \frac{AW(^{63}Cu + ^{65}Cu)}{AW(^{65}Cu)} \times \frac{IR_{sp}\text{-}IR_{meas}}{IR_{meas}\text{-}IR_{nat}} \times (IR_{nat} + 1) \quad (1.3)$$

where: R = total ^{65}Cu* added to soil during spiking (mg kg^{-1} soil); AW(Cu_{nat}) = atomic weight of natural Cu; AW(^{65}Cu) = atomic weight of ^{65}Cu isotope; IR_{nat} = natural abundance ratio of

$^{63}Cu/^{65}Cu$ in plant; IR_{sp} = abundance ratio of $^{63}Cu^*/^{65}Cu^*$ in spiking solution; IR_{meas} = measured abundance ratio of $(^{63}Cu+^{63}Cu^*)/(^{65}Cu+^{65}Cu^*)$ in plant tissue; and an asterisk (*) indicates Cu sourced from the added ^{65}Cu spike.

Oliver et al. (2006) concluded that the derived L values were not statistically different to E values derived using equilibration periods up to and including the growth period of plants in the L value method.

1.5 Aging of metals and radionuclides within soil

Upon addition of metal to the soil, a significant fraction is rapidly and reversibly adsorbed to the solid phase within 24 hours (Roig et al., 2007; Juhasz et al., 2008). Following this initial rapid formation of a pseudo-equilibrium between the metal in the solid phase and solution phase, a slow and irreversible adsorption phase will proceed on a timescale of up to several years (Arai and Sparks, 2002). The result is a decline in the availability of metal over time, commonly termed aging (Ma et al., 2006).

Intra-particle diffusion is recognised as a key rate-limiting factor in the slow adsorption phase, where rapid adsorption to the external surface of a solid phase component is suceeded by slow adsoprtion along surface sites of the micropore walls (Axe and Trivedi, 2002). Amorphous (hydrous) oxides of Fe, Al and Mn possess significant microporosity, which is important for intra-particle diffusion and adsorption; it has been demonstrated that internal surfaces constitute up to 40, 50 and 90% of total adsorption sites for Fe, Al and Mn, respectively (Trivedi and Axe, 1999). Surface diffusivities of ions are reported in the range of 10^{-16} to 10^{-19} cm^2 s^{-1} (Axe and Trivedi, 2002).

The formation of inner sphere complexes will also contribute to the slow adsorption phase. For example, Zhang and Sparks (1990) reported that after initial outer-sphere complexation at the β-layer, selenite undergoes inner-sphere complexation through ligand-exchange with the goethite surface after entering the α- layer. Further processes which contributed to aging include cavity entrapment, occlusion within solid phases by co-precipitation, and surface precipitation (Cavallaro and McBride, 1978; Schosseler et al., 1999; Elzinga and Reeder, 2002; Ma et al., 2006).

Aging of radiocaesium (Cs) within clayey soils is attributed to adsorption and fixation to illitic clay minerals (Squire and Middletone, 1966; Cremers et al., 1988; Noordijk et al., 1992). The small hydrated radii of Cs cations mean that they can adsorb to internal interlayer surfaces of illite. Hird et al. (1996) describe how if sufficient quantities of Cs cations are adsorbed, the charge on the internal surfaces of the clay becomes neutralised, thereby reducing the repulsive forces between layers. Furthermore, dehydration of Cs cations upon adsorption produces an interlayer solution that is hypotonic (dilute) relative to the external or bulk soil solution, and the resulting osmotic potential triggers a net flow of water out of the interlayer region causing the interlayers to collapse around the Cs cations. Wetting and drying cycles are reported to accelerate dehydration of the clay interlayers and subsequent interlayer collapse (Hird et al., 1995; Rigol et al., 1999; Roig et al., 2007).

Several kinetic equations have been developed and applied to model the aging of metals and metalloids within soil (Guo et al., 2011; Wang et al., 2015). For example, a number of studies have demonstrated that a parabolic diffusion equation derived from Fick's second law can effectively describe the kinetics of the slower reactions governing the aging process (Ma and Uren, 1997; Ma et al., 2006; Di Tullo et al., 2016). Under such scenarios, the slow diffusion of species into microporous mineral and organic particles and/or between aggregates is concluded to be the rate-limiting mechanism controlling aging.

The rate law of chemisorption was first established by Zeldowitsch (1934), where the rate of adsorption of carbon monoxide on manganese dioxide was shown to decrease exponentially with an increase in the amount of gas adsorbed. This function has since been known as the Elovich equation, and a simplified version has been used to describe second order kinetics of chemisorption of both inorganic and organic pollutants on solid surfaces over a range of timescales. In the soil system, it has been applied to describe the sorption of both P (Chien and Clayton, 1980) and Se (Li et al., 2016).

A pseudo-second-order rate expression was developed to describe both ion exchange and chemiosorption where covalent bonding occurs between the adsorbent and adsorbate (Ho, 1995). It has been widely applied to describe the adsorption of a range of metals to a number of different adsorbents including activated carbon (Basso et al., 2002), peat (Ho and McKay, 1999) and tree fern (Ho et al., 2004) amongst others. Recently, the model has been successfully applied to describe the aging of As (Wang et al., 2015) and Se (Li et al., 2016) in soils.

The rate and extent of aging of radionuclides in soil is important in determining the long-term radiation dose to humans and other biota by influencing the magnitude of transfer of radionuclides to plants and crops (Krouglov et al., 1997). For example, following contamination of upland Cumbrian soils with Cs deposited in fallout from the Chernobyl Nuclear Power Plant accident in 1986, sheep in the area exhibited levels of radioactivity exceeding the 1000 Bq kg^{-1} (fresh weight) intervention limit prompting restrictions to be imposed on the movement and slaughter of livestock (IAEA, 2006). Such restrictions remained in place for unexpectedly long periods of time, in some places up to 26 years (BBC, 2012), as unsafe activity levels persisted within sheep. The very slow aging of Cs in the upland Cumbrian soils is attributed to their predominantly acidic nature, in combination with a low clay content and high organic matter content. The associated high ion exchange capacity and large

proportion of non-specific adsorption sites is responsible for the sustained availability of Cs (Cremers et al., 1990; CEC, 1992; Nisbet and Shaw, 1994).

1.6 Plant uptake of radionuclides

A wide range of plant species have been documented throughout the scientific literature to accumulate substantial quantities of radionuclides from contaminated soils via root uptake, which represents the primary entry route of radionuclides into the biosphere. For example, Coughtrey et al. (1989) reported that up to 19% of the Chernobyl ^{137}Cs fallout deposited in the UK was accumulated by the *Festuca/Agrostis* plant community. Once penetration of the root epidermis has been achieved, the radionuclides are distributed in various parts of the plant through the sap of xylemic and phonemic channels, and subsequently compartmentalised within cells (Ansoborlo and Adam-Guillermin, 2012). Uptake is commonly quantified in terms of a soil-to-plant transfer factor (TF), an empirical quantity which is defined as the activity concentration ratio of a radionuclide between the dry plant mass and dry soil within the rooting zone as defined in Equation (1.4) (Ehlken and Kirchner, 2002):

$$\mathrm{TF_i} = \frac{\text{activity concentration of radionuclide i per kg dry plant mass}}{\text{activity concentration of radionuclide i in dry soil within the rooting zone}} \qquad (1.4)$$

Table 1.1 lists soil-to-plant transfer factor ranges for a number of radionuclides taken from a comprehensive compilation given in a recent UNSCEAR (2011) report. Given that Cs^+ and Sr^{2+} are structural analogues of the nutrient ions K^+ and Ca^{2+}, respectively, with highly similar geochemical behaviour, this is likely to explain their considerably greater transfer to plants than for non-essential elements such as Pu and Am (Nisbet and Shaw, 1994).

Table 1.1. *Illustrative ranges of soil-plant transfer factors (Bq kg^{-1} plant dry mass per Bq kg^{-1} soil dry mass) for different radionuclides [adapted from Ansoborlo and Adam-Guillermin (2012)].*

Element	Concentration ratio (soil/plant)	Aggregated transfer factor
Strontium (Sr)	0.01-1	4×10^{-5} to 4×10^{-3}
Caesium (Cs)	0.001-0.1	4×10^{-5} to 4×10^{-4}
Cs*	0.1-10	4×10^{-4} to 4×10^{-2}
Iodine (I)	0.001-1	4×10^{-6} to 4×10^{-3}
Technetium (Tc)	0.1-10	4×10^{-4} to 4×10^{-2}
Lead (Pb)	0.001-0.01	4×10^{-6} to 4×10^{-5}
Radium (Ra)	0.001-0.1	4×10^{-6} to 4×10^{-4}
Uranium (U)	0.001-0.1	4×10^{-6} to 4×10^{-4}
Neptunium (Np)	0.001-0.1	4×10^{-6} to 4×10^{-4}
Plutonium (Pu)	10^{-5}-10^{-3}	4×10^{-8} to 4×10^{-6}
Americium (Am)	10^{-5}-10^{-3}	4×10^{-8} to 4×10^{-6}
Curium (Cm)	10^{-5}-10^{-3}	4×10^{-8} to 4×10^{-6}

**Observed range in natural and semi-natural ecosystems on acid sandy soils poor in potassium.*

Table 1.1 reveals that TFs for Tc are among the highest for routinely measured radionuclides; Cataldo et al. (1984) and Echevarria et al. (1997) report TFs up to 1,000, but the IAEA (2010) recommend a maximum TF of five in food crops and 20 in pasture. The similarity in chemical structure between the plant-available pertechnetate (TcO_4^-) and phosphate ($H_2PO_4^-$) species is likely to explain the observed high concentrations of Tc in a number of plant species. In comparison, TFs for Se added to soil in the form of selenate or selenite span several orders of magnitude from 0.01 to 100, with most in the range from 1 to 10 (Bitterli et al., 2010). Such TFs derived from studies centred on Se-amended soils are generally found to be at least an order of magnitude higher than for those conducted with native soil Se for a given plant species and plant part (Bitterli et al., 2010).

As evident in Table 1.1, significant variability is reported in TFs, even for individual soil-plant combinations (Nisbet and Woodman, 2000). For example, following an extensive literature

survey, Vandenhove et al. (2009) reported that TFs to grass for ^{238}U spanned more than four orders of magnitude. Such variability can be the result of factors including climate, plant type and species, the part of the plant concerned, the physico-chemical form of the radionuclide in the soil and the presence of competing species. Soil characteristics such as pH, redox conditions and water chemistry that influence transport to the root and subsequent adsorption are expected to contribute the most, however (Bettencourt et al., 1988).

Ehlken and Kirchner (2002) make the point that interpretation of decreasing TFs over time as an effect of aging can be complicated by the redistribution of the radionuclide within the rooting zone. Following initial deposition, downward migration of the radionuclide within the soil profile to horizons where roots are less dense will result in reduced uptake and consequently lower TFs over longer timescales of several years to decades. For deep-rooting plants such as trees, the redistribution of the radionuclide may even give rise to an increase in TFs over time (Belli et al., 1996). Despite their crudeness, TFs are widely used in radiological assessment models as the most practical means of quantifying plant uptake and for assessing potential bioavailability.

1.7 DGT technique and principles

Diffusive gradients in thin-films (DGT) is a dynamic speciation technique based upon the principles of Fick's first law of diffusion, initially developed for the in situ quantitative determination of labile trace metals in aqueous solution (Davison and Zhang, 1994; Zhang and Davison, 1995). A selective binding agent is employed within a plastic assembly to passively accumulate the target component, which can subsequently be analytically quantified directly in the laboratory or indirectly following elution from the binding agent. The binding agent itself is typically an ion-exchange resin, such as Chelex-100, a strong metal complexing agent that acts as a sink by rapidly binding free and/or kinetically-labile cationic metal species

(Paulson, 1986). Since its conception over 20 years ago, the technique has been developed to determine concentrations and fluxes of labile or bioavailable trace metals in sediments (Harper et al., 1998) and soils (Zhang et al., 1998). The continuous development of new binding agents has allowed for the extension of the range of analytes, which now include: cationic trace metals (Denney et al., 1999); major cations (Dahlqvist et al., 2002); anionic metals (Stockdale et al., 2010); phosphate (Zhang et al., 1998); rare earth elements (Garmo et al., 2003); radionuclides (Chang et al., 1998; French et al., 2005); and more recently organic compounds (Chen et al., 2012).

Figure 1.4 shows a schematic cross-section of a DGT device, alongside an image of an assembled device ready for deployment. The DGT device comprises a binding layer containing the binding agent, overlain by a polyacrylamide diffusive gel layer of well-defined thickness (conventionally 0.78 mm). On top is a cellulose nitrate filter membrane (pore size 0.45 µm), which behaves like an extension of the diffusive gel and separates the diffusive gel from the surrounding media (Zhang and Davison, 1995). The membrane prevents the adherence of fine particles to the diffusive gel as well as restricting their passage. The three layers are mounted on a plastic cylindrical base within a piston-type assembly and are held in place by a tight-fitting cap. The cap has an exposure window of 2.54 cm^2 for deployment in soil, or 3.14 cm^2 if deployed in solution.

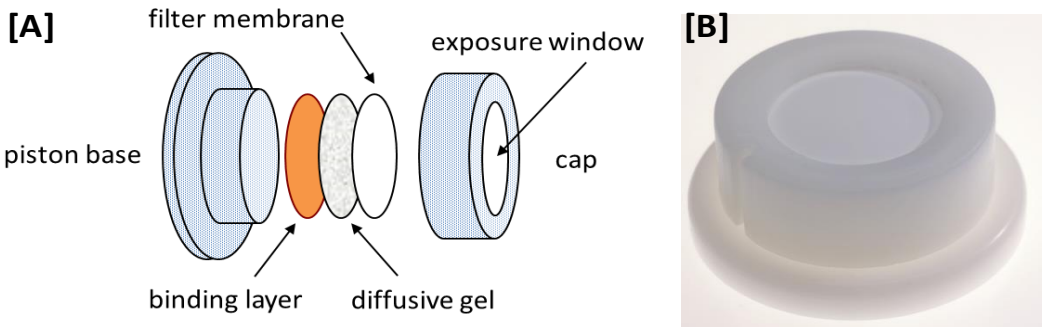

Figure 1.4. *Schematic cross-section of a DGT device* ***[A]****; image of an assembled DGT device ready for deployment* ***[B]****.*

Zhang and Davison (1995) describe how free metal ions and kinetically-labile species (those capable of rapid transfer to solution from a solid phase component or solubilised complexes that readily dissociate) in the surrounding media undergo molecular diffusion across the filter membrane and diffusive gel layer before being removed by the binding agent within the binding layer. By applying Fick's first law of diffusion, the flux (F) though the filter membrane and diffusive gel layer can be expressed in Equation (1.3):

$$\mathrm{F} = \frac{\mathrm{DC}}{\Delta \mathrm{g}} \tag{1.5}$$

where: D is the temperature-corrected diffusion coefficient of the free metal ion in the diffusive gel; C is the concentration of the labile metal in the bulk solution; and Δg is the combined thickness of the diffusive gel and filter membrane (Zhang and Davison, 1995). Since flux is equal to mass (M) per unit area (A) per unit time (t), Equation (1.5) can be re-written as Equation (1.4):

$$\mathrm{M} = \frac{\mathrm{DCtA}}{\Delta \mathrm{g}} \tag{1.6}$$

Provided that the capacity of the binding agent is not exceeded and rapid removal of the accumulated component occurs, a concentration of effectively zero is maintained at the interface between the binding layer and diffusive gel throughout the period of deployment. A steep concentration gradient is consequently established across the material diffusion layer (MDL) which comprises the diffusive gel layer and filter membrane, as depicted in Figure 1.5.

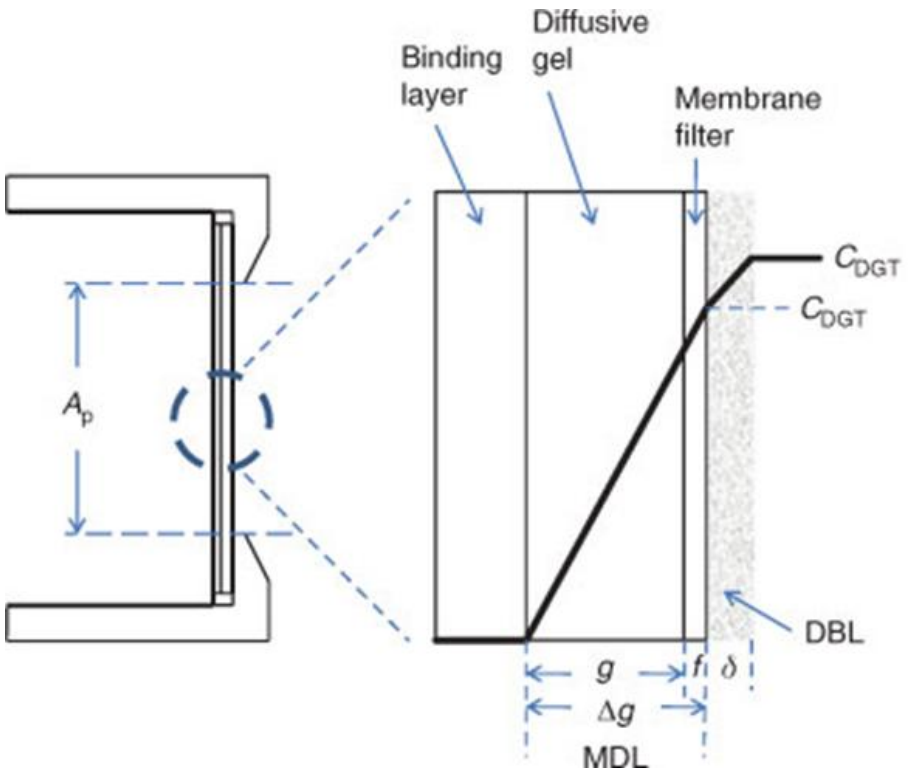

Figure 1.5. *Schematic cross-section of a DGT device deployed in solution showing the binding layer, diffusive gel layer (thickness = g) and membrane filter (thickness = f). MDL = material diffusion layer of thickness ⊿g (g + f); DBL = diffusive boundary layer of thickness δ. From: Davison and Zhang (2012).*

If the concentration gradient remains constant during the deployment time, such that depletion of the diffusing species in the vicinity of the DGT exposure window does not occur, the quantity of accumulated ions in the binding layer can be directly related to the concentration in the surrounding media through re-arranging Equation (1.6) to yield Equation (1.7):

$$C_{DGT} = \frac{M\Delta g}{DtA} \qquad (1.7)$$

where: C_{DGT} is the DGT-labile ion concentration in the bulk solution; M is the mass of ions accumulated by the binding agent; Δg is the thickness of the diffusive gel plus the filter

membrane; D is the diffusion coefficient; A is the exposed surface area of the DGT device; and t is the deployment time.

When deployed in solution, C_{DGT} represents the time-averaged concentration at the interface between the DGT device and solution of the free ion or labile complex species that contribute to the DGT-induced diffusive flux. In well-stirred solutions, rapid mixing ensures that depletion of the diffusing species in the immediate vicinity of the DGT device is negligible, and C_{DGT} is therefore equal to the bulk concentration of the DGT-labile species in solution (Degryse et al., 2009). Figure 1.5 depicts a diffusion boundary layer (DBL), a region in the solution adjacent to the DGT where the transport of metal ions and complexes undergoes a rapid transition from advective to diffusive control, which acts as an extension of the diffusion pathway (Warnken et al., 2006). Below a certain flow threshold, the thickness of the DBL is deemed significant relative to the thickness of the MDL and must therefore be corrected for through deployment of DGT devices with differing thicknesses of diffusion layer.

Zhang and Davison (1999) demonstrated that the diffusion coefficient (D) of a metal ion within the polyacrylamide diffusive gel is indistinguishable from its corresponding value in water. It is typically determined using a diffusion cell, whereby a 0.8 mm-thick diffusive gel disc is interposed between a source and receptor compartment and aliquots are taken from either side at regular time intervals (Luo et al., 2010). Values for D are dependent on temperature since this affects the solution viscosity.

1.8 DGT deployment in soil

Figure 1.6 provides a schematic illustration of DGT deployment in soil with respect to the concentration gradient of the diffusing species. During soil deployment, accumulation of the target species by DGT results in a localised depletion in the soil solution concentration (C_{soln})

in the immediate vicinity of the interface between the DGT device and the soil (Zhang and Davison, 2006).

This depletion in C_{soln} induces the localised release of labile species from the solid phase to buffer the solution concentration, in addition to the dissociation of metal complexes in solution in attempt to re-establish the state of equilibrium that has been perturbed (Zhang et al., 1998). All labile species capable of dissociating sufficiently rapidly to contribute to the flux to the device will be included in the DGT measurement (Zhang and Davison, 2000).

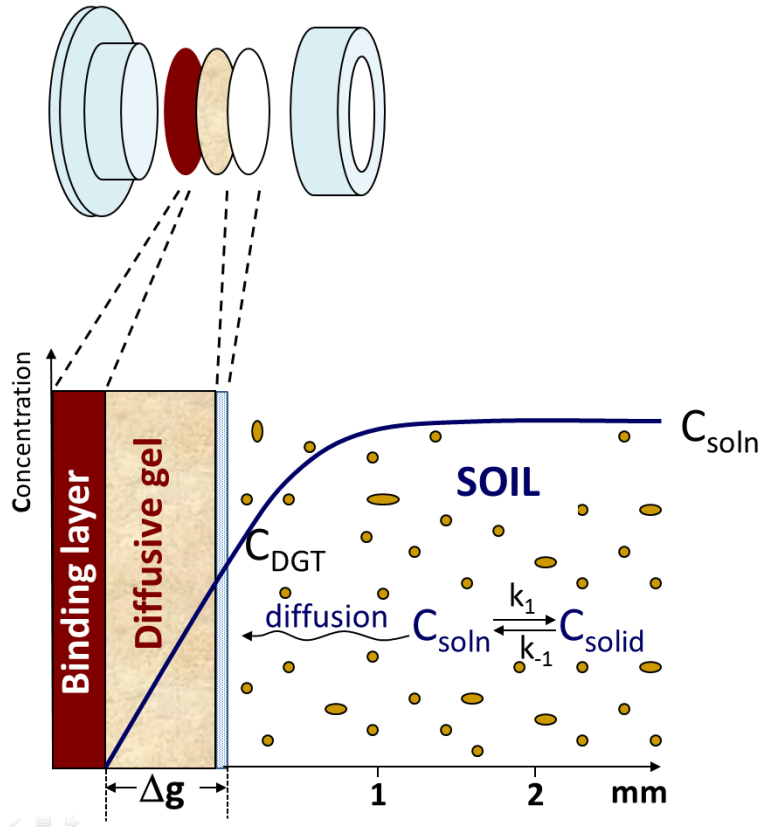

Figure 1.6. *Cross-sectional schematic of DGT deployment in soil showing the concentration gradient across the DGT device and extension into the adjacent soil solution.*

Zhang et al. (1998) describe how the rate of release of this labile component associated with the solid phase determines the extent of depletion in C_{soln} in response to removal by DGT, and identify three scenarios as described below and depicted diagrammatically in Figure 1.7:

- Case (i) *Fully sustained*. Minimal depletion of C_{soln} occurs as the rate of release from the solid phase is rapid to the extent that supply from this pool effectively buffers C_{soln}. Depletion will only occur when the accumulating component associated with the solid phase is eventually used up.

- Case (ii) *Unsustained*. Negligible buffering due to resupply from the solid phase occurs under this scenario, either because the solid phase pool is small or because desorption is slow. Supply to the DGT device is therefore confined to diffusion of the labile species within the soil solution. The DGT-induced flux diminishes fairly rapidly with time as the localised labile pool in solution becomes depleted. Under this scenario, the diffusion gradient may extend several centimetres into the soil (Ernstberger et al., 2002).

- Case (iii) *Partly sustained*. In this intermediate case, which in reality is applicable to the majority of soils, some resupply occurs from the solid phase at an appreciable rate but it is insufficient to fully sustain C_{soln} in the vicinity of the DGT device and thereby satisfy the DGT demand.

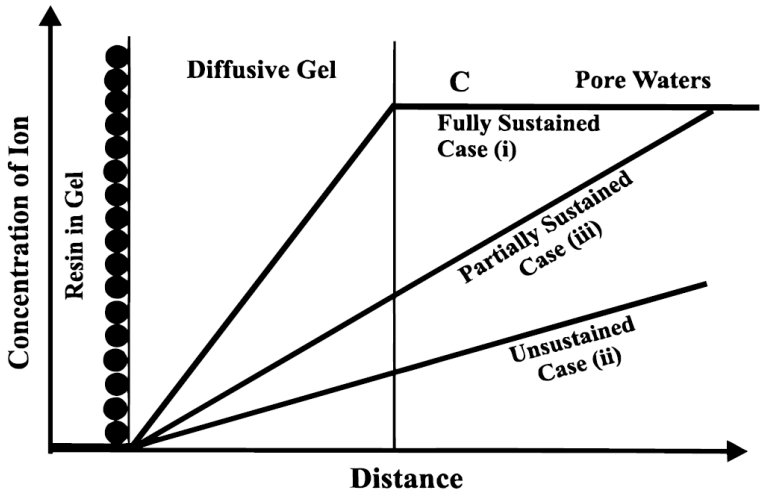

Figure 1.7. *Schematic representation of the effect of three differing scenarios of solid phase resupply on the extent of soil solution depletion at the DGT interface with the soil and the consequent magnitude of the concentration gradient across the device. From: Zhang et al. (1998).*

The three cases described above can be distinguished from one another by expressing C_{DGT} as a ratio (R) relative to C_{soln} [Equation (1.8)]. C_{soln} is usually determined by extracting the porewater after centrifuging the soil.

$$R = \frac{C_{DGT}}{C_{soln}} \tag{1.8}$$

where:

- R > 0.8. Rapid and sustained resupply from the solid phase is occurring.
- R < 0.1. Unsustained case where virtually no resupply from the solid phase occurs.
- 0.1 < R < 0.8. Some resupply occurs but it is insufficient to fully sustain R.

Harper et al. (1998) developed a numerical model describing the DGT-soil system which simulates the response of a homogeneous soil following DGT deployment. The model, known as DGT-induced fluxes in soils and sediments (DIFS), couples removal and diffusional transport

within the DGT device with diffusive transport and exchange between the solid and solution phases in the adjacent soil, as illustrated in Figure 1.8. The basis for the model is a pair of linked parabolic partial differential equations describing dissolved and adsorbed trace metal concentrations in the soil and DGT device. These are solved by the Method of Lines using standard ordinary differential equation solvers.

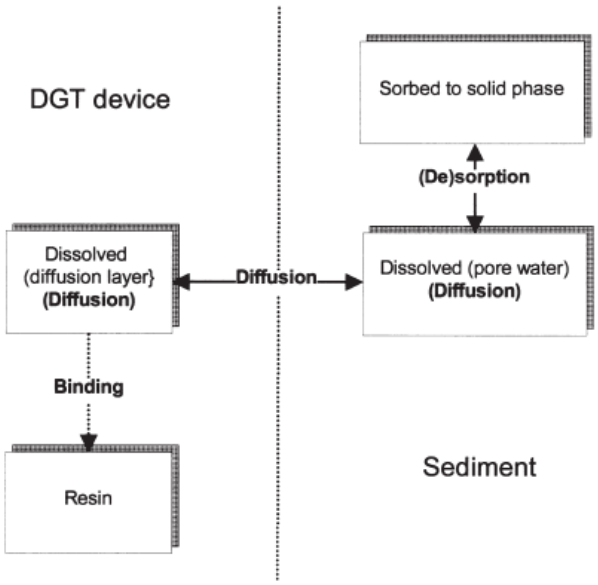

Figure 1.8. *DIFS model components. From: Harper et al. (2000).*

The model allows for prediction of soil parameters including the proportion of labile trace metal in the solid phase (K_D) and the response time (T_c) in which the equilibration of metal between the solid and solution phase occurs (Ernstberger et al., 2002). The kinetics of the interaction are taken into account by adsorption and desorption rate constants (k_1 and k_{-1}), whilt transport through the system is diffusion-controlled.

Initially, DIFS was developed as a one-dimensional (1D) model that assumed that DGT devices could be represented by an infinite planar surface extending along an axis perpendicular to the DGT interface. Later, the model was advanced and refined to consider the diffusion of solutes in two dimensions (2D-DIFS) (Sochaczewski et al., 2007) using a finite element

discretisation (FED) method. It was demonstrated that the 2D-DIFS is likely to more accurately simulate real DGT deployments than 1D-DIFS, especially in cases where there is significant depletion of trace metal by the DGT device (Lehto et al., 2008).

1.9 DGT as an indicator of bioavailability

The supply of metal from soil to plants is controlled by a range of processes including diffusional and convective transport through solution to the root, the root encountering fresh soil surfaces during growth, in addition to the influence of root micro-environments and exudates (Marschner, 1995; McLaughlin et al., 1998; McLaughlin et al., 2000). Barber (1995) demonstrated that these processes do not operate in isolation however, with supply to the plant likely to occur simultaneously from the solid phase and dissolved complexes. Unless one of these processes is dominant it is unlikely that any single chemical surrogate could mimic plant uptake (Zhang et al., 2001; Zhang and Davison, 2006).

Bioavailability should ideally be assessed in situ using a procedure capable of mimicking the dynamic action of the plant to account for the labile component associated with the solid phase and dissolved complexes, as well as reflecting the transport rate of ions through the soil. This is the approach that DGT takes, which aims to perturb the soil system in a similar manner as a plant by depleting the soil solution concentration at the root surface (Zhang et al., 2001; Zhang and Davison, 2006). By superimposing a layer of diffusive hydrogel onto a binding agent, a controlled flux of metal is established through the soil and device on a similar spatial scale to that of a plant (Zhang and Davison, 2015). The removal of metal from the soil by DGT and the induced diffusive flux is analogous to the action of a plant root. Lehto et al. (2006) presented a DGT-parameterised dynamic plant uptake model and demonstrated quantitatively the similarity between fluxes to plant membranes and DGT through simulating Zn uptake by a Zn hyper-accumulator (*Thlaspi caerulescens*) and a non-accumulator (*Thlaspi*

arvense). The thickness of the diffusion layer established under diffusion-limited plant uptake conditions is generally similar to the thickness operating during dynamic techniques for assessing speciation and bioavailability, and for DGT the agreement is particularly good (van Leeuwen et al., 2005). As a result, the timescale of DGT measurements is considered to be comparable with the timescale of plant uptake, and the kinetic perturbation of the element concentrations in the soil system is therefore likely to be analogous to the perturbation induced during plant root uptake (Zhang and Davison, 2015).

DGT is expected to perform well as a surrogate for plant uptake in well-buffered soils where the solid phase has a substantial capacity to store labile metal, which can also be readily desorbed to the solution phase such as in soils with a high clay content (Lehto et al., 2006). DGT can only be expected to reliably mimic plant uptake under scenarios where the proportion of metal supplied by mass flow relative to total uptake by the plant is low however (Lehto et al., 2006). In soils where the solid phase resupply is low, for example those with a high sand content and/or low pH, supply of metal to the plant by advection can be significant, and the ability of DGT to physically mimic plant uptake will be limited. DGT will consequently underestimate the total uptake by the plant.

Rhizospheric influences represent a further potential constraining factor on the ability of DGT to successfully act as a surrogate for plant uptake. DIFS fails to consider the effect that root exudates or microbial activity may have on the speciation of the metal being accumulated and its subsequent availability, which can be significant (McLaughlin, 2002; Puschenreiter et al., 2005). Furthermore, the root may encounter fresh surfaces as it grows through the soil, which cannot be accounted for in the DIFS model (Lehto et al., 2006). To ensure the effectiveness of DGT in predicting plant uptake, these processes must make a minimal contribution relative to diffusional supply and associated solid phase buffering (Zhang and Davison, 2006).

The bulk soil solution concentration (C_{soln}) of a metal does not represent the effective concentration in soil that a sink like DGT or a plant root is exposed to soil during the general case of solution and solid phase resupply. Consequently, Zhang et al. (2001) proposed the concept of an effective concentration (C_E), which incorporates C_{soln} and an additional term that represents metal supplied from the solid phase. C_E can be conceptualised as the hypothetical concentration in solution that would be needed to provide the analytically-determined mass of metal accumulated by the binding layer if there was no solid phase buffering (i.e. supply was solely by diffusion) (Degryse et al., 2009). C_E is calculated by dividing the mean interfacial concentration (C_{DGT}) by R_{diff} as shown in Equation (1.9):

$$C_E = \frac{C_{DGT}}{R_{diff}} \quad (1.9)$$

R_{diff} is defined in Equation (1.10):

$$R_{diff} = \frac{C_{diff}}{C_{soln}} \quad (1.10)$$

where: C_{diff} represents the mean DGT-soil interfacial concentration in the case of solely diffusional resupply; and C_{soln} is the concentration in the bulk soil solution. R_{diff} can be calculated using the DIFS model, and is influenced by parameters including the geometry of the DGT device, deployment time, as well as the soil porosity and tortuosity (Harper et al., 2000). For a 24-hour deployment period, using a standard diffusive layer thickness of 0.93 mm, C_E is approximately 13 times larger than C_{DGT}, although this may vary slightly according to the water holding capacity of the soil (Degryse et al., 2009).

Figure 1.9 illustrates the concept of C_E through a schematic representation of the DGT-soil system during deployment in terms of the concentration of metal with respect to lateral distance across the DGT device and adjacent soil solution. Case (i) represents the scenario of

metal supply by diffusion only, whilst in case (ii) some resupply from the solid phase is occurring which is incorporated by C_E.

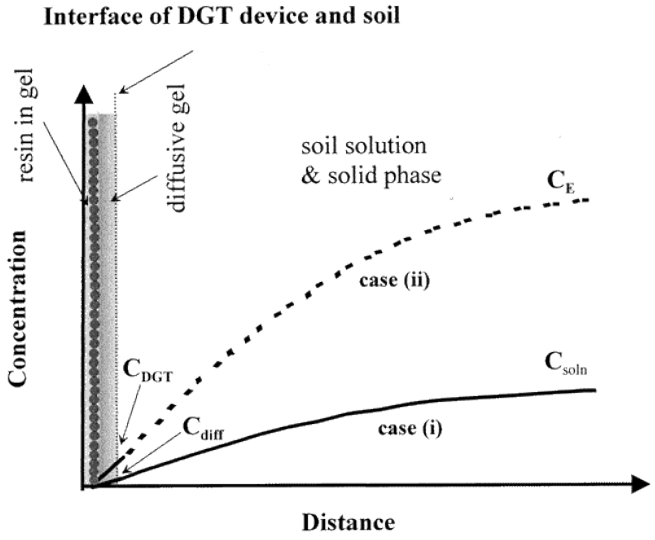

Figure 1.9. *Cross-sectional schematic through the DGT device and adjacent soil solution illustrating how the effective concentration (C_E) relates to the concentration in the soil solution (C_{soln}) and the DGT-measured concentration (C_{DGT}). From: Zhang et al. (2001).*

Zhang et al. (2001) found that that C_E was highly correlated ($r^2 = 0.98$) with concentrations of Cu in the plant material of *Lepidium heterophyllum* grown in 29 different soils covering a range of Cu concentrations. Over the entire Cu concentration range, the other bioavailability indices tested (C_{soln}, the free Cu^{2+} activity, EDTA extraction) were found to be either very poorly correlated or nonlinear with respect to the plant tissue concentration. This study demonstrated the significance of labile metal release in addition to diffusional supply when considering plant uptake and was pioneering in highlighting the potential of DGT and the associated C_E term as a quantitative measure of the bioavailable pool of trace elements in soils.

Since the study by Zhang et al. (2001), approaching 100 published studies can be found in the scientific literature which have sought to further test the relationship between metal uptake by plants and DGT from soil. Varying degrees of success are reported. Most of these

bioavailability studies make a comparison based upon measured concentrations as opposed to considering uptake fluxes. Commonly, the focus has been on uptake of micronutrients, including P, Zn, Ni and Cu, in amended (contaminated) soils in which plants of agricultural significance, such as wheat, barley and vegetable crops, are grown (Koster et al., 2005; Bravin et al., 2010; Black et al., 2011; Tandy et al., 2011). Non-essential elements such as Pb (Nolan et al., 2005; Agbenin and Welp, 2012), Cd (Perez and Anderson, 2009; Williams et al., 2012), As (Williams et al., 2011) and Hg (Liu et al., 2012) have also been investigated. Only a small number of studies have utilised the DGT technique at low metal concentrations where theoretically it is expected to perform best in mimicking plant uptake (Menzies et al., 2005; McBeath et al., 2007; Mason et al., 2010; Tandy et al., 2011).

Application of DGT for assessing bioavailability of radionuclides for plant uptake is confined to a pair of studies by Vandenhove et al. (2007) and Duquene et al. (2010), both of which investigated the ability of DGT to predict uptake of U by ryegrass compared to other measures of bioavailability including various chemical extractions, free ion activities and E values obtained through isotopic dilution. Only one study can be found in the peer-reviewed scientific literature which considers Se (Sogn et al., 2008), whilst there are no examples of experimental work involving DGT and Tc in soils.

The majority of studies comparing plant and DGT uptake of metals have reported significant correlation between the two, thus highlighting the substantial potential of DGT for assessing bioavailability for plant uptake (Nowack et al., 2004; Song et al., 2004; Koster et al., 2005; Six et al., 2012; Puschenreiter et al., 2013; Six et al., 2013). For example, Zhang et al. (2004) found the C_E of Zn as measured by DGT in soils contaminated to varying degrees to be strongly correlated with the shoot concentration in cress (*Lepidium sativum)*, whilst Nolan et al. (2005) observed shoot concentrations of Cd, Zn and Pb in wheat (*Triticum aestivum* L.) to be better-correlated with C_E than other measures including total and soluble metal concentrations, free

metal activities, 0.01 M $CaCl_2$-exchangeable metal and E values measured through isotopic dilution. More recently, Liu et al. (2012) found that DGT was successfully able to predict uptake of methylmercury by rice plants (*Oryza sativa* L.) as interpreted through significant correlation between the soil-to-plant uptake flux and the DGT-measured flux ($R = 0.853$, $p < 0.01$). Collectively, these studies suggest that the same soil parameters responsible for mediating metal supply to DGT also govern uptake of the metal by the plants investigated in the corresponding soils (Lehto et al., 2006).

The soil solution can contain significant quantities of metal in the form of inert colloids or complexes, in particular at higher pH values (Lombi et al., 2003), which are unlikely to contribute to plant uptake (Degryse et al., 2009). In such soils, C_{DGT} will be more closely related to plant uptake than C_{soln} as these inert complexes and metal-bearing colloids do not contribute to the DGT flux (Degryse et al., 2003), and yet are still typically measured as part of the total soil solution. This point is illustrated in a study by Smolders et al. (2004) in which an absence of correlation between C_{soln} and Zn concentrations in the shoots of wheat plants grown for 21 days on a sandy loam soil was observed at lower Zn application rates, despite the existence of strong positive correlation between C_{DGT} and plant concentrations across the entire dose range. The higher porewater concentrations of Zn at lower dose rates were attributed to the presence of Zn-bearing colloids that are unavailable to plants or DGT.

Various scenarios are recognised where DGT does not perform well in simulating plant uptake of metals. For example, Almås et al. (2006) found that the linear relationship between C_E values and the concentration of Cd and Zn in both spinach and ryegrass observed at lower porewater concentrations of these elements did not prevail when the plants were exposed to concentrations at a level considered toxic. The C_E provided an overestimate of the plant concentration as plant uptake diminished at the correspondingly toxic porewater concentrations, whereas accumulation by DGT did not decrease.

DGT is only expected to provide an accurate assessment of bioavailability in soils where the diffusional transport of metal through the soil solution is rate-limiting for its uptake, i.e. where the uptake rate exceeds the rate of supply (Degryse et al., 2009). Through a modelling approach using DIFS, Degryse et al. (2009) demonstrated quantitatively how uptake is not limited by diffusion at high soil concentrations where the plant's demand, as modelled through Michaelis-Menten kinetics, is less than the diffusion flux. In other words, plant uptake is saturated. Furthermore, Oporto et al. (2009) demonstrated experimentally that DGT-measured fluxes of Cd could explain NaCl-enhanced uptake by spinach at lower supplies of Cd but not at high Cd supply.

Plant uptake may not be diffusion-limited at low soil concentrations of metal where the plant has little affinity for the metal (Degryse et al., 2009). If uptake is governed by the plant's demand, uptake may be impeded by the effect of competitive cations when demand is low, but these competing cations do not affect the DGT flux. Under the scenario where diffusional supply is not uptake-limiting, labile complexes do not contribute to the plant uptake, which is instead governed by the free metal ion activity and that of competing ions. Since these labile complexes are measured by DGT, DGT will not in this instance provide an accurate prediction of uptake. Luo et al. (2010) were able to distinguish between the two scenarios on the basis of plots describing plant metal versus soil and DGT measurements and concluded that uptake of Ni from two Ni-amended soils was only diffusion-limited for a Ni hyper-accumulator (*Thlaspi goesingense*). The biotic ligand model (BLM) was more appropriate for describing uptake by the non-hyper-accumulator (*Thlaspi arvense)*, which was not diffusion limited. The greatly reduced uptake of Ni by the non-hyper-accumulator at elevated soil Ni concentrations for the soil with higher Ca and Mg porewater concentrations suggested a different uptake mechanism to that operating for the hyper-accumulator, in which the increase of Ni in the shoots correlated with increasing soil Ni concentration for both soils.

DGT and soil solution concentrations measured in contrasting soil types are usually found to co-vary (Degryse et al., 2009). As a result, correlation observed between metal concentrations in plant tissue and those measured by DGT may simply be an artefact of this covariance as opposed to diffusional-limited plant uptake. Muhammad et al. (2012) decided to calculate concentration factors to investigate whether the correlation observed between Zn and Cd concentrations in plantain shoots and the DGT-measured and soil solution concentration could be the result of such covariance. In general, concentration factors describing transfer between the soil solution and plantain shoots were found to be less than 100, which indicated that supply via mass flow would have been sufficient to explain the observed shoot concentrations (Degryse et al., 2009). It is likely that Cd and Zn uptake would have been diffusion-limited had hyper-accumulator species been used owing to their higher uptake demand.

1.10 Rationale

The increasing global inventory of ^{99}Tc, ^{79}Se and U as components of nuclear waste, coupled to the legacy of contaminated sites, means that increasing attention has been centred on understanding the environmental behaviour of these nuclides. Very limited research has been conducted which addresses the aging of Tc, Se and U in soils, however. Quantifying the aging of Tc, Se and U within different soil types is imperative for making informed assessments regarding the magnitude of the radiological risk associated with transfer to the biosphere over time following a contamination event and will aid in informing environmental safety cases for geological disposal of radioactive waste.

The soil environment represents an important sink for ^{99}Tc, ^{79}Se and U following migration from a geological repository via groundwater, fallout from nuclear weapon detonation or reactor accidents, and localised contamination associated with facilities related to various

stages of the nuclear fuel cycle. Soil may become indirectly contaminated following application of contaminated groundwater for agricultural irrigation. Knowledge of the bioavailability of these nuclides in soils is fundamental when it comes to ascertaining the potential for transfer of radioactivity to the biosphere as a result of plant uptake (Koch-Steindl and Prohl, 2001). Once the radionuclides have entered the biosphere then there is significant potential for redistribution throughout the food chain, including human consumption of contaminated agricultural produce and livestock.

1.11 Thesis aims and objectives

The overarching objective of this thesis is to utilise the DGT technique to advance our knowledge and understanding on the bioavailability and aging of ^{99}Tc, ^{79}Se and U in a range of soil types, in order to further inform the safety case for geological disposal. DGT measurements of Se and U throughout this thesis were made simultaneously using a Chelex-ferrihydrite mixed binding layer (MBL) DGT. The MBL had not previously been validated for measurement of these analytes, and so initially a series of tests were conducted with the aim of demonstrating the suitability of the MBL for this purpose.

A central component of the research presented in this thesis was an 18-month incubation of 20 different soils, during which a series of DGT deployments were made at progressively-increasing time intervals. The aim is to establish a clearer understanding of the rate and extent of aging of these radionuclides within the soil and elucidate the key properties responsible. In addition to this primary 18-month incubation, a secondary incubation was set-up to examine the effects of contrasting moisture regimes and microbial activity on availability and aging of these three elements. The cyclic wetting and drying of the soils associated with DGT deployments may potentially induce a methodological artefact within the acquired DGT dataset.

The final stage of this thesis seeks to validate the DGT technique as a suitable tool for assessing the bioavailability of Tc in soil by examining the correlation between DGT uptake and ryegrass uptake across several soil types. As part of this work, an experimental DGT deployment was made in situ with the ryegrass, a novel approach to investigate whether DGT uptake in situ during active plant growth correlates with the observed ryegrass uptake.

In brief, the three main objectives of this thesis can be summarised as follows:

- Validate the performance of the MBL DGT for measurement of Se and U within soil (Chapter 3)
- Assess the availability and aging of Tc, Se and U within a range of soil types (Chapters 4, 5 and 6)
- Validate DGT as a tool to predict plant uptake of Tc from contrasting soils (Chapter 7)

Chapter 2: Materials and methods

This chapter serves to outline the experimental and analytical methods adopted throughout this thesis. More specifically, it details the primary incubation procedure upon which this thesis is largely based, in addition to the short-term secondary incubation. Finally, calculation of and analysis for the DGT datasets are described.

2.1 Reagents and incubation approach

2.1.1 Preparation of DGT and DET devices

DGT devices with two different types of binding layer were used for the experimental work in this thesis: a TEVA resin binding layer and a mixed Chelex-ferrihydrite binding layer (MBL DGT). For measurement of Tc, a binding layer utilising TEVA resin as the binding agent (TEVA DGT) was used, as developed by French et al. (2005). One gram (dry weight) of TEVA resin was hydrated in ultrapure milli-Q (MQ) water (18.2 MΩ.cm at 25°C) and mixed with 20 mL of polyacrylamide gel solution. By volume, the polyacrylamide gel solution comprised 47.5% MQ water, 37.5% acrylamide solution (40% w/v) and 15% cross-linker. Ammonium persulphate initiator (240 µL of 10% w/v solution) and N,N,N',N'tetramethylethylenediamine (TEMED) catalyst (120 µL) were added to the resin-gel mix, and the resin-gels cast between glass plates in an oven at 60°C for ~1.5 hours. The gels were hydrated in MQ water over a 24-hour period, and subsequently stored in a 0.01 M $NaNO_3$ solution. The thickness of the TEVA binding layer described in French et al. (2005) was increased by 0.2 mm to improve the ease of handling as TEVA gels of the standard 0.4 mm thickness were found to be overly fragile and difficult to handle.

For measurement of Se and U, a mixed binding layer (MBL DGT) incorporating freshly-precipitated ferrihydrite and Chelex-100 ion-exchange resin as binding agents for Se and U, respectively, was used. Chapter 3 details the production and performance validation of the MBL DGT.

All DGT devices contained a diffusive gel layer of standard thickness (0.8 mm), which was prepared according to published procedures (Zhang and Davison, 1995). In brief, 10 mL of polyacrylamide gel solution was mixed with 70 µL of ammonium persulphate initiator (10% w/v) followed by 25 µL of TEMED catalyst and pipetted between glass plates separated by a 0.25 mm plastic spacer. The gels were cast at 42-46°C for approximately one hour and subsequently hydrated over an ~24-hour period in MQ water. The water was changed four to five times during this hydration period and the gels were then stored in a 0.01 M $NaNO_3$ solution. Binding layer and diffusive gels were cut into 25 mm-diameter discs using the aperture of a 30-mL plastic tube. Plastic mouldings, consisting of a cylindrical base and cap, were used to hold the binding and diffusive layers in place. A 0.45 µm pore size cellulose nitrate filter membrane (0.13 mm-thickness) was interposed between the diffusive gel layer and cap. Two types of cap were used, each having different exposure window areas; soil devices have an exposure area of 2.54 cm^2 and solution devices have an area of 3.14 cm^2.

Initially, triplicate TEVA DGT devices from each batch were tested to ensure reproducibility and consistency in performance between batches of resin-gel and diffusive gel. This testing comprised the simultaneous deployment of devices in a 2.3-L low ionic strength solution (0.01 M $NaNO_3$) spiked with 10 µg L^{-1} ^{99}Tc for 24 hours. Uptake of Tc by the DGT devices was assessed through comparison of the DGT-measured solution concentration (C_{DGT}) with the solution concentration measured directly by inductively coupled plasma mass spectrometry (C_{soln}). Uptake was deemed to be acceptable where the ratio of C_{DGT}:C_{soln} was between 0.8 and 1.2. The testing procedure for the MBL DGT is described in more detail in Section 3.3.2.

Diffusive equilibrium in thin films (DET) devices are the same as DGT devices, but without the binding layer. DET was used to determine the concentration of radionuclide species within the soil solution that are physically small enough to diffuse into the polyacrylamide gel, and therefore be measured by DGT. A slightly thinner cap was used for DET devices to compensate for the absence of a binding layer and therefore ensure a tight and secure fit of the diffusive gel layer and filter membrane between the base and cap.

All glassware, including the glass plates and spacers used for casting gels, in addition to DGT base and cap mouldings were subjected to a wash cycle consisting of 5% (v/v) Decon solution followed by 10% (v/v) HNO_3, with a final thorough rinse in MQ water. All reagents used were of analytical grade. Gel preparation, handling and assembly of devices was carried out in a class-100 laminar flow hood to ensure the cleanest possible working conditions.

2.1.2 Soil samples and characterisation of properties

The primary incubation (Section 2.1.3) was conducted in collaboration with colleagues at Nottingham University. Both groups worked on the same set of spiked soils. The Nottingham group implemented a sequential extraction procedure for Se, Tc and I to quantify the kinetics of speciation changes for these elements, while the work presented in this thesis assessed the aging of Tc, Se and U by use of DGT.

Twenty soils representing a range of physico-chemical properties and land use types were selected to form the basis of this incubation. Sixteen of the soils were collected across Leicestershire, Derbyshire and Nottinghamshire (Figure 2.1) from sites comprising woodland, moorland, grassland and arable land. These sites were pre-selected by aid of soil maps and were the closest sites to the University of Nottingham Sutton Bonnington campus with the desired land use type and soil characteristics. The remaining four soils were sampled from

sites within the Chernobyl Exclusion Zone (CEZ) that received relatively low levels of ^{99}Tc, ^{79}Se and U deposition from the nuclear fallout associated with the 1986 reactor accident. These CEZ soils were included on the basis that soils from other parts of the CEZ receiving relatively high levels of fallout would be used to validate the kinetic speciation models parameterised from the spiked soils. Unfortunately, logistical difficulties meant that these highly contaminated soils could not be returned to the UK.

To obtain representative samples from each location, soil was sampled from each corner of a roughly 10 m x 10 m square, plus the centre point. The 20 soils were sampled from the field with clean stainless-steel spades, augers and trowels, and sealed in clear plastic bags for transport. It is understood that the soils from the CEZ were oven-dried at ~100°C prior to shipment (despite instructions to the contrary). Soils sampled in the UK were stored unsealed in a cold room (~10°C) prior to sieving to < 2 mm particle size. The soils were prevented from drying out completely in order to maintain microbial activity.

Determination of soil properties, with the exception of soil alkalinity, was performed entirely by Nottingham University on unspiked sub-samples. A compilation of measured soil properties is presented in Appendix A.1. Prior to use, all laboratory glassware and plasticware was subjected to a wash cycle consisting of 5% (v/v) Decon solution followed by 10% (v/v) HNO_3, with a final thorough rinse in MQ water. All reagents used were of analytical grade.

Soil Code	Soil Location	Coordinates (DMS) N	W	Land Use
M1-T	CEZ	—	—	meadow topsoil
M2-T	CEZ	—	—	meadow topsoil
F1-T	CEZ	—	—	forest topsoil
F3-T	CEZ	—	—	forest topsoil
BC-M	Sherwood Forest Nature Reserve	53°12'52	1°05'30	moorland
BH-G	Breedon on the Hill	52°48'25	1°23'58	grassland
BH-W	Breedon on the Hill	52°48'22	1°24'05	woodland
BY-W	woodland N of Ticknall	52°49'26	1°27'58	woodland
CO-A	Sutton Bonington	52°49'23	1°14.05	arable
DY-G	Longshaw Country Park	53°18'54	1°36'02	grassland
FD-G	West Leake (nr. Sutton Bonnington)	52°49'53	1°13'35	grassland
IH-W	Ives Head (nr. Shepshed)	52°44'57	1°17'26	woodland
NP-A	Bunny	52°51'36	1°07'26	arable
SB-G	Southwood (S of Ticknal)	52°47'20	1°27'59	grassland
SR-A	Pasture Fm (nr. Stoke Rochford)	52°51'11	0°40'31	arable
SR-G	Pasture Fm (nr. Stoke Rochford)	52°50'59	0°40'41	grassland
SR-W	Pasture Fm (nr. Stoke Rochford)	52°50'58	0°40'34	woodland
TK-G	Stanley's Barn Farm (nr. Ticknal)	52°47'36	1°28'26	grassland
WK-A	Sutton Bonington	52°49'49	1°14'28	arable
WS-A	Bunny	52°51'16	1°07'41	arable

Figure 2.1. *Sample locations and land use descriptions for the 16 UK soils and four Chernobyl Exclusion Zone (CEZ) soils. Coordinates for CEZ soils are not known.*

The soils were broadly categorised as a sand, loam or clay based upon a visual inspection. Soil pH was measured using a pH meter (Model pH 209, HANNA Instruments) with combined glass electrode (Ag/AgCl) on a suspension of 5 g (± 0.5 g) air-dried soil (< 2 mm) in 12.5 mL of MQ water after shaking end-over-end for 30 minutes at 27 rpm (Mathers et al., 2017). Triplicate samples for each soil were analysed to calculate the mean, and the relative standard deviation in all cases was less than 10%.

Soil alkalinity was measured on 10 mL filtered (< 0.45 µm) samples of soil solution obtained through centrifuging after the soils had been saturated in MQ water for ~24 hours. The soil solution was titrated with 0.01 M HCl, and methyl orange indicator was used to monitor the pH change (Rowell, 1994). The end point for the titration was when the methyl orange turned to orange/red at pH ~4.5. Triplicate samples for each soil were analysed to calculate the mean, and the relative standard deviation in all cases was less than 10%.

Soil organic carbon was calculated as the difference between total soil carbon measured using an elemental analyser (CE Instruments Flash EA1112) and inorganic carbon determined using a Shimadzu TOC-Vcph CN analyser with a SSM-5000a solids module (Mathers et al., 2017). Triplicate samples for each soil were analysed to calculate the mean, and the relative standard deviation in all cases was less than 10%. In propagating the errors (standard deviation) associated with total soil carbon and inorganic carbon measurements, Equation (2.1) was used:

$$\sigma_{SOC} = \sqrt{(\sigma_{SC})^2 + (\sigma_{IC})^2} \qquad (2.1)$$

where: SOC = soil organic carbon; SC = total soil carbon; and IC = inorganic carbon.

The total Fe, Al and Mn content of each soil was determined following a nitric-hydrofluoric-perchloric acid (HNO_3-HF-$HClO_4$) total digestion for triplicate soil samples (Mathers et al., 2017). A pre-digestion step for soil organic matter was adopted by adding 4 mL of concentrated HNO_3 ($cHNO_3$) to 0.2 g of soil and heating at 80°C overnight using a Teflon-coated graphite heating block. Concentrated HF (2.5 mL), $cHNO_3$ (2 mL) and $cHClO_4$ (1 mL) were subsequently added, and an overnight stepped heating programme reaching 160°C was applied to fully digest silicate and oxide phases. After heating to dryness, the residue was re-constituted after warming with 2.5 mL MQ water and 2.5 mL $cHNO_3$, and the concentration of Fe, Al and Mn in this residual solution determined via inductively coupled plasma mass spectrometry (ICP-MS). Section 2.2.1 details the ICP-MS analysis. Triplicate reagent blanks were prepared in the same manner as for soil samples and analysed via ICP-MS in the same run as the soil samples. The relative standard deviation in all cases was less than 10%, and reagent blank concentrations were below the instrument detection limit.

2.1.3 Primary incubation: soil spiking and set-up

The soils were spiked at Nottingham University. A ^{99}Tc standard containing 794 kBq mL^{-1} ^{99}Tc as NH_4TcO_4 in MQ water, plus a 10,000 mg L^{-1} U standard in 5% HNO_3 were used for spiking. Radioactive ^{79}Se is not available as a standard in either liquid or solid form, so an isotopically-enriched (≥ 99.20%) stable ^{77}Se standard [259 mg L^{-1} $^{77}Se(VI)$] was used instead. Although not relevant to this thesis, the soils also received a ^{129}I spike from an ^{129}I standard containing 8.1 kBq mL^{-1} ^{129}I as NaI in 0.1 M NaOH. Spike concentrations were 100 µg ^{99}Tc and ^{77}Se, 200 µg ^{129}I and 5000 µg ^{238}U per kg of soil (dry weight). In terms of activity, these concentrations equate to 63.1 kBq ^{99}Tc, 1.3 kBq ^{129}I and 0.1 kBq U per kg of soil. The Tc and I spikes were added directly to the bulk air-dry soil, whereas both the Se and U primary standards were diluted four-fold in MQ water before adding to the soil. A food blender was used to mix the spike throughout the soil to ensure a homogenous distribution. At the same time, MQ water was

added to obtain the desired consistency of 'ground coffee'. The final moisture content achieved for each soil is listed in Appendix A.2.

Two-hundred grams of each freshly-spiked soil was transferred to a 600-mL plastic rectangular container (dimensions 16.5 x 11 x 6 cm) with a removable lid and incubated in a cold storage room at 10-15°C. This temperature was chosen as it represents approximately the mean annual temperature for the UK. During incubation, a small gap was maintained between the container and the lid to aid circulation, and the soils received no input of water during the period between DGT deployments.

The first set of DGT deployments was made at three days following spiking, with a series of nine further deployments conducted thereafter at progressively increasing time intervals (23, 46, 72, 100, 143, 192, 262, 346 and 549 days), accompanied by the simultaneous determination of the concentration of each element within the soil solution (C_{soln}). The incubation was concluded at 549 days following spiking, at which point DET deployments were made within all the soils immediately following the completion of the final set of DGT deployments. Additionally, all the soils were subjected to a 0.01 M $CaCl_2$ extraction in parallel with a 0.01 M KNO_3-0.016 M KH_2PO_4 sequential extraction to determine the exchangeable concentration of each element. Details concerning the incubation soil sampling procedures can be found in Section 2.1.5. Table 2.1 summarises the sampling procedures for the 549-day primary incubation.

Table 2.1. *Summary of sampling procedures at each time point for the duration of the primary incubation.*

Incubation time point (days)	**Sampling procedure details**	
3, 23, 46, 72, 100, 143, 192, 262 and 346	1)  2) 	1) DGT deployment (x3 MBL and x3 TEVA) 2) Soil centrifuged for measurement of C_{soln}
549	1)  2)  3)  4) 	1) DGT deployment (x3 MBL and x3 TEVA) 2) Soil centrifuged for measurement of C_{soln} 3) DET deployment 4) Soil extractions: 0.01 M $CaCl_2$; 0.01 M KNO_3/0.016 M KH_2PO_4

2.1.4 Secondary incubation: soil spiking and incubation set-up

A secondary incubation, comprising four of the soils used in the primary incubation (BH-G, BY-W, SR-W and WK-A), was established to investigate the effect of microbial activity and the moisture regime during incubation on the availability and aging of Tc, Se and U. These four soils were chosen as between them they represented a range of physico-chemical characteristics. Fresh soil was sampled from the field and air-dried in clear plastic sample bags for several weeks at 10-15°C before sieving to ≤ 2 mm particle size. The maximum water holding capacity (MWHC) of each soil was determined by comparison of the wet weight of 10 g of soil after soaking for two hours in a filter funnel, with the wet weight after the soil was allowed to drain under gravity for two hours. The difference in weight between the 10 g of

air-dried soil prior to wetting and the soaked soil minus the water held in the filter paper corresponds to the amount of water a free draining soil can hold under gravity (100% MWHC).

Each of the four soils comprised three subsamples that were incubated simultaneously under two different moisture regimes, with two subsamples subject to biological sterilisation via autoclaving. Approximately 200 g of each air-dry soil was placed in a 1 L Duran bottle and autoclaved on a 2-hour programme comprising multiple cycles of steaming at 121°C for 10 minutes followed by 20 minutes of sterilisation. The various combinations for each subsample are described below:

- Biological sterilisation; incubation at 40% MWHC.
- Biological sterilisation; extensive drying during incubation (no addition of water).
- No sterilisation; incubation at 40% MWHC.

One-hundred-and-fifty grams (dry weight) of each sample was transferred to a 600 mL plastic container (dimensions 16.5 x 11 x 6 cm). Stock solutions used for spiking comprised sodium selenate (1000 ppm Se in MQ water), a U atomic absorption spectroscopy standard (992 ppm U in 1.1 wt.% HNO_3) and a pertechnetate tracer (53 ppm Tc in 0.1 M HNO_3). To ensure that the soils possessed sufficient buffering capacity to absorb the added acidity from the Tc and U spikes, the pH of a dummy sample of each soil was measured before and after addition of the same volume of HNO_3 at the same concentration used for spiking. Each stock solution was diluted in half the volume of MQ water needed to raise the moisture content of each soil to 20% MWHC. The diluted stock solution was poured uniformly over the surface of the soil. To ensure the complete transfer of each element from the glass container, the remaining volume of water required to achieve a soil moisture content of 20% MWHC was used to rinse the container three times, and a metal spatula was used to thoroughly homogenise the soil with the added spike. The final spiking concentrations achieved were 88.6 µg ^{99}Tc (55.8 kBq), 100 µg Se and 5000 µg U (100 Bq) per kg of soil (dry weight).

The first set of DGT deployments were made two days after spiking, with a series of three further deployments made at 23, 44 and 112 days. The two incubation moisture regimes differed in the extent of drying that each soil was subjected to. Following saturation for DGT deployment, two of the subsamples were carefully air-dried to a moisture content of 40% MWHC and were maintained at this level by routinely monitoring the total mass of the container plus the soil, with MQ water being added where necessary. The remaining subsample was subjected to a greater extent of drying between deployments as it did not receive any input of water during this period. All samples were incubated in a laboratory incubator at 12°C.

2.1.5 Incubation sampling procedures

2.1.5.1 DGT/DET deployments

All soil samples were pre-equilibrated for ~24 hours at the moisture content at which the DGT deployments were to be made. The precise wetting strategy differed slightly between the primary and secondary incubations, however. For the primary incubation, soils were wetted subjectively from an air-dry state within their container by adding MQ water, such that the resulting slurry resembled the consistency of a paste. Thorough homogenisation of the slurry was achieved using a metal spatula to ensure that all the soil pores were filled with water and that no air pockets remained. The final weight of the container plus the soil slurry was noted, such that for subsequent wetting events the same moisture content could be accurately attained. It was not necessary to adopt a more accurate approach to saturating the soils according to the maximum water holding capacity since a good degree of precision has been demonstrated in measured DGT fluxes over a range of moisture contents above the field capacity (Hooda et al., 1999). In the secondary incubation, soils were wetted precisely to 100% of their pre-determined MWHC.

DGT devices were deployed in triplicate within each soil sample under the corresponding incubation conditions described in Sections 2.1.3 and 2.1.4. A small portion of soil was gently smeared across the filter membrane to ensure complete contact, and the device then lightly pushed into the soil in a twisting motion such that the interfacial contact between the DGT and the soil was a few millimetres below the soil surface. DET deployments were conducted in the same manner, for the purpose of quantifying the concentration of Tc, Se and U species within the soil solution that are physically small enough to diffusively equilibrate with the polyacrylamide gel. To ensure negligible evaporation during the deployment period, the lid was placed on the container leaving a small gap to aid circulation of air.

Deployment and removal of the DGT devices was carried out in the laboratory at room temperature; however, use of a benchtop laboratory incubator for interim storage of samples ensured that the time each sample spent outside of the deployment temperature was kept to a minimum. Temperature fluctuation within the timeframe of the DGT deployment in the cold storage room was less than 1°C. Longer-term fluctuation during the incubation period was on the order of a few degrees, such that the ambient temperature was generally maintained within the range 10-15°C. However, an approximately 72-hour power cut on day 378 of the primary incubation (day 40 of the secondary incubation) meant that the temperature within the cold store rose to around 18°C during this period. Following the restoration of power, the temperature dropped to 4°C as the period of defrosting resulted in a marked improvement in the efficiency of the cooling system. DGT deployments at day 44 of the secondary incubation were therefore carried out at 4°C. The temperature re-equilibrated at 10-15°C within the ensuing ~2-week period.

DGT and DET devices were removed from the soil after 17-24 hours deployment and rinsed with MQ water to remove adhering soil particles. After disassembling, TEVA binding layers were eluted with 1 mL of 4 M HNO_3 in either 20 mL glass scintillation vials (for liquid

scintillation counting) or 1.5 mL microcentrifuge tubes (for inductively coupled plasma mass spectrometric analysis). MBL gels were eluted in 1.5 mL microcentrifuge tubes with 1 mL of 1 M HNO_3. Sections 3.2.3.1 and 3.3.1 describe the testing of various combinations of acid type, acid concentration, elution time and temperature to optimise the elution efficiency for both Se and U. Diffusive gels from DET devices were eluted in 0.1 M HNO_3. All acids used for elution were of trace analysis grade.

2.1.5.2 Determination of soil solution concentration

The concentration of Tc, Se and U in the soil solution was determined at each DGT deployment by centrifuging the soil slurry in a 50-mL centrifuge tube at 3200 rpm for 10 minutes. The resulting supernatant was filtered using a 0.45 µm syringe disc filter into a microcentrifuge tube and acidified with 15 µl of 6 M HNO_3 (trace analysis grade). Soil samples were subsequently returned to an air-dry state through overnight storage in a fume hood, followed by mixing and disaggregation by use of a spatula to prevent the onset of anoxic conditions.

2.1.5.3 Soil extractions

Following completion of all DGT and soil solution measurements at the final sampling time point for the primary incubation, the soils were subjected to an extraction procedure in order to quantify the labile fraction of Se, U and Tc within the soils for input to the 2D DIFS model (Section 2.3.1).

Labile Tc and U was extracted with 0.01 M $CaCl_2$ since this method is widely-adopted for assessing available fractions of metals in soil (Houba et al., 2000). Triplicate (2 ± 0.05 g) samples of air-dry soil were weighed into 50-mL centrifuge tubes followed by 20 mL of freshly-prepared 0.01 M $CaCl_2$ (1:10 soil:extractant ratio). The tubes were shaken overnight on an end-over-end shaker. One millilitre of the supernatant from the resulting suspension was

filtered using a 0.45 µm syringe disc filter into a microcentrifuge tube and acidified with 15 µL of 6 M HNO_3.

A sequential 0.01 M KNO_3-0.016 M KH_2PO_4 extraction was used to assess the 'soluble' and 'adsorbed' fractions of Se, respectively, according to a procedure used by colleagues at Nottingham University. Exchangeable Se is commonly quantified using a phosphate-based extractant (Wang et al., 2012; Liu et al., 2015). Triplicate (4 ± 0.05 g) samples of air-dry soil plus 20 mL of 0.01 M KNO_3 (1:5 soil:extractant ratio) were shaken (end-over-end) overnight, after which 1 mL of the supernatant was filtered using a 0.45 µm syringe disc filter into a microcentrifuge tube and acidified with 15 µL of 6 M HNO_3. The remaining KNO_3 solution in the centrifuge tube was carefully decanted so as to minimise loss of soil particles and 20 mL of 0.016 M KH_2PO_4 was added to the tube. The samples were shaken (end-over-end) for one hour and 1 mL of the supernatant was subsequently filtered using a 0.45 µm syringe disc filter into a microcentrifuge tube and acidified with 15 µL of 6 M HNO_3. All chemical reagents used for the soil extractions, including salts and acids, were of analytical grade.

2.2 Sample analysis

2.2.1 Inductively coupled plasma mass spectrometry (ICP-MS)

Concentrations of Se and U in all samples were determined exclusively through ICP-MS analysis. Concentrations of Tc in soil extraction, DET and soil solution samples were also determined through ICP-MS, in addition to approximately half of DGT samples. Initially, analytical support was provided by Nottingham University, who granted use of their instrument (Thermo-Fisher iCAP-Q) for analysis of all samples acquired up to and including day 192 from the primary incubation. Thereafter, analysis was carried out at Lancaster University on a Thermo-Fisher X-Series 2 instrument. All samples were diluted by an appropriate factor (typically 10-fold) to ensure that the sample matrix for instrumental uptake

was approximately 0.1 M HNO_3. Procedural laboratory blanks (≥ 3) were prepared and analysed for every analytical run. Blank samples were also inserted randomly between samples for each analytical run to monitor for carryover between samples. All laboratory plasticware and glassware used for ICP-MS analysis was subjected to a wash cycle consisting of 5% (v/v) Decon solution followed by 10% (v/v) HNO_3 (analytical reagent grade), with a final thorough rinse in MQ water. All acids used for procedural blanks and for diluting samples were of trace analysis grade.

The X-Series 2 required manual injection of 20 µL of internal standard (50 µg Rh L^{-1}) to all samples including blanks (0.1 M HNO_3). Multi-element calibration standards (0, 1, 2, 5, 10, 20, 50 and 100 µg Se and U L^{-1}) were prepared from 1000 mg L^{-1} certified standards. A duplicate set of standards were prepared which also contained 0.75 (plus 1 µg Se and U L^{-1}), 1.5 (2), 3.75 (5), 7.5 (10) and 15 (20) µg ^{99}Tc L^{-1}, diluted from a 53 mg L^{-1} Tc standard. Detection limits for each analytical run were calculated as three times the standard deviation of replicate blank samples (0.1 M HNO_3) plus the mean of the blank samples.

Sample analysis on the iCap-Q was carried out by aid of an autosampler. Internal standards used for quantification of Tc, Se and U were Rh, Ge and Ir, respectively. Single element calibration standards were prepared from certified standards. These comprised a 259 mg L^{-1} isotopically-enriched ^{77}Se standard, plus 1000 mg U L^{-1} and 2493 mg Tc L^{-1} standards. Sample concentrations of Se were measured in kinetic energy discrimination (KED) mode using helium as the cell gas. Detection limits were calculated in the same manner as per the X-Series 2.

To validate the comparability of results between the two instruments, 10 samples (both DGT and soil solution extracts) were analysed on both instruments using a different set of calibration standards for each instrument. The results are shown in Figure 2.2. In general, sample concentrations for all three elements were found to be within 20% of each other. The

best agreement was found for Tc (mean of all sample concentration ratios = 1, standard deviation = 0.03), followed by Se ($\bar{x}$ = 0.97, σ = 0.22) and lastly U ($\bar{x}$ = 1.19, σ = 0.19). The data presented in Figure 2.2 inspired a good degree of confidence that the results attained from both instruments were comparable.

To ensure the accuracy of the calibration standards prepared at Lancaster, certified ICP-MS standard solutions of a known concentration for each element used at Nottingham were sent for analysis at Lancaster. The Se and U standards were diluted to 50 µg L^{-1} and the Tc standard to 20 µg L^{-1} for analysis. The best agreement was found for Tc [mean concentration ratio ($\bar{x}$) = 0.99, σ = 0.02], followed by Se ($\bar{x}$ = 1.09, σ = 0.06) and lastly U ($\bar{x}$ = 0.85, σ = 0.05).

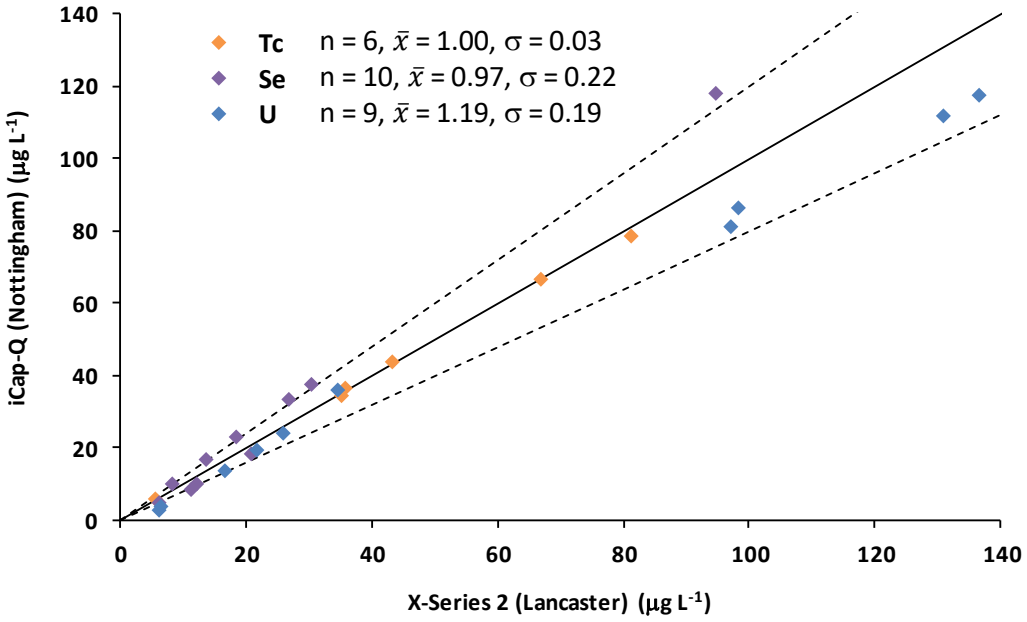

Figure 2.2. *A comparison of sample concentrations for Tc, Se and U obtained from ICP-MS analysis at Lancaster (X-Series 2) and Nottingham (iCap-Q) using different sets of calibration standards. The solid black line represents a concentration ratio of 1 between instruments; dashed lines represents a 20% deviation from this ratio; n = number of samples;* $\bar{x}$ *= mean of all sample concentration ratios;* σ *= standard deviation.*

2.2.2 Liquid scintillation counting (LSC)

The ^{99}Tc activity of all DGT samples acquired from the secondary incubation, along with DGT samples from deployment at day 262 through to day 549 inclusive in the primary incubation, was radiometrically determined through liquid scintillation counting (LSC) using a Packard Tri-Carb 3170 instrument. TEVA resin-gels plus the eluent (1 mL of 4 M HNO_3) were analysed directly in 20 mL glass scintillation vials after the addition of 10 mL of cocktail (Meridian Gold Star LT^2). Each vial was given a brief but vigorous shake to ensure that the gel and resin were disaggregated. Background samples were prepared by eluting blank TEVA resin-gels in the same manner as for experimental samples. All samples were counted for 20 minutes on an open counting window (0-300 keV), with one background sample inserted per rack of 12 samples. The extent of quenching was monitored through the Transformed Spectral Index of the External Standard (tSIE) parameter. Quenching was consistent between analytical runs and no quench correction was deemed necessary.

The spectra derived from each analytical batch of samples were subjected to a post-count tuning procedure to minimise the contribution of background counts to the total integrated count rate. This process involved trimming the counting window to obtain the highest value for the figure of merit (FoM), where the FoM is calculated using Equation (2.2):

$$\mathrm{FoM} = \frac{\left(\frac{\mathrm{N}}{\mathrm{N_{total}}}\right)^2}{\mathrm{B}} \tag{2.2}$$

where: N is equal to the number of counts over the selected counting window (e.g. 10-120 keV); N_{total} is the total number of counts over the entire energy window (0-150 keV); and B is the number of counts in the background sample over the selected counting window.

Figure 2.3 shows an example of a sample spectrum produced from an open counting window over the energy range 0-150 keV. The highest FoM value was obtained for the 6-65 keV energy window (highlighted by red dashed lines), so only counts produced in this window were used to calculate the total ^{99}Tc count rate of the sample. This procedure was adopted for each analytical run, resulting in the use of marginally different counting windows between the associated batches of samples. A net count rate for each sample (counts per minute) (CPM) was obtained after subtracting the mean count rate of all background samples from the same analytical run as the sample.

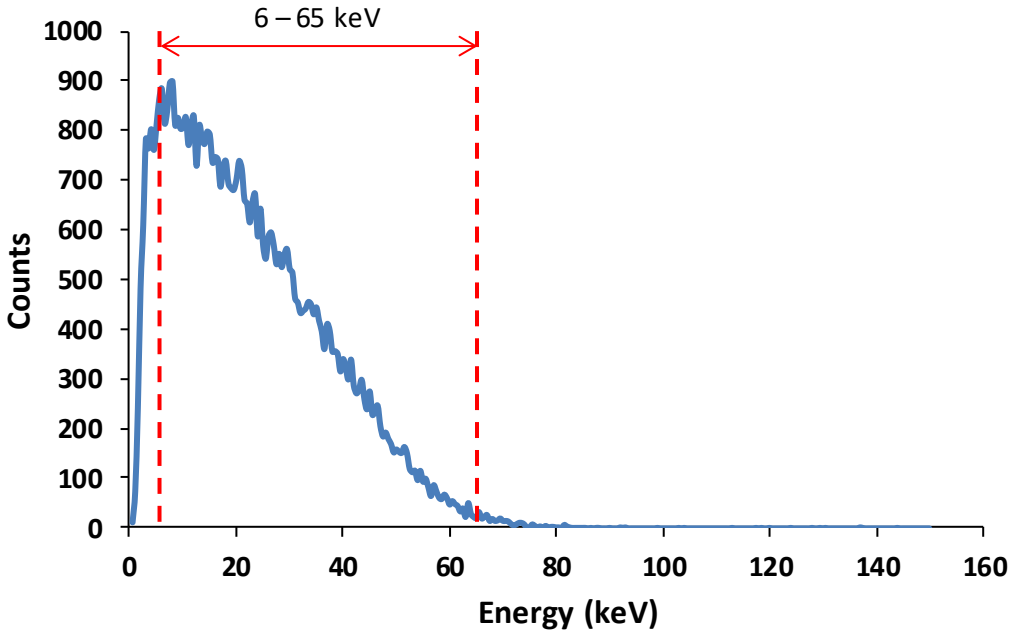

Figure 2.3. *Sample spectrum produced from counting a sample containing ^{99}Tc over an energy window of 0-150 keV. Red dashed lines indicate the portion of the spectrum (5-65 keV) that yields the highest figure of merit value.*

The counting efficiency for the sample matrix (TEVA resin-gel disc, 1 mL 4 M HNO_3 and 10 mL cocktail) was determined through a mass balance approach, whereby 1 mL aliquots of a ^{99}Tc-spiked 0.01 M $NaNO_3$ solution (10 mL) were taken before and after immersion of a TEVA gel disc in the solution for ~24 hours. The difference in activity between the before and after

aliquots was taken to represent the activity of ^{99}Tc bound to the TEVA resin-gel. The ratio between the count rate measured directly for eluted TEVA resin-gels and the activity determined through mass balance was taken to represent the counting efficiency. The counting efficiency of the 0.01 M $NaNO_3$ matrix was in turn determined through directly spiking vials containing 1 mL of 0.01 M $NaNO_3$ with a known activity of ^{99}Tc. Background samples with a matrix identical to both sample types (eluted TEVA gels and 0.01 M $NaNO_3$) were also counted.

An overall mean counting efficiency of 0.72 (72%) was derived from the analysis of 8 resin-gels, with a standard deviation of 0.04 (% RSD = 5.71). This value was comparable to that obtained by French et al. (2005), who reported a counting a efficiency of 74.5 ± 2.0 %. Prior to the addition of cocktail, French et al. (2005) placed gel-bearing vials on an orbital shaker for ~24 hours to facilitate the separation of the resin beads from the gel. However, the figure presented here (72 ± 5.71 %) was derived without shaking the gels, so it can be concluded that shaking the resin-gels before counting does not yield a significant improvement in the counting efficiency. The counting efficiency was adjusted according to the counting window over which batches of DGT samples were counted. For example, where sample count rates from a particular run were tuned to an energy window of 10-80 keV, count rates for samples used to derive the counting efficiency were likewise tuned to the same counting window.

Surman (2014) reported that the TEVA resin-gel exhibited a 19.2 ± 1.5% uptake efficiency for ^{129}I from a 0.01 M NaCl solution over 24 hours. Iodine-129 undergoes pure β^- decay with an E_{max} of 154 keV, compared to an E_{max} of 294 keV for ^{99}Tc (Lehto and Hou, 2011). Since the soils in the primary incubation were co-spiked with ^{129}I (Section 2.1.3), there is the potential for ^{129}I bound to the TEVA resin-gel to contribute to the observed count rate and produce an artificially elevated ^{99}Tc activity. To assess the potential interference of ^{129}I, the spectra of analysed TEVA resin-gels were compared between DGT deployments made in the soils of the

primary incubation containing ^{129}I and subsamples of their counterparts from the secondary incubation that did not contain ^{129}I. The comparison was made between samples acquired from similarly-aged soils. Both spectra were subdivided into energy windows and the number of counts within each window was calculated as a proportion of the total number of counts over the entire spectrum to obtain a 'count ratio' (Figure 2.4). This method can be used because the endpoint of the ^{129}I spectrum is lower than that for ^{99}Tc, so any contribution of ^{129}I counts to the ^{99}Tc spectrum will alter the count ratio. Figure 2.4 reveals that for all energy windows of the spectra, the count ratios were within error of each other for all the soils tested. Based upon this finding, the uptake of ^{129}I and resulting spectral interference was deemed negligible.

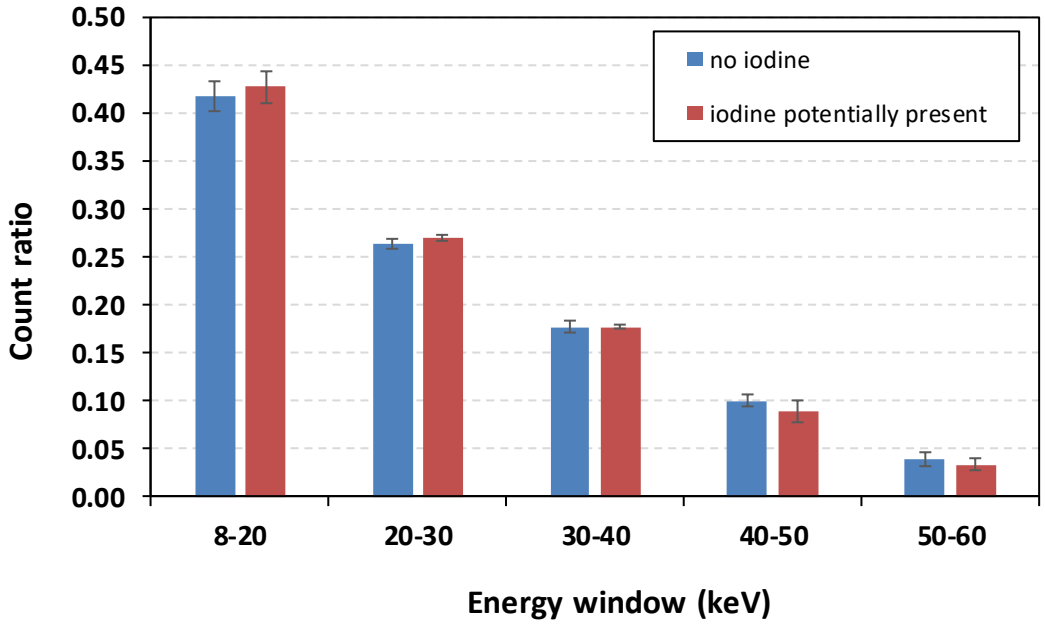

Figure 2.4. *A comparison of mean count ratios (energy window counts/total spectrum counts) for a batch (n = 6) of TEVA DGT resin-gels deployed in soil samples containing iodine and those without iodine.*

2.2.3 Cross-validation of ICP-MS and LSC analytical techniques

To ensure comparability between the data acquired from ICP-MS and LSC analysis, nine samples were subjected to analysis by both analytical techniques to demonstrate that sample concentrations were within an acceptable degree of error of each other. Differences in the precise analytical approach between the two methods meant that the most convenient means of comparison was through calculating C_{DGT} values, which are shown in Figure 2.5. Measurements by LSC were in excellent agreement with measurements derived through ICP-MS analysis, with a mean LSC:ICP-MS ratio of 1.03 (standard deviation = 0.04) between the calculated C_{DGT} values.

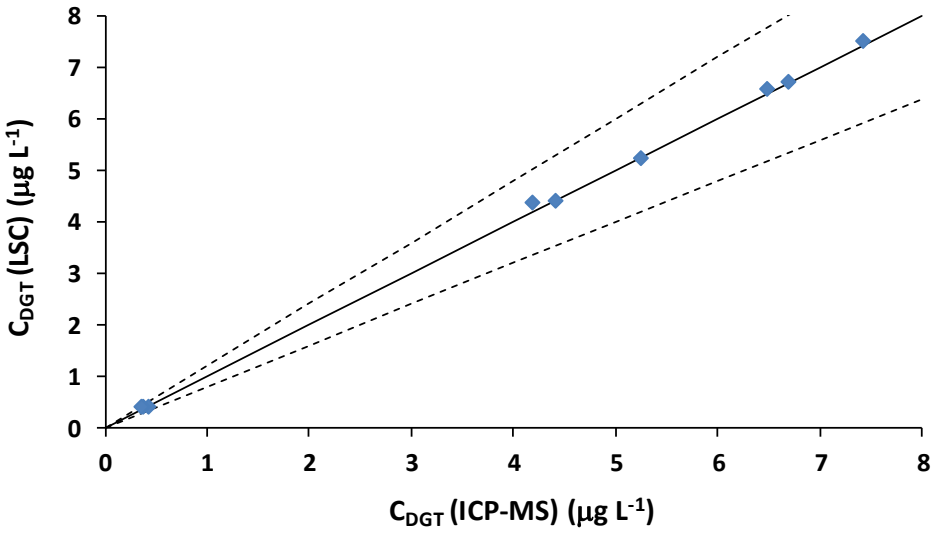

Figure 2.5. *Comparison of Tc C_{DGT} values for nine samples analysed via liquid scintillation counting (LSC) and inductively coupled plasma mass spectrometry (ICP-MS). The solid black line represents a concentration ratio of 1; dashed lines represent a 20% deviation from this ratio.*

2.3 Data analysis

2.3.1 Statistical approach

Every dataset subjected to correlation analysis was assessed for normality through visual examination of a histogram plot. In all cases normality was not observed, so correlation between datasets was calculated using the nonparametric Spearman's rank correlation method to obtain a correlation coefficient (r_s) describing the strength of the correlation. The formula for calculating r_s is given in Equation (2.3):

$$r_s = 1 - \frac{6 \sum d_i^2}{n(n^2 - 1)} \quad (2.3)$$

where: n = the number of sets of paired data; and d_i is the difference between pairs of ranked data.

The significance of each correlation coefficient was examined at the 95% ($\alpha < 0.05$) and 99% ($\alpha < 0.01$) confidence level through comparison with calculated critical values obtained from Ramsey (1989).

2.3.2 Calculation of C_{soln}, C_{DGT} and other DGT-derived parameters

2.3.2.1 C_{soln} calculation

As discussed in Section 2.1.5.2, the soil solution concentration of element (C_{soln}) was determined by centrifuging the soils to separate the soil solution following saturation for the preceding DGT deployment. The analytically-determined concentration within the extracted soil solution is therefore expressed per litre of soil solution (μg L^{-1}). Different volumes of water were added to each soil to achieve saturation, with the organic matter and clay contents being

the most significant physico-chemical properties in influencing how much water was added. The variability in the volume of soil solution between soils therefore complicates the comparison of C_{soln} (µg L^{-1}) between different soil types. By determining the mass of air-dry soil particles per litre of soil solution (kg L^{-1}), it is possible to express C_{soln} per mass of air-dry soil (µg kg^{-1}) by dividing C_{soln} (µg L^{-1}) by the soil particle concentration (kg L^{-1}) as shown in Equation (2.4):

$$C_{soln} = \frac{S_c}{P_c} \quad (2.4)$$

where: S_c is the analytically-determined element concentration in the extracted soil solution (µg L^{-1}); and P_c is the soil particle concentration (µg L^{-1}).

To reliably determine the mass of air-dry soil within each container, the weight of the empty container was subtracted from the weight of the soil-bearing container after the soils had been extensively air-dried simultaneously for one month in a cold store at 10-15°C.

2.3.2.2 C_{DGT} calculation

The time-averaged interfacial concentration of the target element at the DGT interface with the soil during the period of deployment (C_{DGT}) was calculated according to Zhang and Davison (1995) using Equation (2.5):

$$C_{DGT} = \frac{M\Delta g}{DtA} \quad (2.5)$$

where: M is the total mass (or activity) of the element accumulated within the binding layer (ng or Bq); Δg is the total thickness of the lateral diffusive pathway through the diffusive gel

layer and filter membrane (cm); D is the diffusion coefficient of the element within the diffusive gel layer ($cm^2\ s^{-1}$); t is the deployment time (s); and A is the area of the DGT exposure window in contact with the soil (cm^2). The mass (M) of element bound within the binding layer is calculated by applying Equation (2.6):

$$M = \frac{C_e(V_g + V_e)}{f_e} \quad (2.6)$$

where: C_e is the analytically-determined concentration of the element in the gel eluent (μg L^{-1} or Bq L^{-1}); V_g is the volume of gel in the binding layer (mL); V_e is the volume of eluent (mL); and f_e is the ratio of the eluted to bound element, expressed as an elution factor.

Diffusion coefficients used for calculation of C_{DGT} for Tc, Se and U are given in Table 2.2. The diffusion coefficients were corrected for temperature by use of Equation (2.7), the derivation of which is described by Zhang and Davison (1995).

$$log\ D_t = \frac{1.37023(t-25) + 8.36 \times 10^{-4}(t-25)^2}{109 + t} + log\frac{D_{25}(273+t)}{298} \quad (2.7)$$

where: D_{25} is the diffusion coefficient at 25°C; and D_t is the diffusion coefficient at the desired temperature (t).

Table 2.2. *Tc, Se and U diffusion coefficient values (measured in diffusive gels) obtained from the literature. Values are reported at 25°C.*

Element	D ($cm^2\ s^{-1}$) at 25°C	Reference
Tc	9.93 x 10^{-6}	French et al. (2005)
Se	5.83 x 10^{-6}	Zhang (pers. comm.)
	7.10 x 10^{-6}	Price et al. (2013)
U	5.56 x 10^{-6}	Zhang (pers. comm.)

2.3.2.3 Correction of C_{soln} and C_{DGT} for cumulative depletion

Repeated sampling of the incubated soils over time meant that they experienced a cumulative depletion of Tc, Se and U as a result of their accumulation within the DGT binding layer during deployment, plus removal of the soil solution for determining the dissolved concentration of each element. A mass balance was conducted to determine the extent of depletion within each soil. The starting mass of each element could be deduced through knowledge of the precise starting mass of each air-dry soil and the spike concentration. Equation (2.6) was used to calculate the mass of each element removed by individual DGT devices. The mass of each element removed during extraction of the soil solution was determined after sample analysis to measure the concentration per litre of soil solution. One millilitre of filtered soil solution was obtained for analysis, and the volume of solution retained within the syringe was estimated to be 0.5 mL. The mass fraction of Tc and Se remaining within the soil at each incubation time point prior to sampling is listed in Appendix B.2 and Appendix C.2, respectively. This figure was used as a correction factor to account for the depletion through sampling by normalising all measured values of C_{DGT} and C_{soln} for Tc and Se obtained from the primary incubation. Data for U were not corrected as across the range of soils the total mass of U removed accounted for < 0.001% of the spike.

2.3.2.4 R, R_{diff} and DIFS-derived rate constants

The ratio (R) of C_{DGT} to the concentration of metal measured in the soil solution (C_{soln}) determined through an independent method can be expressed in terms of an R value using Equation (2.8), which reflects the contribution of labile metal from the soil solid phase (Zhang et al., 1998):

$$R = \frac{C_{DGT}}{C_{soln}} \quad (2.8)$$

The hypothetical ratio where there is no solid phase contribution and supply to the DGT device is confined to diffusion only (R_{diff}) was computed through use of the 1D DGT-induced fluxes in soils and sediments (DIFS) model (Harper et al., 2000), as is common practice. The DIFS model is introduced and described in Section 1.8. To simulate this diffusion-only scenario, the system response time (T_c) was set to 1 x 10^{10} s and K_D was set to 0 L kg^{-1}.

The 2D version of the DIFS model (Sochaczewski et al., 2007) was used to derive estimates for T_c in addition to the desorption (k_{-1}) and sorption (k_1) rate constants for every combination of soil and element after 549 days of aging. Data for these parameters complement and aid in interpretation of the DGT data.

At equilibrium, the ratio of the adsorbed to dissolved concentration is defined by a distribution ratio, K_D (cm^3 g^{-1}), as defined in Equation (2.9):

$$K_D = \frac{C_s}{C_{soln}} = \frac{1}{P_c}\frac{k_1}{k_{-1}} \quad (2.9)$$

where: k_1 and k_{-1} are the adsorption and desorption rate constants, respectively; and P_c (g cm^{-3}) is the soil particle concentration. The extraction procedures used to find the sorbed concentrations of Tc, Se and U are described in Section 2.1.5.3.

It is convenient to express the rate constants as a response time, T_c (s), for the exchange reaction, as defined in Equation (2.10):

$$T_c = \frac{1}{k_1 + k_{-1}} \quad (2.10)$$

The response time (T_c) represents the characteristic time for the perturbed system (after deployment of the DGT device) to reach 63% of its equilibrium position (Jannasch et al., 1988).

The 2D-DIFS model requires input data for: soil particle concentration (P_c) and porosity (Φ_s); diffusion coefficients for the soil (D_s) and DGT diffusion layer (D_d); diffusion layer porosity (Φ_d) and thickness (Δg); DGT deployment time; and the dissolved element concentration (C_{soln}). Key input parameters are listed and described in Table 2.3. Of the three parameters (K_D, T_c and R), two are supplied as inputs and DIFS calculates the other parameter. Input values of each parameter are tabulated for every modelled soil in the Appendices for Tc (Appendix B.5), Se (Appendix C.5) and U (Appendix D.3).

Table 2.3. *Summary of key input parameters for the 2D-DIFS model plus a brief description of their derivation.*

Parameter	Units	Description
Soil particle concentration (P_c)	g cm^{-3}	$= \frac{\text{dry wt. of soil (g)}}{\text{volume of } H_2O \text{ (mL)}}$
Soil porosity (ϕ_s)	dimensionless	$= \frac{\text{volume of } H_2O \text{ (mL)}}{\text{volume of } H_2O \text{ (mL)} + \left(\frac{\text{dry wt. of soil (g)}}{p\ (g\ cm^{-3})}\right)}$
Soil diffusion coefficient (D_s)	$cm^2\ s^{-1}$	$= \frac{D_{gel}}{1 - \ln \phi^2}$
Sorbed concentration (C_s)	µg kg^{-1}	0.01 M $CaCl_2$ (Tc and U) and 0.016 M KH_2PO_4 (Se) extraction
Dissolved concentration (C_{soln})	µg L^{-1}	Measured using DET
Soil-solution distribution ratio (K_D)	L kg^{-1}	$= C_s/C_{soln}$

p = mean soil particle density = 2.65 g cm^{-3}; D_{gel} = hydrogel diffusion coefficient.

2.3.3 Kinetic modelling of the aging process

A simplified Elovich model (Chien and Clayton, 1980), parabolic diffusion model (Ma and Uren, 1997), pseudo-second-order model (Ho, 2006) and natural exponential function were fitted to the DGT data to describe the kinetics of the decrease in availability (C_{DGT}) of Tc, Se and U within each soil during the aging process. These models were introduced in Section 1.5.

The standard error (SE) of the modelled values for Q_t was calculated using Equation (2.11) and used as a criterion for judging the best fit of the models to the experimental C_{DGT} data for each soil:

$$SE = \sqrt{\frac{\sum(Q_t - Q_t')^2}{n-2}} \quad (2.11)$$

where: Q_t and Q'_t are the experimental and modelled values of Q (C_{DGT}), respectively, at time t (days); and n is the number of experimental time points.

2.3.3.1 Elovich

The equation for the Elovich model (Chien and Clayton, 1980) is given as:

$$Q_t = a + b \ln(t) \quad (2.12)$$

where: Q_t is the modelled availability (μg L^{-1}) at time t (days); and a and b are both constants obtained by plotting the experimentally-derived values for Q_{t3}-Q_{ti} against ln(t) (where t_3 is equal to the availability at day 3, and t_i the availability at any subsequent time point i). A linear relationship should be produced, where the slope of the straight line of best fit represents b, which is related to the aging rate constant, and a is the y-intercept.

2.3.3.2 Parabolic diffusion

The form of the parabolic diffusion equation (Ma and Uren, 1997) used is given in Equation (2.13):

$$Q_t = \sqrt{k_{pd}} + c \tag{2.13}$$

where: Q_t is the modelled availability (µg L^{-1}) at time t (days); k_{pd} is the parabolic diffusion constant; and c is a further constant related to the diffusion layer. Qt_3-Qt_i can be plotted against $\sqrt{t}$ to obtain a linear relationship, where the slope of the straight line of best fit represents k_{pd}, and c is given by the y-intercept.

2.3.3.3 Pseudo-second-order

The pseudo-second-order expression (Ho, 2006) is given as Equation (2.14):

$$Q_t = \frac{t}{\left(\frac{1}{k}\right)Q_e^2 + \left(\frac{t}{Q_e}\right)} \tag{2.14}$$

where: Q_t is availability (µg L^{-1}) at time t (days); Q_e is availability at equilibrium (µg L^{-1}); and k is the pseudo-second-order rate constant, which in this context corresponds to the aging rate constant (µg L^{-1} d^{-1}).

The linear form of Equation (2.14) is given as Equation (2.15):

$$\frac{t}{Q_t} = \frac{1}{kQ_e^2} + \frac{1}{Q_e}t \tag{2.15}$$

By plotting $t/(Q_{t3}-Q_{ti})$ against t, a linear relationship can be obtained with a slope of $1/Q_e$ and an intercept of $1/kQ_e^2$ (where Q_{t3} is equal to the availability at day 3, and Q_{ti} the availability at any subsequent time point where i corresponds to days). The values for the slope and intercept can then be substituted into Equation (2.14) to calculate Q_t.

2.3.3.4 Natural exponential function

The natural exponential function is given as Equation (2.16):

$$Q_t = A\, e^{-Bt} + C \tag{2.16}$$

where: Q_t is the modelled availability (μg L^{-1}) at time t (days); and A, B and C are all constants. The constants A and C represent the initial availability at time zero and at equilibrium (negligible rate of aging) respectively. The constant B is synonymous to the rate constant of the aging process, and an availability 'half-life' was calculated through dividing ln(2) by this value. The SOLVER function in Microsoft Excel was used to the optimise the constant values for each soil by minimising the sum of the squared difference between data points and the function describing the data using an iterative algorithm.

Chapter 3: Development of the Chelex-ferrihydrite mixed binding layer (MBL) DGT for measuring selenium and uranium

3.1 Introduction

Conventionally, DGT devices contain a single binding agent for measurement of the target species. Initially, this binding agent was Chelex-100 cation-exchange resin, which is used for determination of a range of cationic trace metals. To extend the range of analytes measured from a single DGT deployment, two binding agents can be simultaneously incorporated, commonly referred to as a 'mixed' binding layer. For example, the Chelex-ferrihydrite mixed binding layer (herein referred to as MBL) incorporates both nano-oxide ferrihydrite, an amorphous iron oxyhydroxide precipitate, and Chelex-100 resin within the same binding layer to allow for the simultaneous measurement of both anionic and cationic species. It was initially developed and its performance validated for measurement of a handful of essential trace cations (Cd, Cu, Mn, Zn) and anions (Mo, P) in soils (Mason et al., 2005). Since then, its application has been extended to include Pb and As for use in studying mining-impacted waters and soils by Huynh et al. (2012). More recently, mixed binding layers have been tested and validated which combine Chelex resin with the titanium dioxide-based adsorbent Metsorb^{TM} (Panther et al., 2014) and zirconium oxide (Sun et al., 2015) for the simultaneous measurement of cations and oxyanions including As, P, V, Mo, Sb and W.

Measurement of Se by ferrihydrite (Luo et al., 2010) and U by Chelex (Li et al., 2006; Li et al., 2007; Turner et al., 2012) as individual binding phases has already been validated. Se(IV) (selenite) is understood to adsorb to ferrihydrite through inner sphere complexation, but

adsorption of Se(VI) (selenate) occurs through outer sphere complexation and is strongly influenced by the surface charge characteristics of the oxide surface (Balistrieri and Chao, 1990). In addition to Chelex, several additional binding phases have been successfully used for the quantitative determination of labile U species. These include the titanium-based adsorbent Metsorb^{TM} (Hutchins et al., 2012), as well as a range of ion-exchange resins such as Whatman DE 81 and Dowex 2x8-400 (Li et al., 2007), Spheron-Oxin® (Gregusova and Docekal, 2011), Diphonix (Drozdzak et al., 2015) and a polyphenol-impregnated weak base anion-exchange resin (PIWBA) (Drozdzak et al., 2016).

As discussed in Section 1.1.2, it is predicted that both ^{79}Se and ^{233}U will make significant contributions to the long-term (> 100,000 years) total activity of spent fuel, and are therefore integral to radiological and environmental safety assessments surrounding the geological disposal of such waste (NDA RWMD, 2010). Combined with the potential releases associated with interim storage and reprocessing, both Se and U represent important components of current and future environmental monitoring programmes of soil and groundwater in the vicinity of such facilities. DGT is recognised as an ideal tool for such monitoring programmes. It offers a method for in situ, passive monitoring of groundwater in the field, alleviating the need for collection of voluminous samples. Its capacity to provide mean concentrations over defined and more extended periods of time is particularly advantageous, where conventional sampling techniques can only provide instantaneous measurements. Furthermore, the selectivity of the binding layer and its ability to pre-concentrate the target analyte aids in simplifying sample analysis, which represents a significant saving in time. In situ soil deployment in the field has not yet proven to be feasible, although new advances in the technology may change this.

Use of the MBL DGT to measure both Se and U simultaneously avoids the deployment of separate Chelex and ferrihydrite DGT devices, thus providing a more time-efficient and cost-

effective approach to sampling. A significant saving in time is achieved as a result of halving the number of DGT devices to be produced and consequently the number of samples acquired for processing and analysis. Critically, the saving in time is facilitated by the fact both elements can be analysed simultaneously by inductively coupled plasma mass spectrometry. The MBL approach also represents a reduction in expenditure on reagents and consumables. In a regulatory capacity, should the MBL DGT be used as a tool for environmental monitoring of soil and groundwater in the vicinity of geological disposal facilities, then a significant financial saving could be achieved through halving outlay on DGT devices and reducing the number of samples for processing and analysis. As a guide, individual Chelex and ferrihydrite DGT devices supplied by DGT® Research for commercial use are currently (January 2017) priced at £13.50 each (DGT Research, 2017).

To date, the use of DGT in the radionuclide field is dwarfed by its application in the trace metal field. Generally, the binding layers which have been developed for measurement of radionuclides are highly specific and therefore less versatile than Chelex and ferrihydrite. The use of Chelex in the MBL over the aforementioned alternative binding agents for U is advantageous because Chelex has been validated for measurement of other elements with radioactive isotopes including Pu (Cusnir et al., 2014) and Ra (Leermakers et al., 2009).

The experimental work presented in this chapter aims to demonstrate the compliance of Se and U uptake by the MBL with DGT theory and test various aspects of its performance in relation to deployment within soil. The MBL DGT will be used throughout this thesis to simultaneously measure Se and U, so validation of its performance is essential to underpin its use.

3.2 Methods and materials

3.2.1 Preparation of Mixed Binding Layer

A ferrihydrite slurry was prepared by titrating a 0.1 M solution of iron nitrate [$Fe(NO_3)_3$] with 1 M sodium hydroxide (NaOH). The solution was continuously and vigorously stirred, and a pH electrode was used to ensure that the pH of the solution did not exceed 7 at any point. A dark brown-red ferrihydrite precipitate was formed, with the resultant slurry being stored in a refrigerator at 4°C for up to six months. Chelex-100 resin was initially washed and hydrated in MQ water under static conditions, with the water being changed two to three times over a ~24-hour period.

For the MBL, the ferrihydrite and Chelex cation-exchange resin were incorporated into a gel layer with a 2:1 ratio, with 3 g of ferrihydrite and 1.5 g of Chelex resin (both wet weight) used for every 10 mL of polyacrylamide gel solution. Mason et al. (2005) reported this binding agent ratio to be optimal, yielding uptake efficiencies of > 98% for the anions and cations tested. By volume, the gel solution comprised 47.5% MQ water, 37.5% acrylamide solution (40% w/v) and 15% cross-linker. Ninety-six micro-litres of ammonium persulphate initiator and 26 µL of N,N,N',N'tetramethylethylenediamine (TEMED) were added to catalyse polymerisation and the gels were cast at 42-46°C for at least one hour. The total thickness of the fully-hydrated MBL gel sheet was 0.6 mm.

MBL gel sheets were washed and hydrated in MQ water for a 24-hour period during which the water was changed three times. The sheets were subsequently stored in a 0.01 M $NaNO_3$ solution prior to cutting. Standard DGT solution mouldings (3.14 cm^2 exposure area) were used for assembly, which also included a 0.8 mm-thick diffusive gel layer and 0.13 mm-thick cellulose nitrate filter membrane of 0.45 µm pore size. Assembled MBL devices were stored in the refrigerator within sealed bags containing a few drops of 0.01 M $NaNO_3$.

3.2.2 Instrumental analysis and DGT detection limits

After elution of both analytes from the binding layer in 1.5 mL microcentrifuge tubes, all samples were analysed for Se and U by inductively coupled plasma mass spectrometry (ICP-MS), as detailed in Section 2.2.1. A range of elution techniques were investigated, as described in Section 3.2.3.1.

DGT detection limits were established through analysis of 'blank' DGT devices. Blank devices were handled in the same manner as for normal samples but were placed in sealed plastic bags containing a few drops of 0.01 M $NaNO_3$ during the experimental deployment period. At the end of this deployment period, the devices were removed from the bags, dismantled and the gels eluted using the same procedure as for all other samples. The measured mass of Se and U for each blank MBL gel (ng per device) was used to obtain a minimum detection limit (MDL) for each device, calculated as the mean value of the blank plus three times the standard deviation between blanks. These masses were used to derive a solution concentration (μg L^{-1}) that would give a DGT-accumulated mass indistinguishable from the MDL based on a 24-hour deployment period at 25°C, assuming diffusive gel and filter membrane thicknesses of 0.8 and 0.14 mm, respectively.

For spiking, a 1000 ppm Se(VI) stock solution was prepared by dissolving sodium selenate (Na_2SeO_4) in MQ water, and for U a 992 ppm U atomic absorption spectroscopy standard in 1.1 wt.% HNO_3 was used. Bulk solutions prepared for the experimental work detailed in this chapter were thoroughly pre-equilibrated overnight on a magnetic stirrer with the pH monitored to ensure equilibrium between all species and the atmosphere. Solutions were stirred continuously to negate the effects of the diffusive boundary layer (Warnken et al., 2006). Unless otherwise stated, all experimental solutions had an ionic strength of 0.01 M,

prepared using $NaNO_3$. DGT devices were suspended in solution by aid of Perspex racks with the exposure window facing the centre of the container.

3.2.3 Characterisation of DGT performance

3.2.3.1 Elution efficiency

A mass balance approach was used to determine the elution efficiency of Se and U from the MBL. Gel discs were immersed individually (one gel per solution) in triplicate 10 mL solutions (0.01 M $NaNO_3$) containing 100 µg L^{-1} of both Se and U. The mass of each element bound to the gel was deduced through analysis of 1 mL aliquots taken from the solutions before and after immersion of the gels. The mass of each element in the gel eluent was divided by the calculated mass on the gel to obtain an elution factor. Various combinations of different acids (HNO_3, HCl and H_2SO_4) of varying concentration (up to 4 M) were sequentially investigated at elution times ranging from 24 hours up to 30 days, until a good degree of recovery (> 80%) could be attained for both elements. A summary of tested combinations is given in Table 3.1, which were based largely on published procedures in the DGT literature. Initially, increasing concentrations of HNO_3 were tested at 24 and 72 hours, followed by experimentation with alternative acids (H_2SO_4 and HCl). The elution time for HNO_3 was then extended to 10 and 30 days, and finally the effect of an increased elution temperature (70°C) was tested.

Table 3.1. *Tested combinations of acid, acid concentration, elution time and temperature for assessing the elution efficiency of Se and U from the MBL.*

Acid	Concentration (M)	Elution time	Elution temperature
HNO_3	1	24 & 72 hrs; 10 & 30 days	ambient and 70°C
	2	24 & 72 hrs; 10 & 30 days	ambient
	4	72 hrs	ambient
H_2SO_4	0.3	72 hrs	ambient
HCl	1	72 hrs	ambient

3.2.3.2 Uptake efficiency from solution

Assembled MBL DGT devices were deployed in 8 L of a solution containing 100 μg L^{-1} Se and U to ensure that uptake of Se and U agreed with the theoretical mass that would be predicted to be accumulated according to the C_{DGT} equation [Equation (1.7)]. DGT devices were removed in triplicate after 1, 2, 4 and 24 hours exposure, and the gels eluted in 1 mL of 1 M HNO_3 at 70°C for ~72 hours. Unfiltered aliquots (1 mL) were taken from the bulk solution at the start of the deployment period and each subsequent time point at which a DGT device was removed. The DGT uptake efficiency was subsequently assessed by comparison of the DGT-measured concentration (C_{DGT}) with the ICP-MS-measured solution concentration (C_{soln}), where a C_{DGT}:C_{soln} ratio of 0.8-1.2 is indicative of acceptable uptake. The solution temperature was periodically monitored such that the diffusion coefficient could be appropriately corrected using Equation (2.7). A 2 L control tank containing 100 μg L^{-1} U and Se but with no DGT devices was prepared to monitor for sorption within the tank or precipitation. Unfiltered and filtered (0.2 μm filter) aliquots (1 mL) were taken at the start and finish of the experimental timeframe, and the aliquots subsequently acidified with 20 μL of 6 M HNO_3.

3.2.3.3 Aging of MBL gels

Aging in this context refers to the length of time that freshly-prepared binding layer gels can be stored until their performance with respect to Se and U uptake diminishes to an unacceptable level. At 14, 28, 43, 57 and 100 days following initial production of the MBL, four DGT devices were deployed for ~24 hours in a 2.3 L solution containing 100 μg L^{-1} of both Se and U. After deployment, the gels were eluted in 1 mL of 1 M HNO_3 at 70°C for ~72 hours. Comparison of C_{DGT} with the concentration of each element measured in 1 mL aliquots taken from the bulk solution and analysed via ICP-MS allowed the DGT performance to be validated,

where a C_{DGT}:C_{soln} ratio of 0.8-1.2 is indicative of acceptable uptake. A fresh solution was prepared at each time point.

3.2.3.4 Binding kinetics

To assess the kinetics of binding of both Se and U to the MBL, individual gel discs were immersed in 10 mL of 0.01 M $NaNO_3$ solution in centrifuge tubes (one gel per tube), spiked with 100 µg L^{-1} each of Se and U, for various lengths of time. During this immersion period, the tubes were placed on an orbital shaker at 180 rpm to ensure a thoroughly-mixed and uniform solution. MBL gel discs were removed from the tubes in triplicate at the following time intervals: 5, 10, 15, 30, 60, 120, 240 and 600 minutes. Aliquots (1 mL) were taken from each tube prior to immersion of the gel discs and after removal to determine the mass of each element bound to the gel. MBL gels were eluted in 1 mL of 1 M HNO_3 at 70°C for ~72 hours. A control tube consisting of spiked solution, but no gel disc, was used to monitor sorption of Se and U to the tube.

3.2.3.5 Gel capacity

Twenty-one MBL DGT devices were deployed simultaneously in an 8 L solution containing 100 µg L^{-1} Se and U for up to 18 days to establish the temporal trend for Se and U accumulated by the MBL. DGT devices were removed in triplicate after 1, 2, 4, 7, 11, 15 and 18 days deployment, and the gels eluted in 1 mL of 1 M HNO_3 at 70°C for ~72 hours. The capacity of the binding layer is inferred to be exceeded at the point at which the relationship between mass uptake and time deviates from linearity. Aliquots (1 mL) were taken periodically from the solution to measure the change in concentration with time due to the combined effects of evaporation and removal by DGT.

3.2.3.6 Effect of pH and ionic strength on Se and U uptake

Three 2.3 L solutions (0.01 M $NaNO_3$) of varying pH (3.40, 6.66 and 7.34) were prepared by incremental additions of 0.1 M NaOH or 0.1 M HNO_3 over a ~48-hour period, with constant stirring and exposure to the ambient atmosphere. A further three 2.3 L solutions of varying ionic strength (10, 100 and 200 mM) were prepared by dissolving $NaNO_3$ in MQ water. After equilibration, each solution was spiked with 50 µg L^{-1} U and Se before triplicate deployment of DGT devices for ~24 hours within each solution. MBL gels were subsequently eluted in 1 mL of 1 M HNO_3 at 70°C for ~72 hours. Unfiltered aliquots (1 mL) were taken from the bulk solution at both the start and end of the deployment period, and DGT performance was subsequently assessed by comparison of C_{DGT} with the measured solution concentration.

3.2.3.7 Alkalinity

Four 2.3 L solutions (0.01 M $NaNO_3$) with varying concentrations of HCO_3^- (0.16-4.18 mM) were prepared using a freshly-prepared 0.5 M sodium bicarbonate ($NaHCO_3$) stock solution. Each solution was subsequently spiked with 50 µg L^{-1} Se and U and equilibrated overnight with constant stirring and exposure to the ambient atmosphere. DGT devices were deployed in triplicate for 24 hours, after which MBL gels were eluted in 1 mL of 1 M HNO_3 at 70°C for ~72 hours. Unfiltered aliquots (1 mL) were taken from the bulk solution at both the start and end of the deployment period, and DGT performance was assessed by comparison of C_{DGT} with the measured solution concentration. The concentration of HCO_3^- species within each solution was calculated using the Henderson-Hasselbalch equation [Equation (3.1)]:

$$\mathrm{pH} = \mathrm{pK_a} + \log\frac{[\mathrm{A^-}]}{\mathrm{K_H p_{CO_2}}} \qquad (3.1)$$

where: $[A^-]$ is the molar concentration of the conjugate base (HCO_3^-); $K_H p_{CO_2}$ is Henry's Law constant for CO_2 in water at the requisite water temperature; and K_a is the carbonic acid dissociation constant (which includes dissolved CO_2).

3.3 Results and discussion

3.3.1 Elution efficiency

Table 3.2 presents a summary of the elution efficiencies obtained for both Se and U for a range of elution conditions. Recoveries of both Se and U were found to be particularly sensitive to the elution timeframe, the type and concentration of acid used, as well as the elution temperature. Increasing the elution time using 1 M HNO_3 from 24 hours to 10 days yielded a dramatic improvement in the recovery of Se from 2.7 ± 0.8% to 80.4 ± 6.4%. A 10-day elution timeframe is not particularly pragmatic however, especially where a fast turnaround time for attaining experimental results is required. Increasing the concentration of HNO_3 to 2 or 4 M had no effect on U recoveries, but did slightly improve the recovery of Se. However, this improvement is likely to be outweighed by the loss of sensitivity during analysis that arises as a result of the higher dilution factors required. Eluting for 72 hours with 0.3 M H_2SO_4 yielded good recoveries for both Se (80.7 ± 1.4%) and U (81.1 ± 8.2%) but heating the gels at 70°C in 1 M HNO_3 was found to be the optimal elution procedure, offering excellent recoveries of 92 ± 3.2% for Se and 86 ± 1.1% for U within a pragmatic timeframe (72 hours).

The poor recovery of Se (2.7 ± 0.8%) after eluting with 1 M HNO_3 for 24 hours is unexpected but was found to be reproducible. Although no elution efficiencies of Se from the MBL are reported in the DGT literature, Luo et al. (2010) reported an elution efficiency of 0.79 ± 0.023 (79%) for Se from precipitated ferrihydrite gels also using 1 M HNO_3. However, Luo et al.

(2010) do not state exactly how long the gels were eluted for prior to analysis, other than that gels were eluted for a minimum of 24 hours.

Table 3.2. *Elution efficiencies (%) of Se and U from MBL gels.*
Error values represent the standard deviation of the mean.

Se	**1 M HNO_3**		**2 M HNO_3**	**4 M HNO_3**	**0.3 M H_2SO_4**	**1 M HCl**
	ambient	**70°C**				
24 hrs	2.7 ± 0.8	42.1 ± 4.9	31.0 ± 2.6	—	—	—
72 hrs	54.2 ± 4.9	92.1 ± 3.2	58.6 ± 1.5	61.4 ± 1.3	80.7 ± 1.4	68.5 ± 3.5
10 days	80.4 ± 6.4	—	71.4 ± 2.4	—	—	—
30 days	89.1 ± 10.5	—	76.0 ± 4.4	—	—	—
U	**1 M HNO_3**		**2 M HNO_3**	**4 M HNO_3**	**0.3 M H_2SO_4**	**1 M HCl**
	ambient	**70°C**				
24 hrs	88.1 ± 2.3	38.0 ± 4.3	39.7 ± 1.4	—	—	—
72 hrs	64.1 ± 0.4	86.5 ± 1.1	66.4 ± 0.6	66.8 ± 1.6	81.1 ± 8.2	1.07 ± 9.5
10 days	69.7 ± 1.9	—	68.4 ± 0.2	—	—	—
30 days	70.2 ± 4.4	—	74.6 ± 0.9	—	—	—

The data presented in Table 3.2 demonstrate the criticality of time in determining the elution efficiency of Se from the MBL, so it could be that the greater recoveries achieved in these studies were the result of leaving the gels to elute for up to 10 days.

3.3.2 Uptake efficiency from solution

Figure 3.1 demonstrates that the MBL DGT-measured concentration (C_{DGT}) of Se when deployed in solution from one up to 24 hours is within 20% of the solution concentration as measured via ICP-MS (C_{soln}). In contrast, the C_{DGT}/C_{soln} ratio for U is only 0.38 ± 0.02 for a one-hour deployment, which increases slightly to 0.56 ± 0.08 after deployment for four hours. Only after a 24-hour deployment is U uptake sufficient to yield a C_{DGT}/C_{soln} ratio (0.81 ± 0.03) within the ± 20% error margins considered as acceptable for DGT performance.

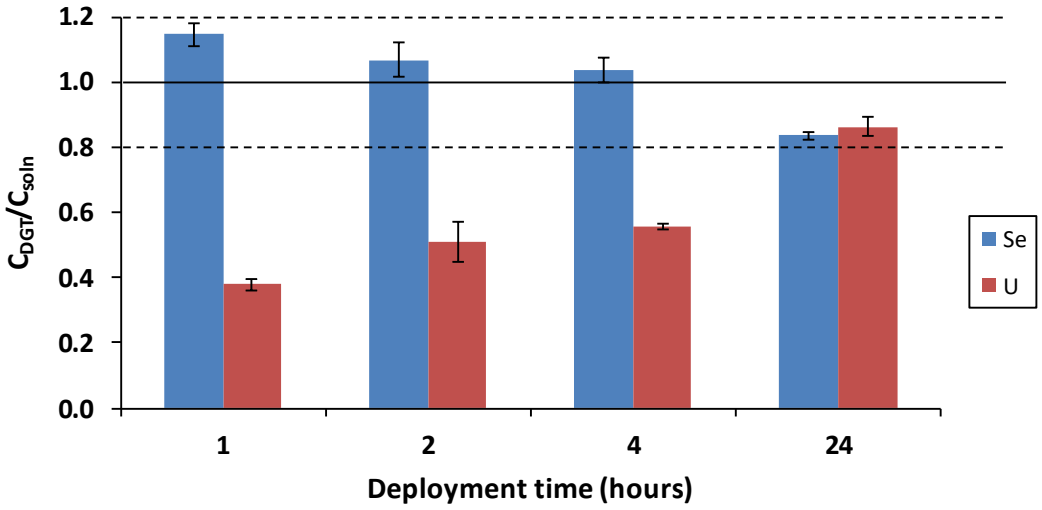

Figure 3.1. *Ratio of DGT-measured concentration (C_{DGT}) of Se and U to solution concentration (C_{soln}) for MBL DGT devices deployed in solution (100 µg L^{-1} Se and U) for 1, 2, 4 and 24 hours. Solid horizontal line represents 1:1 C_{DGT}/C_{soln} ratio, and dashed horizontal lines represent 20% deviation from this ratio. Error bars represent the standard deviation of the mean for triplicate deployments.*

The inadequate uptake of U by the MBL at shorter deployment times (≤ 4 hours) is seemingly related to the slower kinetics of binding of U to the Chelex resin in the presence of ferrihydrite. As presented in Figure 3.3, the mass of U bound to the gel after 60 minutes is only 56% of that for Se, although after four hours this has narrowed to 85%. The reason for the slower kinetics of U binding relative to Se is not immediately obvious, but the ferrihydrite particles clearly serve to interfere with the process. Mason et al. (2005) reported cation uptake by the MBL to be on the order of 6-10% lower than for anions, which was attributed to the longer diffusion pathway experienced by cations within the MBL due to the presence of ferrihydrite particles between the gel surface and the Chelex beads. In this scenario, the diffusion layer thickness (Δg) would be underestimated and consequently lead to an underestimate for C_{DGT}. This phenomenon is likely to contribute to the inferior U uptake demonstrated in Figure 3.1.

3.3.3 Aging of MBL gels

Figure 3.2 reveals that MBL gels could be stored for up to 57 days following binding layer production, with no reduction in uptake of Se observed. C_{DGT} was found to be within 20% of the solution concentration as measured directly through ICP-MS, which is deemed acceptable to be compliant with DGT theory. A marked decline in the C_{DGT}/C_{soln} ratio was measured at 100 days after production of the MBL gels for both Se and U, so on this evidence MBL gels should be used within ~8 weeks following production to ensure acceptable performance.

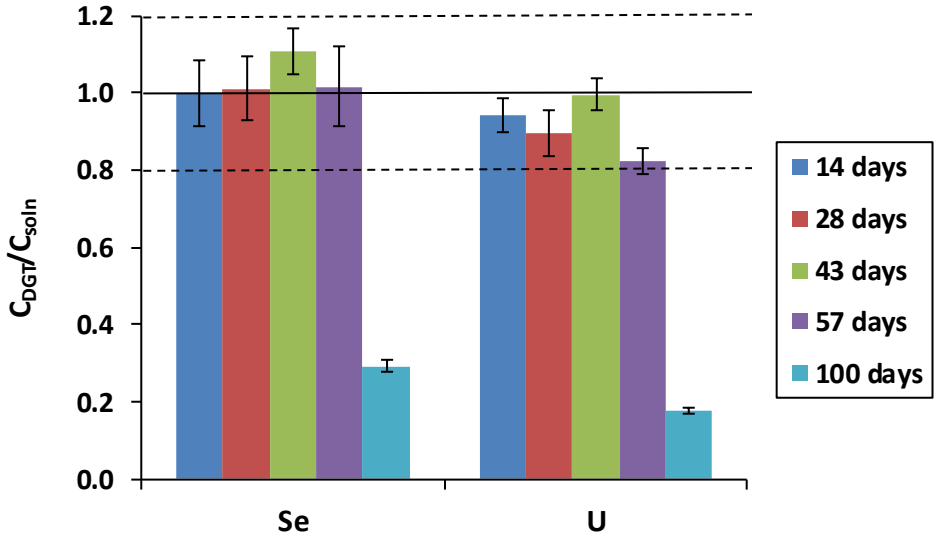

Figure 3.2. *Ratio of DGT-measured concentration (C_{DGT}) of Se and U to solution concentration (C_{soln}) for MBL DGT devices of varying binding layer age. Error bars represent the standard deviation of the mean for triplicate DGT deployments. Solid horizontal line represents 1:1 C_{DGT}/C_{soln} ratio, and dashed horizontal lines represent 20% deviation from this ratio.*

The eight-week shelf-life does not take into consideration the age of the ferrihydrite however, which was precipitated several weeks before the MBL gels were prepared. Ferrihydrite is metastable under oxic conditions and undergoes gradual transformation to more crystalline and stable Fe(III) oxide phases including goethite and hematite (Das et al., 2011). These phases possess a smaller surface area with a consequent reduction in binding capacity. Had the

ferrihydrite been freshly-precipitated immediately prior to its incorporation within the MBL, then it is likely that the shelf-life of the MBL gels could be extended beyond eight weeks.

3.3.4 Binding kinetics

Figure 3.3 shows uptake of Se and U by the MBL for gels immersed in solution for increasing lengths of time. Uptake of both elements occurs at a rapid rate within the first couple of hours, although the binding kinetics of U to Chelex are found to be slower than the binding kinetics of Se to ferrihydrite. The rate of binding levels off after 4-5 hours as the mass of element remaining in solution becomes significantly depleted and a state of equilibrium is reached between the concentration of element in solution and that bound to the gel. The initial period of fast uptake demonstrates that binding of both elements to the gel is rapid in accordance with DGT theory, which requires the concentration of the free unbound target species in solution at the interface between the binding layer and diffusive gel to be zero.

3.3.5 DGT blanks and detection limits

Table 3.3 presents blank MBL DGT sample concentrations for both Se and U. The MBL Se blank (0.058 ± 0.033 ng/device) is over four times that of U (0.013 ± 0.003 ng/device). The calculated MDL solution concentrations for both Se (0.008 μg L^{-1}) and U (0.001 μg L^{-1}) are below the typical environmental surface water concentrations encountered for both elements, at 0.01-0.3 μg L^{-1} for Se (Fordyce, 2005) and 0.1-500 μg L^{-1} for U (Zavodska et al., 2008). If the concentration of labile Se and U in the soil solution is close to the solution MDL then the deployment time can be increased.

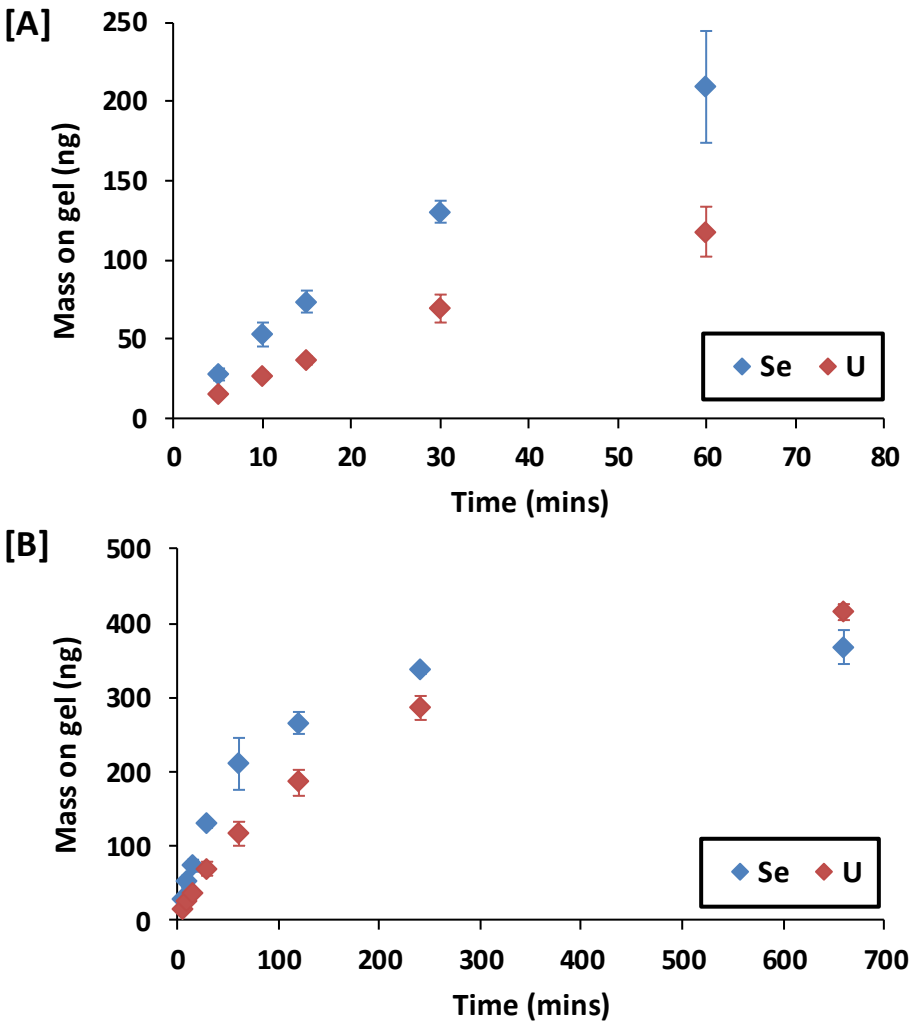

Figure 3.3. *Uptake of Se and U by MBL gels immersed in 100 µg L^{-1} U and Se solutions for varying lengths of time; 5-60 minutes* ***[A]*** *and 5-660 minutes* ***[B]****. Error bars represent the standard deviation of the mean, for triplicate samples.*

Table 3.3. *MBL blank sample concentrations (ng/device) and calculated method detection limits (MDL) per device. The reported error represents the standard deviation of the mean of 12 samples. The deployment solution concentration (µg L^{-1}) required to achieve the MBL MDL based upon a 24-hour deployment of a MBL DGT with a standard 0.8 mm-thickness diffusive gel layer is also given.*

	MBL blank (ng/device)	MBL MDL (ng/device)	MBL MDL (µg L^{-1} solution)
Se	0.058 ± 0.033	0.157	0.008
U	0.013 ± 0.003	0.022	0.001

3.3.6 Gel capacity

Figure 3.4 presents the MBL DGT mass uptake of Se and U over time. A linear response was obtained for Se up to 264-hours deployment, beyond which the relationship deviated from linearity. The point at which this deviation occurs would imply that the Se capacity of the MBL has been exceeded, but a mass balance calculation reveals that this deviation is instead the result of depletion of Se from the deployment solution due to cumulative removal by the DGT devices. It is therefore not possible to determine the Se capacity for the MBL, but on the evidence presented in Figure 3.4 a minimal capacity of 17 µg can be deduced. For comparison, Huynh et al. (2012) report a MBL capacity for As of 15 µg. Price et al. (2013) report the ferrihydrite binding affinity of both major As species to be superior than for selenate and selenite, which would imply that the Se capacity should be less than the reported 15 µg for As. Elsewhere, Luo et al. (2010) report a Se capacity of 22 µg for precipitated ferrihydrite gels, so at 17 µg the MBL would appear to be close to capacity. Mason et al. (2005) found that the Chelex resin does not interfere with the capacity of ferrihydrite within the MBL to adsorb P, which if also applicable to Se would suggest that the Se capacity of the MBL may be close to 22 µg.

For U, a linear relationship between mass uptake and time is observed in Figure 3.4 over the complete timescale of the deployment period (up to 437 hours), which suggests that the capacity of the MBL for U has yet to be reached. Nonetheless, a minimum capacity of 27 µg can be deduced. Comparatively, MBL capacities for a variety of other cations are reported to be on the order of 70 µg, depending on the selectivity of the Chelex resin for the target element (Mason et al., 2005; Huynh et al., 2012). Huynh et al. (2012) reported that their measured cation capacities for certain elements were an order of magnitude less than those measured for pure Chelex binding layers. They speculated that this reduction was due to

coating of the Chelex resin by ferrihydrite within the MBL. Li et al. (2006) estimated the U capacity for a pure Chelex disc to be 133 µg, but the MBL capacity is likely to be lower.

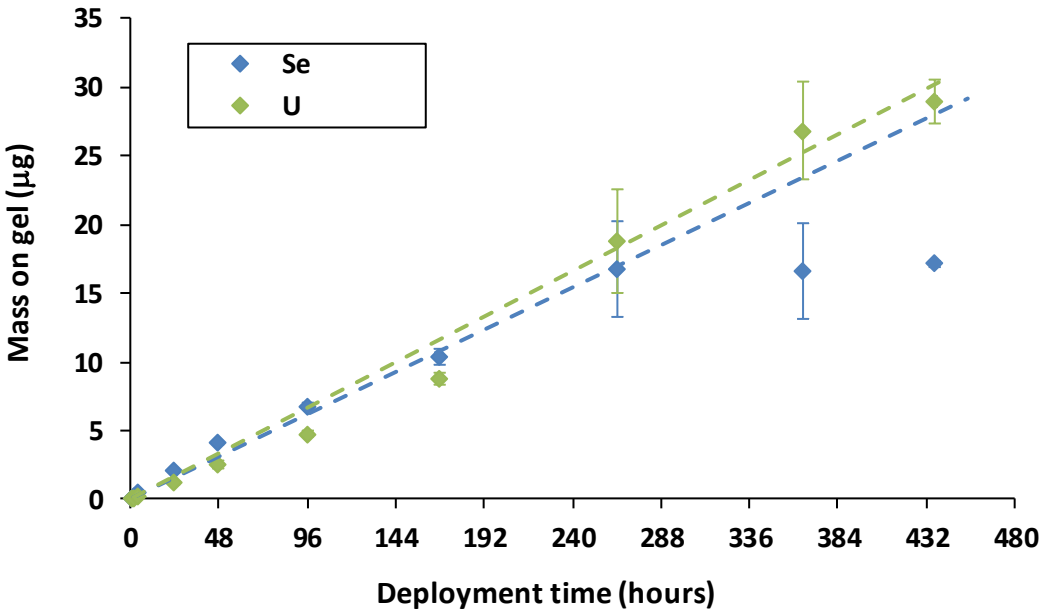

Figure 3.4. *Measured mass (µg) of Se and U on MBL gels according to DGT deployment time (hours). Error bars represent the standard deviation of the mean for triplicate deployments. Green and blue dashed lines are linear regression fits forced through the origin.*

Increasing the initial solution concentration of Se and U would have avoided the problem of Se depletion by DGT and accelerated the mass uptake of U. A caveat to increasing the solution concentration is that it increases the potential for precipitation of Se and U phases. An alternative approach to circumvent both the aforementioned issues would have been to deploy DGT devices in triplicate within a smaller volume of solution.

3.3.7 Solution pH and ionic strength

Figure 3.5 demonstrates that no inhibition in U uptake by the MBL DGT was observed over the pH range tested (3.40-7.34). Good uptake of Se (C_{DGT}/C_{soln} > 0.8) was observed at pH 3.40 and 6.66, but uptake diminished to an unacceptable level at pH 7.34 (C_{DGT}/C_{soln} = 0.56).

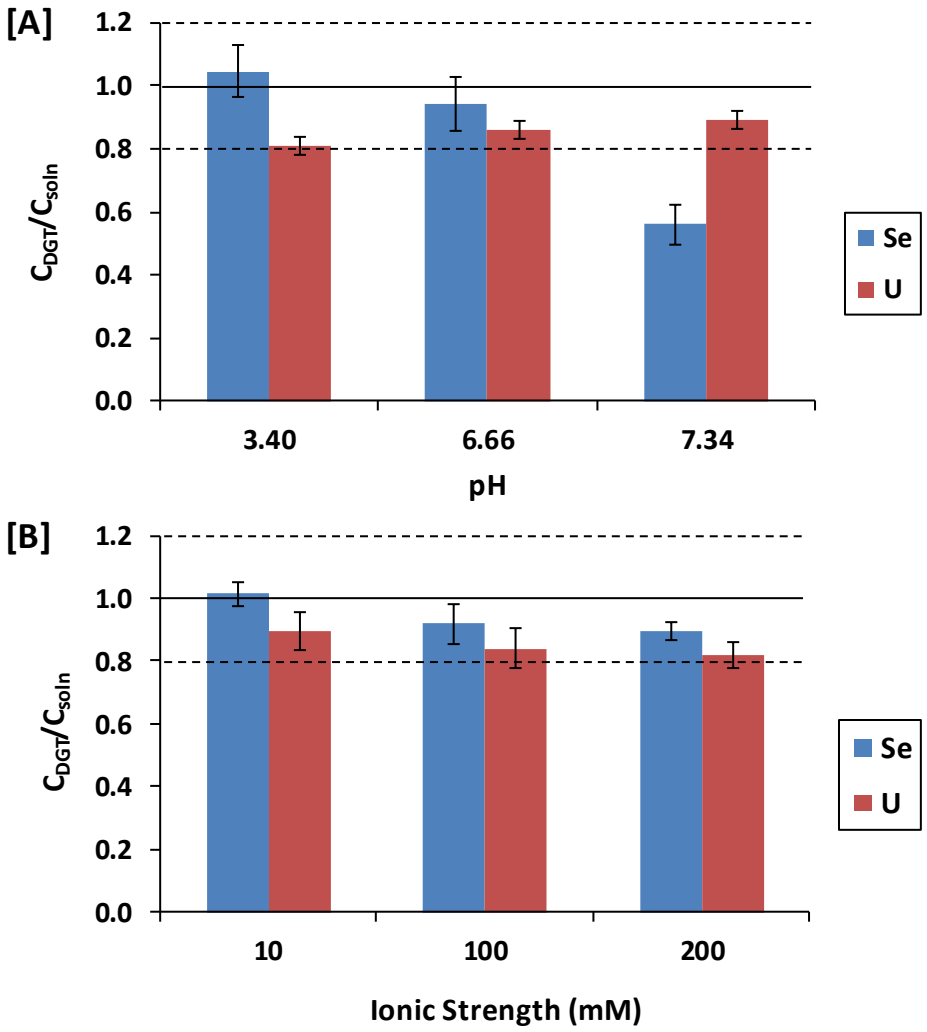

Figure 3.5. *Ratio of DGT-measured concentration (C_{DGT}) of Se and U to solution concentration (C_{soln}) for MBL DGT devices at varying solution pH **[A]** and ionic strength **[B]**. Error bars represent the standard deviation of the mean for triplicate DGT deployments. Solid horizontal line represents 1:1 C_{DGT}/C_{soln} ratio, and dashed horizontal lines represent 20% deviation from this ratio.*

The finding of decreased Se uptake at pH > 7 has been previously reported for both pure ferrihydrite (Luo et al., 2010; Price et al., 2013) and the MBL (Mason et al., 2005). Lower uptake of Se at higher pH has been attributed to the reduction in adsorption of anionic selenate to ferrihydrite (Price et al., 2013) as the concentration of positively-charged sites on the ferrihydrite diminishes approaching the point of zero charge. Pure synthetic ferrihydrite

phases are reported to have a point of zero charge at pH 8.0-8.3 (Schwertmann and Fechter, 1982), above which the net surface charge becomes negative.

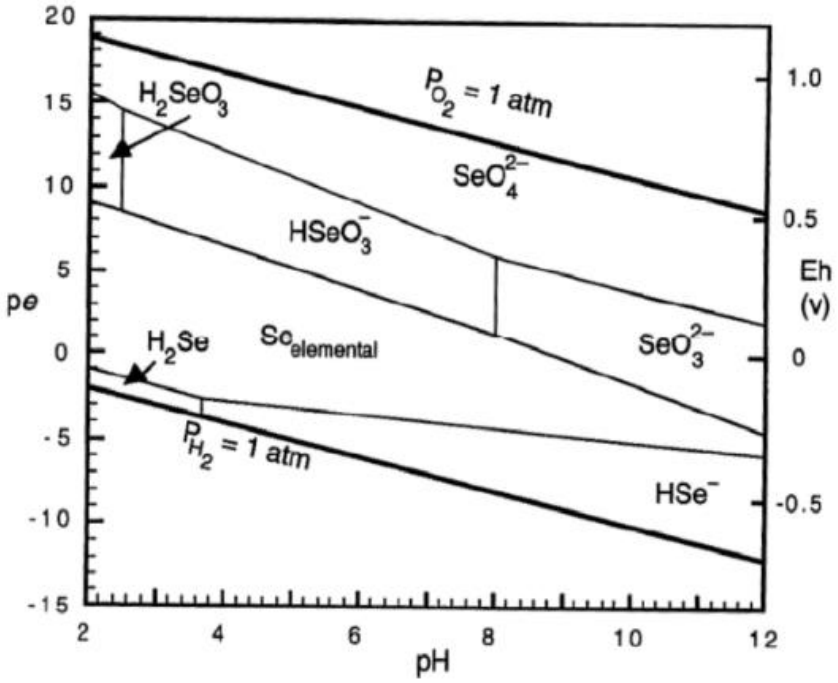

Figure 3.6. *Eh-pH speciation diagram for Se. From: Drever (1997).*

Figure 3.7 shows that at low pH (< 5), the speciation of U under oxidising conditions is dominated by the uranyl cation (UO_2^{2+}). At around pH 3-4, uptake of U is expected to diminish as the Chelex-100 resin transitions from a cation exchanger to an anion exchanger (Bio-Rad, 2017). Conflicting evidence is presented in the literature as to the performance of Chelex DGT for measuring U over the pH 3-4 window. Li et al. (2006; 2007) found reduced uptake of U at pH < 5, yet Turner et al. (2012) found no inhibition in uptake down to pH 3, in support of the data presented in Figure 3.5 whereby uptake remains acceptable at pH 3.40. At pH 7.34, in the absence of complexing ligands aside from hydroxide, neutral $UO_2(OH)_2^0$ species will dominate (Figure 3.7). These uncharged species are unable to participate in ion exchange with the Chelex resin, so C_{DGT} values would be expected to diminish accordingly. This is not reflected in Figure 3.5A, however, where uptake remains good (C_{DGT}/C_{soln} = 0.89 ± 0.05). This

observation is supported by Li et al. (2006), who noted that uptake of U by Chelex gels over the pH range 1-9 peaked between pH 6 and 8.

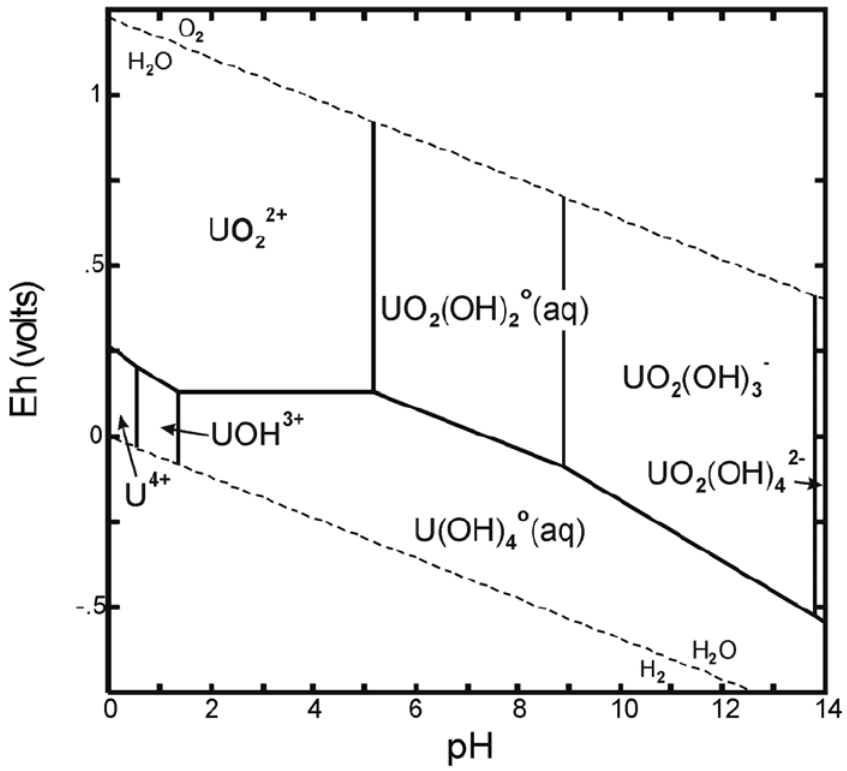

Figure 3.7. *Eh-pH speciation diagram for U in the absence of complexing ligands except for hydroxide. From: Krupka and Serne (2002).*

Figure 3.5B reveals that uptake of neither Se nor U is affected by the solution ionic strength over the range 10-200 mM $NaNO_3$. Increasing the ionic strength of the solution may hinder the diffusion of both elements through the gel as opposed to interfering with binding. Previous studies that investigated Se uptake by ferrihydrite DGT with increasing ionic strength did not consider ionic strengths above 100 mM $NaNO_3$ but concur with the findings in Figure 3.5. Conflicting evidence is presented in the literature regarding the effect of ionic strength on uptake of U by Chelex DGT; Turner et al. (2012) reported consistent uptake up to 1 M $NaNO_3$, while Price et al. (2013) reported reduced uptake (C_{DGT}:C_{soln} < 0.6) at 200 mM $NaNO_3$.

3.3.8 Alkalinity

Figure 3.8 reveals that uptake of both Se and U is suppressed with increasing alkalinity beyond 0.16 mM HCO_3^-. At 1.03 mM, C_{DGT}/C_{soln} drops to 0.16 ± 0.02 and 0.72 ± 0.03 for Se and U, respectively. The C_{DGT}/C_{soln} ratio shows minimal further decline for Se with increasing HCO_3^-, whereas C_{DGT}/C_{soln} for U continues to decline in a more linear manner, falling to 0.38 ± 0.04 at 4.18 mM HCO_3^-.

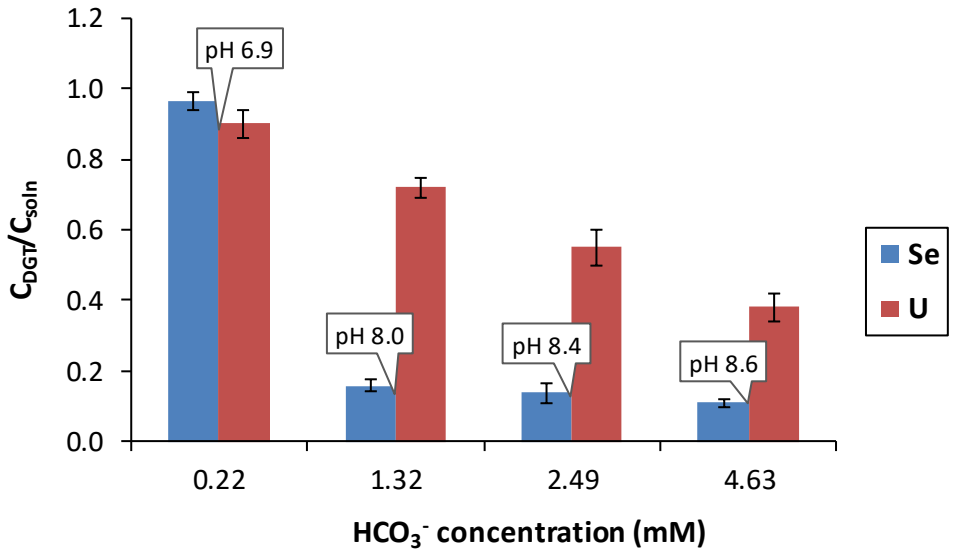

Figure 3.8. *Effect of solution alkalinity (HCO_3^- concentration) on the ratio of concentrations of Se and U measured by DGT (C_{DGT}) to deployment solution concentrations (C_{soln}). Measured solution pH is also shown. Error bars represent the standard deviation of triplicate DGT deployments. Solid horizontal line represents 1:1 C_{DGT}/C_{soln} ratio, and dashed horizontal lines represent 20% deviation from this ratio.*

The suppressed uptake of Se at 1.03 mM HCO_3^- is likely to be explained mostly by the high pH of the solution (8.0) leading to a reduction in Se adsorption to ferrihydrite as discussed in Section 3.3.7. Furthermore, ferrihydrite is able to adsorb a range of anions and cations, and so introduction of HCO_3^- anions into the system will introduce competition with Se for binding sites therefore further suppressing uptake of Se. Balistrieri and Chao (1990) report that the

adsorption affinity of HCO_3^-/CO_3^{2-} is greatly superior to both selenate and selenite, and will therefore outcompete these anions for adsorption sites.

Other studies have also noted a decrease in U uptake by Chelex DGT in the presence of increasing concentrations of HCO_3^-/CO_3^{2-} (Gregusova and Docekal, 2011; Turner et al., 2012). Gregusova and Docekal (2011) found accumulation of U to diminish when the total carbonate concentration exceeded 30 ppm (0.49 mM). The relative increase in anionic uranyl carbonate species over neutral uranyl hydroxide and carbonate species at higher alkalinity, as discussed in Section 1.2.3, is likely to be responsible for the reduction in uptake since anionic species are unable to bind to Chelex at pH > 4.

3.4 Conclusions

In summary, uptake of Se and U by the Chelex-ferrihydrite MBL is compliant with DGT theory. Deployment of the MBL in soil for measuring Se and U simultaneously will offer a significant saving in time and financial outlay for the experimental work conducted in this thesis. Some limitations in the performance of the MBL are recognised, however. Firstly, due to the slower kinetics of binding for U relative to Se, uptake of U by DGT at shorter deployment times (< 24 hours) is not quantitative. Therefore, a minimum deployment time of 24 hours must be adhered to. A longer deployment time is favourable since it will lower the method detection limits for both elements. Second, deployment does not appear to be suitable for alkaline soils since uptake of both Se and U was found to be inhibited in the presence of higher concentrations of HCO_3^- and CO_3^{2-} (≥ 1.03 mM). Since the work in this thesis is primarily concerned with relative temporal trends in the availability of both elements however, the absolute measured values of C_{DGT} are not essential. A correction factor could be applied where necessary to account for reduced uptake. Further work should aim to establish the effect of

other competing ions on Se uptake, in particular anionic species commonly found in soils including phosphate, fluoride and sulphate.

This page intentionally left blank

Chapter 4: Availability and aging of technetium-99 within spiked soils

4.1 Introduction

Increasing attention has been centred on understanding the environmental behaviour of the long-lived radionuclide ^{99}Tc, due to the progressively increasing global inventory associated with spent nuclear fuel coupled to a substantial legacy of terrestrial and marine contamination. As reviewed in Section 1.2.1, the speciation of Tc in aerobic soils is dominated by the highly-soluble, mobile and bioavailable pertechnetate (TcO_4^-) anion (Bennett and Willey, 2003), which is reduced at lower redox potentials to hydrous TcO_2 species exhibiting greatly enhanced adsorption to the soil solid phase (Sheppard et al., 1990).

Throughout the scientific literature, the availability of Tc in soils has been predominantly assessed through plant uptake studies. Knowledge of the aging of Tc is limited, although several studies have reported that soil-to-plant transfer factors diminish over time following addition of Tc to the soil in the form of pertechnetate (TcO_4^-) (Mousny and Myttenaere, 1982; Garten et al., 1984; Echevarria et al., 1997). Echevarria et al. (1997) found that bioavailability decreased with biomass production as opposed to incubation time following spiking. Conversely, Ewers et al. (2011) concluded that aging of Tc was the most important factor in determining plant uptake. They suggested that Tc was in a predominantly chemically reduced form at four months following contamination and consequently proposed separate transfer factors for both reduced and non-reduced forms accordingly.

Meanwhile, chemical extraction methods have been used very sparingly to assess available Tc. Calcium chloride (typically 0.05 M) is the extractant of choice in such studies (Echevarria et al., 1997; Tagami and Uchida, 1998; Tagami and Uchida, 1999). Echevarria et al. (1997)

found that that a $CaCl_2$ extraction was able to predict ryegrass uptake of Tc in two inceptisols at various Tc application rates (up to 250 Bq g^{-1}) in two different chemical forms (NH_4TcO_4 and Tc bio-incorporated in wheat leaves).

Significant gaps exist in the scientific literature concerning the aging of Tc, in particular with respect to how fast Tc ages and which soil properties are most influential in determining the kinetics of aging. To date, no previous studies have utilised DGT to investigate Tc dynamics in soil. The objective of the work in this chapter therefore was to utilise DGT to advance knowledge and understanding surrounding ^{99}Tc availability in a range of soil types. As detailed in Section 2.1.3, the approach taken to achieve this objective was an 18-month incubation of 20 different soils that were subjected to a series of DGT deployments at progressively increasing time intervals. The aim was to establish a clearer understanding of the rate and extent of aging of Tc within the soil and elucidate the key soil properties influencing the aging process. Three different kinetic models and a natural exponential function were then applied to the DGT dataset to quantitatively analyse the data with respect to aging. A description of these models can be found in Section 1.5, whilst Section 2.3.3 explains how they were fitted to the primary incubation DGT dataset presented in this chapter. In addition to the primary incubation experiments, a secondary incubation was set-up to investigate the effects of microbial activity on Tc availability and aging, as well as the impact of different moisture regimes during the incubation period, as described in Section 2.1.4.

4.2 Results and discussion

In this section, the availability and aging of Tc are assessed through two datasets derived from the primary incubation: firstly, the concentration of Tc measured in soil solution (C_{soln}), and secondly the DGT-measured concentrations (C_{DGT}). A quantitative assessment of the aging processes is made by fitting a selection of kinetic models to the DGT dataset. The solid phase

resupply of Tc is then addressed by examining R values (C_{DGT}/C_{soln}) in combination with soil response times calculated through the 2D-DIFS model. Lastly, the effects of microbial activity, and in particular the incubation moisture regime, on Tc aging are examined through data acquired from the secondary incubation.

4.2.1 Availability and aging assessed by soil solution measurements

4.2.1.1 Aging process and kinetics

Figure 4.1 shows the concentration of Tc measured in soil solution (C_{soln}) over time for all 20 incubated soils after C_{soln} at each time point has been normalised to the first measurement for C_{soln} made at day 3. Measured values of C_{soln} expressed per litre of soil solution (μg L^{-1}) have been converted to concentrations expressed per kg of air-dry soil (μg kg^{-1}), and subsequently normalised to account for the cumulative depletion of Tc from the soil associated with DGT deployments and extraction of the soil solution (Section 2.3.2.3). Data from Appendix B.2 demonstrate that, prior to the final DGT deployment at 549 days aging, the mass of Tc removed from the soil ranged from 4 to 33% with a mean and median of 20 ± 10 and 23% respectively.

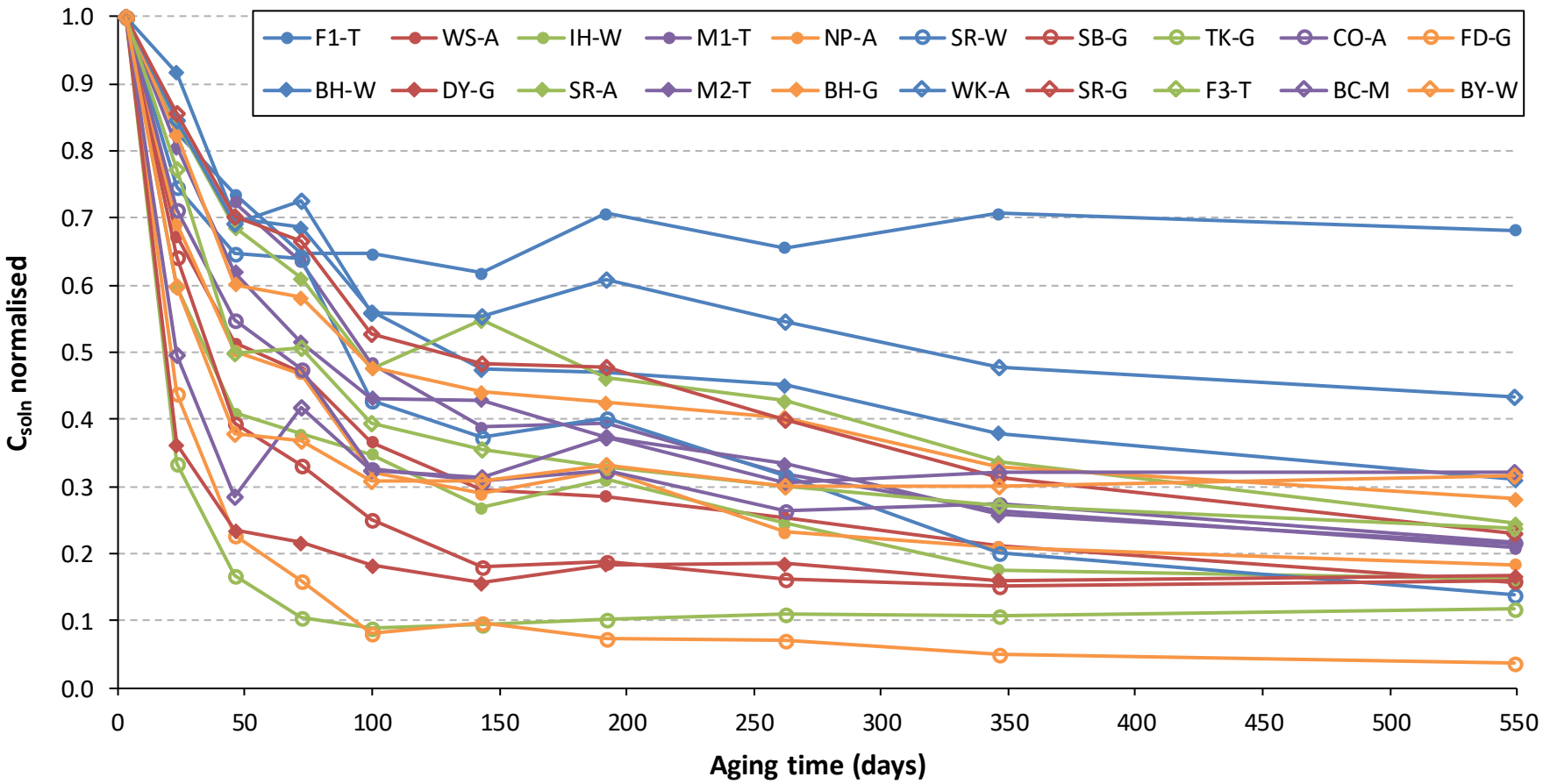

Figure 4.1. *Concentration of Tc measured in the soil solution over 549 days incubation time for all 20 soils after normalising to day 3.*

In general, Figure 4.1 reveals a biphasic trend of removal of Tc from solution whereby removal occurs most rapidly over the first 3-100 days, followed by a much slower phase of removal. The observation of decreasing availability of Tc over time in Figure 4.1 is reported elsewhere from both laboratory (Mousny and Myttenaere, 1982; Tagami and Uchida, 1998) and field studies (Hoffman et al., 1982; Garten et al., 1984). After 100 days incubation, C_{soln} is less than 50% of the measured concentration at day 3 in all but four of the soils. After 549 days incubation, C_{soln} is between 4 and 67% of C_{soln} measured at day 3, with a mean and median of 23 and 20% respectively.

The decrease in Tc measured in solution with time is often explained through the reduction of TcO_4^- to lower oxidation states, including Tc(IV) hydrous oxides such as $TcO_2.nH_2O$ [abbreviated as $TcO_2(s)$], and eventually sulphides and high molecular weight organic complexes (Sheppard et al., 1990; Tagami and Uchida, 1996). Anoxic conditions are ultimately responsible for initiating these transformations in speciation, yet the soils in this study were incubated in an air-dry state under conditions unlikely to promote anoxia. It is well-established, however, that anaerobic microsites can develop even in well-drained soils considered uniformly aerobic as a result of oxygen depletion through hot spots of microbial activity in small water-filled pores (Greenland and Hayes, 1981; Parkin, 1987). Such microbially-produced anaerobic microsites within aerobic soils are recognised to play an important role in denitrification and the concomitant production of ammonia for example, and several authors have implicated their role in TcO_4^- reduction (Hoffman et al., 1982; Henrot, 1989; Echevarria et al., 1997; Abdelouas et al., 2005). On this evidence it is possible that such anaerobic microsites could contribute to the reduction of a small fraction of the TcO_4^- within the soils which could explain the slow phase of removal of Tc from solution. However, the removal of Tc from solution is most likely to be explained by the adsorption of

anionic TcO_4^- to the positively-charged surfaces of inorganic soil components, in particular, hydrous oxides of Al and Fe, as discussed in Section 4.2.1.2.

4.2.1.2 Effect of soil properties on availability

Spearman's rank correlation coefficients (r_s) describing the correlation between C_{soln} and a range of soil properties at 3, 100 and 549 days aging are listed in Table 4.1. Organic carbon (C_{org}) is found to exhibit the strongest correlation of any soil property with C_{soln}, where a significant negative relationship ($\alpha < 0.01$) is observed at 3 ($r_s = -0.56$) and 549 days, and a highly significant relationship ($\alpha < 0.01$) at 100 days ($r_s = -0.64$). The relationship between C_{org} and C_{soln} is illustrated in Figure 4.2 where availability is clearly observed to be greater in soils with a lower C_{org} content.

Table 4.1. *Spearman's rank correlation coefficients (r_s) relating the concentration of Tc measured in solution determined by centrifugation (C_{soln}) to soil properties after 3, 100 and 549 days aging (N = 20).*

	Days of aging		
	3	**100**	**549**
Organic carbon	-0.56*	-0.64**	-0.56*
pH	0.51*	0.50*	0.34
Fe	0.19	0.05	-0.03
Al	-0.01	-0.29	-0.40
Mn	0.46	0.36	0.35
Al + Fe	0.19	0.05	-0.03

**Indicates significant relationship at α < 0.05; **Indicates significant relationship at α < 0.01*

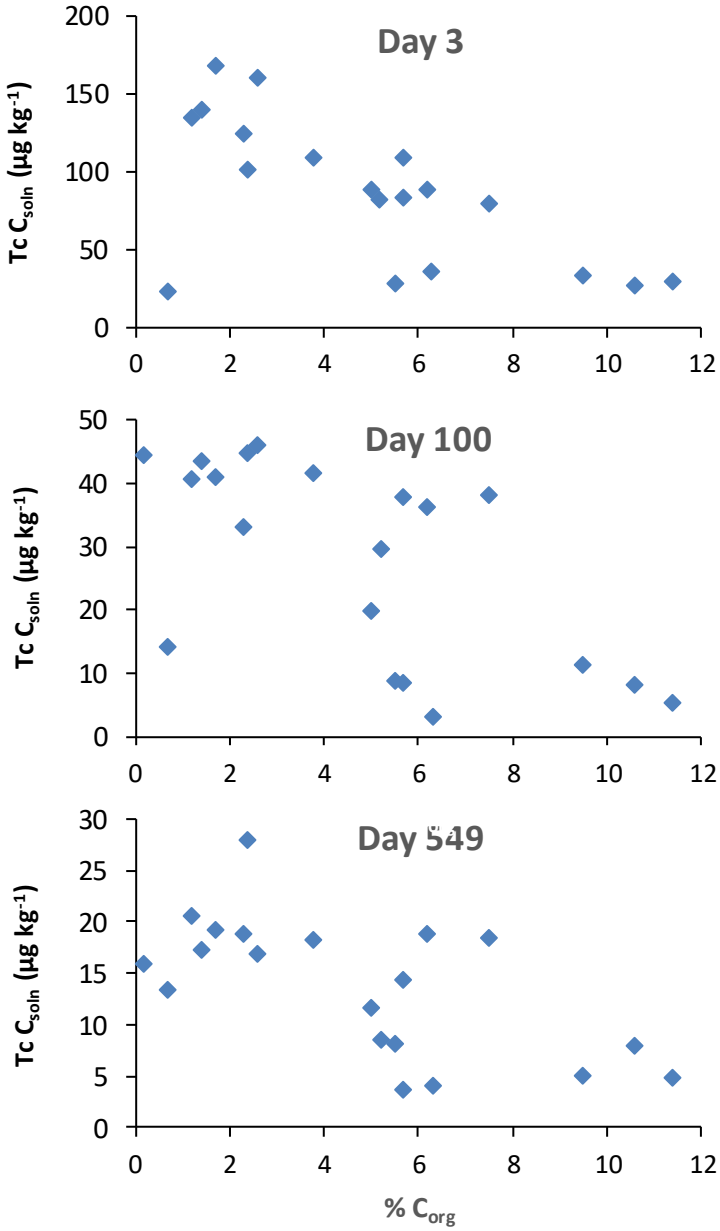

Figure 4.2. *Relationship between the concentration of Tc measured in the soil solution (C_{soln}) (µg kg^{-1}) and soil organic carbon content (C_{org}) at 3, 100 and 549 days aging.*

The organic matter (OM) fraction of soil is widely recognised as an important geochemical sink for Tc in soils by a number of studies (Balogh and Grigal, 1980; Sheppard et al., 1983; Wildung et al., 1995; Kaplan, 2003; Ewers and Brown, 2014), in support of the highly significant relationship reported here between C_{org} and C_{soln}. Under locally-reducing conditions, Tc is reported to complex with humic acid (HA) to form Tc(IV)-humic acid complexes characterised

by relatively slow ligand exchange rates (Stalmans et al., 1982; Geraedts et al., 2002; Gu and Ruan, 2007; Boggs et al., 2011). Negligible complexation of Tc was observed by Sanders (unpublished data) in a pure HA system of high redox potential over an incubation period of ~150 days, which supports the notion that reducing conditions are required for complexation. As previously discussed however, reduction of Tc within the soils of this study is not expected to be significant given the strongly aerobic conditions of incubation, and so sorption of Tc to organic matter is likely to be the primary removal mechanism as observed by Wildung et al. (1986).

Table 4.1 reveals that soil pH was also found to be well-correlated with C_{soln}, where a significant relationship ($\alpha < 0.05$) was identified after 3 ($r_s = 0.51$) and 100 ($r_s = 0.50$) days aging. At lower pH, the number of positively-charged sorption sites associated with variably-charged oxides of Fe and Al, plus organic matter, is greater (Yu, 1997), which in turn promotes enhanced adsorption of soluble anionic TcO_4^-. A moderate degree of negative correlation is calculated between the soil total Al content and C_{soln} at 100 ($r_s = -0.29$) and 549 ($r_s = -0.40$) days aging, yet correlation with Fe is largely absent. Several studies have noted the significance of the oxidic Al and Fe fraction in the sorption of Tc in soils, usually in combination with C_{org} (Schulte and Scoppa, 1987; Wildung et al., 1995; Icenhower et al., 2010).

4.2.1.3 Effect of soil properties on aging kinetics

To ascertain the influence of different soil properties on the kinetics of Tc aging, C_{soln} at each time point has been normalised to C_{soln} at day 3 for all the soils, and the soils highlighted according to their C_{org} content (Figure 4.3) and total Al + Fe content (Figure 4.4). Figure 4.3 reveals that, in general, the rate of removal of Tc from solution is faster in soils of higher C_{org} content. A 'rapid' phase of binding with C_{org} occurs over the first 50 days of aging for soils of high C_{org}, followed by a 'slow' phase of binding during which the rate of decrease in C_{soln} is

considerably slower. The onset of the slow phase is significantly delayed in soils of low C_{org} (< 4%) until ~100-150 days. Soils of high Al + Fe content (> 80 g kg^{-1}) in Figure 4.4 can be identified by a faster rate of decline in C_{soln}, where rapid aging occurs over the first 100 days after spiking. For soils with a concentration of < 80 g kg^{-1} however, there is no clear correlation between the Al + Fe content and the rate of decline in C_{soln}.

Wildung et al. (1995) investigated the sorption of Tc in a range of soils over a period of 1050 hours (~43 days) and reported that sorption within the first 48 hours was most strongly influenced by pH-dependent sorption sites on both oxidic Fe and Al fractions. Beyond 48 hours, the C_{org} content was found to dictate sorption. Here, the first measurement of C_{soln} in the primary incubation was not taken until day 3, where strong correlation was identified with C_{org} (r_s = -0.56, α < 0.05). In contrast, correlation between C_{soln} and total Al + Fe (r_s = 0.19) was very weak (Table 4.1). After 23 days aging, strong correlation with C_{org} (r_s = -0.70, α < 0.01) persisted and correlation with Al + Fe remained absent, in support of the findings of Wildung et al. (1995).

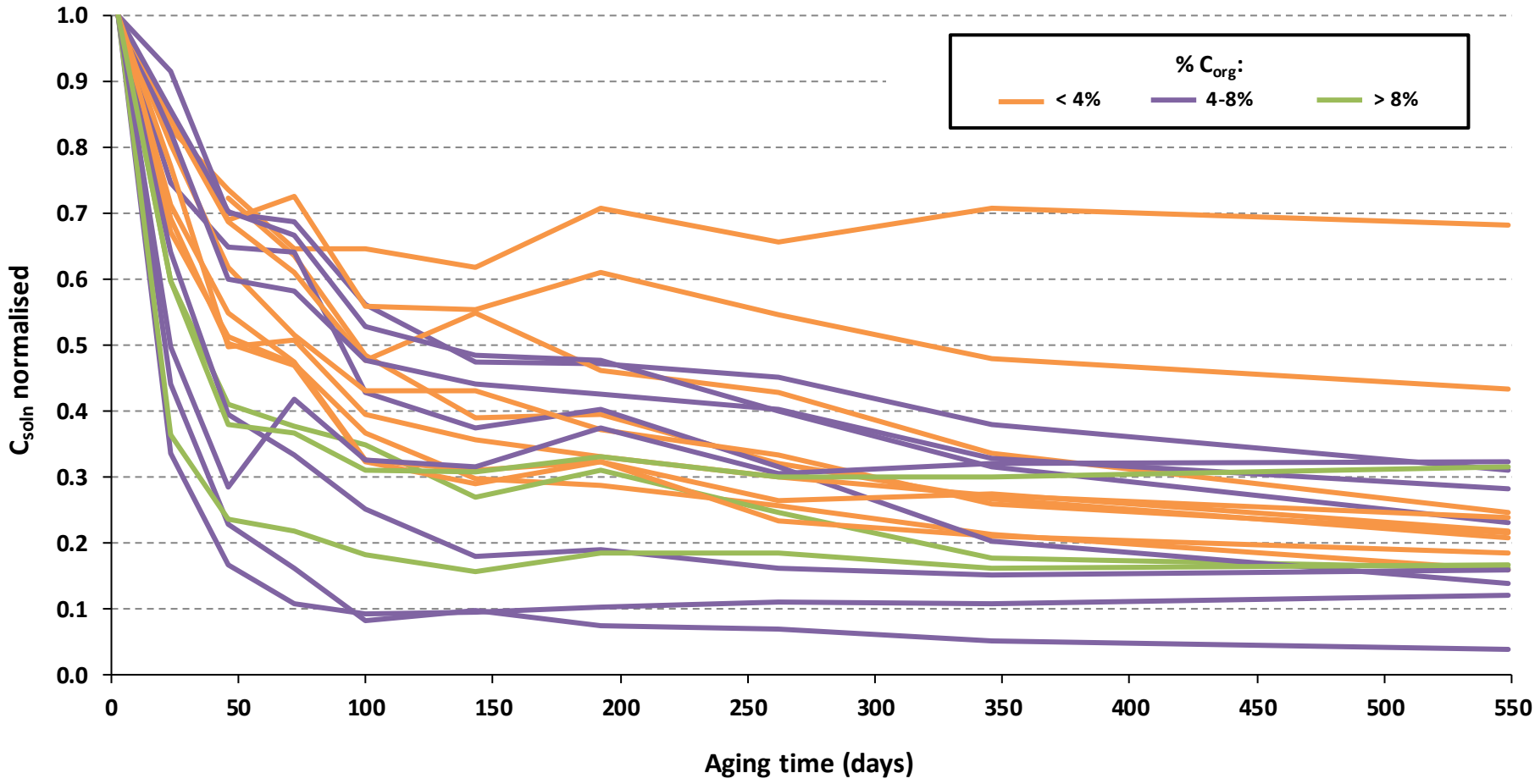

Figure 4.3. *Concentration of Tc in the soil solution (C_{soln}) for all 20 soils after normalising to day 3. C_{soln} determined by centrifugation. Soils are highlighted according to organic carbon (C_{org}) content.*

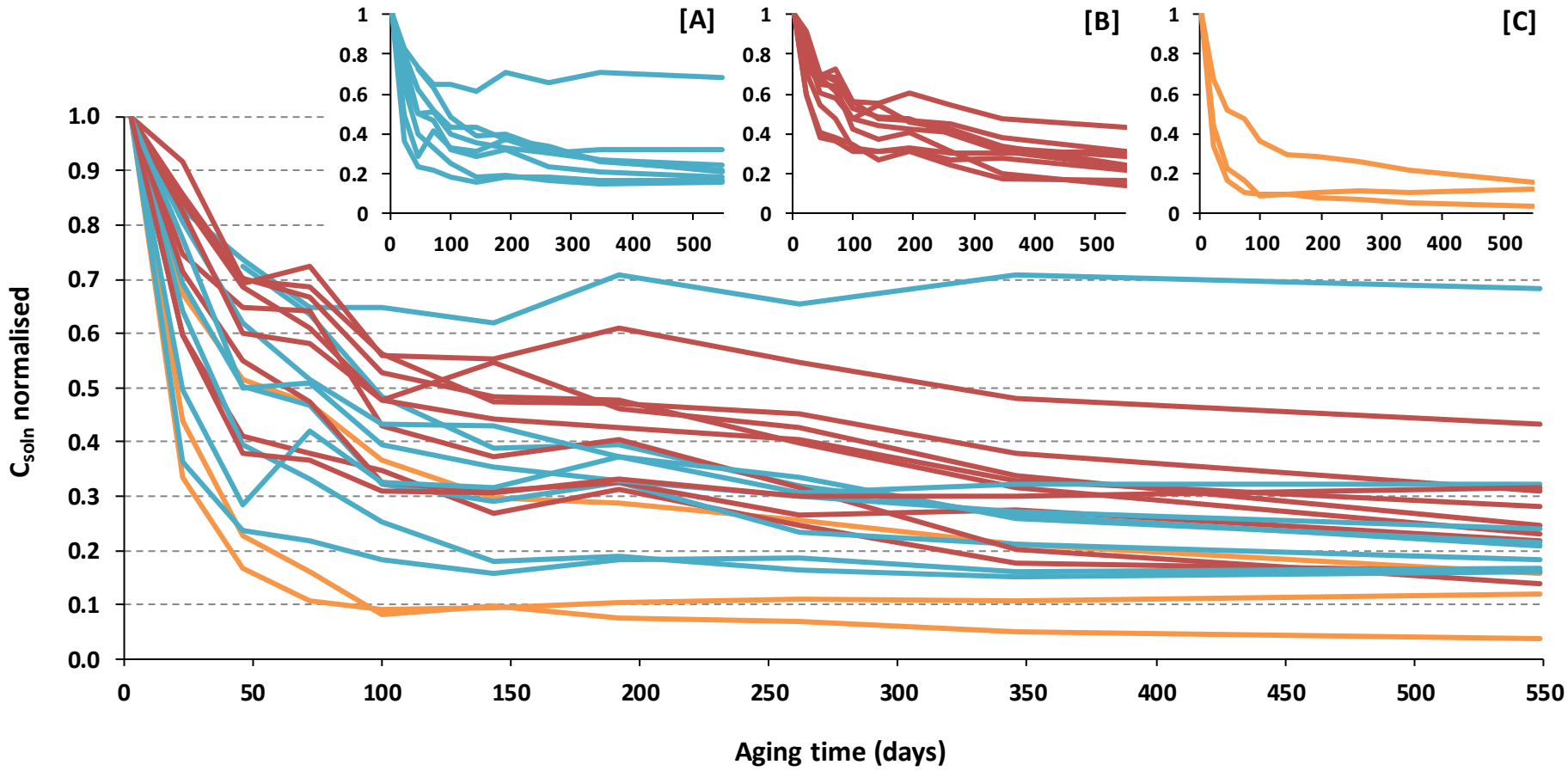

Figure 4.4. *Concentration of Tc in soil solution (C_{soln}) for all 20 incubated soils after normalising to day 3. Soils are highlighted according to their total Al + Fe content. C_{soln} determined by centrifugation. The three inset graphs exclusively highlight soils with a total Al and Fe content of < 40* ***[A]****, 40-80* ***[B]*** *and > 80 g kg^{-1}* ***[C]****.*

4.2.2 Availability and aging assessed by DGT

4.2.2.1 Aging process and kinetics

Presented in Figure 4.5 are the DGT-measured concentrations of Tc (C_{DGT}) within all 20 incubated soils throughout the primary incubation after normalising C_{DGT} at each time point to the first measurement for C_{DGT} at day 3. C_{DGT} values were initially corrected to account for the cumulative depletion of Tc from the soil (Section 2.3.2.3). The general trend of decreasing C_{DGT} over time is almost identical to that for Tc in solution. The distinctive biphasic trend which characterised the removal of Tc from solution in Figure 4.1 can likewise be discerned for C_{DGT} in Figure 4.5. After 100 days incubation, C_{DGT} is less than 50% of the measured concentration at day 3 in 15 out of 20 soils, in comparison to 16 of the 20 soils for C_{soln} (Figure 4.1). After 549 days incubation, C_{DGT} is between 3 and 41% of C_{DGT} measured at day 3, with a mean and median of 18 and 19% respectively.

The broad similarity in the trends over time between C_{soln} and C_{DGT} for the incubated soils is expected, since DGT measures both dissolved species in soil solution and resupply from the solid phase. However, as discussed in Section 1.4, a simple measurement of dissolved species is unlikely to provide an accurate assessment of availability. One of the key attributes of DGT is its ability to integrate the component of available Tc associated with the soil solid phase and labile complexes, which can be examined through the relationship between C_{DGT} and C_{soln}. This point is explored in Section 4.2.3

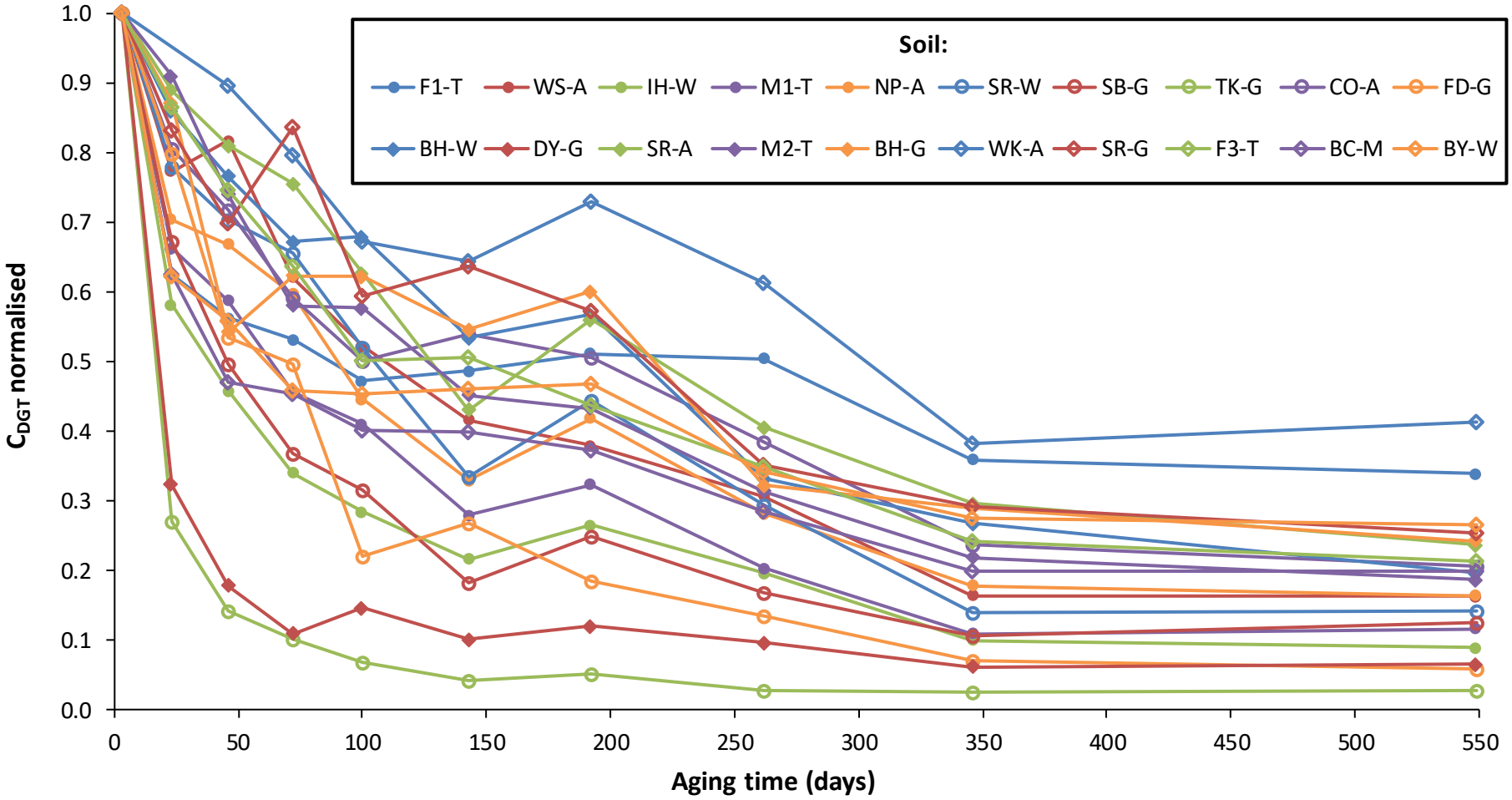

Figure 4.5. *DGT-measured concentration of Tc (C_{DGT}) in all 20 incubated soils after normalising to day 3.*

From consulting the published scientific literature, our knowledge of Tc aging is largely based on measurements of soil-to-plant transfer factors (TFs) over time. Interpreting temporal changes in TFs and relating these to measurements of DGT availability in soil over time is somewhat complicated, mainly due to the significant differences in values reported between species and taxonomic position (Cataldo et al., 1983; Cataldo et al., 1984), but also because of the potential for the migration and redistribution of Tc within the rooting zone (Ehlken and Kirchner, 2002). Further complication arises from the fact that plants have been observed to remove a substantial portion of the Tc spike in lysimeter studies (Grogan et al., 1986; Echevarria et al., 1997), and so TFs may evolve to appear deceptively low.

In a review of the literature concerning soil-to-plant transfer of Tc, Ewers et al. (2011) concluded that Tc was considered to be in a reduced form at four months following initial contamination, and consequently proposed separate TFs for both reduced and non-reduced forms accordingly. After a similar period of incubation time (143 days), C_{DGT} measured across all soil types was on average 39 ± 17% of the availability at three days following spiking, and so this extent of aging would appear to support the conclusions of Ewers et al. (2011) that Tc could be considered to be in a reduced form four months after its application as TcO_4^-. Tagami and Uchida (1998) reported a much slower rate of aging, however, for Tc within two soils of low C_{org} based upon a series of 0.05 M $CaCl_2$ extractions. After six months, the extractable activity was found to have diminished to no more than 80% in one of the soils, and 50% in the other.

Coefficient and parameter values obtained after fitting a pseudo-second-order (Ho, 2006), Elovich (Chien and Clayton, 1980) and parabolic diffusion equation (Ma and Uren, 1997) to the DGT dataset derived for all 20 incubated soils are presented in Table 4.2. Table 4.3 lists coefficient and parameter values after fitting the natural exponential function. Section 1.5 introduces the four models and Section 2.3.3 describes how they were fitted to the

experimental data. The relevant parameters and coefficients are described in the captions of both Table 4.2 and Table 4.3.

In general, all the models could adequately describe the aging of Tc across the range of soils. This is illustrated in Figure 4.6 where all four models are fitted to the experimentally-derived C_{DGT} values, using soil SR-A as an example. Using the calculated standard error to describe the closeness of fit for each of the modelled values to the experimental data, the pseudo-second-order equation provided the best fit for seven of the soils, followed by the Elovich (6), natural exponential (3) and lastly parabolic diffusion equation (2).

Also presented in Table 4.3 is an availability half-life for each soil, calculated by dividing ln(2) by the rate constant (B). The half-lives range from just 10 days (TK-G) up to 156 days (SR-G), with a median of 78 days. A mean half-life of 72 ± 46 days is calculated. Vandecasteele et al. (1989) investigated the long-term availability of Tc in an accidentally-contaminated lysimeter soil through monitoring of soil-to-plant concentration ratios over a 4-year period. The study proposed a bioavailability half-life of about one month for the majority (96%) of the Tc present in the soil, which was characterised as a neutral (pH 6.9) clay soil with an C_{org} content of 3.81%. The soil from the primary incubation with the most similar properties is SR-G, but this soil is found to exhibit the longest half-life of any of the incubated soils at 156 days. Nevertheless, one month is still comparable to the range of half-lives presented in Table 4.3, with a mean and median of 54 and 59 days respectively.

Table 4.2. *Parameter and coefficient values for three different kinetic models (pseudo-second-order, Elovich and parabolic diffusion) used to describe the aging of Tc in all 20 incubated soils. Q_t is the DGT-available concentration of* Tc *at time t (days); a, b and c are all constants; k_p is the parabolic diffusion rate constant (μg L^{-1} $d^{-1/2}$); k is the pseudo-second-order rate constant that also represents the Tc aging rate constant (μg L^{-1} d^{-1}); Q_e is the quantity of available Tc at equilibrium time (μg L^{-1}); SE is the standard error of the modelled values of Q_t, used to judge the best fit of the models to the experimental data [see Equation (2.11)].*

Soil	Pseudo-second-order $Q_t = \frac{t}{\left(\frac{1}{k}\right)Q_e^2 + \left(\frac{t}{Q_e}\right)}$			Elovich $Q_t = a + b \ln(t)$			Parabolic Diffusion $Q_t = \sqrt{k_{pd}} + c$		
	k	**Q_e**	**SE**	**a**	**b**	**SE**	**k**	**c**	**SE**
F1-T	0.219	0.72	0.27	0.591	0.636	0.18	0.107	2.326	0.17
WS-A	0.049	1.75	1.02	-11.310	4.393	1.53	0.695	2.969	5.34
IH-W	0.181	0.90	0.06	-0.193	0.884	0.05	0.139	2.415	0.16
M1-T	0.033	3.93	1.89	-8.516	5.863	1.60	0.898	10.572	9.34
NP-A	0.047	2.38	1.72	-7.911	4.273	1.64	0.685	5.859	6.09
SR-W	0.069	1.33	0.76	-7.453	3.090	0.89	0.515	1.050	1.18
SB-G	0.089	1.84	0.19	-1.949	2.115	0.48	0.327	4.198	1.34
TK-G	0.136	2.89	0.02	4.243	0.532	0.08	0.078	5.841	0.16
CO-A	0.066	1.42	0.92	-6.907	3.077	0.74	0.518	1.503	0.84
FD-G	0.169	0.71	0.12	-2.508	1.291	0.17	0.201	1.222	0.47
BH-W	0.082	0.89	0.38	-6.984	2.512	0.57	0.430	-0.209	0.39
DY-G	0.299	1.11	0.01	1.864	0.245	0.02	0.037	2.590	0.04
SR-A	0.063	1.11	0.82	-9.453	3.304	0.91	0.551	-0.360	1.25
M2-T	0.044	1.75	0.89	-12.904	4.802	0.46	0.782	0.544	2.37
BH-G	0.098	0.91	1.38	4.240	1.977	1.20	0.334	1.147	0.04
WK-A	0.077	0.76	1.26	-8.911	2.748	1.20	0.408	-0.514	1.26
SR-G	0.096	0.73	0.71	-5.322	1.997	0.92	0.346	0.005	0.67
F3-T	0.058	1.51	0.36	-9.603	3.766	0.33	0.617	0.900	1.33
BC-M	0.263	0.58	0.07	-0.078	0.581	0.02	0.096	1.532	0.04
BY-W	0.331	0.07	0.07	0.077	0.434	0.03	0.073	1.264	0.03

Table 4.3. *Coefficient and parameter values for a natural exponential function used to describe the aging of Tc in all 20 incubated soils. Availability half-life (days) is calculated as ln(2)/-B; Se is the standard error of the modelled values of Q_t, used to judge the fit of each model to the experimental data.*

	Natural exponential function: $Q_t = A*e^{-Bt} + C$				
Soil	**SE**	**A**	**B**	**Half-life (days)**	**C**
F1-T	0.45	4.10	-0.044	16	3.03
WS-A	0.93	16.04	-0.007	94	2.70
IH-W	0.35	4.87	-0.024	29	0.97
M1-T	1.88	24.80	-0.013	55	4.66
NP-A	1.45	16.91	-0.010	70	4.24
SR-W	0.87	11.45	-0.007	95	1.76
SB-G	0.48	10.36	-0.020	35	1.81
TK-G	0.21	8.65	-0.068	10	0.37
CO-A	1.06	11.61	-0.007	100	3.52
FD-G	0.29	5.18	-0.014	49	0.47
BH-W	0.57	9.56	-0.005	147	1.44
DY-G	0.10	3.86	-0.067	10	0.35
SR-A	0.85	11.68	-0.006	112	3.30
M2-T	0.82	16.84	-0.008	88	3.87
BH-G	1.15	7.63	-0.006	111	2.62
WK-A	1.19	9.69	-0.005	128	5.23
SR-G	0.77	7.93	-0.004	156	1.63
F3-T	0.66	13.48	-0.008	87	3.85
BC-M	0.33	3.19	-0.025	27	1.28
BY-W	0.30	2.53	-0.029	24	1.41

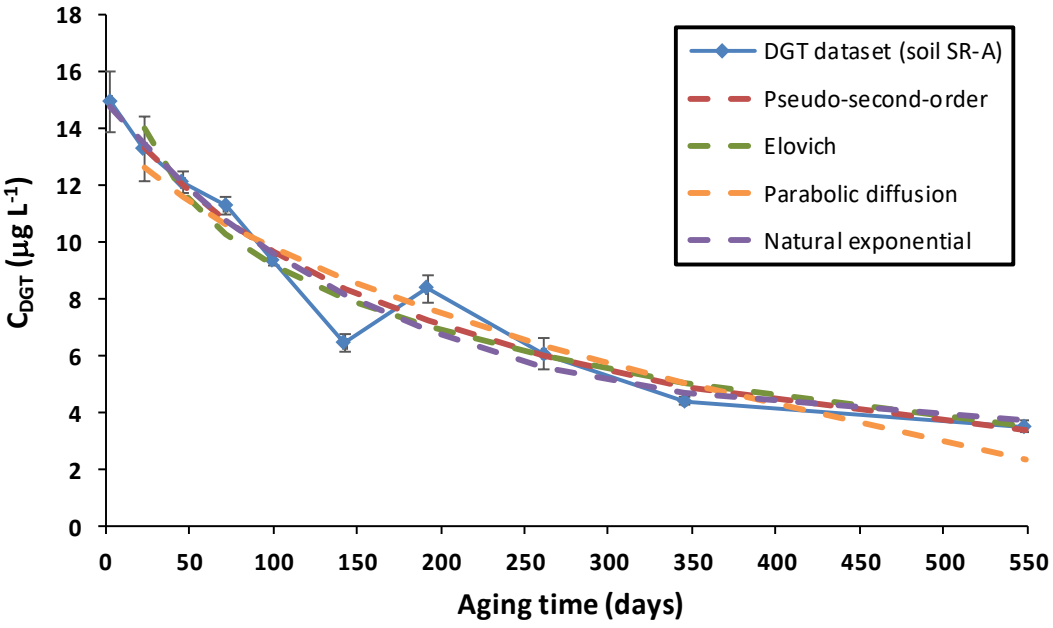

Figure 4.6. *Comparison of model fits (pseudo-second-order, Elovich and parabolic diffusion) for experimentally-acquired DGT data for soil SR-A over 549 days of aging. Error bars represent one standard deviation of the mean of triplicate DGT deployments.*

4.2.2.2 Effect of soil properties on availability

Spearman's rank correlation coefficients (r_s) describing the correlation between C_{DGT} and various soil properties at 3, 100 and 549 days aging are listed in Table 4.4. As was the case for Tc in solution (C_{soln}), a highly significant relationship ($\alpha < 0.01$) is observed between C_{org} and C_{DGT} throughout the incubation period. This strong negative correlation is illustrated in Figure 4.7 and Figure 4.8, where higher values of C_{DGT} are clearly observed in soils of lower C_{org}. The limited solubility of the organic matter compounds to which the Tc is adsorbed owing to their high molecular weight can explain their inability to be measured by DGT.

Table 4.4. *Spearman's rank correlation coefficients (r_s) relating C_{DGT} to soil properties after 3, 100 and 549 days aging (N = 20).*

	Days of aging		
	3	**100**	**549**
Organic carbon	-0.77**	-0.73**	-0.77**
pH	0.50*	0.47*	0.27
Fe	-0.14	-0.10	-0.14
Al	-0.32	-0.38	-0.48*
Mn	0.25	0.24	0.17
Al + Fe	-0.14	-0.10	-0.14

**Indicates significant relationship at α < 0.05; **Indicates significant relationship at α < 0.01*

Additionally, a significant relationship ($\alpha < 0.05$) is observed between soil pH and C_{DGT} after 3 ($r_s = 0.50$) and 100 ($r_s = 0.47$) days aging (Table 4.4). The significance of this relationship between pH and C_{DGT} reported at 3 and 100 days aging is likely to be attributed to the acidic nature of soils of higher C_{org} owing to the abundance of humic and fulvic acids. For example, the three soils with the highest C_{org} content in this incubation have a pH of 3.88, 3.90 and 3.41. At the same time, soil organic matter will contain a higher concentration of positively-charged sorption sites at lower pH, the result being greater retention of TcO_4^- and in turn lower availability should sorption be a significant process in the retention of TcO_4^- by organic matter.

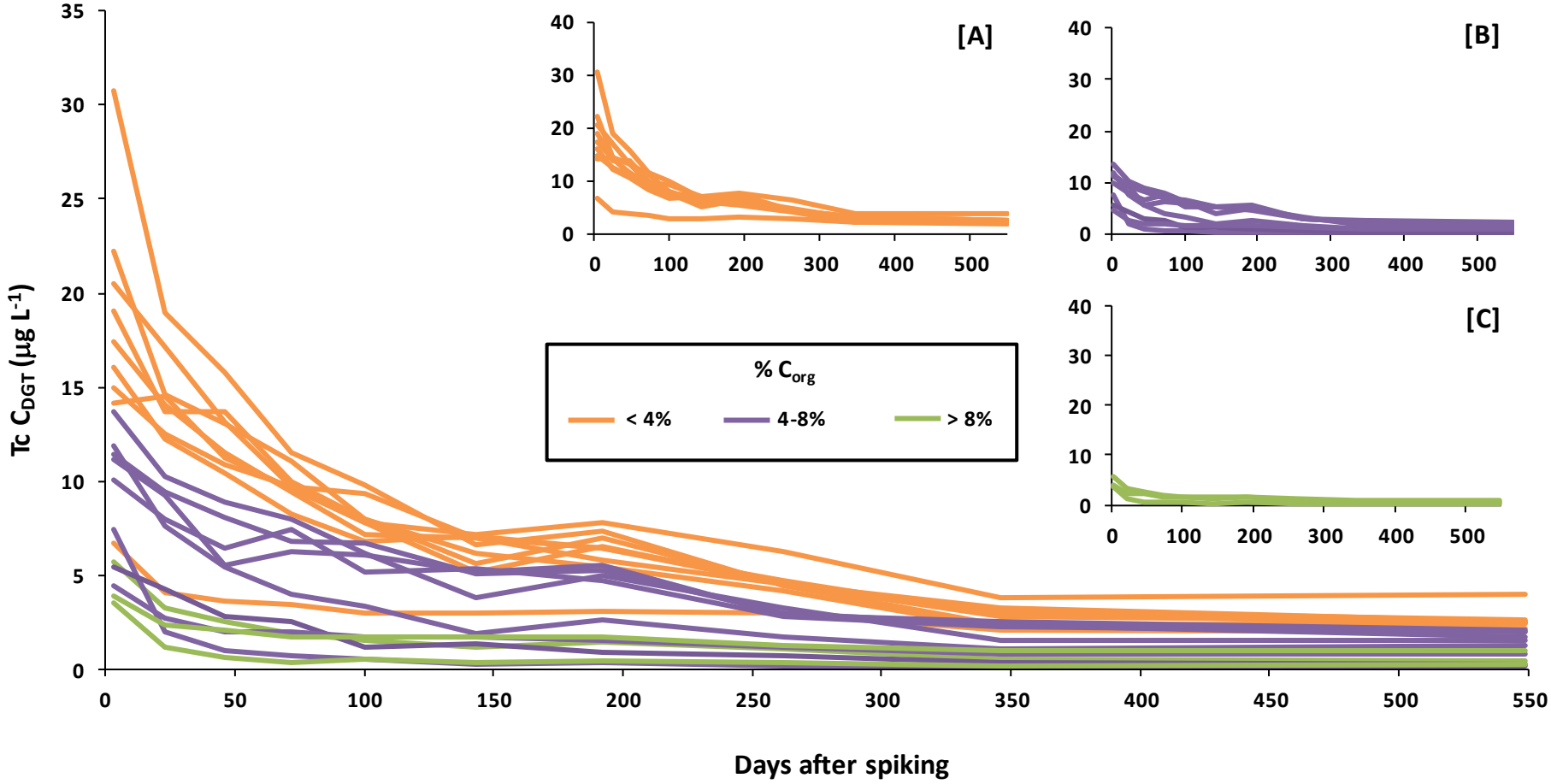

Figure 4.7. *DGT-measured concentration (C_{DGT}) of Tc in all 20 incubated soils over 549 days aging. Soils are highlighted according to organic carbon (C_{org}) content. The three inset graphs exclusively highlight soils with an organic carbon content of < 4%* ***[A]****, 4 – 8%* ***[B]*** *and > 8%* ***[C]****.*

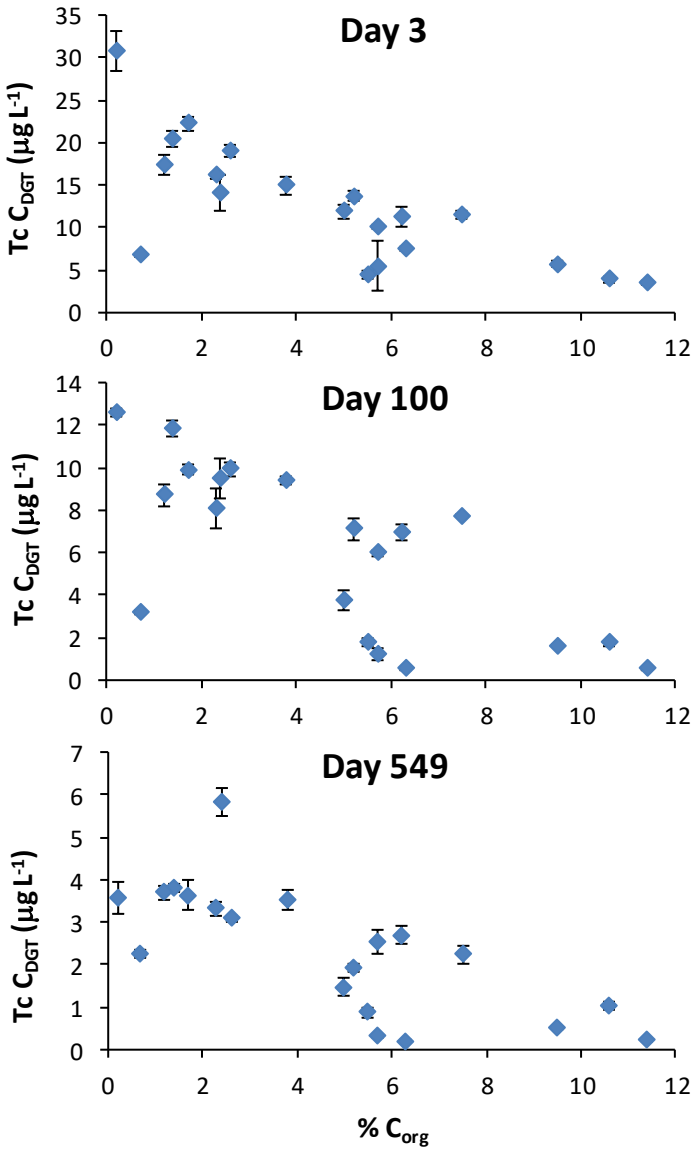

Figure 4.8. *Relationship between the DGT-measured concentration of Tc (C_{DGT}) (µg L^{-1}) at 3, 100 and 549 days aging, and soil organic carbon (C_{org}) content.*

A moderate degree of negative correlation can be found between C_{DGT} and Al, which is significant (r_s = -0.48, $\alpha < 0.01$) after 549 days aging, but correlation with Mn and Fe is largely absent. The correlation between C_{DGT} and Al is comparable to the correlation reported in Table 4.1 between C_{soln} and Al.

4.2.2.3 Effect of soil properties on aging kinetics

The relationships between soil properties and the rate constants associated with the natural exponential function, Elovich and pseudo-second-order equations were investigated, since between them the three models could best describe the rate of aging for all but one of the soils. Spearman's rank correlation coefficients (r_s) relating soil properties to the pseudo-second-order (k) and Elovich rate constants (b), plus the availability half-life derived from the natural exponential function are presented in Table 4.5.

Table 4.5. *Spearman's rank correlation coefficients (r_s) describing the correlation between various soil properties and the rate constants for the pseudo-second-order (k) and Elovich (b) equations, plus the availability half-life derived from the natural exponential function;*

	k	***b***	***Half-life***
Organic carbon	0.71**	0.73**	-0.18
pH	-0.56*	-0.55*	0.71**
Fe	0.09	0.08	0.51*
Al	0.26	0.27	0.13
Mn	-0.30	-0.31	0.75**
Al + Fe	0.09	0.08	0.51*

**denotes significant relationship at α < 0.05, **denotes significant relationship at α < 0.01.*

Strong positive correlation (α < 0.01) is calculated between organic carbon (C_{org}) and k (r_s = 0.671, α < 0.01), which suggests that aging of Tc occurs more rapidly in soils of higher C_{org} Likewise, strong and negative correlation is calculated between C_{org} and B (r_s = 0.73, α < 0.01). Figure 4.9 illustrates the rate of aging across all 20 incubated soils after normalising C_{DGT} to day 3. Here, availability of Tc appears to decline faster in soils of higher C_{org}, in support of the correlation identified between k and C_{org}. The onset of the slow phase of aging in Figure 4.9 occurs after 25-100 days in soils of greater than 8% C_{org}, but for soils with less than 4% C_{org} this slow phase does not proceed until after at least 200-300 days aging. The observation that Tc ages faster in soils of higher C_{org} is supported by the work of Ewers and

Brown (2014), who reported that TFs in a peat soil declined much faster than in a loam soil, which suggested a more rapid rate of chemical reduction of Tc in the presence of C_{org}.

Correlation between C_{org} and the availability half-life is very weak however (r_s = -0.18). The absence of correlation between C_{org} and the availability half-life may be attributed to the fitting approach taken for the natural exponential function. This point is illustrated in Figure 4.10 using a soil of very low C_{org} (0.7%), F1-T, as an example. Function A has been fitted by minimising the sum of the squares, the approach taken for all the soils (Section 2.3.3), but the fitted function overestimates the rate of aging, yielding an unsuitably short half-life. Function B, meanwhile, has been fitted by fixing the value of the constant (C) to equal the measured C_{DGT} value at 549 days aging, and consequently seems to better model the rate of aging.

Table 4.5 reveals that soil pH is also found to correlate strongly with k (r_s = -0.56, $\alpha < 0.05$), b (r_s = 0.55, $\alpha < 0.05$) and the availability half-life (r_s = 0.71, $\alpha < 0.01$). The correlation suggests that Tc ages faster in soils with a lower pH. Figure 4.11 illustrates the aging of Tc in exclusively acidic (pH < 5.5) and alkaline (pH > 7) soils. Soils of pH 5.5 - 7 are omitted for clarity. In general, Tc appears to age faster within acidic soils, in particular over the first 50-100 days after spiking, in support of the relationships identified in Table 4.5. However, the three acidic soils in Figure 4.11 in which Tc ages the fastest (IH-W, DY-G and TK-G) are all characterised by a relatively high content of C_{org} (9.5, 11.4 and 6.3% respectively). If these soils are ignored, then it is impossible to discern any distinction in the rate of aging between acidic and alkaline soils, especially over longer periods of aging (> 100 days). Soils with higher contents of C_{org} are typically acidic due to the presence of humic and fulvic acids. On this evidence, it would appear that soil pH is insignificant in controlling the rate of Tc aging.

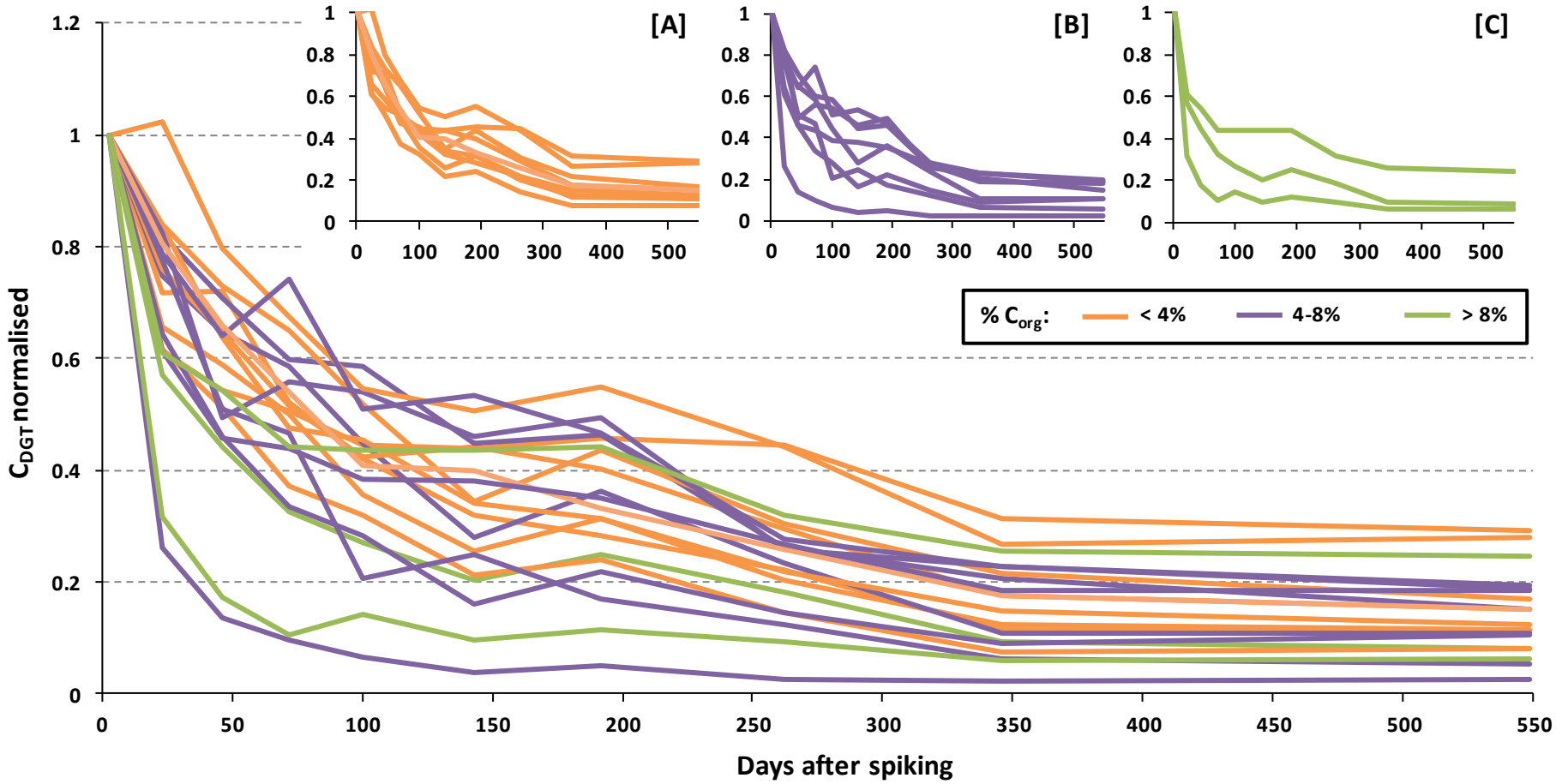

Figure 4.9. *DGT-measured concentration of Tc (C_{DGT}) in all 20 incubated soils after normalising to day 3. Soils are highlighted according to organic carbon (C_{org}) content. The three inset graphs exclusively highlight soils with an organic carbon content of < 4%* ***[A]****, 4 – 8%* ***[B]*** *and > 8%* ***[C].***

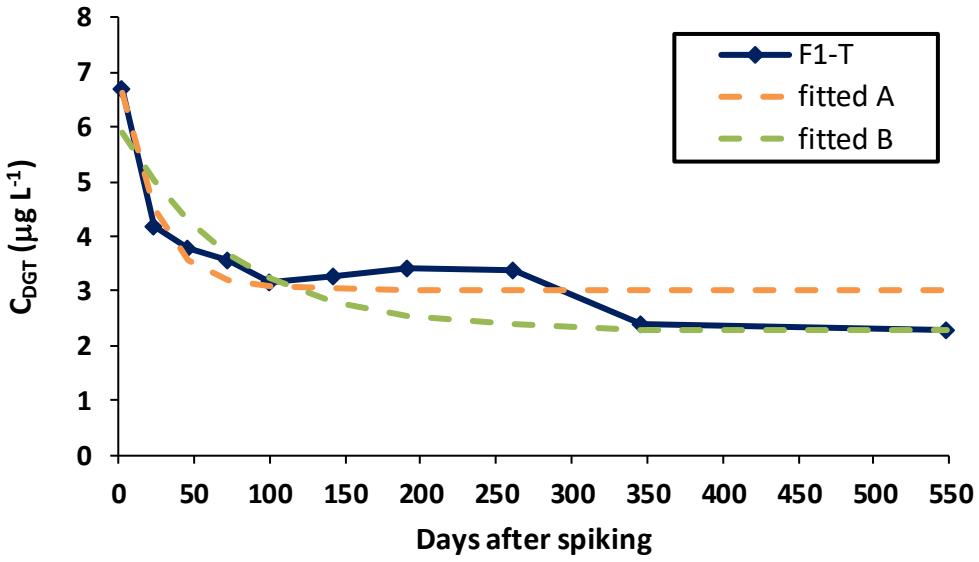

Figure 4.10. *Comparison of two natural exponential functions of the form $C_{DGT} = Ae^{-Bt} + C$ fitted to experimentally-acquired DGT data for soil F1-T. For function A, the value of the constant C is calculated using Microsoft Excel's SOLVER feature, whereas for function B the value of C is set to match the value for C_{DGT} at day 549.*

Table 4.5 also reveals strong correlation between the availability half-life and both Mn ($r_s = 0.75$, $\alpha < 0.01$) and Fe ($r_s = 0.51$, $\alpha < 0.05$). Figure 4.12 illustrates the relationship between the half-life and both Mn and Fe through scatter plots. The positive correlation suggests that Tc ages faster in soils characterised by a lower concentration of Fe and Mn oxides, rather than at higher concentrations as would be expected. No correlation was identified between C_{DGT} and either of these soil phases at any stage of the incubation (Table 4.4), so the relationship is again unexpected. The absence of any correlation between either k or b and both Fe or Mn would suggest that the correlation between the availability half-life and these phases should be treated with caution.

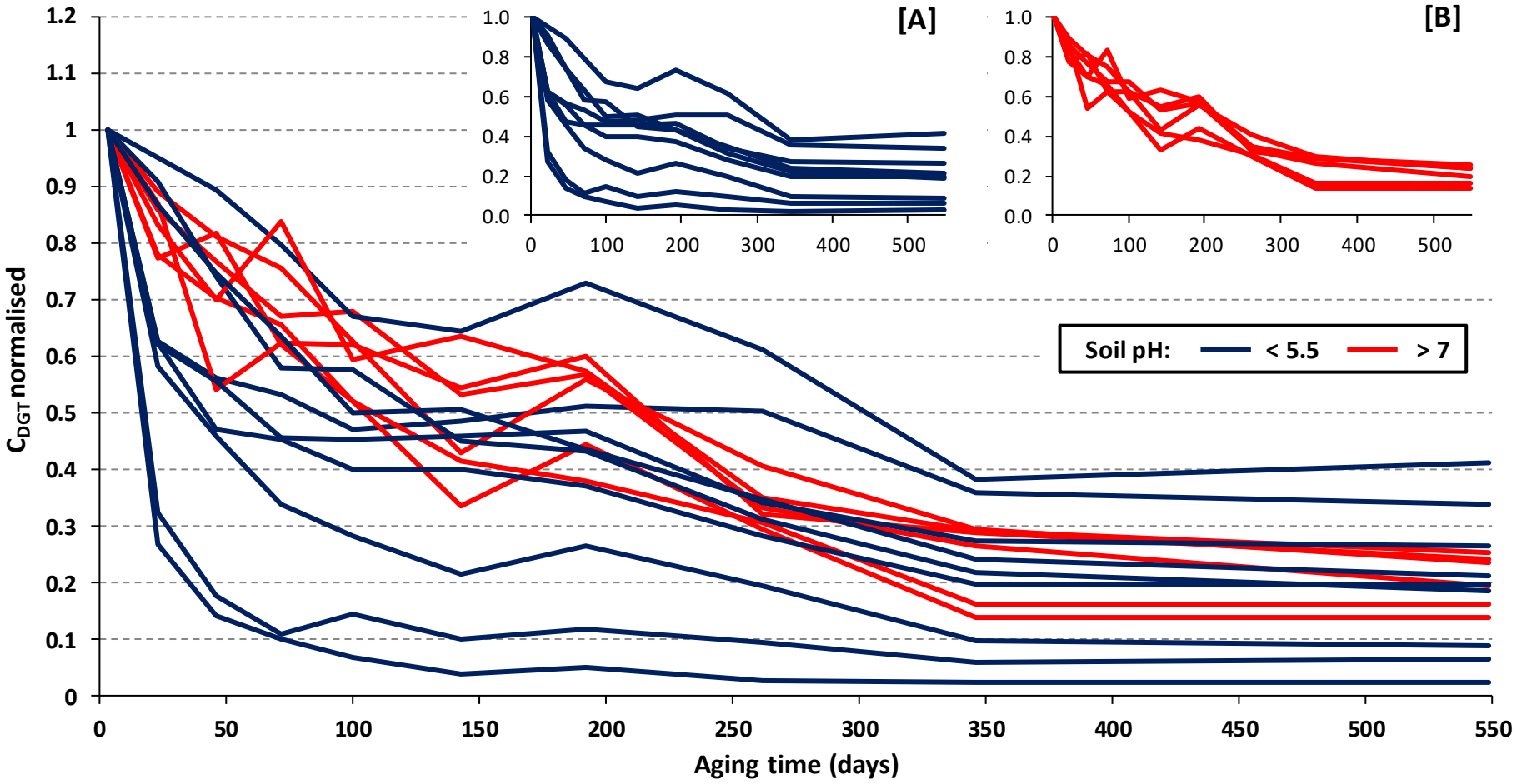

Figure 4.11. *DGT-measured concentration of Tc (C_{DGT}) in acidic (pH < 5.5) and alkaline (pH > 7) soils after normalising to day 3. The two inset graphs exclusively highlight soils with a pH of < 5.5* ***[A]*** *and > 7* ***[B]****.*

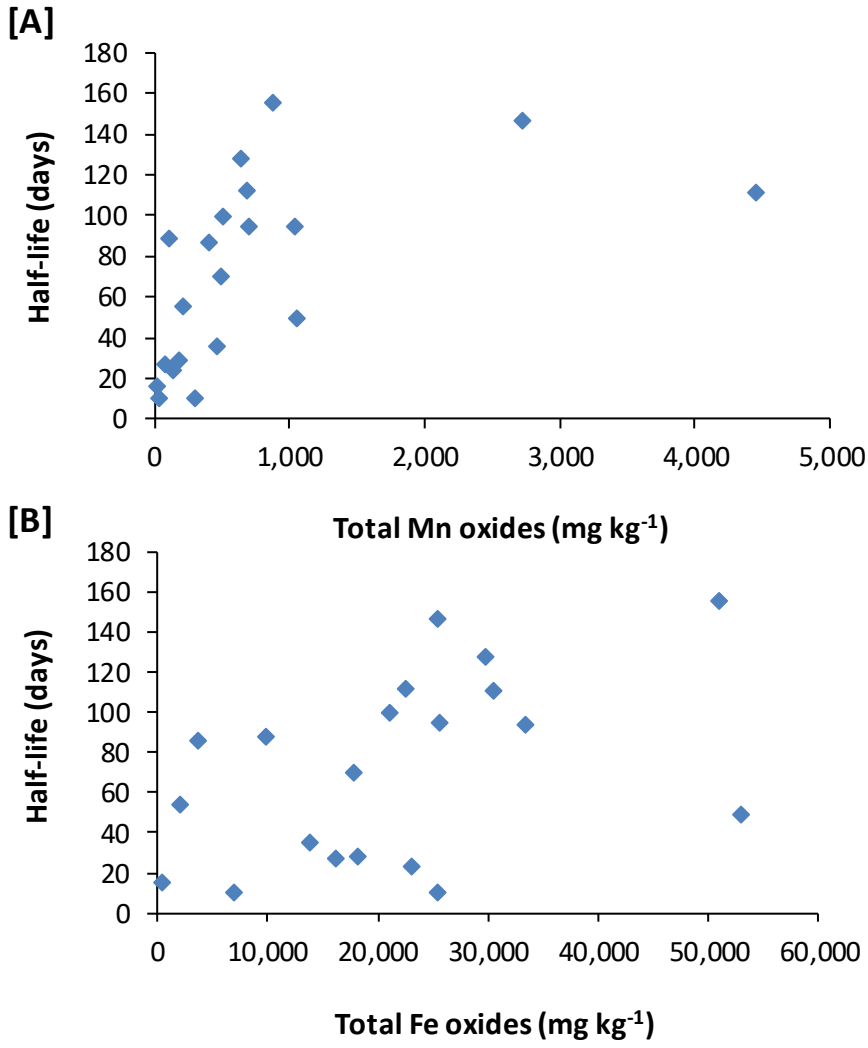

Figure 4.12. *Relationship between the availability half-life derived from the natural exponential function, and both total Mn* ***[A]*** *and Fe* ***[B]*** *oxides.*

4.2.3 Resupply of Tc from the soil solid phase

Figure 4.13 shows R values at the start (day 3) and end (day 549) of the incubation for all 20 soils. As detailed in Section 1.8, an R value expresses the ratio between the concentration of a species measured by DGT (C_{DGT}) and the concentration measured in the bulk soil solution (C_{soln}). As R increases, the capacity of the solid phase to resupply Tc to the soil solution in response to the DGT-induced depletion increases, and C_{soln} is more effectively buffered within the vicinity of the DGT device. Where resupply is absent, Tc supply to the DGT is confined to

diffusional transport, which is influenced by the soil porosity and tortuosity, and the R value is referred to as R_{diff}. Values of R_{diff} for all 20 soils are also plotted in Figure 4.13.

Figure 4.13 reveals that R values are low (< 0.15) across all soil types. For most of the soils, R values at day 3 were found to be comparable in magnitude to R_{diff} values, with R values in the remaining soils only marginally higher. No relationship was evident between any of the soil properties and the associated R values. Likewise, no relationship was identified between the soil properties and R-R_{diff}, which is used as a quantitative indicator of the ability of the soil to resupply Tc.

Such low values of R imply a kinetic limitation operating within the soils whereby resupply of Tc from the soil solid phase is kinetically constrained (Zhang et al., 1998) or the size of the labile pool on the solid phase (available to resupply Tc) is very small and close to zero. Some resupply may be occurring, but it is at a rate insufficient to sustain the soil solution concentration and satisfy the demands of the DGT. It seems likely that the solid phase pool of labile Tc is very small, which would imply that most of the Tc is still in solution or in less-labile forms.

A very low DGT response (i.e. a low R value) could also be explained by a significant fraction of Tc being present in the solution phase as colloidal material with an inherently large particle size exceeding the pore size of the polyacrylamide diffusive gel. The DGT diffusive gel layer employed in this work will only permit the free diffusion of inorganic labile species and Tc-organic complexes of lower molecular weight. Measurements of Tc in solution performed by centrifugation and filtration (C_{soln}) include colloidal species as the filter pore size is 0.45 µm, and so exceptionally low R values may arise where such colloidal species unavailable to DGT are incorporated in measurements of Tc in soil solution.

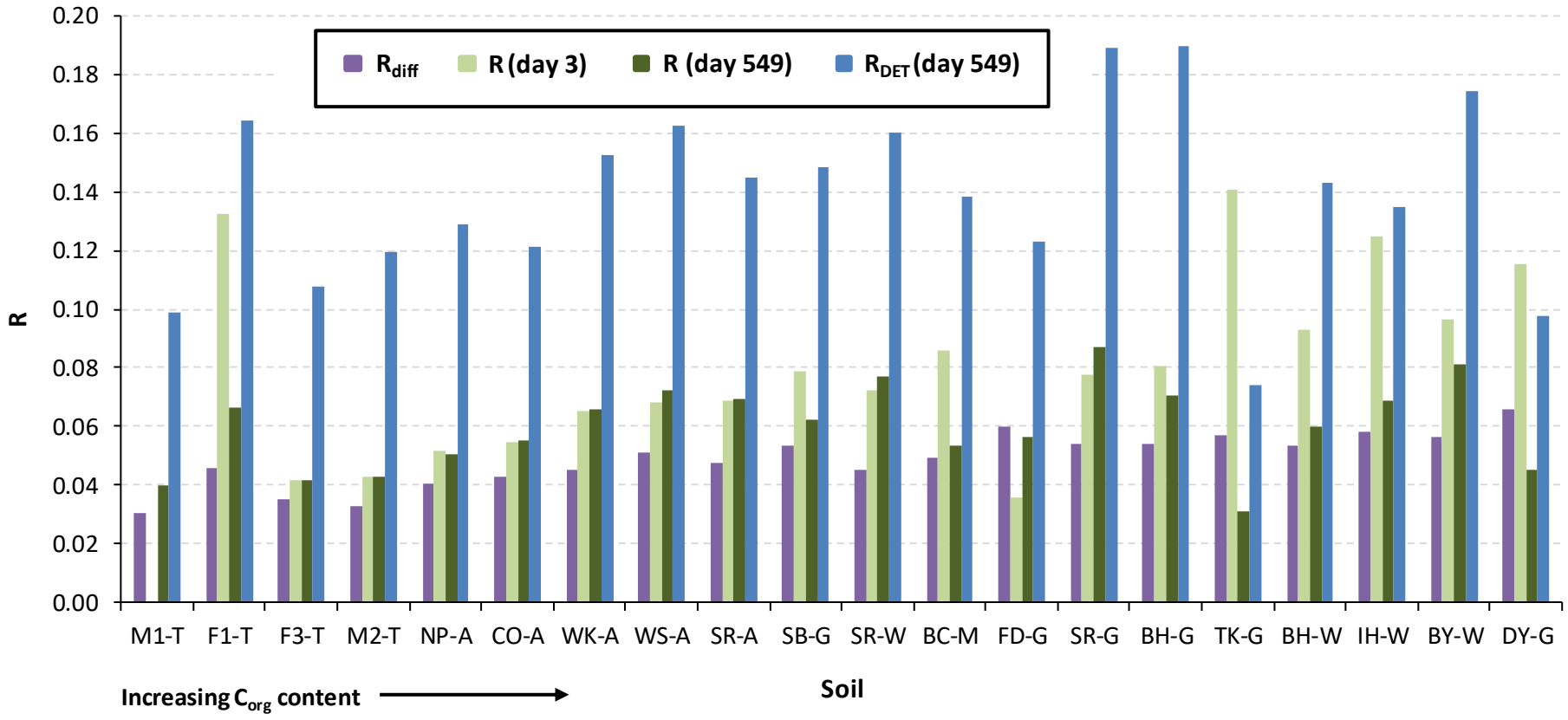

Figure 4.13. *R values at day 3 and 549 for all 20 incubated soils, in addition to the corresponding R_{diff} value for each soil. Also plotted are R values at day 549 using DET to determine Tc soil solution concentration. Soils are listed in order of increasing C_{org} content. No R (day 3) data for soil M1-T.*

Also plotted in Figure 5.13 are R values for day 549 calculated using DET (diffusive equilibrium in thin-films) to determine Tc in solution (R_{DET}) as opposed to via centrifugation (R). Across all soils, R_{DET} values were found to be between ~2 and 2.5 times greater than R values, which suggests that there may be a sizeable fraction of Tc associated with colloids in the size range ~100-450 nm.

Low R values can also be explained by a substantial fraction of Tc being present in solution in the form of inert organic complexes of high stability. DGT will discriminate between species on a kinetic basis since the resin is assumed to bind exclusively with the free metal ion. Therefore, only labile complexes that can dissociate within the timeframe (on the order of minutes) it takes for the species to be transported through the diffusive layer will be bound and measured. A way of investigating the Tc-humic complex lability would be to deploy DGT devices of increasing diffusion layer thickness so as to manipulate the time frame for dissociation (Scally et al., 2003). Such Tc complexes are reported to be of fairly low lability (Geraedts et al., 2002; Gu and Ruan, 2007), and therefore unlikely to dissociate rapidly enough to bind to the TEVA resin within the diffusion timeframe. Significantly, the absence of any correlation between $R\text{-}R_{diff}$ and C_{org} would suggest that Tc-humic complexes of high stability may not fully explain the low R values, since higher R values would be expected in soils with a low content of C_{org}.

Soil response times (T_c) (s) for all 20 soils after 549 days aging calculated using the 2D version of the DIFS (DGT-induced Fluxes in Soils/Sediments) model (Sochaczewski et al., 2007) are presented in Table 4.6, alongside the desorption rate constants (k_{-1}). Key input parameters for the model are described in Section 2.3.2.4, and the values listed in Appendix B.5. In brief, T_c integrates the capacity of labile Tc associated with the solid phase as well as its rate constant of release in response to localised depletion by DGT (Lehto et al., 2008).

Table 4.6. *Soil response times (T_c) plus sorption (k_1) and desorption rate constants (k_{-1}) for all 20 incubated soils after 549 days aging. Values were calculated using 2D-DIFS.*

Soil	T_c (s)	k_1 (s^{-1})	k_{-1} (s^{-1})
F1-T	16.88	0.04	0.01
WS-A	22.74	0.03	0.01
IH-W	6.96	0.10	0.04
M1-T	10.82	0.06	0.03
NP-A	10.92	0.05	0.03
SR-W	10.82	0.07	0.03
SB-G	12.31	0.06	0.02
TK-G	5.28	0.14	0.05
CO-A	7.48	0.06	0.07
FD-G	4.80	0.15	0.05
BH-W	15.00	0.04	0.02
DY-G	5.23	0.13	0.06
SR-A	15.79	0.04	0.02
M2-T	15.89	0.04	0.02
BH-G	20.36	0.04	0.01
WK-A	15.79	0.04	0.03
SR-G	17.78	0.04	0.02
F3-T	8.79	0.06	0.05
BC-M	8.41	0.09	0.03
BY-W	12.10	0.06	0.02

The response times presented in Table 4.6 are considerably shorter than those reported other trace metals in similar DGT/DIFS studies, which are typically on the order of several minutes or more (Ernstberger et al., 2002; Lehto et al., 2008). Such short response times would usually imply a fast rate of release of Tc from the soil, but in the soils of this study it seems that a very small labile pool of Tc is a more plausible explanation, especially given the low R values presented in Figure 4.13. No correlation could be identified between the response times or either rate constants and soil properties.

4.2.4 Effect of microbial activity and contrasting moisture regimes

The objectives of the experimental work discussed in this section are two-fold: firstly, to elucidate the significance that soil microbes play in the reduction of TcO_4^- to insoluble TcO_2 species, and secondly to investigate the effect that extensive drying of the soils in between saturation for DGT deployments has on the kinetics of Tc aging. Details relating to the secondary incubation approach can be found in Section 2.1.4. Figure 4.14 and Figure 4.15 reveal the effect of autoclaving and contrasting moisture regimes on C_{DGT} and C_{soln}, respectively, for Tc in four soils (BH-G, BY-W, SR-W and WK-A) over a 120-day incubation. In order to incorporate the data for C_{DGT} from the primary incubation (microbes/extensive drying), all C_{DGT} values were normalised relative to the first sampling point at day 2.

In general, it is difficult to identify any systematic trends between soils regarding the effect of the moisture regime or autoclaving on Tc availability. The trends observed for C_{DGT} in Figure 4.14 are replicated in Figure 4.15 for C_{soln}. The only soil in which autoclaving appears to have any clear effect on availability is WK-A, where availability is lower in samples subjected to autoclaving and availability declines at a faster rate. Subsamples which were incubated at a constant moisture show a good level of agreement in terms of Tc availability for all four soils minus WK-A, regardless of autoclaving. The only differences in Tc availability between the two moisture regimes are seen in soils BH-G and SR-W, where extensive drying appears to reduce availability and accelerate the aging of Tc. No obvious effect can be seen in soils BY-W and WK-A, however.

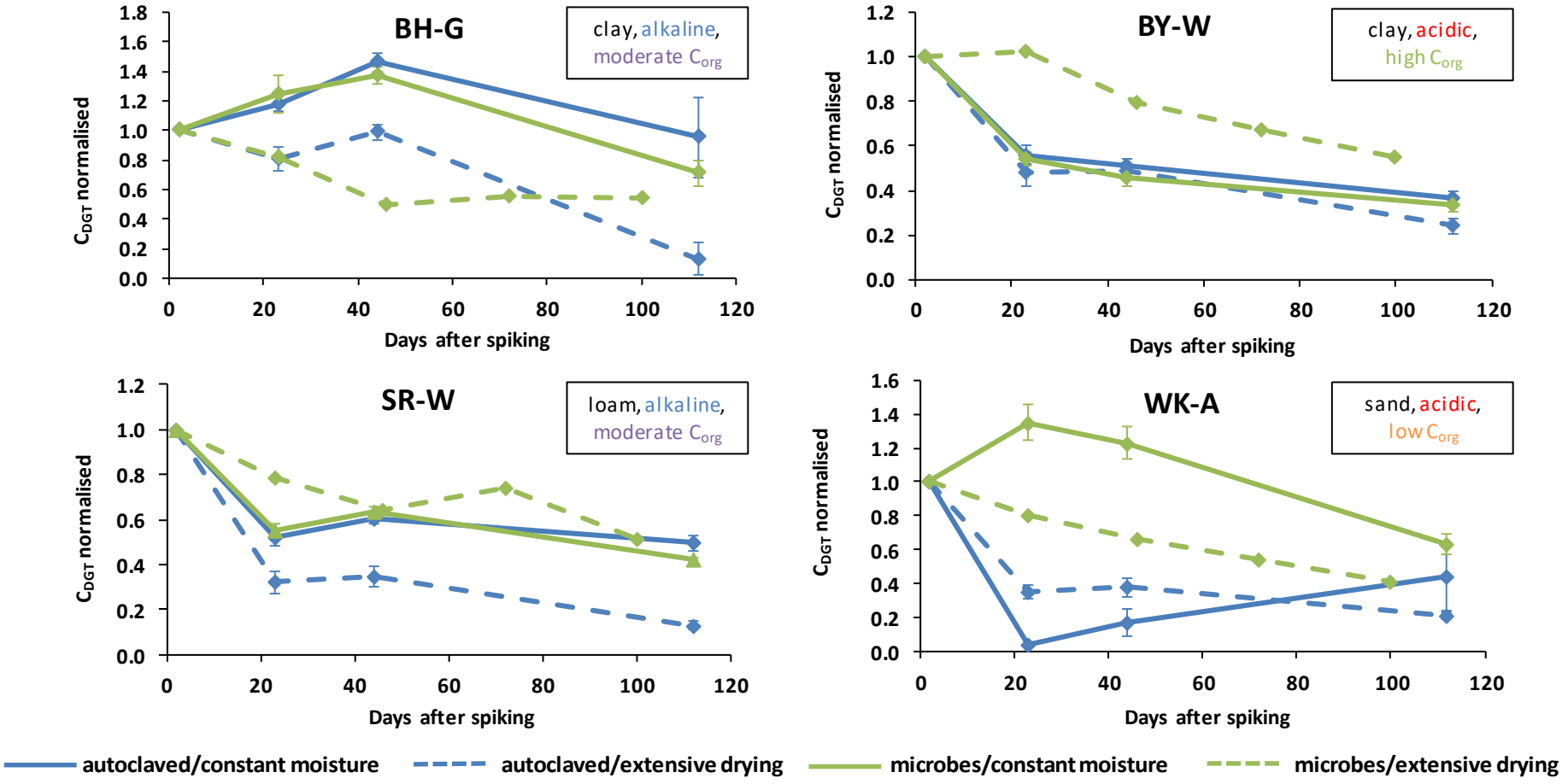

Figure 4.14. *C_{DGT} normalised to the first time point (day 2) in autoclaved and non-autoclaved (microbes present) subsamples of four different soils (BH-G, BY-W, SR-W and WK-A) incubated for 120 days at contrasting moisture regimes.*

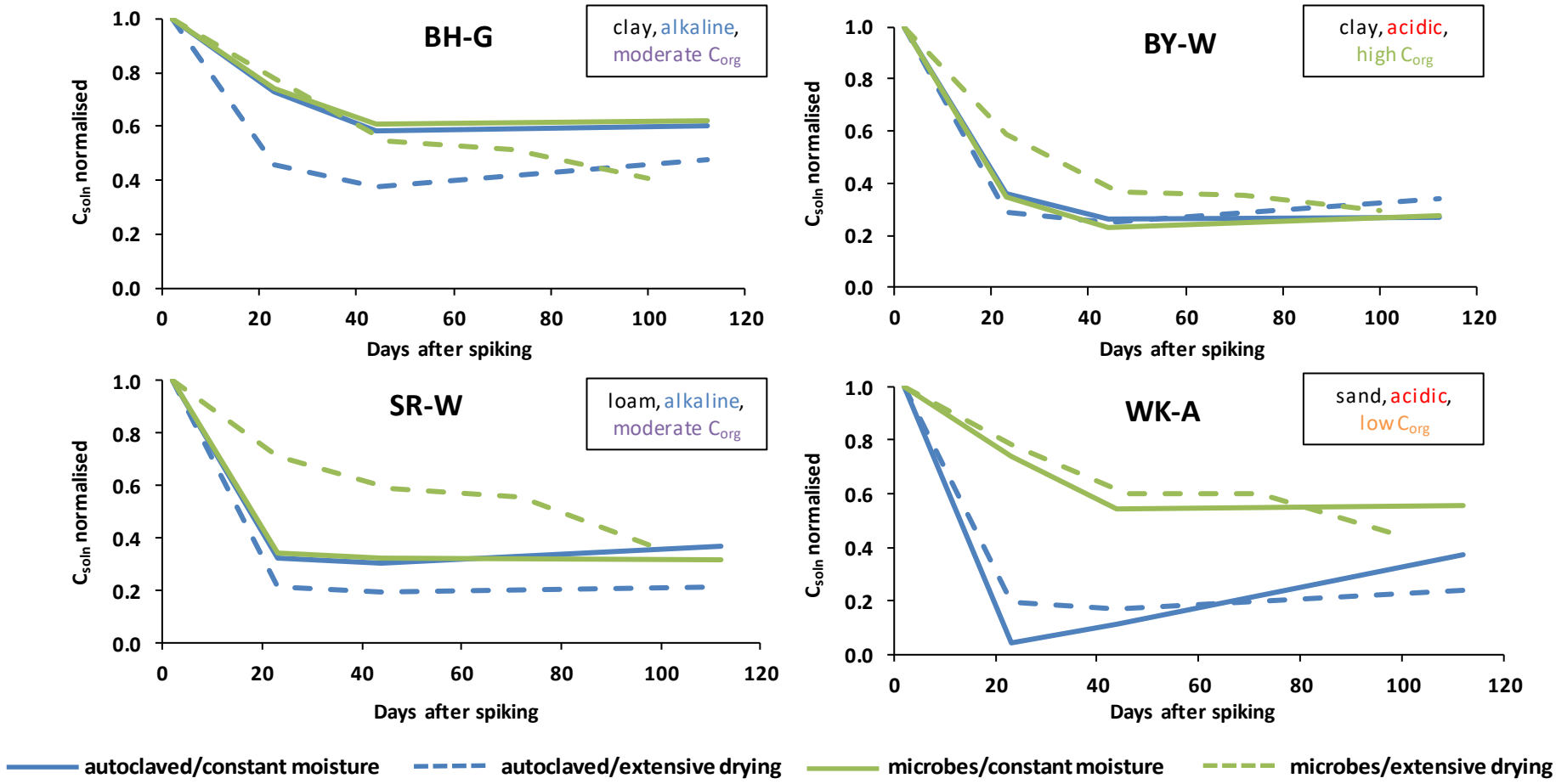

Figure 4.15. *Concentration of Tc measured in soil solution (C_{soln}) (µg L^{-1}) normalised to the first sampling point (day 2) in autoclaved and non-autoclaved (microbes present) subsamples of four different soils (BH-G, BY-W, SR-W and WK-A) incubated for 120 days at contrasting moisture regimes.*

Throughout the literature, a range of microbes, in particular Fe-reducing *Shewanella putrefaciens* and *Geobacter metallireducens*, have demonstrated the capacity to enzymatically reduce soluble Tc(VII) to sparingly-soluble hydrous $Tc(IV)O_2$ under anaerobic conditions (Lloyd and Macaskie, 1996; Lloyd et al., 1998; Lloyd et al., 2000). Data from the secondary incubation presented in Figure 4.14 and Figure 4.15 imply that the soil microbial community does not play a significant role in mediating the reduction of Tc(VII) to insoluble Tc(IV) under the conditions which the primary incubation was conducted. Should the microbes play a role in the reduction of Tc(VII), then we should expect to observe systematically higher values for C_{soln} and C_{DGT} in the autoclaved soil samples, yet this is not the case. Furthermore, C_{soln} within autoclaved soils is lower for three of the four soils investigated, an observation which again does not implicate the soil biota in the reduction of Tc(VII).

In light of the findings presented in Figure 4.14 and Figure 4.15 that the rate of aging of Tc within autoclaved soils is not dissimilar to aging within non-autoclaved soils, and given the preceding discussion concerning the significance of microbes in mediating the reduction of Tc, the efficiency of the autoclaving procedure in sterilising the soils should be questioned. A straightforward test to verify the sterility should have been performed whereby a small aliquot of soil prepared in a sterile saline dilution is incubated on nutrient agar for several days to monitor for the growth of colony forming units (Trevors, 1996). In hindsight, to allow for maximum penetration of steam throughout the soil, a more effective approach may have been to spread the soil out in a thinner layer in a tray as opposed to filling a glass Duran bottle.

It is also important to consider the potential alteration to the soil's physical and chemical structure as a result of autoclaving. Autoclaving is a frequently used method of soil sterilisation, but changes to the chemical structure of soil organic matter and/or the physical structure of soil particles and aggregates could cause additional unwanted effects, making biotic and abiotic processes harder to distinguish. For example, Berns et al. (2008) observed

that autoclaving yielded an increase by over an order of magnitude in the dissolved organic carbon (DOC) fraction, with up to 11% of the C_{org} solubilised in one soil. At the same time, an increase in the surface area of the clay fraction was observed due to disaggregation. Autoclaving is also recognised to release ammonium-N and amino acids (Alef and Nannipieri, 1995).

Soil undergoes a plethora of interrelated physical, chemical and biological changes associated with drying and subsequent re-wetting (Soulides and Allison, 1961; Utomo and Dexter, 1982). In the context of the data derived from the secondary incubation, it is the impact that extensive drying between re-wetting events has on the availability of Tc which is most important to consider, since all the soils are subjected to re-wetting. The effect of wet-dry (WD) cycles on the OM structure is likely to be the key consideration here since C_{org} is observed to be the dominant property controlling Tc availability. Generally, an increase in dissolved organic carbon (DOC) with soil drying is reported (Sorensen, 1974; Denef et al., 2001), primarily as a result of microbial cell lysis induced by osmotic shock upon re-wetting the dried soils (Kieft et al., 1987; Zsolnay et al., 1999). The release of protected organic matter by disruption of macroaggregates during rewetting may also contribute (Denef et al., 2001).

A number of studies have demonstrated that the availability of organic compounds aged within soils subject to WD cycles is lower than for soils aged at a constant moisture (Shelton et al., 1995; White et al., 1998; Kottler et al., 2001). The shrinking and expansion of organic matter induced by drying and re-wetting the soil is speculated to facilitate the migration of such compounds into highly inaccessible sites within the soil (White et al., 1998), whilst the drying could expose binding sites associated with the OM that were previously inaccessible (Shelton and Parkin, 1991). Data from soil BY-W with the highest C_{org} content (11.6%) of the four incubated soils would suggest that such processes associated with C_{org} do not facilitate

the aging of Tc since an almost identical rate of aging is observed between subsamples of both moisture regimes.

Several studies have investigated the immobilisation and re-oxidation of Tc in soils which have been flooded to induce anoxia and then restored to aerobic conditions (Tagami and Uchida, 1999; Ashworth and Shaw, 2005; Haudin et al., 2011). The mechanisms operating in such soils may not be directly relatable to those occurring in the incubated soils of this study since the soils here were not saturated for long enough to establish fully anoxic conditions. In any case, it is the extent of drying on Tc availability which is the key factor here, something which these studies do not address. Although not concerned with Tc, perhaps the most relevant study to aid in understanding of the data acquired here is that of Li et al. (2015), who used DGT to investigate metal availability in two soils subject to two different moisture regimes. In the calcareous soil, the availabilities of Cd and Zn after two cycles of wetting and moderate drying from saturated conditions to 50% of the MWHC were found to be less than half of what they were in the same soil that underwent severe drying to 30% MWHC. No such effect on availability was seen for Cu and Ni however, and the same trend for Cd and Zn was not observed in the acidic soil. No explanation was offered by Li et al. (2015) as to why availability was lower in soil that underwent moderate drying, and this observation is the inverse to what is presented in Figure 4.14 and Figure 4.15 where availability is lower after more severe drying.

Assuming that the soils in this study were effectively sterilised after autoclaving, the lower availability of Tc cannot be explained in terms of the effect of microbial activity, but a concomitant increase in DOC accompanying microbial death as a result of autoclaving may facilitate the removal of Tc from solution. Alternatively, Tc may be partitioned into less accessible sites within the soil that were exposed upon drying. Cyclic wetting and drying of soil has been to shown to cause a shrinkage and swelling of the structure which may facilitate

such partitioning (Makeyeva, 1989), but a more detailed understanding of the size fractionation and mineralogy of the soils is needed to explore this hypothesis further.

4.3 Conclusions

The data presented in this chapter highlight the interaction of Tc with C_{org} as being instrumental in governing the availability and rate of aging of Tc in soils. Soil pH and the total Al oxide content are also observed to exert an influence on availability, but these are secondary to C_{org}.

Conflicting evidence is presented regarding the reduction of Tc(VII) to less available Tc(IV) however, which, based upon work reported from other studies, is presumed to be a prerequisite for binding with soil humic substances. Localised anaerobic conditions established through microbial activity, enhanced in the presence of higher concentrations of OM, would appear to promote this reduction, in combination with direct biological reduction in soils of higher OM content. In contrast, data attained from the autoclaved soils in the secondary incubation suggest that microbes are not responsible in driving the reduction of Tc(VII) however, where the aging of Tc occurs at an almost identical rate within both autoclaved and non-autoclaved subsamples. Furthermore, appreciable aging of Tc is still observed in autoclaved and thoroughly-dried soil samples assumed to be fully oxic, which hints at alternative reduction mechanisms. The reproducibility of such observations recorded from the secondary incubation should be explored however, in particular with regard to the effect of biological sterilisation on Tc availability and the efficiency of the autoclaving process, before disregarding the role of microbial activity in controlling Tc availability and aging.

The kinetics of aging of Tc across throughout the range of soils can best described by a natural exponential function, however the simplified Elovich and pseudo-second-order equations

provide similarly good fits to the experimental data. Based on the derived aging rate constants, C_{org} is implicated as the most important soil property in controlling the rate of Tc aging, where aging is accelerated in soils of increasing C_{org}. Availability half-lives derived from the natural exponential function range from 10 to 156 days, with a median and mean of 78 and 72 ± 56 days respectively. However, it seems that fitting the function by minimising the sum of the squares is not suitable for every soil, where the function fails to suitably model the aging trend in certain soils.

Resupply of available Tc from the solid phase was found to be minimal across all soil types after both short and longer periods of aging, which suggests that the solid phase pool of available Tc is very small since most of the Tc is still in solution or in less-labile forms. After 549 days aging, at least half of the Tc in solution was found to be in a colloidal form unavailable to DGT. No correlation was evident however between R_{DET} - R_{diff} and C_{org}, which would appear to rule out non-labile Tc-humic substance complexes in reducing the availability of Tc. The nature of this colloidal matter should be further investigated.

Finally, the extent to which the soil is allowed to dry out between DGT deployments does not induce a systematic effect in terms of the kinetics of Tc aging across a range of soil types. However, enhanced aging within both calcareous soils may be related to partitioning within less accessible binding sites exposed upon cyclical extensive drying.

Chapter 5: Availability and aging of selenium-79 within spiked soils

5.1 Introduction

As a constituent of spent nuclear fuel, the fission product selenium-79 represents an important component of safety assessments informing the case for geological disposal of nuclear waste owing to its long half-life (~3.5 x 10^5 years) and high environmental mobility. As reviewed in Section 1.2.1, the speciation of Se in soils under oxidising conditions is dominated by the oxyanions selenate (SeO_4^{2-}) and selenite (SeO_3^{2-}), with selenate being more bioavailable for plant uptake due to its inferior adsorption affinity for the soil matrix than selenite (Goh and Lim, 2004).

Much of our current understanding of Se availability in soils is derived from plant uptake studies (Munier-Lamy et al., 2007; Kikkert et al., 2013). A standard extraction method for assessing the plant-available fraction of Se in soils has yet to be established. Soluble Se is often extracted using KCl solution (Gao et al., 2000) or deionized water (Zhang and Frankenberger, 2003), whilst exchangeable Se is commonly quantified using a phosphate-based extractant (Wang et al., 2012; Liu et al., 2015), since both Se and phosphate are understood to share the same primary adsorption mechanism of ligand exchange.

Application of DGT to investigate Se availability is confined to a single study by Sogn et al. (2008), who measured availability in a loam at two different pH levels (5.5 and 6.0) and four mineral Se fertilization levels. Measured masses of Se by DGT were found to be close to the analytical detection limit, whilst significantly enhanced DGT-measured Se concentrations were found only for the highest input of Se at pH 5.5. Based upon the experimental work

presented in Chapter 3, impaired performance of the mixed binding layer can be expected in calcareous soils with a pH greater than 7.0.

At the time of writing, only a handful of studies investigating the aging of Se with respect to its fractionation and availability in soil over timeframes of several months or more could be found in the published literature (Tolu et al., 2014; Di Tullo et al., 2016; Li et al., 2016). In the first of these studies, Tolu et al. (2014) reported that the soil/liquid distribution (K_D) of Se did not reach a steady state until at least one month following application of Se to a woodland and agricultural soil. In the study by Li et al. (2016), aging of Se was assessed over a 100-day incubation period by combining a sequential extraction approach with measuring uptake by pak choi (*Brassica chinensis* L.). A rapid decrease in availability over the first 42 days was reported, followed by a slow decline thereafter. Finally, Di Tullo et al. (2016) conducted a two-year field study comprising a forest, agricultural and grassland soil, each of which were extracted in parallel to investigate the kinetics of transformations in the speciation of the spiked stable selenite tracer. Their work found that aging was controlled by a combination of chemical and diffusion-controlled processes, and forecast that it would take up to several decades for the solid phase distribution of the added selenite tracer to equilibrate with the naturally present Se.

The objective of the work presented in this chapter was to build on the existing limited knowledge base in the scientific literature concerning the availability and aging of Se within different soil types and explore new insights that DGT may offer into the longer-term availability and aging of Se. The approach is centred on an 18-month incubation of 20 different soils that were subjected to a series of DGT deployments at progressively increasing time intervals, as described in Section 2.1.3. Three kinetic models (pseudo-second-order, Elovich and parabolic diffusion) plus a natural exponential function were fitted to the DGT dataset to provide a quantitative analysis of the data (Section 2.3.3). In addition to the primary

incubation, a secondary incubation was set up to investigate the effects of microbial activity on Se availability and aging, as well as the impact of different moisture regimes during the incubation period (Section 2.1.4)

5.2 Results and discussion

In this section, the availability and aging of Se are assessed through two datasets derived from the primary incubation: firstly, the concentration of Se measured in soil solution (C_{soln}), and secondly the DGT-measured concentrations (C_{DGT}). A quantitative assessment of the aging processes is made by fitting a handful of kinetic models to the DGT dataset. The solid phase resupply of Se is then addressed by examining R values in combination with soil response times calculated through the 2D-DIFS model. Lastly, data from the secondary incubation investigating the effect of microbial activity and the moisture regime on the availability of Se are presented.

5.2.1 Availability and aging assessed by soil solution measurements

5.2.1.1 Aging process and kinetics

Figure 5.1 shows the concentration of Se measured in the soil solution (C_{soln}) for all 20 soils over the course of the 549-day incubation period after normalising C_{soln} to the first measurement for C_{soln} made at day 3. Measured values of C_{soln} expressed per litre of soil solution (µg L^{-1}) have been converted to concentrations expressed per kg of air-dry soil (µg kg^{-1}), and subsequently normalised to account for the cumulative depletion of the Se spike from the soil associated with DGT deployments and extraction of the soil solution (Section 2.3.2.3). The data in Appendix C.2 demonstrate that prior to the final DGT deployment at 549 days aging, the mass of the Se spike removed from the soil ranged from 4 to 18%, with a mean and median of 9 and 7% respectively.

Figure 5.1 reveals, in general, a biphasic trend of Se removal from solution whereby removal occurs most rapidly over the first 75-200 days, followed by a much slower phase of removal. Soil BY-W is an exception to this trend, as C_{soln} does not appear to decrease over the course of the incubation period. Excluding soils BY-W, BC-M and IH-W, at least half of the Se has been removed from solution after ~170 days. After 549 days aging across the range of soils, C_{soln} is between 0.69 and 109% of the concentration measured at day 3, with a mean and median of 18 and 12% respectively (excluding BY-W).

The rate of decline in C_{soln} for Se presented in Figure 5.1 is considerably slower than reported elsewhere, even for soils of comparable properties. For example, Li et al. (2010) investigated the removal of Se from solution in an acidic soil of low C_{org} after Se had been applied as either selenate or selenite, and found that after only nine days ~50 and 3% of these species, respectively, remained in solution. Furthermore, Tolu et al. (2014) observed the water-soluble fraction of added Se(IV) in an agricultural and forest soil to decline exponentially before reaching a steady state after only 21-25 days. The reason for the faster rate of aging observed in these studies is not immediately clear, although the cooler temperature of the primary incubation in this study (10-15°C) may contribute to some degree by retarding physico-chemical and biological activity in the soils.

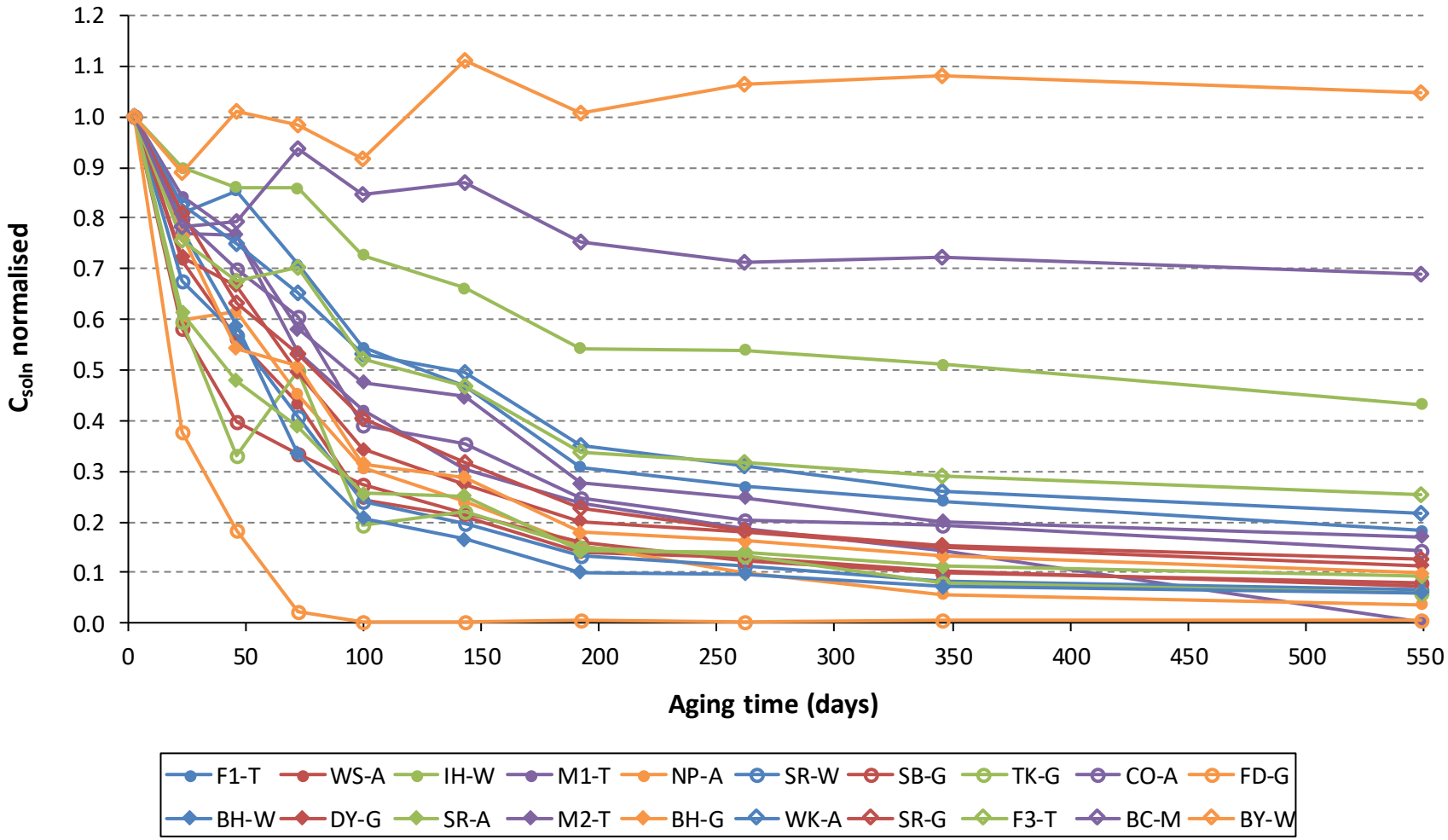

Figure 5.1. *Concentration of Se measured in the soil solution (C_{soln}) for all 20 soils over 549 days aging after normalising to day 3.*

5.2.1.2 Effect of soil properties on availability

Spearman's rank correlation coefficients (r_s) describing the correlation between C_{soln} and soil properties after 3, 100 and 549 days aging are listed in Table 5.1. After three days aging, C_{soln} is found to be strongly and positively correlated with soil pH ($r_s = 0.58$, $\alpha < 0.01$), Fe ($r_s = 0.47$, $\alpha < 0.05$) and Mn ($r_s = 0.63$, $\alpha < 0.01$). After 100 days aging, strong negative correlation with C_{org} ($r_s = -0.47$, $\alpha < 0.05$) emerges, whilst the strong positive correlation with pH that was present at day 3 disappears. Moderate negative correlation is calculated between C_{soln} and Al ($r_s = -0.37$). After 549 days, all measured soil properties were found to exhibit moderate negative correlation with C_{soln}.

Table 5.1. *Spearman's rank correlation coefficients (r_s) relating C_{soln} to soil properties after 3, 100 and 549 days aging (N = 20).*

	Days of aging		
	3	**100**	**549**
Organic carbon	0.00	-0.47*	-0.30
pH	0.58**	0.03	-0.39
Fe	0.47*	-0.18	-0.32
Al	0.27	-0.37	-0.37
Mn	0.63**	-0.05	-0.32
Total Al + Fe	0.47*	-0.18	-0.32

**Indicates significant relationship at α < 0.05; **Indicates significant relationship at α < 0.01*

The first notable observation from Table 5.1 is that no single soil property appears to be dominant in driving aging of Se. The positive nature of the correlation observed with C_{soln} for Fe, Al and Mn at day 3 implies that none of these oxides are responsible for the removal of Se from solution. The strong positive correlation between C_{soln} and pH at day 3 tells us that that greater removal of Se from solution occurs in soils of increasing acidity. Adsorption of negatively-charged selenite and selenate species is expected to be greater in acidic soils where the variably-charged mineral surfaces become protonated to yield a net positive charge (Yu,

1997). However, based on the data presented in Table 5.1 for day 3, it would appear that neither C_{org} or oxides of Al, Mn or Fe are important adsorbent phases for Se across the range of incubated soils. This could implicate clay minerals such as kaolinite and montmorillonite, which have previously been demonstrated as adsorbents for Se (Bar-Yosef and Meek, 1987).

Deprotonation of variably-charged mineral surfaces at higher pH will yield a net negative charge, so such soils may therefore exhibit poor retention of Se (high C_{soln}) despite a high content of Al and Fe oxides. Commonly-encountered Fe oxides in soil such as goethite, ferrihydrite and hematite exhibit points of zero charge (pzc) in the range 7.5 to 9.5 (Sparks, 2003). Oxides of Al have pzc values in a similar range, although values as low as 5.1 are reported for allophane. The correlation between C_{soln} and Fe was recalculated after omitting soils with a pH above 7.5, but this did not yield an improvement in the strength of the correlation between C_{soln} and Fe. Similarly, correlation between C_{soln} and Al was recalculated after omitting soils with a pH in excess of 5.1, with no improvement in the strength of the correlation reported either.

Figure 5.2 illustrates the relationship between C_{org} and C_{soln} over the duration of the incubation. No correlation was calculated between C_{org} and C_{soln} at day 3 in Table 5.1, yet in Figure 5.2 greater removal of Se from solution appears to have occurred in soils of higher C_{org} content. After only three days aging, the difference between the lowest and highest values for C_{soln} in soils of contrasting C_{org} content is around a factor of 10, but this diminishes over time such that after 549 days aging the difference is around a factor of two. The importance of C_{org} in governing the adsorption and availability of Se is supported by a number of studies (Johnsson, 1991; Kang et al., 1993; Seby et al., 1997; Coppin et al., 2009; Dhillon et al., 2010).

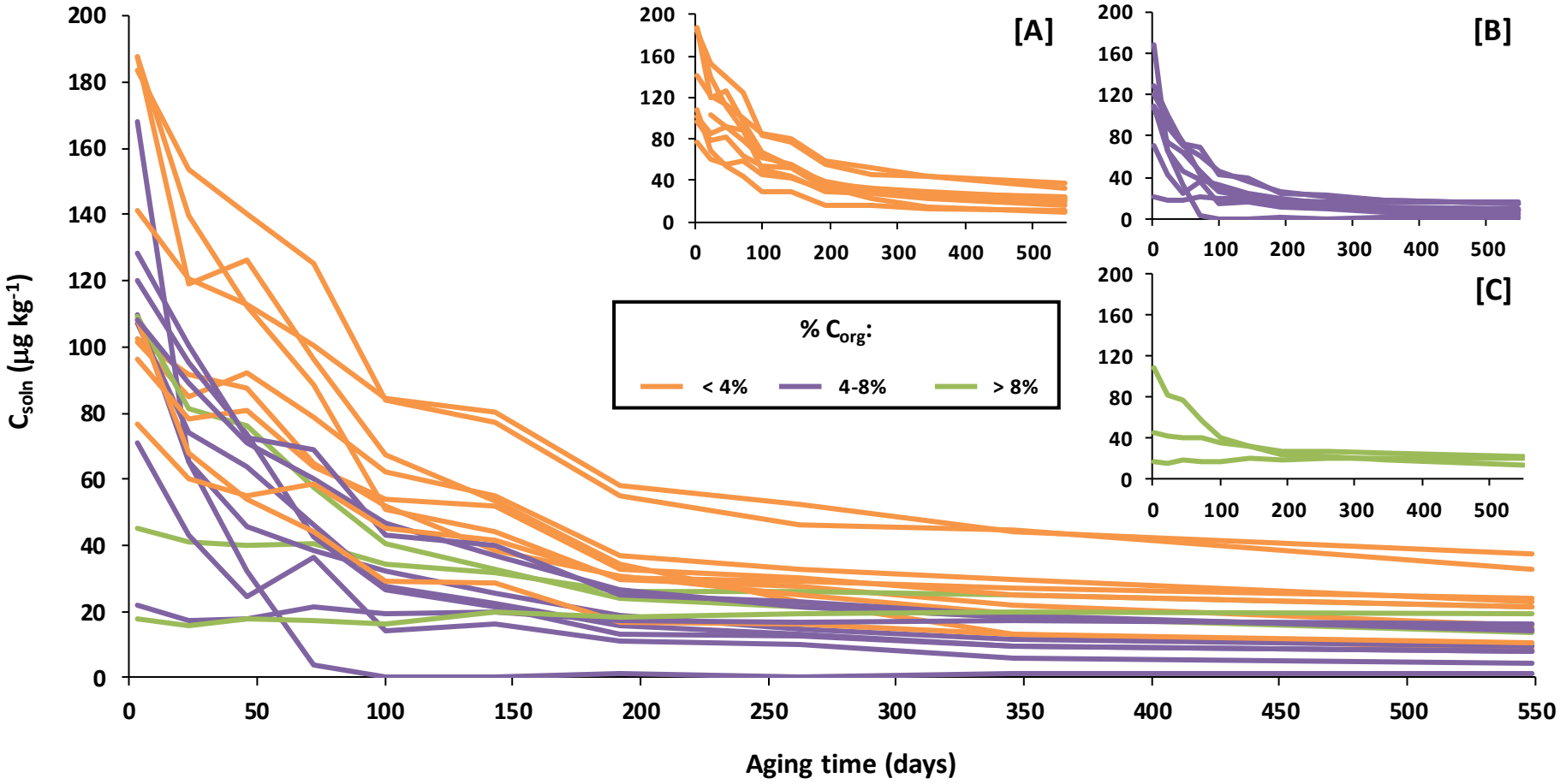

Figure 5.2. *Concentration of Se in soil solution (C_{soln}) (µg L^{-1}) in all 20 soils over 549 days of aging. Soils are highlighted according to organic carbon (C_{org}) content. The three inset graphs exclusively highlight soils of < 4%* ***[A]****, 4 - 8%* ***[B]*** *and > 8%* ***[C]*** *organic carbon.*

5.2.1.3 Effect of soil properties on aging kinetics

In Figure 5.3, all 20 incubated soils are highlighted according to their C_{org} after normalising C_{soln} values to day 3. With the exception of the three outlying soils (BY-W, BC-M and IH-W) with relatively high C_{org} that exhibit the slowest rate of decline in C_{soln}, aging of Se broadly occurs at a faster rate in soils of higher C_{org}. These outlying soils BY-W, BC-M and IH-W are misleading in that they exhibit the lowest values of C_{soln} at day 3 in comparison to all the other soils, which would suggest an initial rapid removal of Se from solution within the first three days after spiking. This is reflected in Figure 5.2 where a range of values for C_{soln} spanning a factor of ~10 can be seen. Correlation between C_{soln} and C_{org} after three days aging was calculated to be virtually absent however (Table 5.1), which would imply that C_{org} plays no role in the initial removal of Se from solution.

Figure 5.4 shows the aging trends for Se within all 20 incubated soils after highlighting the soils according to their Al content. In addition to C_{org}, total soil Al was found to exhibit a moderate degree of negative correlation with C_{soln} after 100 and 549 days aging (Table 5.1). In Figure 5.4, removal of Se from solution over time appears to occur more rapidly in soils characterised by a higher content of Al. The trend is masked to a degree by the three outlying soils (BY-W, BC-M and IH-W) of high Al content, but as previously discussed these three soils had aged substantially within three days of spiking so their inclusion in Figure 5.4 is misleading.

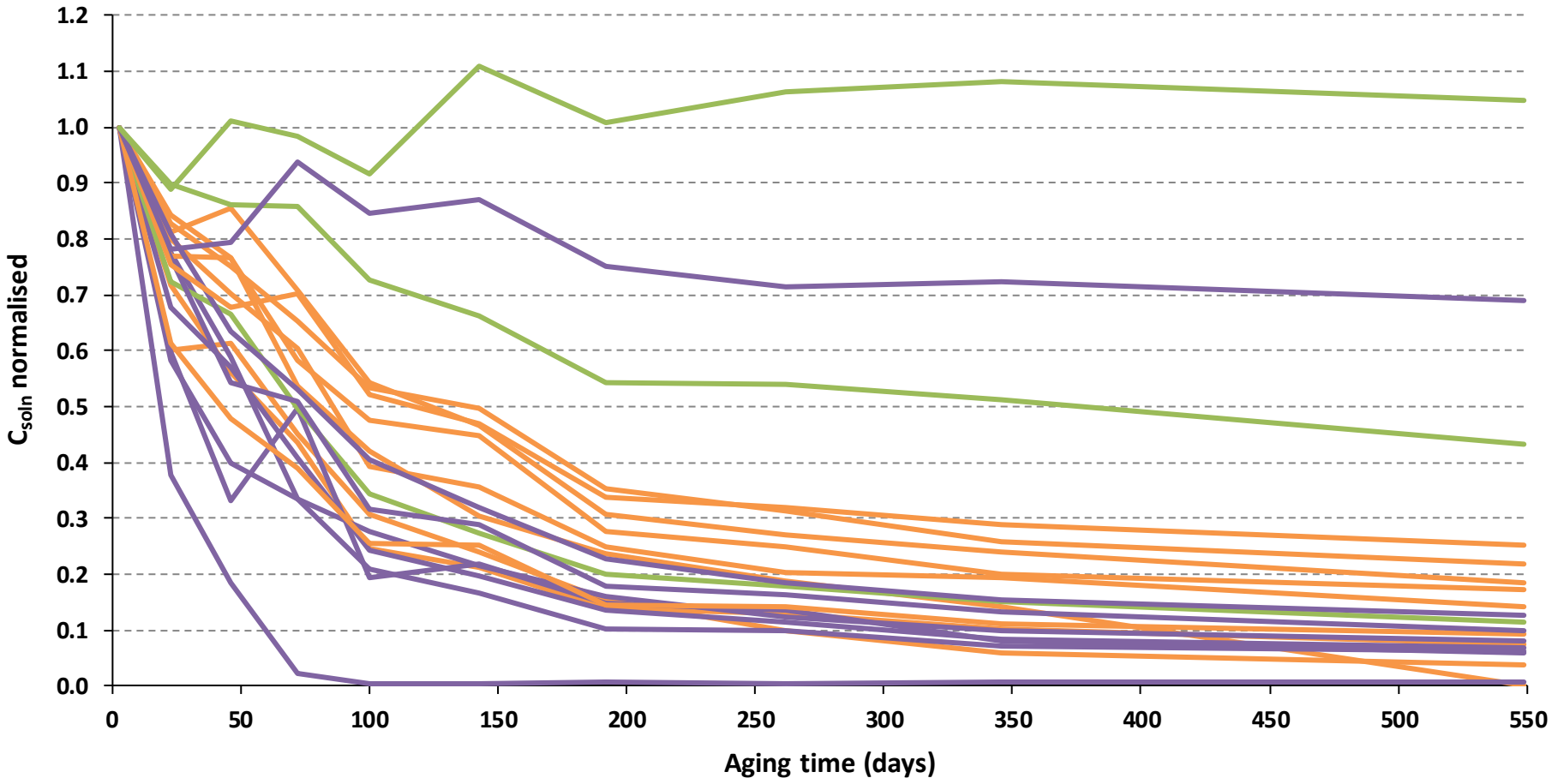

Figure 5.3. *Concentration of Se in the soil solution (C_{soln}) for all 20 soils over 549 days aging after normalising to day 3. Soils are highlighted according to organic carbon (C_{org}) content.*

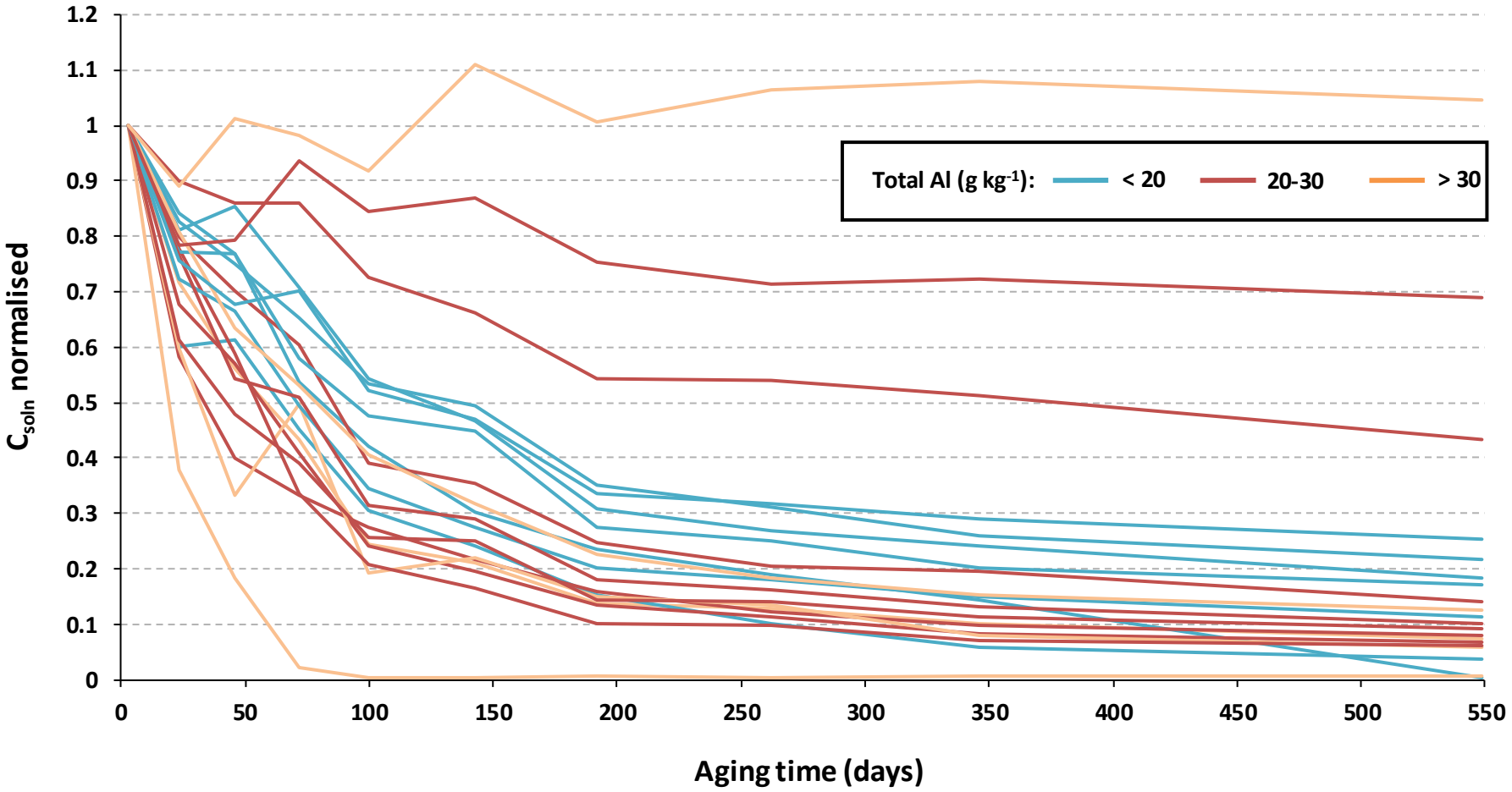

Figure 5.4. *Concentration of Se in the soil solution (C_{soln}) for all 20 soils over 549 days aging after normalising to day 3. Soils are highlighted according to total Al oxide content.*

Initially, after just three days aging, correlation with C_{soln} for Fe, Al and Mn was found to be positive. This observation is unexpected in that it does not implicate any of these oxides in the removal of Se from solution. In contrast, Tolu et al. (2014) speculate that adsorption to oxides and clay mineral phases initially governs this removal from solution. Only after longer periods of aging (≥ 100 days) does negative correlation with C_{soln} emerge for C_{org} and Al, although neither C_{org} or Al would appear to individually govern the removal of Se from solution. Organic matter may adsorb to inorganic phases in the soils which will modify the surface reactivity of Al and Fe oxides, therefore convoluting any correlation which may exist directly between C_{soln} and Al, Fe or Mn.

5.2.2 Availability and aging assessed by DGT

5.2.2.1 Aging process and kinetics

Presented in Figure 5.5 are the DGT-measured concentrations of Se (C_{DGT}) within all 20 incubated soils throughout the primary incubation after normalising C_{DGT} to the first measurement for C_{DGT} made at day 3. Values for C_{DGT} were initially corrected to account for the cumulative depletion of the Se spike from the soil (Section 2.3.2.3). In general, availability declines in a biphasic manner similar to that observed for C_{soln} in Figure 5.1, although the aging curves for C_{DGT} are more saw-toothed in their trend. The fastest rate of aging is seen over the first ~150 days, at which point availability of Se in all the soils is ≤ 60% of the availability at day 3. Beyond 150 days, the rate of aging plateaus, and after 549 days the availability of Se across all 20 soils ranges from 2 to 100% of the availability at day 3, with a mean and median of 27 and 21%, respectively.

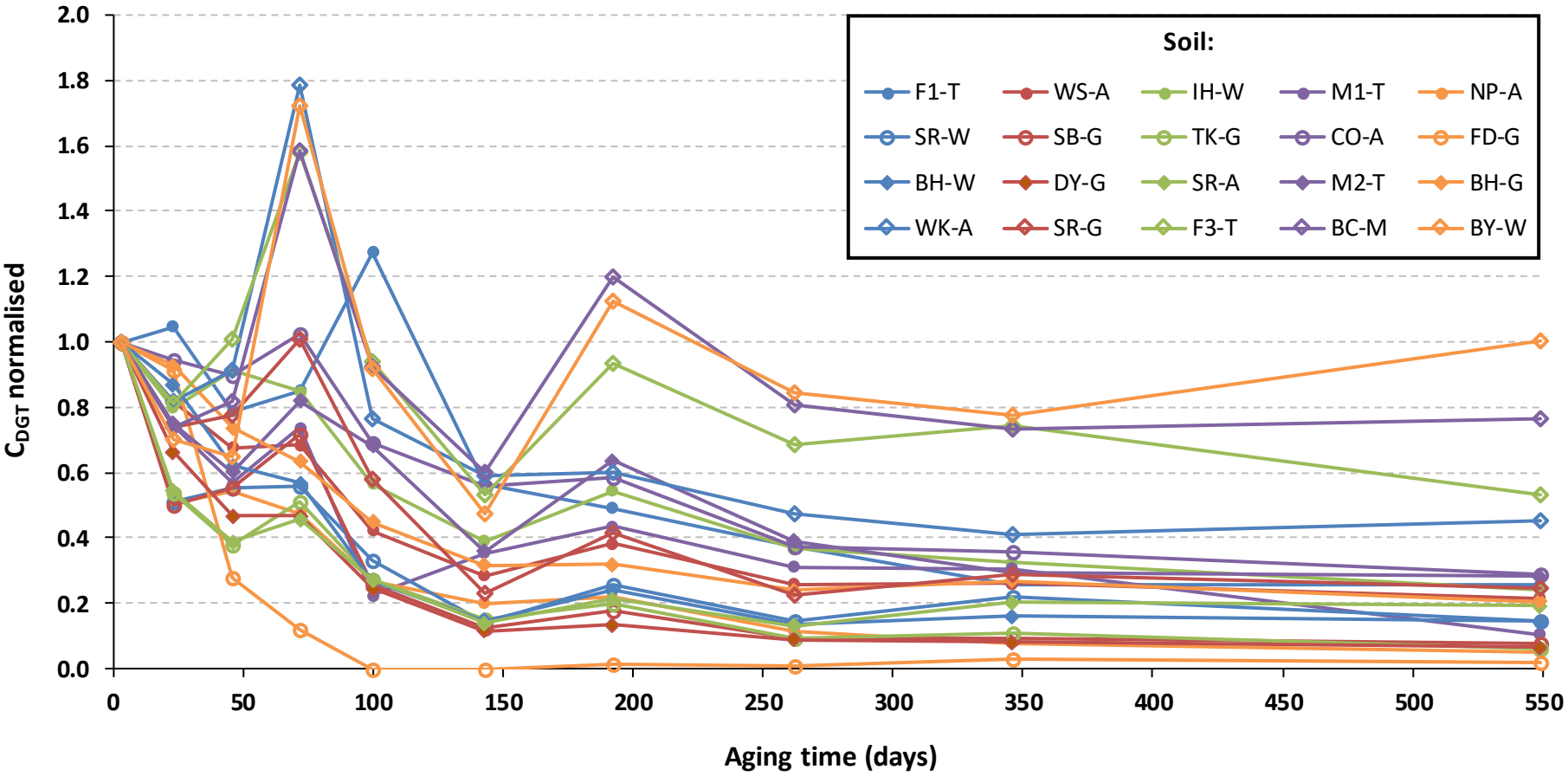

Figure 5.5. *Concentration of Se measured by DGT (C_{DGT}) in all 20 soils over 549 days aging after normalising to day 3.*

The rate of decline in the availability of Se for all the soils presented in Figure 5.5 occurs approximately four times slower than observed by Li et al. (2016), who measured uptake by pak choi in three different soils. They observed a rapid decrease in the concentration of Se measured in the roots and shoots over the initial 42 days, followed by a slow decline thereafter. This pattern was mirrored by a decrease in the size of the exchangeable Se fraction, which occurred on a similar timescale. In contrast, Di Tullo et al. (2016) reported that the distribution and speciation of native and spiked Se were still quite different after two years of in situ incubation. The total ^{77}Se exchangeable fraction was found to be a factor of 1.5 to 1.7 greater than native Se, whilst this factor ranged between two and five, depending on soil type, for the selenite-77 fraction specifically. Despite not knowing the intrinsic availability of the native Se within the soils incubated in this study, it is clear that a slow evolution in the available fraction of Se proceeds beyond 549 days of aging.

As reported in Section 3.3.8, uptake of selenate by the mixed binding layer (MBL) DGT was found to be suppressed at pH > 7, which was predominantly attributed to the reduction in adsorption of anionic selenate to ferrihydrite as the concentration of positively-charged sites on the ferrihydrite surface diminishes approaching the point of zero charge (pH 8.0-8.3). This effect of suppressed uptake of selenate is reflected in Figure 5.6, where systematically low values of C_{DGT} are observed in soils with a pH greater than 7, relative to their concentration measured in the soil solution (C_{soln}). As a result of this effect, the six incubated soils with a pH of greater than 7 are omitted from all further DGT analysis and discussion concerning Se.

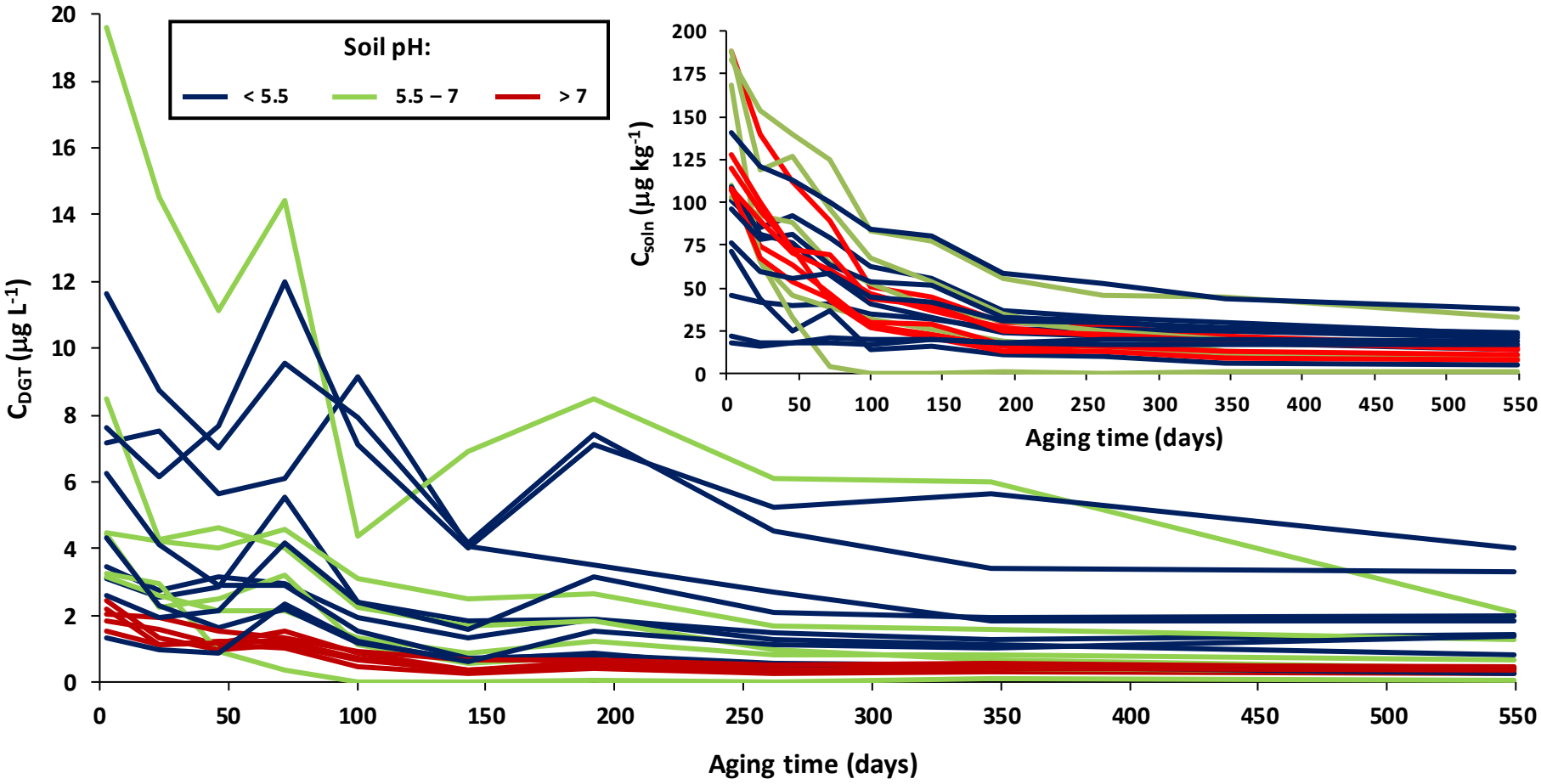

Figure 5.6. *DGT-measured concentration (C_{DGT}) of Se in all 20 incubated soils over 549 days aging. Inset: Concentration of Se in soil solution (C_{soln}) in all 20 soils over the same incubation period. Soils are highlighted according to pH.*

Coefficient and parameter values obtained after fitting the parabolic diffusion, Elovich and pseudo-second-order equations to the 14 acidic (pH < 7) soils are presented in Table 5.2. Table 5.3 lists coefficient and parameter values after fitting the natural exponential function. Section 2.3.1 describes the four models and explains how they were fitted to the experimental data. The relevant parameters and coefficients are described in the captions of both Table 5.2 and Table 5.3.

The models fitted the experimental DGT data for the soils with varying degrees of accuracy. This point is illustrated in Figure 5.7, where all four models are fitted to the DGT datasets for soils IH-W, FD-G and BY-W. In the case of soil IH-W, all four models appear to fit the data with a good degree of accuracy. In contrast, the Elovich, pseudo-second-order and parabolic diffusion models considerably underestimate the rate of aging of Se in soil FD-G. No clear or defined aging trend for Se was visible within the DGT dataset for soils BC-M and BY-W, so the model-fitting exercise for these soils was arguably inappropriate.

Using the standard error (SE) values [Equation (2.11)] as an indicator of the closeness of fit of each model to the experimental data, the natural exponential function provided the best fit across the range of soils as it yielded the lowest SE values for 10 out of the 14 soils. The Elovich equation provided the next best fit as it yielded the lowest SE values for three of the soils, followed by the pseudo-second-order equation which provided the closest fit in one soil. The parabolic diffusion equation provided the least-best fit as it yielded the highest SE values in eight of the soils.

Table 5.2. *Parameter and coefficient values for three different kinetic models used to describe the aging of Se in 14 acidic (pH < 7) soils. Q_t is the DGT available concentration of Se at time t (days); a, b and c are all constants; k_{ip} is the intraparticle diffusion rate constant (μg L^{-1} $d^{-1/2}$); k is the pseudo-second-order rate constant that also represents the Se aging rate constant (μg L^{-1} d^{-1}); Q_e is the quantity of available Se at equilibrium time (μg L^{-1}); SE is the standard error [Equation (2.11)].*

	Pseudo-second-order $Q_t = \frac{t}{\left(\frac{1}{k}\right)Q_e^2 + \left(\frac{t}{Q_e}\right)}$			**Elovich** $Q_t = a + b\ln(t)$			**Parabolic Diffusion** $Q_t = \sqrt{k_{pd}} + c$		
Soil	**k**	**Q_e**	**SE**	**a**	**b**	**SE**	**k**	**c**	**SE**
F1-T	0.11	0.51	0.51	-6.28	1.90	0.46	0.32	-1.09	0.68
IH-W	0.23	0.25	0.41	-2.15	0.76	0.40	0.13	0.06	0.43
M1-T	0.05	1.96	2.77	-5.98	3.57	2.58	0.59	3.92	2.72
NP-A	0.11	1.26	0.65	-1.15	1.51	0.57	0.25	3.03	0.68
SB-G	0.23	0.77	0.33	-0.26	0.74	0.36	0.12	1.85	0.47
TK-G	0.23	0.69	0.35	-0.23	0.71	0.33	0.11	1.77	0.40
CO-A	0.16	0.30	0.32	-3.19	1.02	0.25	0.17	-0.41	0.33
FD-G	0.26	0.44	0.75	-0.86	0.74	0.65	0.10	1.46	0.81
DY-G	0.16	0.99	0.38	-1.58	1.27	0.49	0.20	2.13	0.75
M2-T	0.10	0.88	1.58	-3.80	1.89	1.53	0.33	1.24	1.45
WK-A	0.40	0.18	0.23	-1.31	0.50	0.26	0.08	0.04	0.26
F3-T	0.13	0.25	1.42	-1.90	0.73	1.26	0.14	-0.10	1.19
BC-M	1.56	4.19	0.88	-0.36	0.12	0.84	0.03	-0.15	0.83
BY-W	-113.09	—	0.55	0.24	-0.02	0.52	0.00	0.14	0.52

Table 5.3. *Coefficient values for a natural exponential function used to describe the aging of Se in 14 acidic (pH < 7) soils. Q_t is the DGT-available concentration of Se at time t (days); A, B and C are all constants; Availability half-life (days) is calculated as ln(2)/-B; SE is the standard error [Equation (2.11)].*

	Natural exponential function $Q_t = A*e^{-Bt} + C$				
Soil	**A**	**B**	**Half-life (days)**	**C**	**SE**
F1-T	6.40	-0.006	124	1.27	0.44
IH-W	2.73	-0.006	107	0.78	0.33
M1-T	14.53	-0.014	51	4.86	2.61
NP-A	7.13	-0.014	48	0.80	0.75
SB-G	3.94	-0.020	35	0.46	0.36
TK-G	3.66	-0.018	38	0.49	0.41
CO-A	3.57	-0.006	125	1.08	0.19
FD-G	3.88	-0.025	28	0.00	0.36
DY-G	5.86	-0.017	42	0.47	0.31
M2-T	7.71	-0.006	119	2.92	1.45
WK-A	1.88	-0.006	109	1.22	0.19
F3-T	6.01	-0.001	554	1.20	1.11
BC-M	2.05	-0.715	1	2.38	0.79
BY-W	1.49	0.000	19,995	-0.24	0.49

Ignoring soils BC-M and BY-W, for which the suitability of the model-fitting exercise was previously questioned, availability half-lives calculated from the decay rate constant (B) derived from the natural exponential function ranged from 28 days in soil FD-G to 554 days in soil F3-T. The mean half-life was calculated as 115 ± 144 days, whilst the median was much lower at 79 days. The mean is skewed by the exceptionally long half-life calculated for soil (F3-T); in the absence of this soil the mean half-life is recalculated as 75 ± 41 days, which is marginally greater than that calculated for Tc (72 ± 46 days) in Section 4.2.2.1. Including soil F3-T, the median half-lives for both elements are remarkably similar, differing only by one day (Tc = 78 days).

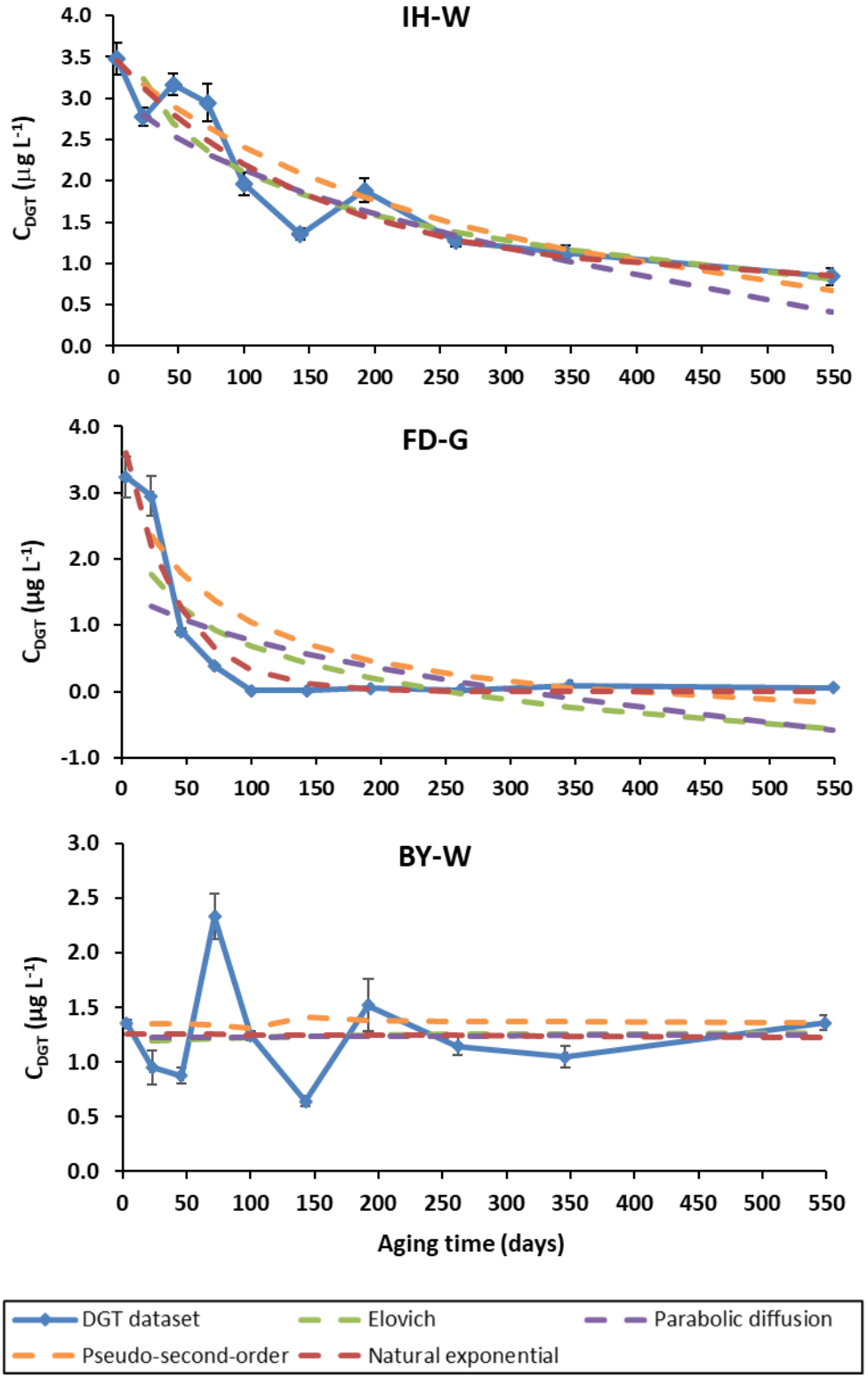

Figure 5.7. *Comparison of model fits (Elovich, parabolic diffusion, pseudo-second-order and natural exponential) to experimental DGT data for soils IH-W, FD-G and BY-W over 549 days of aging. Error bars represent one standard deviation of the mean of triplicate DGT deployments.*

Li et al. (2016) applied the pseudo-second-order, Elovich and parabolic diffusion models to three contrasting selenite-spiked soils and found that aging of the exchangeable Se fraction in all the soils could best be described by the pseudo-second-order equation, followed by the Elovich equation and lastly the parabolic diffusion equation. These observations are in contrast to the findings presented here; ignoring the natural exponential function, the Elovich equation provided the best fit in eight of the 14 soils, followed jointly by the pseudo-second-order (3) and parabolic diffusion (3) equations. Conversely, Di Tullo et al. (2016) reported that the parabolic diffusion equation could best describe the aging of total exchangeable added ^{77}Se and selenite over the Elovich equation. The pseudo-second-order equation was not applied, however.

An advantage of using the pseudo-second-order model is that the equilibrium adsorption capacity (in this context the availability of Se after aging has diminished to a negligible rate) need not be determined experimentally, it can in fact be calculated from the model (Ho, 2006). This parameter is denoted Q_e in Table 5.2. Li et al. (2016) reported that the values of Q_e for exchangeable Se obtained from their dataset were in good agreement with measured values after 100 days aging for all three tested soils. In this study, values of Q_e were lower than measured values of C_{DGT} after 549 days aging for half (7) of the 14 modelled soils, implying that equilibrium was yet to be reached. In the remaining soils, the time point at which Q_e was attained varied within the region of 46 to 262 days.

Despite the natural exponential function yielding the best fit for the majority (10) of the 14 modelled soils, two notable limitations of the function are evident. Firstly, the values of C presented in Table 5.3 representing availability at equilibrium (negligible rate of aging) are not wholly accurate since availability in some of the soils still appears to be decreasing beyond 549 days aging. This is exemplified in Figure 5.8 for soil M1-T. More suitable values for C could be constrained by using DGT to measure the intrinsic availability of native Se within unspiked

soil samples. Secondly, as discussed in Section 4.2.2.3 for Tc, fitting the function by minimising the sum of the squares is not necessarily the most suitable approach to take for every soil. Again, this point can be illustrated using soil M1-T in Figure 5.8 where function A has been fitted by minimising the sum of the squares. Function A appears to overestimate the rate of aging within the soil. Function B has been fitted by fixing the value of C to equal the measured C_{DGT} value (at day 549), and the function consequently seems to better model the rate of aging.

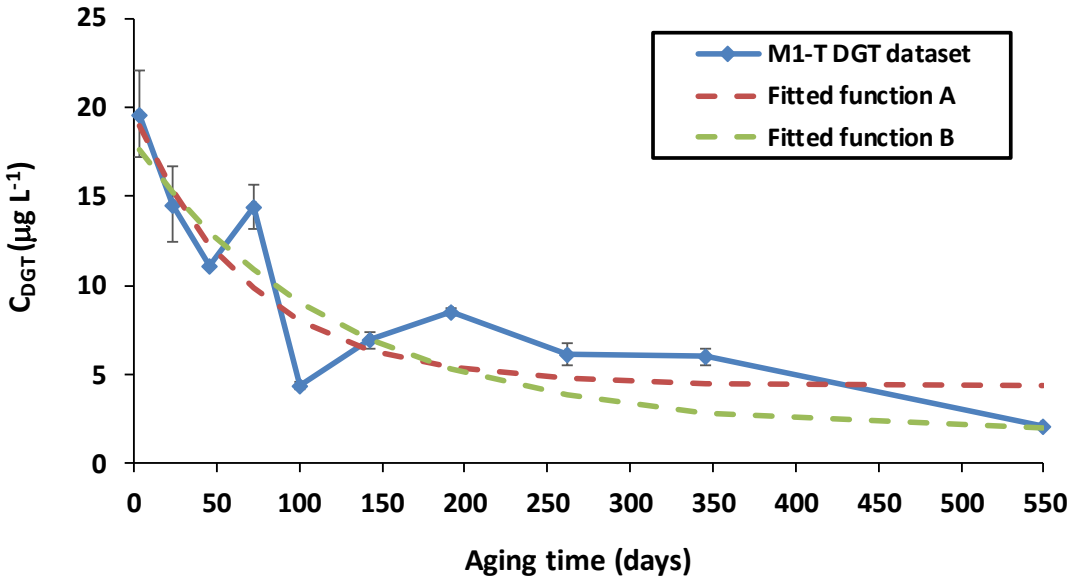

Figure 5.8. *A natural exponential function fitted to experimentally-acquired DGT data for soil M1-T over 549 days of aging. Error bars represent one standard deviation of the mean of triplicate DGT deployments. For function A, the value of the constant C is calculated by minimising the sum of the squares, whereas for function B the value of C is set to match the value for C_{DGT} at day 549.*

5.2.2.2 Effect of soil properties on availability

Spearman's rank correlation coefficients (r_s) describing the correlation between C_{DGT} and individual soil properties after 3, 100 and 549 days aging are listed in Table 5.4, where soils with a pH greater than 7.0 have been excluded. Soil organic carbon in addition to Al and Fe oxides are found to be the most important soil properties in determining the availability of Se

after any given period of aging. Strong negative correlation is calculated between C_{DGT} and C_{org}, with correlation coefficients (r_s) ranging from -0.64 ($\alpha < 0.05$) at 549 days to -0.77 ($\alpha < 0.01$) at 100 days. Similarly, strong and negative correlation is calculated with both Al and Fe. Coefficients for Al range from -0.70 ($\alpha < 0.01$) at 549 days to -0.81 ($\alpha < 0.01$) at 100 days, whilst coefficients for Fe range from -0.56 ($\alpha < 0.05$) at 549 days to -0.71 ($\alpha < 0.01$) at 3 days.

Table 5.4. *Spearman's rank correlation coefficients (r_s) relating C_{DGT} to soil properties after 3, 100 and 549 days aging (N = 14).*

	Days of aging		
	3	**100**	**549**
Organic carbon	-0.71**	-0.77**	-0.64*
pH	0.35	-0.16	-0.25
Fe	-0.71**	-0.65*	-0.56*
Al	-0.73**	-0.81**	-0.70**
Mn	-0.13	-0.37	-0.36
Total Al + Fe	-0.78**	-0.74**	-0.62*

**Indicates significant relationship at α < 0.05; **Indicates significant relationship at α < 0.01*

The significance of Fe and Al oxides and oxyhydroxides in the adsorption of Se is widely-reported (Rajan, 1979; Neal et al., 1987; Parida et al., 1997; Rashid et al., 2002; Duc et al., 2003), and it is adsorption of Se to these phases which is responsible for the reduced availability of Se as measured by DGT in such soils. Similarly, Li et al. (2017) report on the importance of soil organic matter in immobilising Se and the consequent reduction in availability in their review of the interaction between Se and soil organic matter. The combined significance of C_{org} and both Al and Fe oxides in governing availability as presented in Table 5.4 could support the hypothesis that Se is adsorbed indirectly by OM-cation (e.g. Fe, Al) complexes to form a Se-OM-metal ternary system (Gustafsson and Johnsson, 1994; Coppin et al., 2009; Jordan et al., 2009).

5.2.2.3 Effect of soil properties on aging kinetics

The correlation coefficients presented in Table 5.4 for C_{DGT} are incomparable to those presented in Table 5.1 for C_{soln}, which were calculated for all 20 soils including the six soils with a pH < 7.0. In Table 5.1, no single soil property exhibited any persistent correlation with C_{soln} throughout the duration of the incubation. For example, strong negative correlation was calculated between C_{org} and C_{soln} after 100 days aging, yet this correlation was largely absent after 3 and 549 days aging. Similarly, negative correlation with C_{soln} for Fe (-0.18 to -0.32) and Al (-0.27 to -0.37) at 100 and 549 days aging was much weaker, and in complete contrast a positive relationship with C_{soln} for both elements was identified at 3 days aging.

The relationships between soil properties and the rate constants associated with the natural exponential function, Elovich and pseudo-second-order equations were investigated, since between them the three models could best describe the rate of aging for all 14 modelled soils. Spearman's rank correlation coefficients (r_s) relating soil properties to the pseudo-second-order (k) and Elovich rate constants (b), plus the availability half-life derived from the natural exponential function are presented in Table 5.5. Soils BC-M and BY-W were excluded from the correlation analysis because Se did not display any evidence of aging in these soils and consequently the models could not be appropriately fitted to reflect this.

Highly significant ($\alpha < 0.01$) positive correlation with the pseudo-second-order aging rate constant (k) was calculated for C_{org}, ($r_s = 0.76$), Fe ($r_s = 0.82$) and Al ($r_s = 0.80$), which implies that Se ages faster in soils with a higher content of C_{org}, Al and Fe oxides. Similarly, significant ($\alpha < 0.05$) positive correlation is calculated between the Elovich rate constant (b) and Fe ($r_s = 0.69$) and Al ($r_s = 0.62$), although only moderate positive correlation ($r_s = 0.50$) is found between b and C_{org}. No significant relationships could be identified between the half-lives

calculated from the natural exponential function and any of the measured soil properties, although moderate negative correlation was calculated for C_{org} (r_s = -0.57) and Al (r_s = -0.54).

Table 5.5. *Spearman's rank correlation coefficients (r_s) describing the correlation between various soil properties and the rate constants for the pseudo-second-order (k) and Elovich (b) equations, plus the availability half-life derived from the natural exponential function (N = 12).*

	k	***b***	***Half-life***
Organic carbon	0.76**	0.50	-0.57
pH	-0.08	-0.06	-0.34
Fe	0.82**	0.69*	-0.39
Al	0.80**	0.62*	-0.54
Mn	0.53	0.58	-0.22
Al + Fe	0.87**	0.72*	-0.48

**denotes significant relationship at α < 0.05; **denotes significant relationship at α < 0.01*

The relationship between the rate of aging of Se within the 14 acidic (pH < 7.0) soils and C_{org} is illustrated in Figure 5.9, where values for C_{DGT} have been normalised to day 3 and the soils highlighted according to their C_{org} content. In Figure 5.10, the same 14 acidic soils have been highlighted according to their total Al + Fe content. In Figure 5.9 and Figure 5.10, C_{org} and Al + Fe do not appear to be as significant in governing the rate of aging of Se as the relationships identified in Table 5.5 with the rate constants would suggest. As previously discussed, it should be remembered that the models do not accurately describe the aging process in some soils and therefore the aging rate constants themselves are not accurate. Additionally, in some of the soils a significant extent of aging has already occurred within the first three days of incubating, and this is not reflected in the modelled rate constants or the aging curves in Figure 5.9 and Figure 5.10.

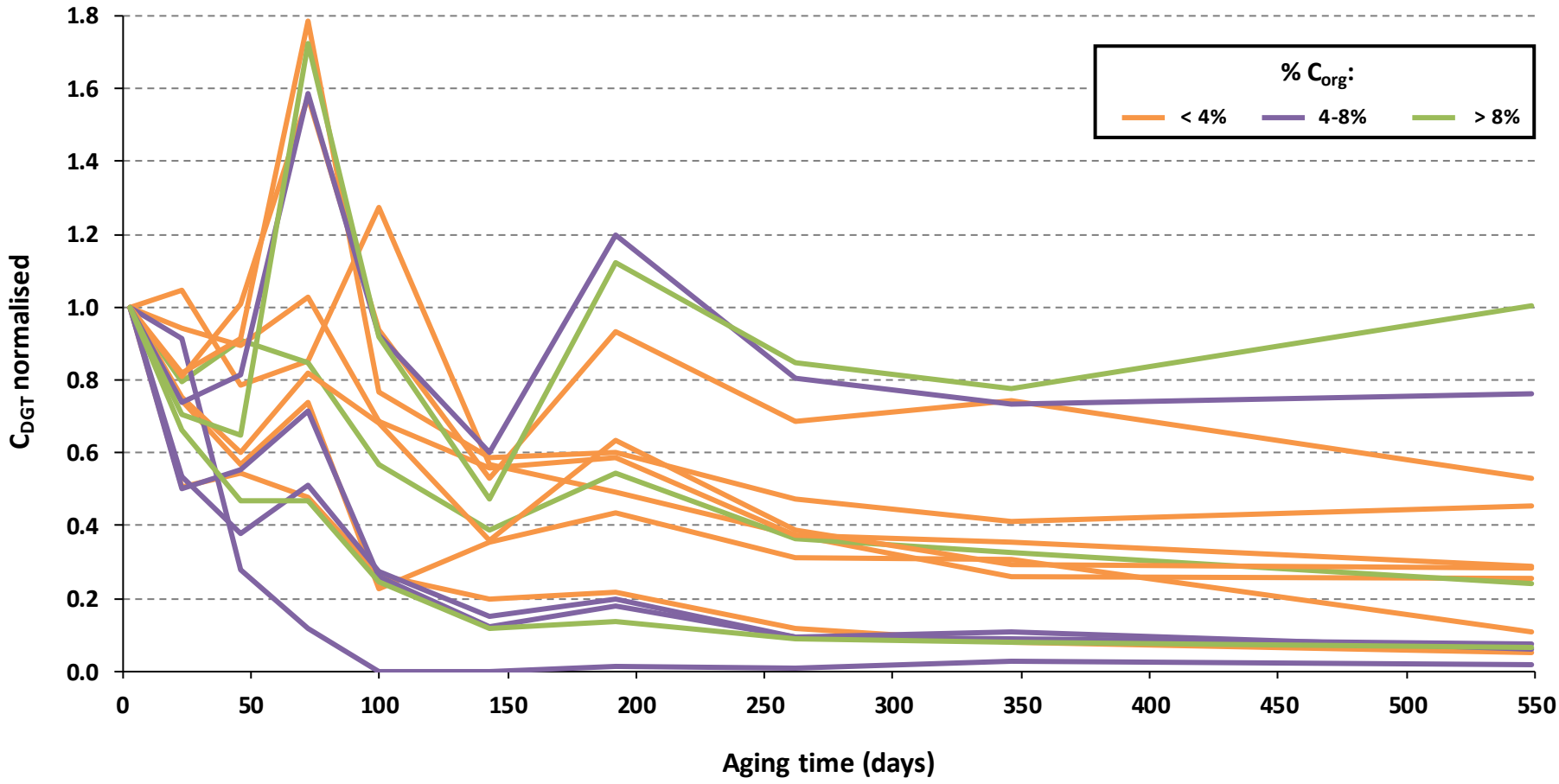

Figure 5.9. *DGT-measured concentration of Se (C_{DGT}) in 14 acidic (pH < 7) soils after normalising to day 3. Soils are highlighted according to organic carbon (C_{org}) content.*

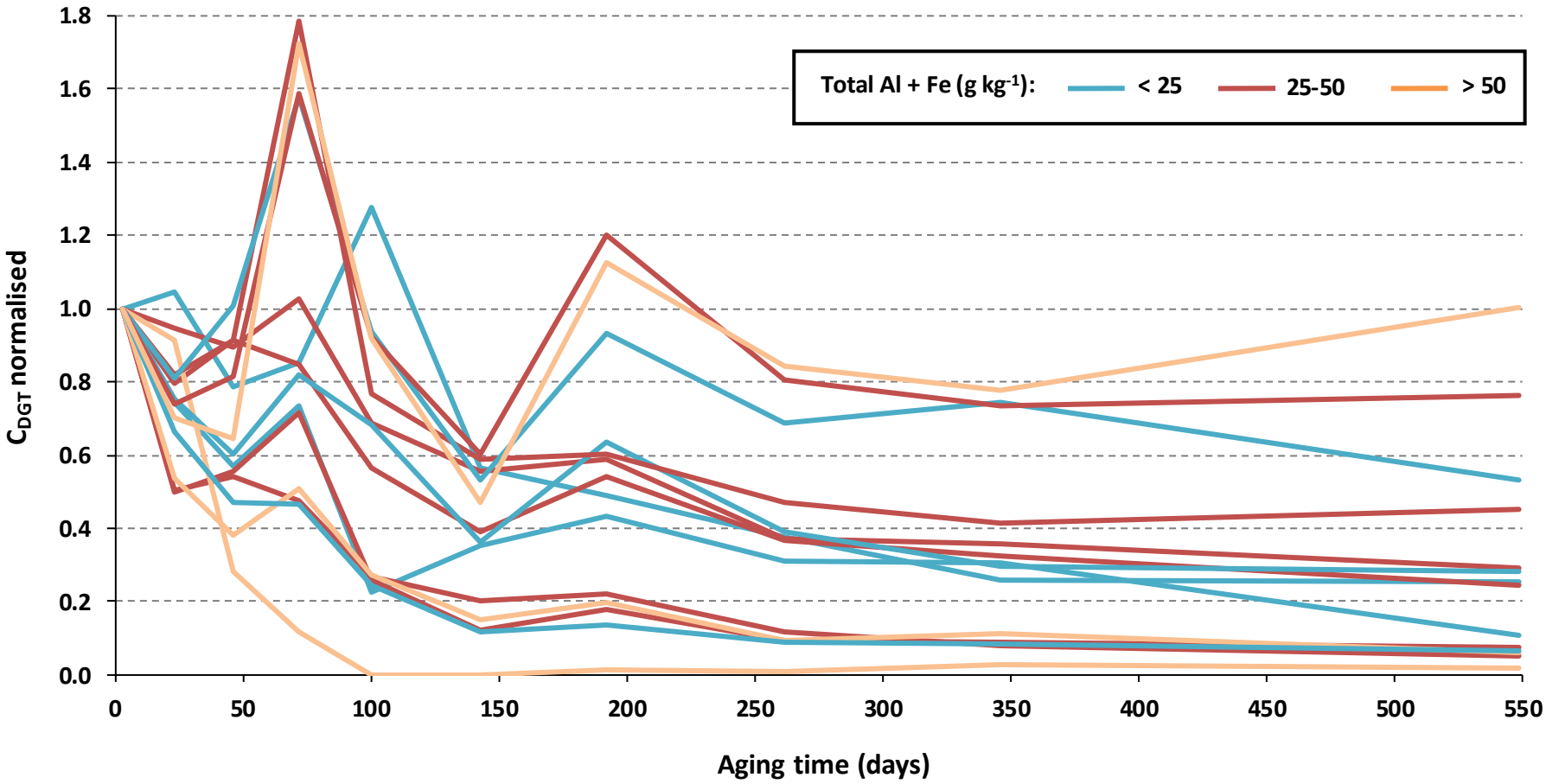

Figure 5.10. *DGT-measured concentration of Se (C_{DGT}) in 14 acidic (pH < 7) soils after normalising to day 3. Soils are highlighted according to total Al + Fe oxide content.*

5.2.3 Resupply of Se from the soil solid phase

Values of R for Se in the 14 acidic soils (pH < 7.0) are presented for day 3 and day 549 in Figure 5.11. As detailed in Section 1.8, an R value expresses the ratio between the concentration of Se measured by DGT and the concentration measured in the bulk solution (C_{soln}). As R increases, the capacity of the solid phase to resupply Se to the soil solution in response to the DGT-induced depletion increases, and the concentration in solution is more effectively buffered within the vicinity of the DGT device. Where resupply is absent, Se supply to the DGT is confined to diffusional transport, which is influenced by the soil porosity and tortuosity, and the R value is referred to as R_{diff}. Figure 5.11 reveals that R values at both day 3 and day 549 across the 14 soils are generally very low, exhibiting a very narrow range between 0.01 and 0.07. For the majority (12) of the soils, R values at both day 3 and day 549 are comparable to or less than the calculated R_{diff} values.

Also plotted in Figure 5.11 are R values for day 549 derived using DET to measure the concentration of Se in the soil solution (R_{DET}). In comparison to the R values at day 549 derived by centrifuging the soil to obtain a measure of C_{soln}, R_{DET} values are between a factor of 1.87 (TK-G) to 2.84 (M2-T) greater across the 14 soils. However, the R_{DET} values in absolute terms are still low, ranging between 0.05 and 0.18, with 9 of the 14 soils exhibiting values of 0.1 or less. Crucially, R_{DET} is found to be greater than or comparable to the corresponding R_{diff} value for each soil.

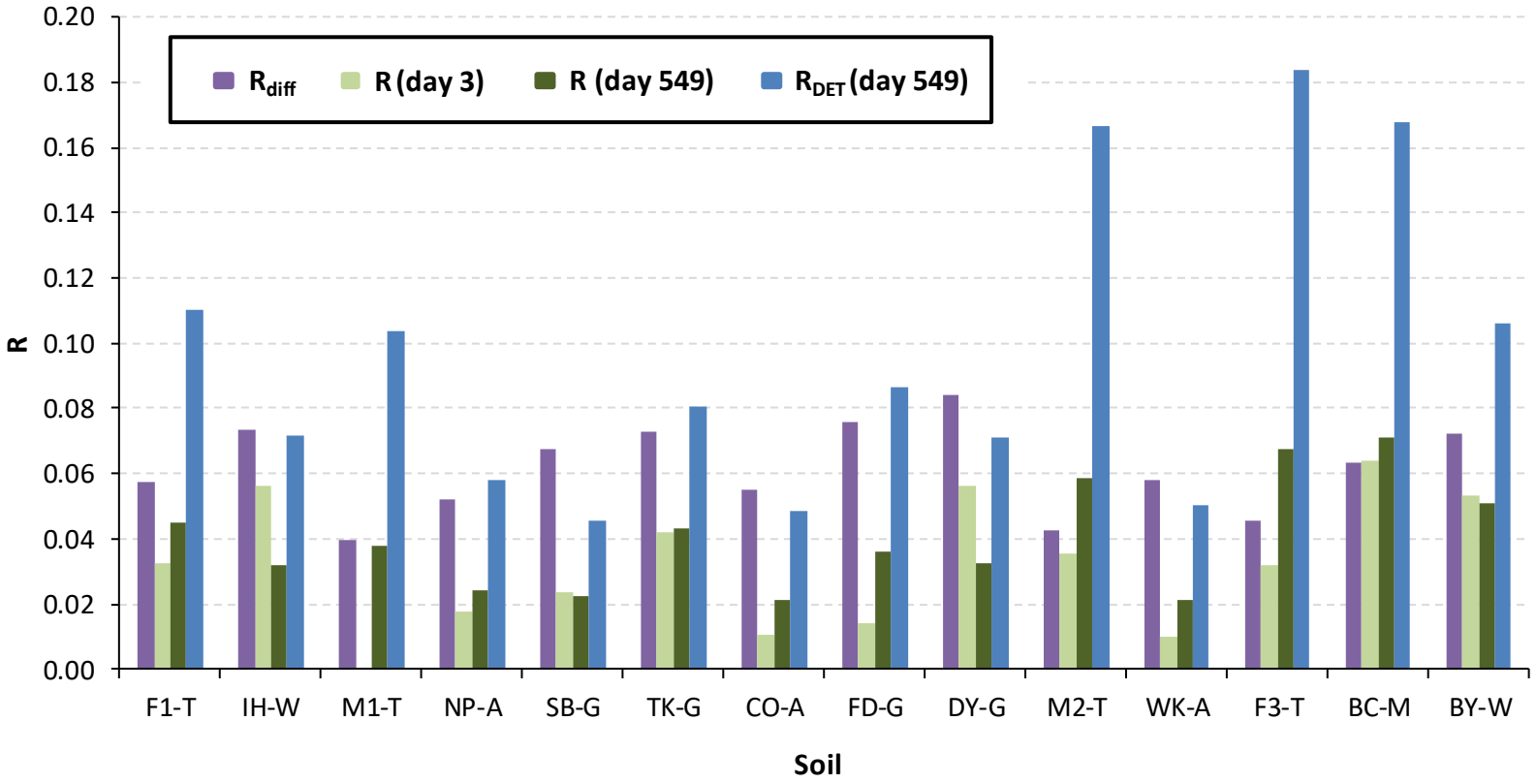

Figure 5.11. *A comparison of R values at day 3 and day 549 for 14 incubated acidic soils (pH < 7.0), in addition to the corresponding R_{diff} values. Also plotted are R values at day 549 using DET to determine C_{soln}. No data are available concerning the R value at day 3 for soil M1-T.*

The use of DET to derive new R values (R_{DET}) by providing a measure of the concentration of Se species in the soil solution which are physically small enough to undergo diffusion through the polyacrylamide hydrogel in DGT, reveals that the exceptionally low R values in Figure 5.11 can be attributed to the presence of a significant fraction of colloidal Se, which is physically excluded from measurement by DGT. Even after accounting for these colloidal species however, R_{DET} is found to be only marginally greater than (up to 0.14), or comparable to, the corresponding R_{diff} value for each of the 14 soils. Granted, DET was only deployed after 549 days aging, so higher R_{DET} values may have been observed after shorter periods of aging, but the conventional R values measured by centrifuging at day 3 do not differ greatly to those at day 549 (Figure 5.11), which would imply a similar trend for R_{DET}.

In Figure 5.12, the concentration of Se species in solution for all 20 soils measured using DET (C_{DET}) is divided by the concentration derived from centrifuging the soil and filtering at 0.45 μm (C_{soln}), and plotted against both C_{org} [A] and the total Al + Fe content [B]. This ratio (C_{DET}/C_{soln}) can be used as an indicator of the concentration of colloidal Se species unavailable to DGT. A visual inspection of the relationship between C_{DET}/C_{soln} and both C_{org} and Al + Fe suggests only a moderate degree of positive correlation. In fact, highly significant correlation (r_s = 0.65, $\alpha < 0.01$) is calculated between C_{DET}/C_{soln} and C_{org} using Spearman's rank correlation test. Correlation between C_{DET}/C_{soln} and Al + Fe is weaker (r_s = 0.40). The strong positive correlation between C_{org} and C_{DET}/C_{soln} in Figure 5.12[B] suggests that the Se colloids can be attributed to interactions with C_{org}.

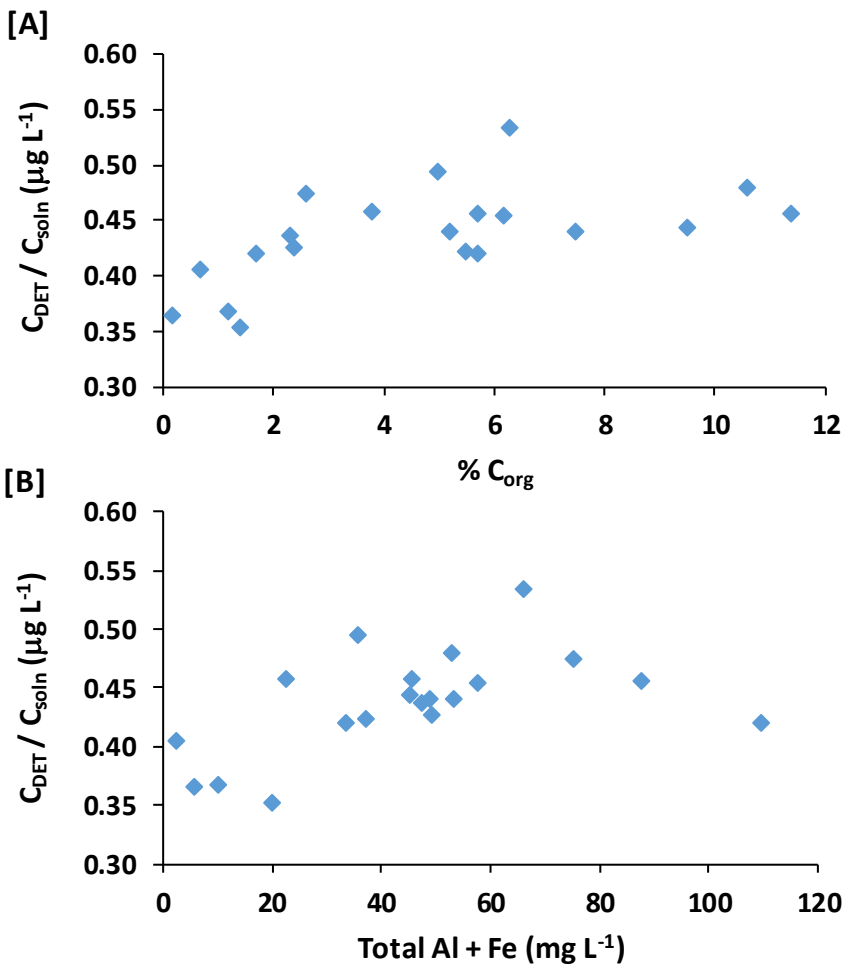

Figure 5.12. *Concentration of Se species in solution for each soil measured using DET (C_{DET}) divided by the concentration derived from centrifuging the soil and filtering at 0.45 µm (C_{soln}), plotted against both soil organic carbon (% C_{org})* ***[A]*** *and the total Al + Fe (g kg^{-1}) content* ***[B]****.*

Other studies report on the significance of Se occurring as colloidal material (Yamada et al., 1998; Weng et al., 2011). For example, Weng et al. (2011) applied an anion Donnan membrane technique to establish that 67-86% of Se in the 0.01 M $CaCl_2$ extracts of a range of grassland soils was colloidal. The study concluded that the colloidal Se was most likely to be bound to or incorporated in colloidal-sized organic matter, rather than Fe and Al oxides, which is in agreement with the data presented in Figure 5.12.

A more accurate determination of the relative contribution of inorganic and organic colloids to Se speciation in solution for the soils in this study would be possible through the use of 'restricted gel' DGT devices, in which a bis-acrylamide cross-linker is used to produce polyacrylamide diffusive gels of smaller pore sizes (< 1 nm) (Zhang and Davison, 2000). The restricted diffusive layer is therefore believed to only measure free ions and small inorganic complexes (Zhang and Davison, 2000).

In Figure 5.13, the R_{diff} value for each soil is subtracted from R_{DET} to derive a quantitative indicator of the capacity of each soil to resupply Se, which in turn is plotted against C_{org}. The trend that emerges is for soils of lower C_{org} to exhibit a slightly greater capacity to resupply Se than soils of higher C_{org}. A Spearman's rank correlation coefficient (r_s) of -0.50 is calculated, which falls narrowly short of being significant at $\alpha = 0.05$. The relationship in Figure 5.13 indicates that the presence and concentration of organic Se complexes may govern the ability of the soil to release Se in response to its removal from solution.

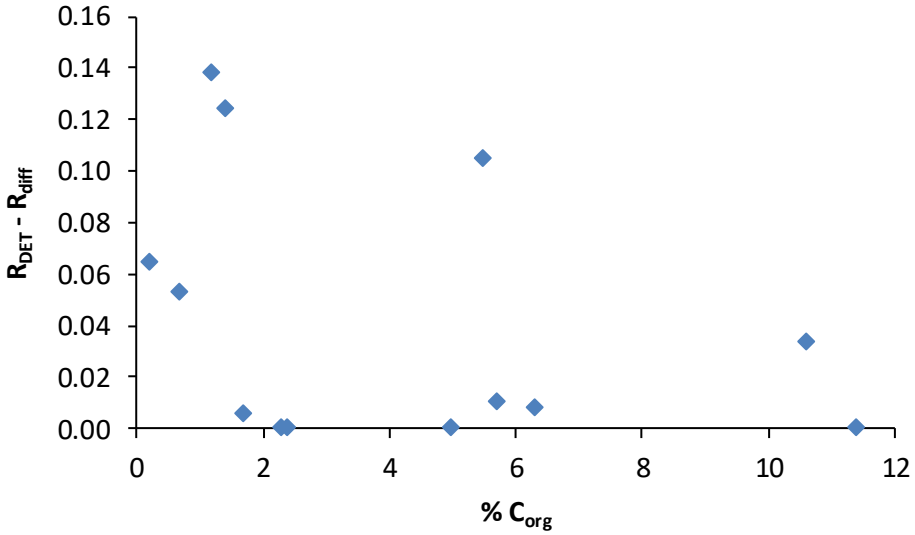

***Figure 5.13**. R_{DET} - R_{diff} plotted against soil organic carbon (C_{org}) for 14 acidic (pH < 7.0) soils after 549 days aging.*

Soil response times (T_c) (s) for the 14 acidic (pH < 7.0) soils after 549 days aging calculated using the 2D version of the DIFS (DGT-induced Fluxes in Soils/Sediments) model (Sochaczewski et al., 2007) are presented in Table 5.6, alongside the desorption rate constants (k_{-1}). Key input parameters for the model are described in Section 2.3.2.4. In brief, T_c represents the capacity of labile Se associated with the solid phase as well as its rate constant of release in response to localised depletion by DGT (Lehto et al., 2008). Response times range from 0.87 s in soil F1-T to 23.35 s in BY-W. Desorption rate constants are greater than sorption rate constants in 9 of the 14 soils.

Table 5.6. *Soil response times (T_c) plus sorption (k_1) and desorption rate constants (k_{-1}) for 14 acidic (pH < 7.0) soils after 549 days aging. Values were calculated using 2D-DIFS.*

Soil	T_c (s)	k_1 (s^{-1})	k_{-1} (s^{-1})
F1-T	0.87	0.11	1.04
IH-W	7.20	0.16	0.08
M1-T	1.84	0.14	0.40
NP-A	6.22	0.08	0.52
SB-G	11.16	0.21	0.04
TK-G	4.90	0.14	0.18
CO-A	7.21	0.15	0.11
FD-G	19.94	0.04	0.06
DY-G	1.51	0.14	0.52
M2-T	5.70	0.12	0.09
WK-A	4.68	0.04	0.25
F3-T	9.13	0.06	0.05
BC-M	14.46	0.05	0.09
BY-W	23.35	0.03	0.65

The very short soil response times (0.87 to 23.35 seconds) presented in Table 5.6 imply both a small capacity of labile solid phase Se plus slow resupply. Desorption rate constants are greater than sorption rate constants in over half (9) of the 14 soils, which suggests that release of Se from the solid phase is either very limited or in fact exceeded by the rate of sorption to

the solid phase. No correlation was observed between soil response times or the sorption/desorption rate constants and any measured soil properties.

5.2.4 Effect of microbial activity and contrasting moisture regimes

Figure 5.14 and Figure 5.15 reveal the effect of autoclaving and contrasting moisture regimes on the solubility and availability, respectively, of Se in four soils (BH-G, BY-W, SR-W and WK-A) over the 120-day secondary incubation. To allow for the inclusion of C_{DGT} data from the primary incubation (microbes/extensive drying), all C_{DGT} values were normalised relative to the first sampling point at day 2. Details relating to the secondary incubation approach can be found in Section 2.1.4.

The data indicate that autoclaved subsamples from soils BY-W and WK-A exhibit a significantly lower availability and solubility of Se relative to the non-autoclaved soils. This effect is also partly seen in soil SR-W, but not in BH-G, where the availability is generally indistinguishable between subsamples. Several studies have indicated that microorganisms in soil are capable of aerobic oxidation of Se^0 to selenite and selenate (Sarathchandra and Watkinson, 1981; Losi and Frakenberger, 1998), which would contribute towards retarding the aging of Se in the non-autoclaved samples relative to the autoclaved samples. This explanation seems unlikely, however, given the very low rates (0.0009 and 0.0117 day^{-1}) associated with these reactions relative to reductive processes.

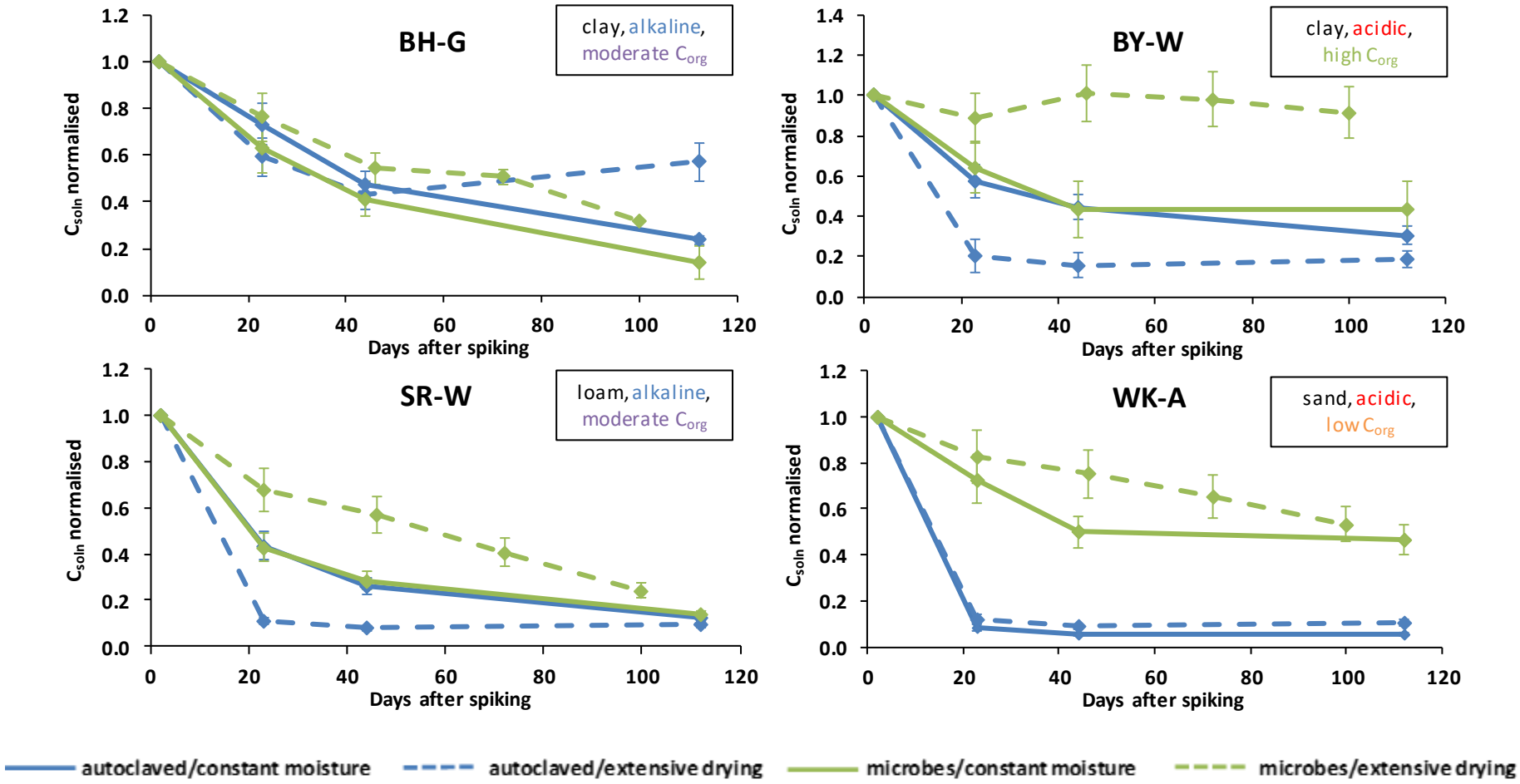

Figure 5.14. *Concentration of Se measured in solution (C_{soln}) normalised to the first time point (day 2) in autoclaved and non-autoclaved (microbes present) subsamples of four different soils (BH-G, BY-W, SR-W and WK-A) incubated for 120 days at contrasting moisture regimes.*

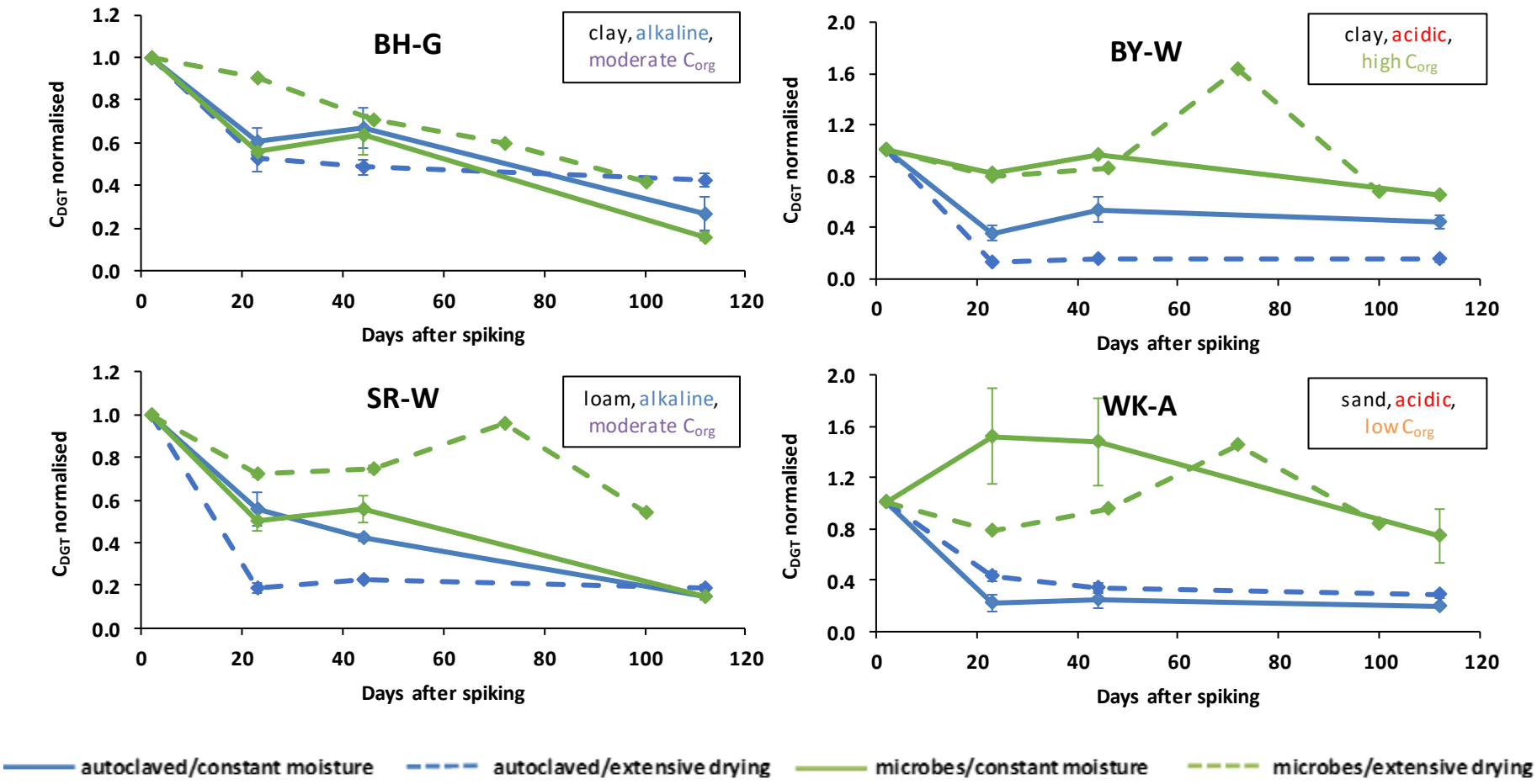

Figure 5.15. *DGT-measured concentration of Se (C_{DGT}) normalised to the first time point (day 2) in autoclaved and non-autoclaved (microbes present) subsamples of four different soils (BH-G, BY-W, SR-W and WK-A) incubated for 120 days at contrasting moisture regimes.*

The observation that both C_{soln} and C_{DGT} are lower for the autoclaved samples would appear to rule out an increase in dissolved organic carbon (DOC) associated with autoclaving (Berns et al., 2008) as being responsible for reducing the availability in such samples. An increase in DOC would result in the dissolution of Se through formation of non-labile and colloidal Se-DOC complexes, which cannot be measured by DGT either due to their size or stability. An alternative hypothesis involves the disaggregation of clays within the soil matrix which could lead to a greater extent of adsorption of Se and eventually fixation due to an increased sorption capacity.

Regardless of the precise mechanism responsible however, the observation that aging does not appear to be microbially-driven is significant in that it hints at the predominance of abiotic processes in the reduction of Se oxyanions. Only a limited number of studies have focussed specifically on an abiotic route of Se incorporation into OM (Gustafsson and Johnsson, 1994; Ferri and Sangiorgio, 1999), or reduction by minerals such as green rusts (Johnson and Bullen, 2003) and sulphides (Hockin and Gadd, 2003) to form Se^0 precipitates or selenides. However, as discussed in Section 4.2.4, the effectiveness of the autoclaving process in achieving microbial sterilisation should be investigated before disregarding the role of microbes in the aging of Se.

In general, no systematic effect on the solubility or availability of Se in the soils could be identified between contrasting moisture regimes. This observation is in contrast to the findings of studies by Zhang and Moore (1997) and Supriatin et al. (2015), in which the concentration of soluble Se in extracts of 0.25 M KCl and 0.01 M $CaCl_2$, respectively, were found to increase following drying and re-wetting. For example, after oven-drying 58 different soil samples at 40°C, Supriatin et al. (2015) reported an increase in soluble Se of between 1.3 and 34-fold compared to the moist control soil. In both studies, the enhanced dissolution was attributed to an increase in DOC following drying, and the concomitant increase in colloidal

organic Se associated with dissolved organic matter (DOM). Oven drying at 40°C would have induced a greater extent of moisture removal than simply air-drying the soils (initially in a fume hood and then at 12°C as conducted here), but Zhang and Moore (1997) still observed a 19-39% increase in soluble Se when samples were dried at 22°C. Granted, both studies by Supriatin et al. (2015) and Zhang and Moore (1997) were not centred on Se-amended soils as in the case of the work in this chapter, so it would be logical to claim that the aging effect could obscure any changes in availability or solubility induced by extensive drying and re-wetting. Nevertheless, a slower rate of aging is expected in samples subject to extensive drying and re-wetting relative to moist soils.

5.3 Conclusions

This chapter presents data concerning the availability and kinetics of aging of Se within a range of soil types. The mixed binding layer (MBL) DGT is shown to be unsuitable for measuring Se availability in soils of pH > 7 due to the exceptionally low values of C_{DGT} observed in these soils when compared to the concentration measured in soil solution. Uptake of Se by the MBL was previously demonstrated in Chapter 3 to be suppressed at pH > 7, which was predominantly attributed to the reduction in adsorption of anionic selenate to ferrihydrite as the concentration of positively-charged sites on the ferrihydrite diminishes approaching the point of zero charge.

Organic carbon, Al and Fe oxide phases are shown to be important in controlling the availability of Se. The combined significance of both properties in governing availability could support the hypothesis that Se is adsorbed indirectly by OM-cation (e.g. Fe, Al) complexes to form a Se-OM-metal ternary system (Gustafsson and Johnsson, 1994; Coppin et al., 2009; Jordan et al., 2009). Resupply of Se from the solid phase is generally negligible or very slow, but there is evidence to suggest that soils of lower C_{org} exhibit a greater capacity to resupply

Se than soils of relatively high C_{org}. This hints at Se forming organic complexes of high stability that are unable to readily dissociate.

For soils of pH < 7, a natural exponential function provides a better fit to the aging curves for the majority of the soils than an Elovich, parabolic diffusion and pseudo-second-order equation, all of which have been used to previously describe the aging of Se. Highly significant ($\alpha < 0.01$) relationships were identified with the pseudo-second-order rate constants derived for each soil for C_{org}, Fe and Al oxides, which suggests that these phases are responsible for driving the aging of Se. The failure of the parabolic diffusion equation to provide the best fit for the experimental data suggests that intraparticle diffusion is not the sole process governing the aging of Se in the soils, but rather a variety of processes including surface nucleation and precipitation, occlusion by organic matter and formation of inner-sphere complexes.

Data from autoclaved soils suggest that microbial activity is insignificant in promoting the binding of Se to organic matter as is proposed in several studies throughout the literature. However, microbial activity is speculated to be responsible for the temporal fluctuations in C_{DGT} observed in a handful of soils. These fluctuations may be linked to the production and cycling of colloidal forms of Se such as uncharged elemental Se^0 or methylated compounds that are physically excluded from measurement by DGT. Meanwhile, extensive drying of the samples between saturation events for DGT deployment does not exert any clear effect on the solubility or availability of Se compared to those incubated at a constant moisture content between deployments.

Chapter 6: Availability and aging of uranium-238 within spiked soils

6.1 Introduction

The chemical speciation of U in soil and in turn its bioavailability is controlled by a complex interplay of factors including the soil solution pH, redox potential, the carbonate, clay and organic matter content, as well as the concentration of amorphous Fe and Al oxides and hydroxides (Koch-Steindl and Prohl, 2001; Gunther et al., 2003). Section 1.2.3 reviews the environmental behaviour of U in addition to its sources of contamination. Although U serves no known biological function, uptake has been demonstrated by a wide range of plants (Mitchell et al., 2013), with lower values for soil-to-plant transfer generally reported in clayey soils (Sheppard and Evenden, 1988; Mortvedt, 1994) and in the presence of organic matter (Sheppard et al., 1983; Ramaswami et al., 2001).

Several different selective extractions are commonly used to assess available pools of U in soil by targeting the 'exchangeable' fraction, with generally limited success. Studies by Shahandeh and Hossner (2002) and Punshon et al. (2003) failed to elucidate a relationship between U transfer to vegetation and extraction with either 0.5 M calcium nitrate ($Ca(NO_3)_2$) or sodium acetate ($NaCH_3COOH$, pH 5). Sheppard and Evenden (1992) reported that uptake of U by radish and beans from spiked soils could not be correlated to the U recovered in 0.5 M sodium bicarbonate ($NaHCO_3$) or 1 M ammonium acetate (CH_3COONH_4) extracts. Vandenhove et al. (2007) found success with using a 0.4 M magnesium chloride ($MgCl_2$) extraction to predict U concentrations in ryegrass shoots, as initially proposed by (Schultz et al., 1998). Significant correlation was also observed after extraction with 0.11 M acetic acid (CH_3COOH).

Three studies can be found in the published literature in which the DGT technique has been utilised in soil to assess U availability, with mixed success. Vandenhove et al. (2007) investigated the capacity of DGT to predict U uptake by ryegrass in six different soils, but concluded that DGT did not offer any significant advantage over the other bioavailability indices (C_{soln}, 0.11M CH_3COOH and 0.4 M $MgCl_2$) tested for assessing plant-available pools, all of which were found to be significantly correlated with concentrations of U in ryegrass roots and shoots. A similar study was conducted by Duquene et al. (2010), however this time none of the tested methods were able to effectively predict U concentrations in the ryegrass shoots (DGT, C_{soln} and CH_3COONH_4), which could be better approximated by the sum of UO_2^{2+}, uranyl carbonate complexes and $UO_2PO_4^-$ species in the soil solution. Mihalik et al. (2012) reported that DGT-measured concentrations of U in a sandy acidic soil of low organic matter correlated well with the concentration taken up by sunflower plants, at various different citric acid treatments. However, DGT-measured fluxes of U were higher than the U fluxes to plants suggesting that DGT did not mimic the plant uptake mechanism for U.

Just a single study can be found in the scientific literature which directly assesses the aging of U in different soil types. The study, by Rout et al. (2016), combines a sequential extraction approach with X-Ray Photoelectron Spectroscopy (XPS) to assess the solid phase fractionation of U in three pedogenetically different soils at one and twelve months after spiking. Significant redistribution of U was reported to occur between soil fractions during this timeframe, where the occlusion of U-Fe oxides and hydroxides due to the precipitation of silica on the ferrihydrite surface was identified as an important mechanism in the aging process. Co-precipitation of U with Fe oxide minerals (Duff et al., 2002) or carbonate mineral phases (Reeder et al., 2000) may represent alternative important processes in the long-term sequestration of U. Furthermore, the formation of reduced layers of U(IV) on U(VI) phases

through the activity of dissimilatory metal-reducing bacteria may also contribute to aging (Fredrickson et al., 2000).

Despite the comprehensive body of research surrounding U behaviour in the soil and its uptake by plants, comparatively few studies have attempted to directly relate the effect of various soil properties on plant uptake, and knowledge surrounding its aging is scarce. By utilising the DGT technique, this chapter aims to develop an understanding of the key soil properties involved in mediating the availability and aging of U in contaminated environments. The 549-day primary incubation will allow a quantitative assessment of the aging of U across a range of soil types to be made, and the effects of contrasting moisture regimes and microbial activity on aging will be elucidated through the secondary incubation.

6.2 Results and discussion

6.2.1 Availability and aging assessed by soil solution measurements

6.2.1.1 Aging process and kinetics

Figure 6.1 shows the concentration of U measured in the soil solution (C_{soln}) for all 20 incubated soils over 549 days aging, where C_{soln} has been normalised to the first measurement for C_{soln} made at day 3. Measured values of C_{soln} expressed per litre of soil solution (μg L^{-1}) have been converted to concentrations expressed per kg of air-dry soil (μg kg^{-1}). In Figure 6.1, C_{soln} appears to gradually increase over time, after initially declining over the first 46-72 days within all but four of the soils (M1-T, NP-A, BC-M, CO-A). After 549 days aging, C_{soln} is on average 1.63 times greater (median = 1.56) than measured at three days aging, ranging from 0.43 to 3.05. C_{soln} is found to be less than that measured after three days aging in only four soils (SR-W, SR-A, WS-A, SR-G).

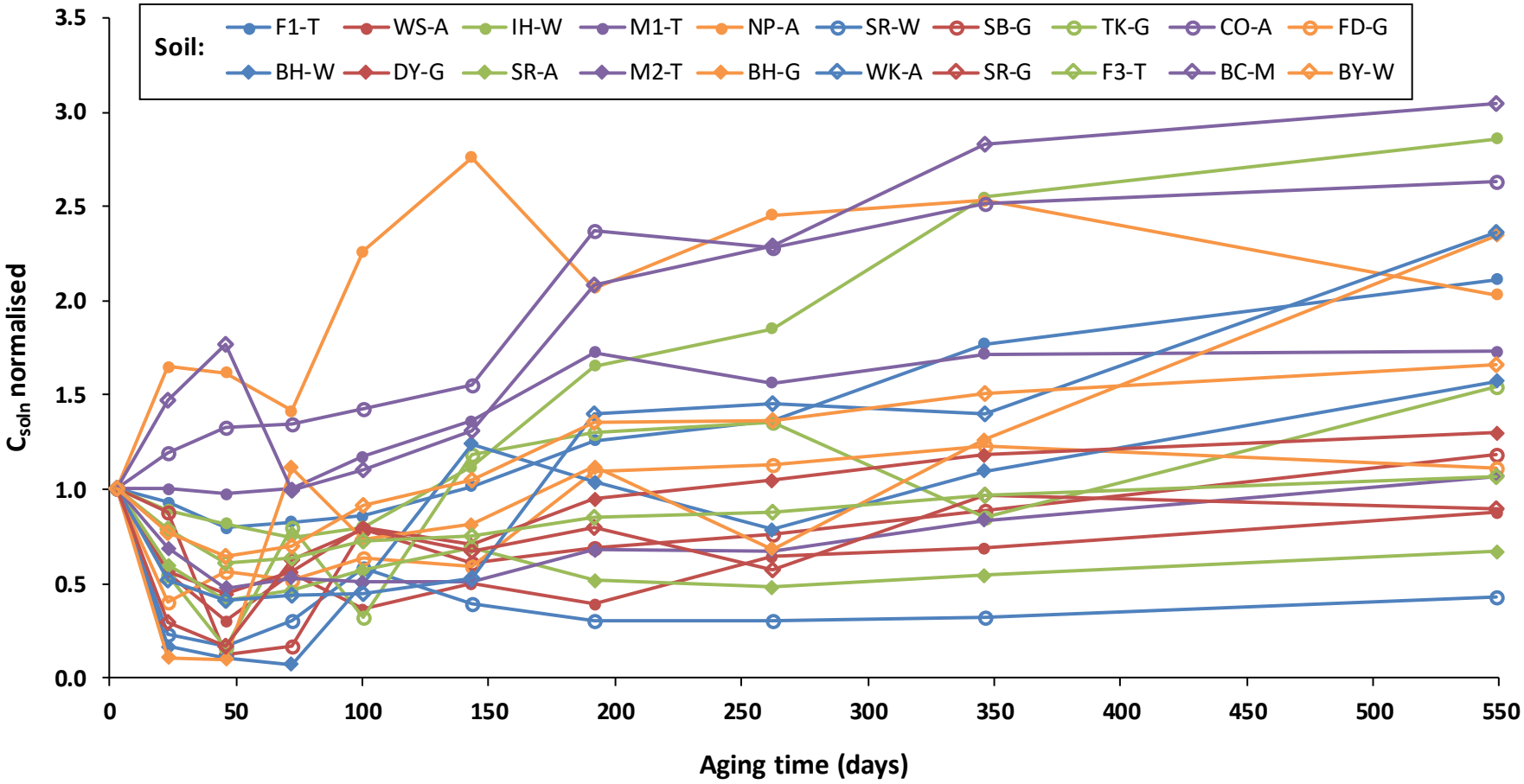

Figure 6.1. *Concentration of U measured in the soil solution (C_{soln}) for all incubated 20 soils over 549 days aging after normalising to day 3.*

6.2.1.2 Effect of soil properties on availability and aging

Spearman's rank correlation coefficients (r_s) describing the correlation between C_{soln} and soil properties at 3, 100 and 549 days aging are listed in Table 6.1. Strong positive correlation is calculated between C_{soln} and alkalinity throughout the incubation period (r_s = 0.70-0.73, $\alpha < 0.05$), whilst moderate positive correlation is calculated between C_{soln} and soil pH over the same period (r_s = 0.36-0.46). No relationship could be identified with C_{soln} for C_{org}, Fe or Al, although a weak to moderate degree of positive correlation is calculated between C_{soln} and Mn (r_s = 0.31-0.33).

Table 6.1. *Spearman's rank correlation coefficients (r_s) relating C_{soln} to soil properties after 3, 100 and 549 days aging (N = 20, except for alkalinity where N = 11).*

	Days of aging		
	3	**100**	**549**
Organic carbon	0.17	0.17	0.28
pH	0.46	0.46	0.36
Alkalinity	0.70*	0.71*	0.73*
Fe	0.20	0.16	0.20
Al	0.18	0.13	0.14
Mn	0.33	0.32	0.31

**Indicates significant relationship at α < 0.05; **Indicates significant relationship at α < 0.01*

The relationship between C_{soln} and soil pH is illustrated in Figure 6.2, where soils with a pH > 7 show considerably greater values for C_{soln} than in soils of pH < 7, typically by a factor of around 10. Using data from day 549 as an example, Figure 6.3 reveals that the positive correlation between C_{soln} and pH over the entire pH range of the incubated soils (3.32-8.00) is influenced to a large degree by the group of six soils with a pH > 7, which also exhibit relatively high alkalinity (> 100 mg L^{-1}).

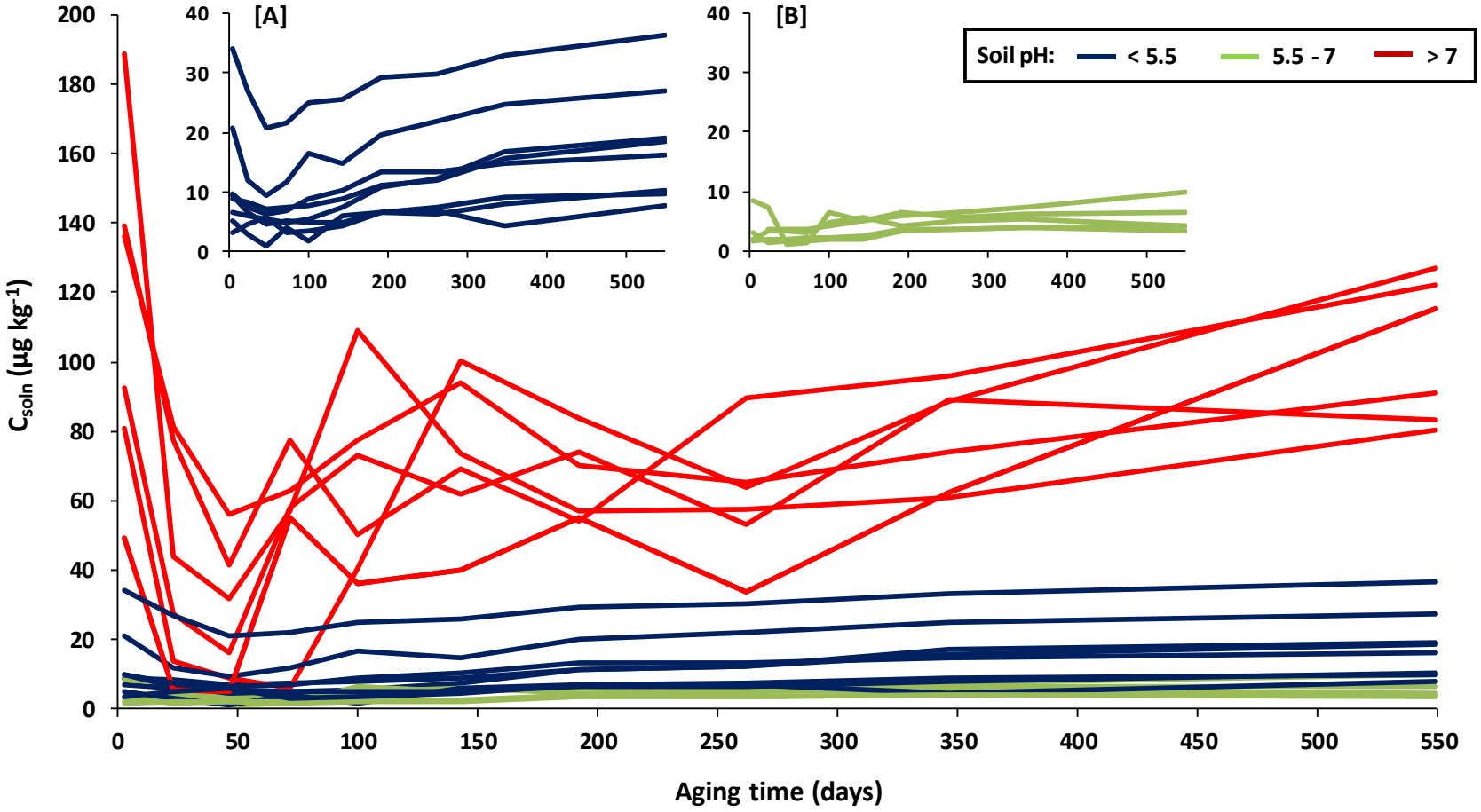

Figure 6.2. *Concentration of U in the soil solution (C_{soln}) (µg kg^{-1}), measured by centrifugation, for all 20 incubated soils over 549 days of aging. Soils are highlighted according to pH. The two inset graphs exclusively highlight soils of pH < 5.5* ***[A]*** *and pH 5.5-7.0* ***[B]****.*

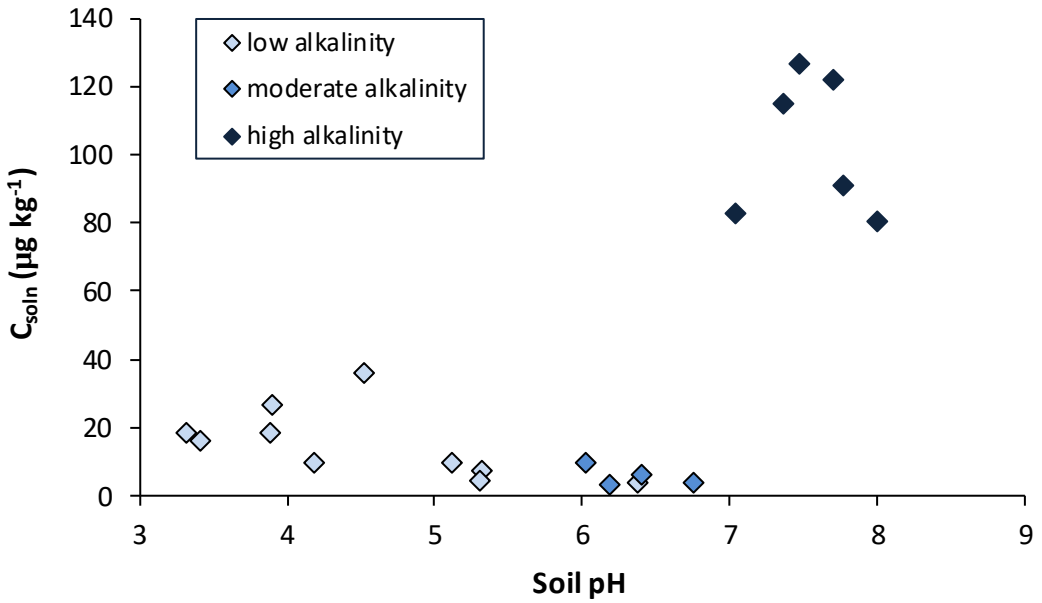

Figure 6.3. *Relationship between U in soil solution (C_{soln}) and soil pH for all 20 incubated soils after 549 days aging. Soils are highlighted according to alkalinity (mg L^{-1}): low (0-20), moderate (20-100) and high (> 100).*

Alkalinity is a measure of the acid-neutralising (buffering) capacity of water, derived from the presence of base anions including bicarbonate, silicate, borate and hydroxide, amongst other species. In soil, the weak acid bicarbonate (HCO_3^-) and carbonate (CO_3^{2-}) anions are the major components of alkalinity (Andrews, 2003), and so alkalinity can be expressed in molar terms as per Equation (6.1):

$$\text{Alkalinity} = [HCO_3^-] + 2[CO_3^{2-}] + [OH^-] - [H^+] \quad (6.1)$$

where: $[HCO_3^-]$ is the concentration of bicarbonate; $[CO_3^{2-}]$ is the concentration of carbonate anions; $[OH^-]$ is the concentration of hydroxyl ions; and $[H^+]$ is the concentration of hydrogen ions.

The relative contributions of the HCO_3^- and CO_3^{2-} species towards alkalinity is a function of the pH of the soil solution. At the same time, the pH of the soil solution is controlled by the relative contribution of dissolved inorganic carbon species (H_2CO_3, HCO_3^- and CO_3^{2-}). As pH decreases below 8, the activity of HCO_3^- declines in parallel with an increase in the activity of H_2CO_3 (carbonic acid), which is produced upon dissolution of CO_2 within the soil solution. Using Equation (6.1), alkalinity is equal to zero at the point of chemical equilibrium between CO_2 in the atmosphere and the pure MQ water applied to the soils; the pH of the resulting weak carbonic acid solution upon dissolution of the CO_2 at atmospheric partial pressure is approximately 5.65. This pH was taken as the reference point only above which alkalinity was measured within the incubated soils.

As discussed in Section 1.2.3, in the presence of carbonate ligands at higher pH (6-10), U forms anionic carbonate complexes (Dementeyev and Syromyatnikov, 1968; Giblin et al., 1981). This is illustrated in the U species fractionation diagram in Figure 6.4, where at pH 7 the most prevalent species of U is the $UO_2(CO_3)_2^{2-}$ anionic complex, followed by $UO_2(CO_3)_3^{4-}$. These U carbonate complexes are reported to be highly soluble (Langmuir, 1978) and are responsible for the significant solubilisation of U observed within the six alkaline soils of pH > 7 in Figure 6.2 and Figure 6.3. Decreased sorption accompanied by increased solubilisation of U at higher pH (> 7) is widely-reported in the scientific literature (Pabalan et al., 1996; Echevarria et al., 2001; Zheng et al., 2003; Vandenhove et al., 2007).

A further notable observation from Figure 6.2 concerns soils in the pH region 5.5 to 7; such soils display uniformly low values of C_{soln} which are in general collectively lower than C_{soln} values in soils of pH < 5.5. This observation hints at adsorption of U to the plastic soil containers upon wetting and mixing. Removal of U from solution in this pH range is reported elsewhere in studies investigating uptake of U from solution by DGT, where adsorption of U to the plastic container has been implicated.

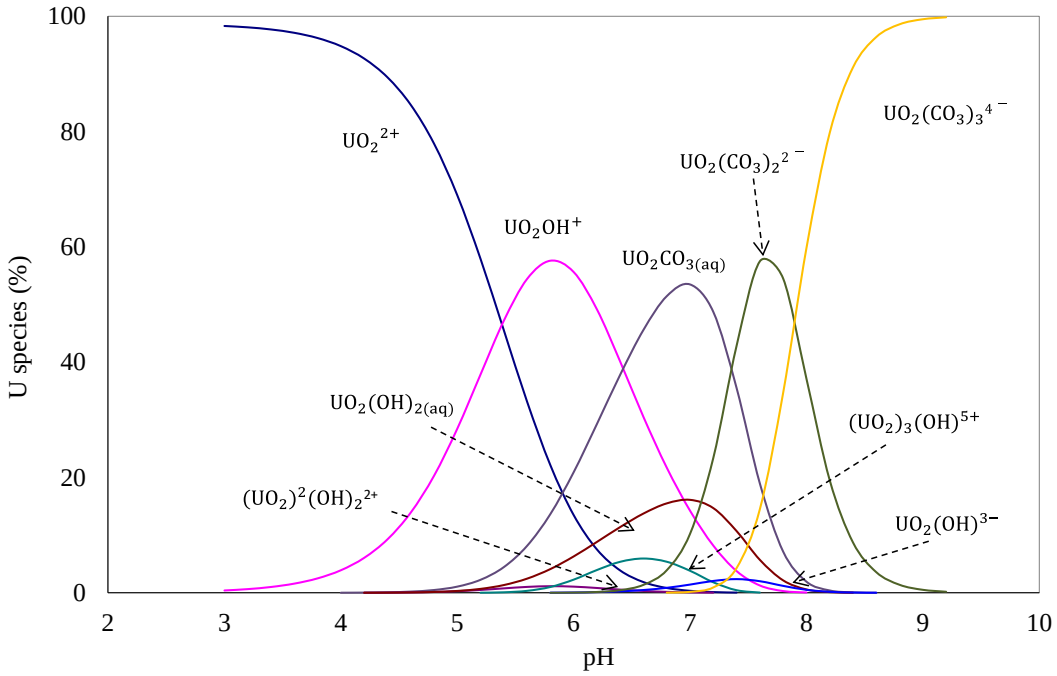

Figure 6.4. *Fractionation diagram illustrating the relative concentrations of different U species in a carbonate system as a function of pH. From: Cheng (2016).*

In Table 6.2, Spearman's rank correlation coefficients (r_s) describing the relationship between C_{soln} and various soil properties are presented after omitting the six soils of higher alkalinity (> 100 mg L^{-1}) These six soils were omitted as it was suspected that the presence of dissolved inorganic carbon at higher pH and its U-complexing ability obscured any relationships that may have been present between C_{soln} and other soil properties for soils of low alkalinity.

After excluding the six soils of high alkalinity (> 100 mg L^{-1}), strong negative correlation emerges between C_{soln} and pH over the range 3.32 to 6.76, which is highly significant at day 549 (r_s = -0.78, $\alpha < 0.01$). This relationship of increasing U in solution with decreasing soil pH is in contrast to the findings of studies by Echevarria et al. (2001) and Vandenhove et al. (2007), in which no relationship could be identified between pH and the K_D for U at lower pH (< 6).

Table 6.2. *Spearman's rank correlation coefficients (r_s) relating C_{soln} to soil properties after 3, 100 and 549 days incubation for soils of low to moderate alkalinity (< 100 mg L^{-1}) (N = 14).*

	Time after spiking (days)		
	3	**100**	**549**
Organic carbon	0.08	0.02	0.14
pH	-0.65*	-0.55*	-0.78**
Fe	-0.65*	-0.64*	-0.57*
Al	-0.41	-0.42	-0.38
Mn	-0.64*	-0.55*	-0.70**

**Indicates significant relationship at α < 0.05; **Indicates significant relationship at α < 0.01*

Strong negative correlation is also calculated with C_{soln} in Table 6.2 for both total Fe (r_s = -0.57 to -0.65, α < 0.05) and Mn [r_s = -0.55 (α < 0.05) to -0.70 (α < 0.01)]. A number of studies corroborate the significance of both Fe (Hsi and Langmuir, 1985; Payne et al., 1996; Lenhart and Honeyman, 1999; Jang et al., 2007) and Mn oxides (Sylwester et al., 2000; Al-Attar and Dyer, 2002; Froideval et al., 2006; Han et al., 2007) as important adsorbents for U. Organic matter is reported to enhance the sorption of U in soils (Thibault et al., 1990; Bednar et al., 2007; Vandenhove et al., 2007), but such a relationship could not be identified from the 14 soils of low to moderate alkalinity analysed in Table 6.2.

Another feature of the trend in C_{soln} for soils of pH > 7 presented in Figure 6.2 is that such soils are also characterised by temporal fluctuations in C_{soln}. Data from the secondary incubation for the two soils of pH > 7 (BH-G and SR-W) presented in Figure 6.5 reveal that the temporal fluctuations in C_{soln} observed in these soils are related to the moisture regime which the soils experienced during incubation. Fluctuations in C_{soln} only occurred within soils which underwent a period of extensive drying in-between ~72-hour saturation events for DGT deployments. In contrast, soils which were incubated at a constant moisture content [~40% of the soil maximum water holding capacity (MWHC)] in-between DGT deployments did not

exhibit such fluctuations, but rather a decline in C_{soln} over time as would be expected due to the effects of aging.

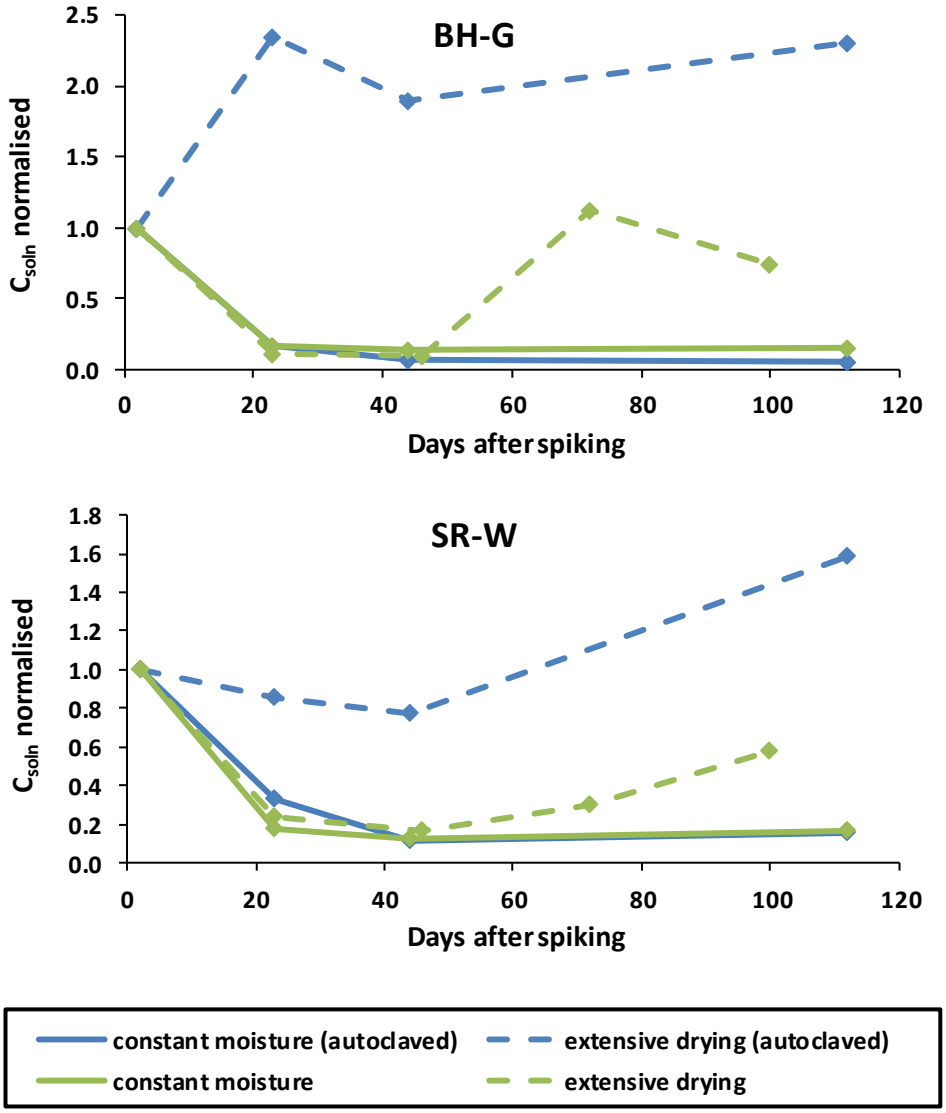

Figure 6.5. *C_{soln} normalised to the first sampling point (day 2) in subsamples of two alkaline soils (BH-G and SR-W) incubated for 120 days at contrasting moisture regimes.*

Drying and subsequent rewetting of soils has been demonstrated to alter the extractability of both major cations such as Al and Fe along with several trace metals (Bartlett and James, 1980; Haynes and Swift, 1991; Koopmans and Groenenberg, 2011). A number of studies have reported significant increases in the dissolved organic carbon (DOC) concentration in water

and weak salt extracts obtained from dried soils relative to moist soils (Kaiser et al., 2001; Peltovuori and Soinne, 2005; Klitzke and Lang, 2007). The accompanying increase in concentrations of total dissolved metals including Ni and Cu are attributed to the complexation of these metals with the elevated levels of humic and fulvic acids (Koopmans and Groenenberg, 2011). The fluctuations observed in C_{soln} for U are unlikely to be due to changes in the concentration of DOC however as the lack of correlation between C_{soln} and C_{org} content implies that C_{org} is not a significant component in the adsorption and binding of U.

The confinement of these fluctuations to soils of pH > 7 implies that variations in the concentration of dissolved carbonate ligands are directly responsible, which in turn must be controlled by the dissolution and precipitation of carbonate mineral phases in the soil. Erich and Hoskins (2011) found the concentration of Ca^{2+} ions in the soil solution to be on average 10% higher in two soils that were extracted at air-dry compared to field-moist conditions. Assuming a substantial fraction of the Ca^{2+} is precipitated as $CaCO_3$, then the release of Ca^{2+} must be accompanied by an increase in CO_3^{2+} ligands which then complex with uranyl cations to form the highly soluble uranyl carbonate complexes. The dissolution and precipitation cycles are driven by changes in pH which are observed to occur with soil drying (van Erp et al., 2001; Erich and Hoskins, 2011) . Drying has been shown to increase the acidity of soil surfaces (Dowding et al., 2005), which is likely to be responsible for the observed increased in extractability of major cations including Ca, Fe and Al (Erich and Hoskins, 2011).

Duquene et al. (2010) present evidence to support the absence of any aging effect for U as presented in this chapter. In their study, C_{soln} and exchangeable U (1 M NH_4OAc) were measured in 18 different soils containing aged U that had been previously used in a study by Vandenhove et al (2007). Across all the soils, C_{soln} was found to have increased on average by a factor of two (range = 0.4-4.5) relative to the values measured by Vandenhove et al. (2007) on freshly-spiked soils. Only two soils were found to have a C_{soln} less than that measured in

the freshly-spiked soils, and these had the highest pH of all the soils tested. This finding is strikingly similar to that observed within the range of soils incubated in this study. Figure 6.6 shows that after 549 days incubation, the four soils to exhibit a C_{soln} less than that measured at the first sampling point (day 2) also had the highest pH (> 7) for the range of soils tested. At the same time, Duquene et al. (2010) observed no decline in the exchangeable U fraction over the three years of storage.

The soils measured in the study by Duquene et al. (2010) had been stored in an air-dry state at ambient temperature for three years before being wetted to 50% of the water holding capacity and maintained at this level for three weeks. Analysis was performed at the end of this three-week incubation period. Duquene et al. (2010) speculated that the diffusion limitations imposed on the soils during the dry storage period may have hindered aging.

The increase in C_{soln} with incubation time, as observed in Figure 6.6, hints at the gradual release of U from the soil solid phase, perhaps due to dissolution of U-bearing mineral phases or precipitates. It is possible that such precipitates may have formed during the spiking of the soil. As detailed in Section 2.1.3, the U spike was added directly to the soil from a highly-acidic (HNO_3, pH 0.55) and concentrated stock solution (2500 mg U L^{-1}). According to the species fractionation diagram for U in Figure 6.4, U carbonate precipitates would be expected to form in those soils with a pH in the range 5.5 to 7.0.

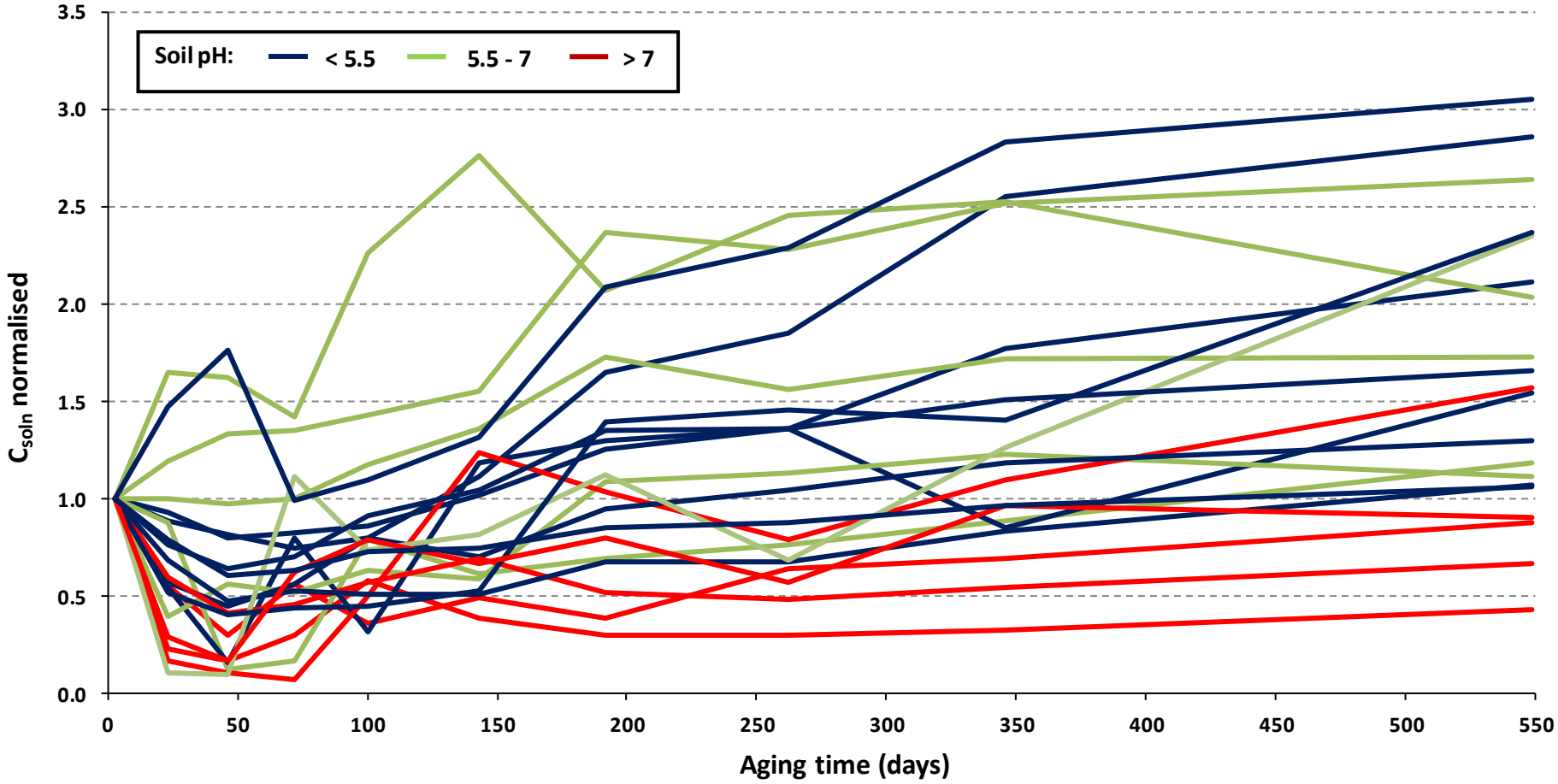

Figure 6.6. *Concentration of U in the soil solution (C_{soln}) for all 20 incubated soils over 549 days aging after normalising to day 3. Soils are highlighted according to pH.*

Alternatively, dissolution of native primary and secondary U-bearing mineral phases in the soil may be occurring since U is in fact fairly ubiquitous; across England for example, the topsoil concentration is typically in the range 1.39 - 3.82 ppm (10^{th}-90^{th} percentile) (UKSO). In the absence of unspiked control soils however, this hypothesis cannot be proven. Given that the absolute increase in C_{soln} within the incubated soils over the duration of the incubation period is only on the order of a few μg kg^{-1}, some degree of dissolution would certainly seem plausible.

Data from the secondary incubation presented in Figure 6.7 for both incubated soils of low pH, BY-W (pH 3.41) and WK-A (5.31), suggest that the cyclical wetting and drying of the soils during incubation may have been responsible for the observed increase in C_{soln} for soils of pH < 5.5. Figure 6.7 reveals that samples which experienced extensive drying between re-wetting events do not exhibit a clear decline in C_{soln}. In contrast, samples which were incubated at a constant moisture content and not subjected to extensive drying display a clear trend of decreasing C_{soln}.

It is hypothesised that following the initial period of rapid adsorption of U to the solid phase within the first few hours after spiking, the slow adsorption phase (aging) is counteracted by the extensive drying and re-wetting episodes which enhance the dissolution of Fe and Al oxides to which the U is adsorbed. The significant negative relationship between C_{soln} and Fe and Al oxides in Table 6.2 highlights the importance of these phases in the adsorption of U, whilst Erich and Hoskins (2011) reported that air-drying significantly increases the extractability of both Al (mean dry/moist concentration ratio = 1.69) and Fe (mean = 2.3) compared to moist soils. This was attributed to a decrease in soil pH that occurred with drying.

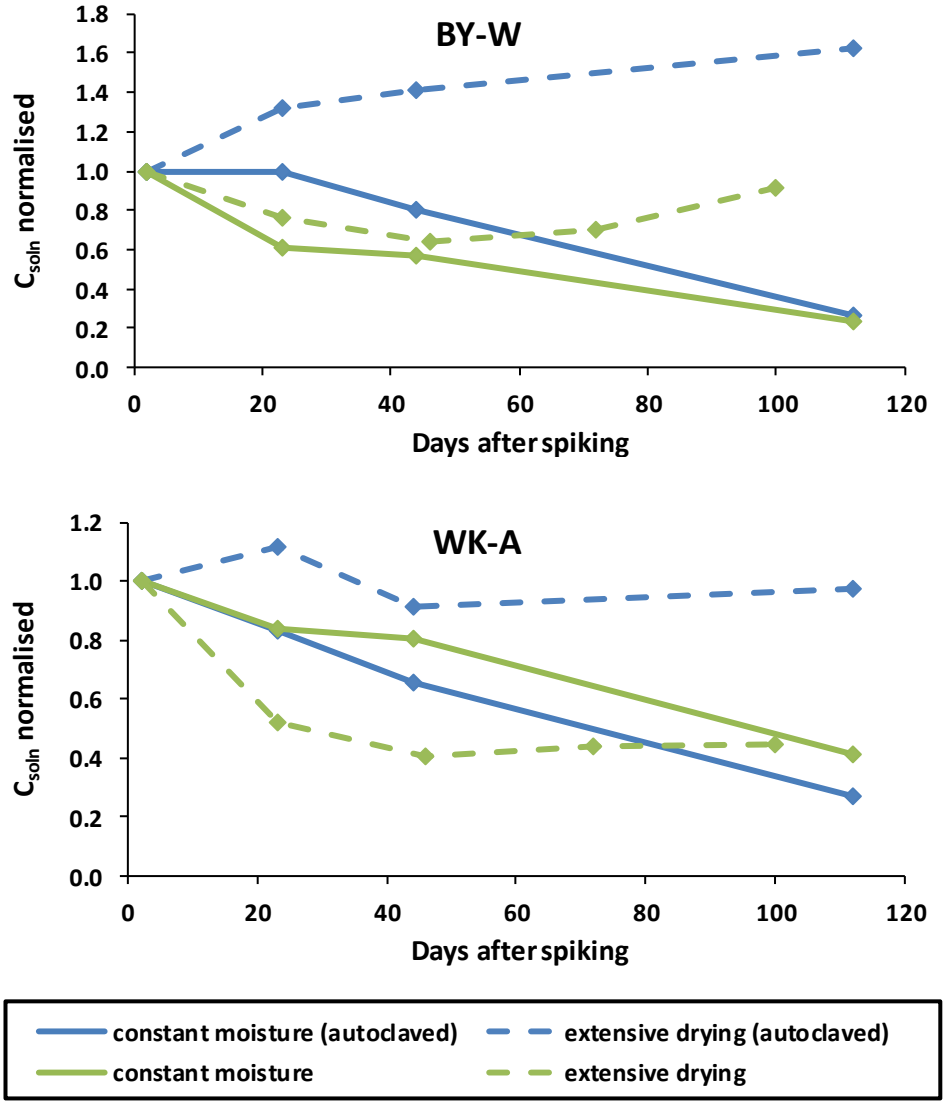

Figure 6.7. *C_{soln} normalised to the first sampling point (day 2) in subsamples of two different soils (BY-W and WK-A) incubated for 120 days at contrasting moisture regimes.*

6.2.2 Availability and aging assessed by DGT

6.2.2.1 Aging process and kinetics

The DGT-measured concentration of U in all 20 incubated soils over the course of the 549-day incubation is presented in Figure 6.8 after normalising to the first measurement for C_{DGT} made at day 3. The general trend is largely similar to that for C_{soln} (Figure 6.1) where minimal evidence for aging was observed in any of the soils. After 549 days aging, C_{DGT} across all 20 soils is between 21 and 273% of the availability at day 3 (median = 91%).

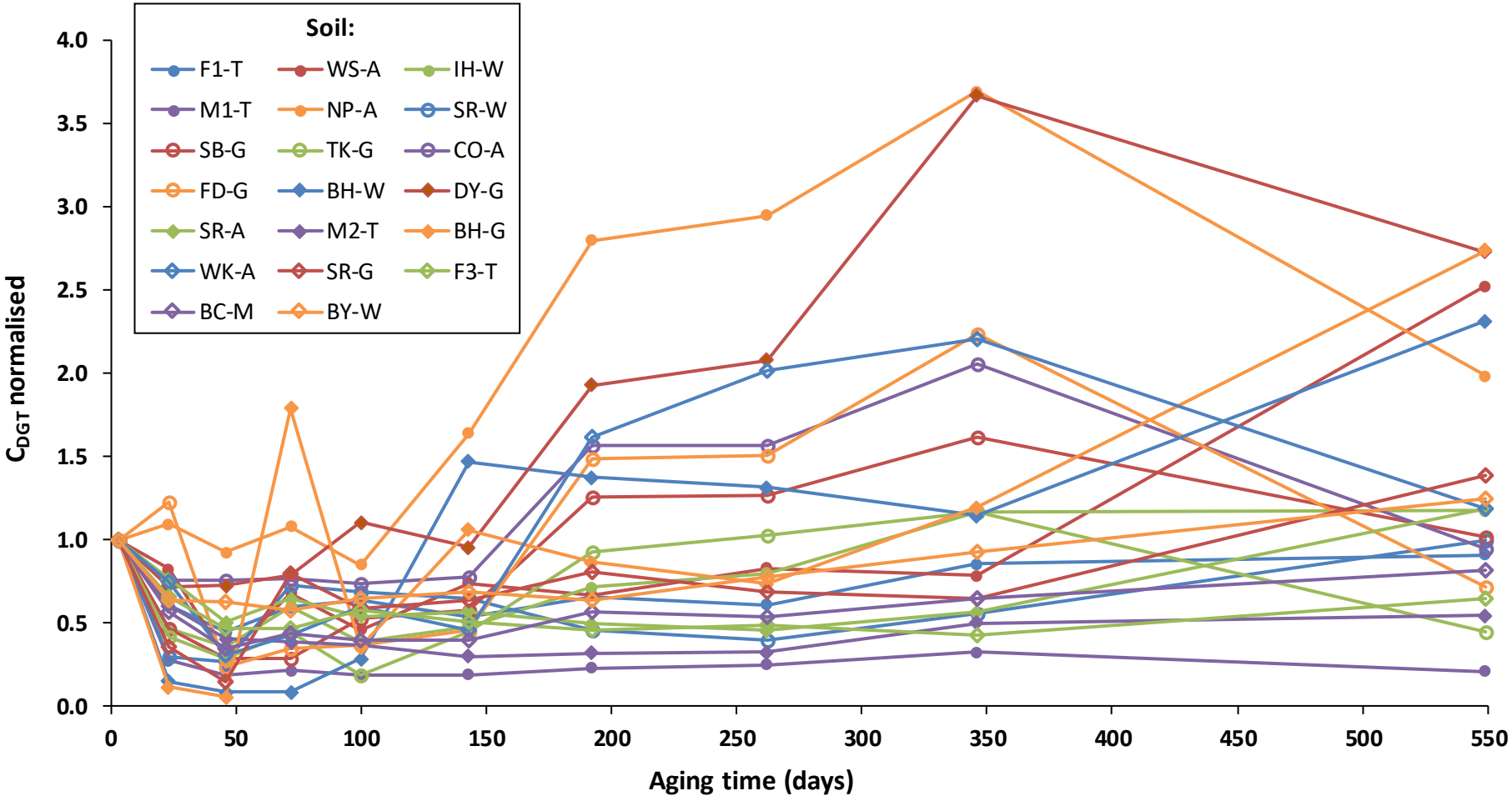

Figure 6.8. *Concentration of U measured by DGT (C_{DGT}) in all 20 soils over 549 days aging after normalising to day 3.*

6.2.2.2 Effect of soil properties on availability and aging

Spearman's rank correlation coefficients (r_s) describing the correlation between C_{DGT} and various measured soil properties for all 20 incubated soils at 3, 100 and 549 days aging are listed in Table 6.3. The findings are similar to those for C_{soln} in Table 6.1. Strong positive correlation is calculated between C_{DGT} and soil alkalinity (r = 0.48-0.70), which is significant at $\alpha < 0.05$ after 549 days aging. Correlation between C_{DGT} and pH is weak to moderate (r = 0.23-0.40), whilst correlation for all other soil properties is either absent or very weak over the three time points tested for the range of soils.

Table 6.3. *Spearman's rank correlation coefficients (r_s) relating C_{DGT} to soil properties after 3, 100 and 549 days incubation (N = 20, except for alkalinity where N = 11).*

	Aging time (days)		
	3	**100**	**549**
Organic carbon	-0.28	-0.28	-0.05
pH	0.32	0.23	0.40
Alkalinity	0.48	0.55	0.70*
Fe	-0.12	-0.16	0.08
Al	-0.14	-0.19	0.02
Mn	0.08	-0.03	0.24

**Indicates significant relationship at α < 0.05; **Indicates significant relationship at α < 0.01*

The strong positive correlation reported between C_{DGT} and alkalinity in Table 6.3 can be explained by the formation of highly soluble and stable anionic uranyl carbonate complexes (Langmuir, 1978). These complexes are reported to be of greater availability than the free uranyl cation (Boileau et al., 1985). For example, Shahandeh and Hossner (2002) investigated the uptake of U in 34 different plant species from nine different soils and observed that plants grown in calcareous soil accumulated a significantly greater quantity of U than those grown in acidic soils. Furthermore, Vandenhove et al. (2007) reported a soil-to-shoot transfer factor for ryegrass grown on alkaline soil 10 times higher than for an acid soil.

Tyler and Olsson (2001) reported that the concentration of U in the roots of *Agrostis capillaris* exhibited a distinct U-shaped trend in relation to soil pH, with a minimum occurring at pH 6.5-7. Figure 6.9 shows that this U-shaped trend is not obvious for the C_{DGT} values obtained for all 20 soils after 549 days incubation. A clear increase in availability occurs with increasing pH, where minimum values for C_{DGT} occur in the pH range 5.3-6.3. An increase in availability is also observed as pH decreases below pH 6, but the rate at which availability increases is significantly less than for soils of higher pH.

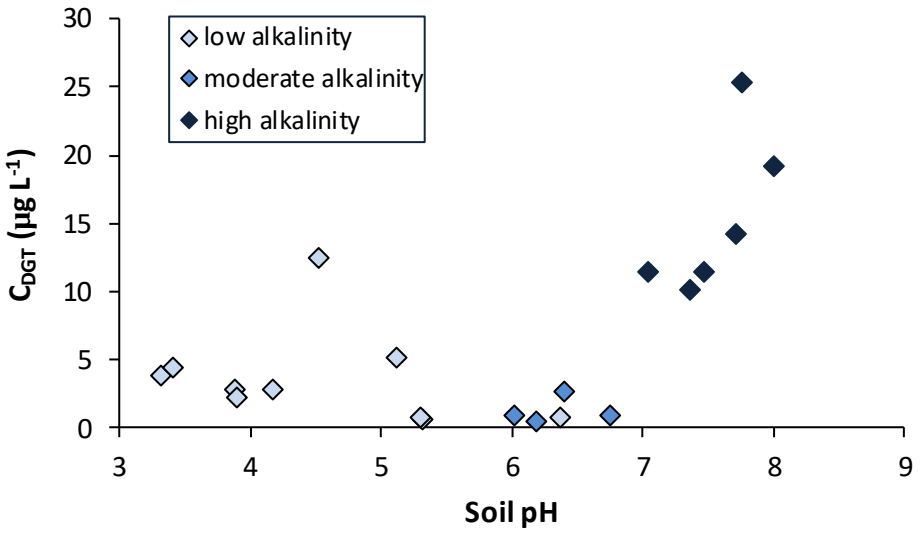

Figure 6.9. *Relationship between pH and C_{DGT} (µg L^{-1}) for all 20 incubated soils after 549 days aging. Soils are highlighted according to alkalinity (mg L^{-1}): low (0-20), moderate (20-100) and high (> 100).*

Table 6.4 presents Spearman's rank correlation coefficients (r_s) between C_{DGT} and soil properties after omitting soils of higher alkalinity (> 100 mg L^{-1}). This approach was taken on the basis that U forms highly soluble uranyl carbonate complexes in systems with significant dissolved inorganic carbon as discussed in Section 6.2.1.2, and this was shown to obscure relationships that were present with other soil properties. After excluding soils of higher alkalinity (> 100 mg L^{-1}), significant relationships are identified with C_{DGT} for Fe, Al and Mn that were not present when soils of higher alkalinity were included in the correlation analysis. The

strongest correlation with C_{DGT} was found for Fe (r_s = -0.62 to -0.77, $\alpha < 0.05$), followed by Mn (r_s = -0.55 to -0.65, $\alpha < 0.05$) and Al (r_s = -0.48 to -0.68). Weak to moderate negative correlation was calculated between C_{DGT} and C_{org} (r_s = -0.27 to -0.46), whilst slightly stronger negative correlation is calculated between C_{DGT} and pH (r_s = -0.40 to -0.60), which is significant at $\alpha < 0.05$ after 549 days aging.

Table 6.4. *Spearman's rank correlation coefficients (r_s) relating C_{DGT} to soil properties after 3, 100 and 549 days aging for soils of low to moderate alkalinity (< 100 mg L^{-1}) (N = 14).*

	Time after spiking (days)		
	3	**100**	**549**
Organic carbon	-0.43	-0.46	-0.27
pH	-0.40	-0.48	-0.60*
Fe	-0.62*	-0.77**	-0.64*
Al	-0.48	-0.68**	-0.54*
Mn	-0.55*	-0.64*	-0.65*

**Indicates significant relationship at α < 0.05; **Indicates significant relationship at α < 0.01.*

Vandenhove et al. (2007) performed DGT measurements of U availability on six soils with differing histories of U contamination and found the highest values for C_{DGT} to occur in soils with a low amorphous Fe and C_{org} content. Further analysis of the C_{DGT} dataset included in Duquene et al. (2010) revealed a significant relationship between C_{DGT} and C_{org} ($r = -0.65$, $p < 0.05$, $n = 14$) for soils of pH < 6.5. Negative correlation with amorphous Fe ($r = -0.52$) over the same pH range was also found, but this was just short of being significant at $p < 0.05$. Both datasets corroborate with the correlation analysis presented in Table 6.4 for the soils of low to moderate alkalinity (< 100 mg L^{-1}) from the primary incubation, although the relationship between C_{DGT} and C_{org} was short of being significant at $\alpha < 0.05$. Similarly, a highly significant negative relationship ($r = -0.72$, $p < 0.01$, $n = 14$) between C_{DGT} and pH for acidic soils of pH < 6.5 could be elucidated from the C_{DGT} dataset of Duquene et al. (2010), in support of the negative correlation calculated in Table 6.4.

Figure 6.4 reveals that the speciation of U in acidic soils (pH < 6.5) is dominated by the positively-charged uranyl (UO_2^{2+}) cation, with a shift towards the formation of hydroxide complexes as the pH approaches neutrality. The strong negative correlation between C_{DGT} and total soil oxides including Fe, Al and Mn in Table 6.4 suggests that adsorption of UO_2^{2+} to these phases is responsible for the removal of UO_2^{2+} from solution. Given the pH range of the soils analysed in Table 6.4 (pH 3.32-6.76), oxide phases of Fe, Al and Mn in the soil are expected to have a net positive charge since oxide phases for these elements have a high point of zero charge (pzc) typically in the pH range 6.7 to 9.0 (Sparks, 2003). Consequently, adsorption through electrostatic attraction is unable to occur. In the literature however, adsorption of UO_2^{2+} to variably-charged oxides is reported to occur under acidic conditions below the pzc for these oxides. For example, (Waite et al., 1994) reported that adsorption of U(VI) to ferrihydrite increased from near zero at pH 3.5 to greater than 99% of the total U(VI) at pH 5.5. Dublet et al. (2017) suggested that the observed adsorption was in fact the result of the formation of covalent bonds between UO_2^{2+} cations and surface oxo or hydroxo sites, and observed themselves the formation of inner-sphere, mononuclear, bidentate UO_2^{2+}-ferrihydrite sorption complexes at pH 4.6.

The weak to moderate negative correlation calculated between C_{DGT} and C_{org} in Table 6.4 (r_s = -0.27 to -0.46) suggests that C_{org} also plays a role in controlling the availability of U for DGT uptake. The surface charge for most natural organic matter in soils is negative over the pH range 2-10 (Hosse and Wilkinson, 2001), so direct adsorption of UO_2^{2+} to organic matter could be occurring in the soils. Several studies have shown a strong association between U, natural organic matter and Fe oxide phases in sediments and groundwaters (Regenspurg et al., 2010; Banning et al., 2013), and under acidic conditions the presence of humic substances has been shown to enhance the adsorption of UO_2^{2+} to the surfaces of Fe oxides (Payne et al., 1996; Lenhart and Honeyman, 1999). However, it is not clearly understood whether UO_2^{2+}

binds to the reactive sites on the oxide surfaces or to organic functional groups in organic matter within these ternary systems.

In Figure 6.10, the rate of aging within all 20 incubated soils is presented after highlighting the soils according to their pH. For soils of pH < 7, C_{DGT} declines over the first 50-100 days after spiking, before increasing over the remainder of the incubation period. The rate of increase in C_{DGT} varies between soils but is generally slower in more acidic soils with a pH < 5.5. Soils of pH > 7 exhibit a rapid decline in availability over the first ~50 days of incubation, but thereafter C_{DGT} fluctuates with a general trend of increasing availability.

Based upon the evidence presented in this chapter, it would appear that any effect of aging is counteracted by the extensive drying of the soils followed by re-wetting. It is not clear what the precise mechanism is that leads to the dissolution of U under such a moisture regime, but as detailed in Section 6.2.1.2, it is hypothesised that an increase in the concentration of Fe and Al oxides in solution to which the U is adsorbed, owing to a decrease in pH that accompanies soil drying, may be responsible.

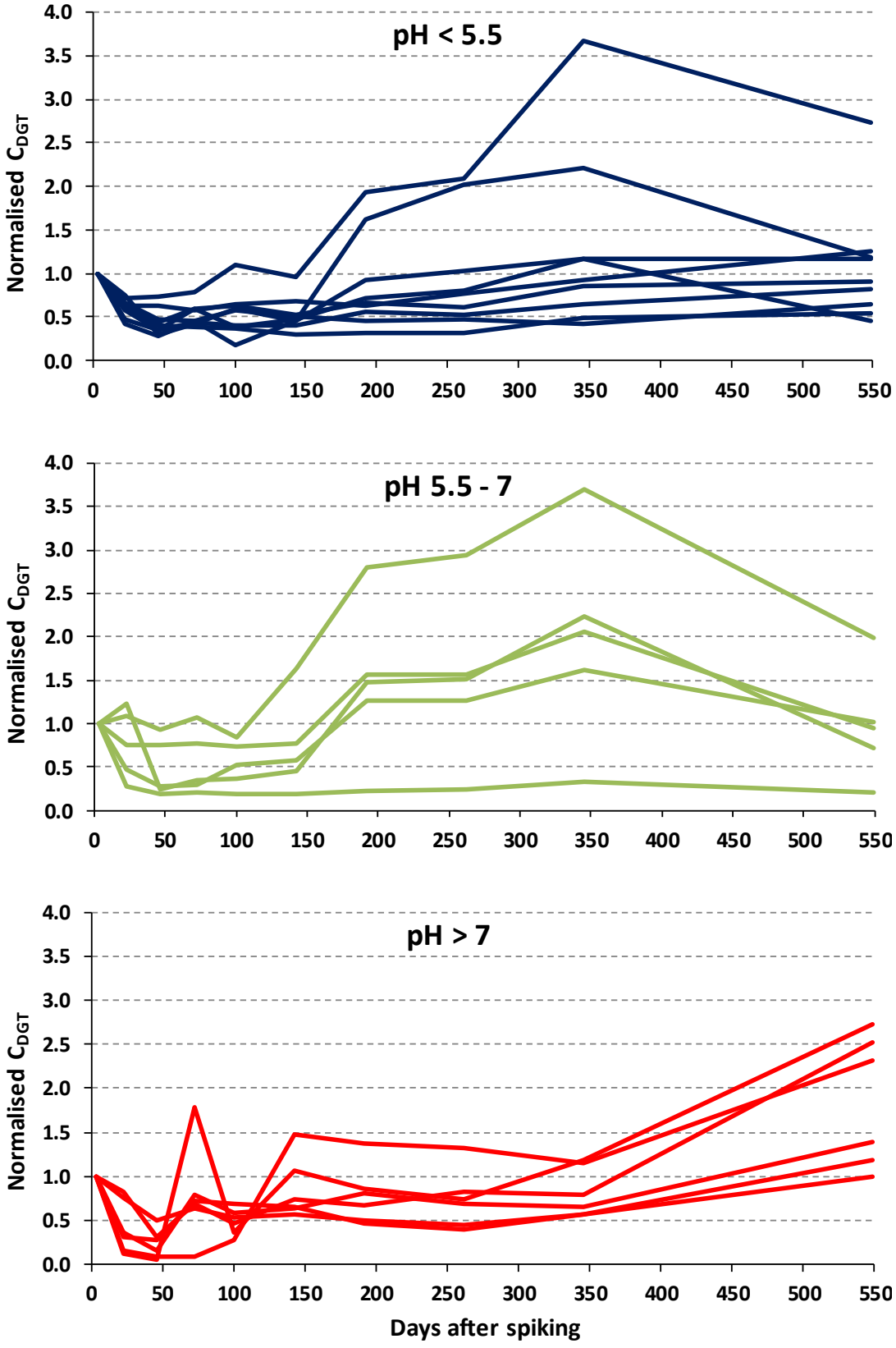

Figure 6.10. *DGT-measured concentration of U (C_{DGT}) over incubation time for all 20 soils after normalising to day 3. Soils are grouped according to pH.*

Rout et al. (2016) reported extensive aging of U over an 11-month incubation period where the exchangeable (0.4 M $MgCl_2$) fraction was found to decrease by 94.86 and 95.64% in two soils of pH 6.9 and 8.1, respectively. The decrease in the exchangeable fraction was attributed to the formation of increasingly stable complexes with organic and carbonate ligands, or adsorption and/or co-precipitation of U on oxides of Fe and Mn. The soils were stored in tubes at an air-dry state with regular exposure to the ambient environment, and therefore would have experienced extensive drying in much the same way as the soils studied by Duquene et al. (2010). A third soil (pH 7.5) did exhibit a slight increase in the exchangeable fraction however, but no attempt was made by Rout et al. (2016) to explain this. It would appear that the length of the re-wetting period may influence the extent of dissolution of U. The soils in the study of Rout et al. (2016) which exhibited aging of U were re-wetted for just one hour during the extraction procedure, yet the soils of this study and those investigated by Duquene et al. (2010) that demonstrate increasing dissolution of U with time were re-wetted for a considerably longer period of ~48 hours and up to three weeks, respectively.

6.2.3 Resupply of U from the soil solid-phase

Figure 6.11 presents R values at day 3 and day 549 for all 20 incubated soils, in addition to the corresponding R_{diff} value. As detailed in Section 1.8, an R value expresses the ratio between the concentration of U measured by DGT and the concentration measured in the bulk solution (C_{soln}). As R increases, the capacity of the solid phase to resupply U to the soil solution in response to the DGT-induced depletion increases, and the concentration in solution is more effectively buffered within the vicinity of the DGT device. Where resupply is absent, U supply to the DGT is confined to diffusional transport, which is influenced by the soil porosity and tortuosity, and the R value is referred to as R_{diff}.

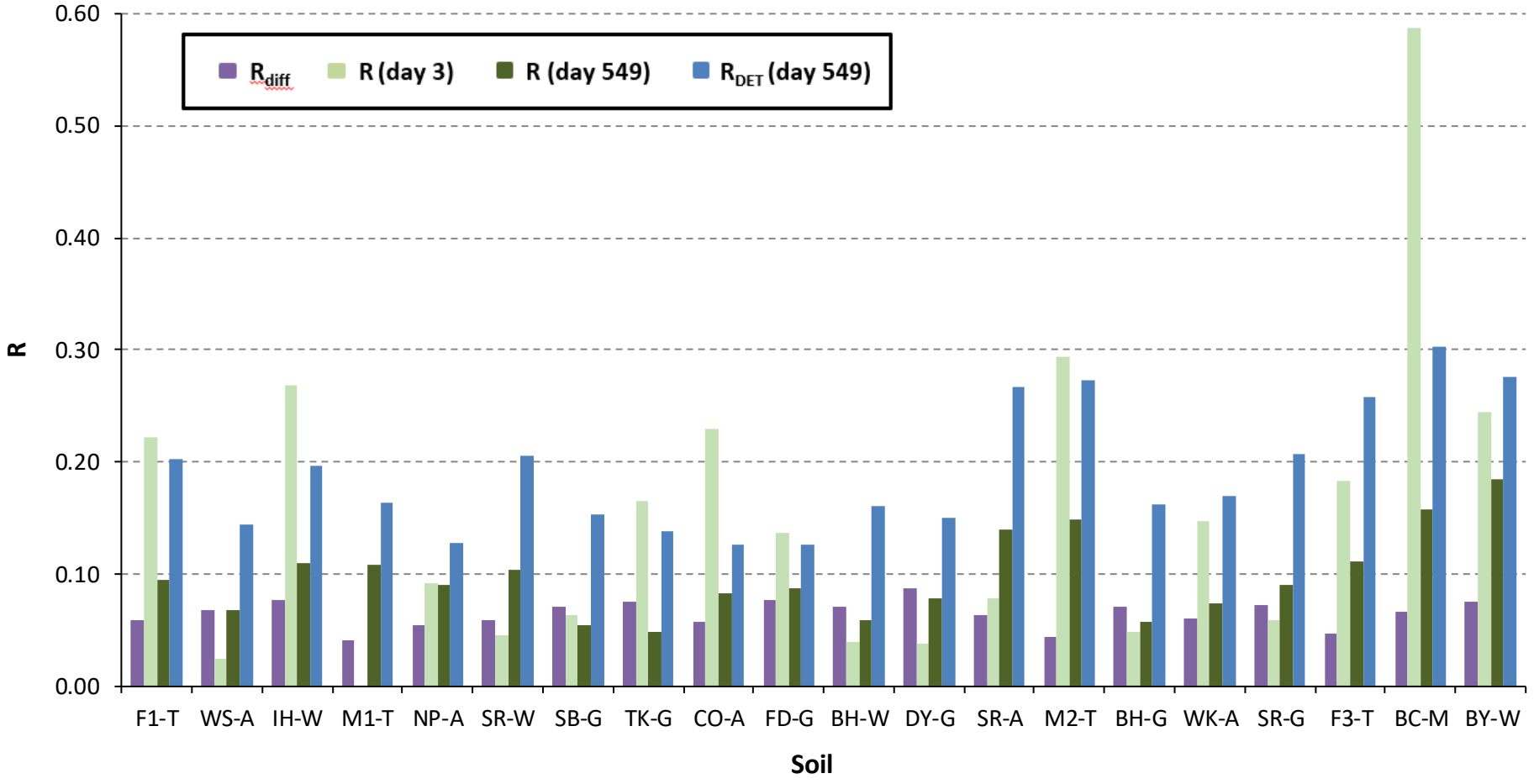

Figure 6.11. *R values at day 3 and day 549 for all 20 incubated soils in addition to the corresponding R_{diff} value for each soil. Also plotted are R values at day 549 using DET to determine U soil solution concentration (R_{DET}).*

Values for R at day 3 in Figure 6.11 range from 0.02 to 0.59 (median = 0.14). Six of the soils (WS-A, SR-W, BH-W, DY-G, BH-G and SR-G) exhibit R values which are comparable to or less than the corresponding R_{diff} values. After 549 days incubation, R values are generally lower, ranging from 0.05 to 0.18 (median = 0.09). However, R values over this period have not necessarily declined in all of the soils, with approximately half staying the same or even increasing slightly. Using DET to determine C_{soln} after 549 days yielded increases in the R values (R_{DET}) for all soils of between 0.04 and 0.15 (median = 0.10). Only the species which are physically small enough to undergo diffusion through the polyacrylamide diffusive gel layer of the DGT will be measured by DET (Davison and Zhang, 1994). Variation in the difference between RDET and R at day 549 could not be explained by any individual soil property.

The generally low R values (R and R_{DET}) across the range of soils at both short (3 days) and longer (549 days) timescales after spiking suggest that the size of the labile fraction of U associated with the solid phase is small, or alternatively the rate of desorption is slow. The absence of any sign of aging across the range of soils presented in Sections 6.2.1 and 6.2.2 is in contrast to the collective decline in R values over the duration of the incubation, which implies that the U is converted to more stable forms that are less available and less labile.

Spearman's rank correlation analysis failed to identify any significant relationships between any one particular soil property and various resupply parameters, which included R, $R–R_{diff}$ and $R_{DET}–R_{diff}$. The same was true even after omission of soils of higher alkalinity (> 100 mg L^{-1}). The two soils exhibiting the highest extent of resupply (BC-M and M2-T) are both sandy and acidic, but at the same time a number of other soils which are also sandy and acidic exhibit a much lower extent of resupply. Clearly a complex interplay of parameters is responsible for governing resupply, with stepwise regression analysis needed to interrogate the data further.

The R values presented for U presented in Figure 6.11 are lower than those reported in the studies by Vandenhove et al. (2007) and Duquene et al. (2010). Vandenhove et al. (2007) calculated R values of between 0.11 and 0.57 (median = 0.19) for six contrasting soils. The highest R value was recorded in an alkaline soil, which was taken to infer that the dissociation of the anionic urnanyl complexes in solution must be rapid. Conversely, the six soils of high alkalinity (> 100 mg L^{-1}) in this study (WS-A, SR-W, BH-W, SR-A, BH-G and SR-G) all exhibit exceptionally low R values in Figure 6.11 which are less than or comparable to the R_{diff} value. This suggests that the uranyl carbonate complexes are extremely stable and unable to dissociate within the timeframe (on the order of minutes) that it takes for the species to be transported through the diffusion layer, since only the free uranyl ion is assumed to bind to the Chelex resin.

Duquene et al. (2010) reported R values ranging from 0.19 to 1.02 (median = 0.39) across 18 contrasting soils that had been aged for approximately three years. No relationship could be elucidated between any single soil parameter and the R values, thus in agreement with the findings of this study. The analysis by Duquene et al. (2010) included several additional soil properties that were not investigated in this study, namely the cation exchange capacity, Olsen P and the concentration of major ions in the soil solution (Mg^{2+}, K^{+}, Ca^{2+}, HPO_4^{2-} and SO_4^{2-}). The U speciation in the soil solution was not able to effectively explain R values either.

In this study, a 0.01 M $CaCl_2$ extraction was used to determine the exchangeable U fraction (C_{sorbed}) in all 20 soils after the final DGT deployment. From this, a K_D describing the distribution of U between the solution and labile solid phase ($K_{D\text{-}labile}$) could be derived by dividing C_{sorbed} by C_{soln}. The $K_{D\text{-}labile}$ values are presented in Figure 6.12, where they have been plotted against $R_{DET} - R_{diff}$. The $K_{D\text{-}labile}$ values cross the range of soils are found to be extremely low, ranging from 0.0009 to 0.0219 (median = 0.0102), which suggests that the size of the labile U fraction is very small relative to C_{soln}. Weak to moderate positive correlation is observed between

$K_{D\text{-labile}}$ and R_{DET}–R_{diff} (n = 14, r_s = 0.32), which implies that the extent of resupply from the solid phase could be directly related to the size of the labile U fraction.

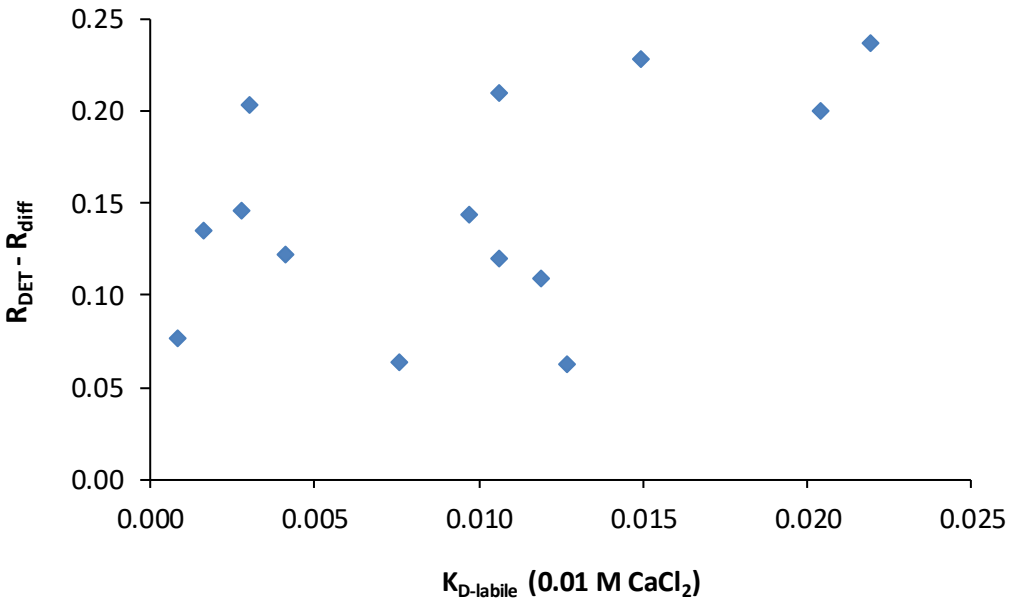

Figure 6.12. *Relationship between R_{DET}–R_{diff} and the U K_D obtained by extraction with 0.01 M $CaCl_2$ ($K_{D\text{-labile}}$). Soils in which the concentration of U in $CaCl_2$ extracts is below the detection limit have been omitted (N = 14).*

A caveat to using R values to assess desorption rates for metals in soils is that the DIFS (DGT-induced Fluxes in Soils/Sediments) model considers all complexes in solution to be fully labile, which in reality is not always the case (Degryse et al., 2009). The exceptionally low R values presented in Figure 6.11 for alkaline soils are likely to be the result of the inherently slow dissociation kinetics of the uranyl carbonate complexes. The consequently low DGT response is reflected through low values of R, which restricts the use of the R value in interpreting desorption kinetics for these soils.

Soil response times (T_c) (s) calculated using the 2D version of the DIFS model are presented in Table 6.5, along with the sorption (k_1) and desorption (k_{-1}) rate constants. The response time embraces the capacity of labile U associated with the solid phase in addition to its rate

constant of release (Ernstberger et al., 2005). Values of T_c for U are very short (0.05 to 0.52 s, median = 0.15 s), and most likely reflect the very small pool size of labile U. Rate constants for k_{-1} are collectively an order of magnitude or two greater than k_1, and so desorption from the solid phase is rapid. No correlation can be identified between T_c or the rate constants (k_1 and k_{-1}) and any of the soil properties, even after omission of soils of higher alkalinity (> 100 mg L^{-1}).

Table 6.5. *Soil response times (T_c), sorption rate constants (k_1) and desorption rate constants (k_{-1}) calculated by the 2D-DIFS model for all 20 incubated soils.*

Soil	T_c (s)	k_1 (s^{-1})	k_{-1} (s^{-1})
F1-T	0.19	0.11	5.15
WS-A	0.09	0.02	11.09
IH-W	0.15	0.10	6.57
M1-T	0.07	0.22	14.07
NP-A	0.11	0.33	10.10
SR-W	0.26	0.02	3.82
SB-G	0.08	0.15	6.67
TK-G	0.05	0.36	19.84
CO-A	0.19	0.22	15.50
FD-G	0.21	0.17	7.11
BH-W	0.34	0.11	4.23
DY-G	0.11	0.07	9.02
SR-A	0.29	0.02	3.43
M2-T	0.28	0.17	3.39
BH-G	0.20	0.31	14.20
WK-A	0.05	0.51	19.65
SR-G	0.09	0.03	10.93
F3-T	0.52	0.06	1.87
BC-M	0.20	0.19	4.71
BY-W	0.32	0.09	3.01

6.3 Conclusions

Soil alkalinity exerts the greatest influence on U availability, which is found to be greatly enhanced in the presence of higher concentrations of dissolved inorganic carbon. This influence can be attributed to the formation of highly soluble and stable anionic uranyl carbonate complexes. For soils of low alkalinity, U availability is found to be strongly correlated with Fe, Al and Mn oxides, whilst weaker correlation is evident with C_{org}. This suggests that U may be adsorbed indirectly by OM-cation (e.g. Fe, Al, Mn) complexes to form a U-OM-metal ternary system, where UO_2^{2+} binds to reactive sites on the oxide surface.

Minimal evidence for aging is presented across the range of soils incubated in this study, with a convoluted temporal trend in availability observed. In general, soils of pH < 7 exhibit an increase in C_{soln} for U over time, whilst soils of pH > 7 are characterised by substantial temporal fluctuations. Both these trends appear to be related to the moisture regime under which the soils were incubated, as soils which were incubated at a constant 'moist' level (~40% MWHC) between the re-wetting events associated with DGT deployments conversely demonstrate a clear decline in C_{soln} and C_{DGT} over time, as would be expected due to the effects of aging. Changes in soil pH driven by cyclic episodes of extensive drying and re-wetting are hypothesised to counteract aging by altering the solubility of Fe, Al and Mn oxides to which the U is adsorbed. Within alkaline soils, fluctuating availability is attributed to variations in the concentration of dissolved carbonate ligands which are driven by the dissolution and precipitation of carbonate mineral phases in the soil. Again, changes in pH are ultimately responsible.

Resupply of U from the solid phase across the range of soil types is low, both at short and longer durations (up to 549 days) of aging, and marginally declines throughout the course of the incubation. The minimal extent of resupply is seemingly attributable to the very small pool

of labile U associated with the solid phase, as determined through extraction with 0.01 M $CaCl_2$, which suggests that the majority of the U in the soil is irreversibly adsorbed and therefore unavailable for uptake. Exceptionally low R values in alkaline soils imply that the kinetics of dissociation for uranyl carbonate complexes are particularly slow, which inhibits their measurement by DGT. No single soil property can explain the observed variation in any of the DGT-derived kinetic parameters.

This page intentionally left blank

Chapter 7: Can DGT predict technetium-99 uptake by ryegrass?

7.1 Introduction

Traditionally, bioavailability of an element for plant uptake has been assessed through equilibrium-based chemical extraction methods. As reviewed in Section 1.4, a plethora of techniques has been developed targetting exchangeable species bound to the solid phase and labile species in solution. The in situ kinetic approach of diffusive gradients in thin-films (DGT) has emerged as a promising tool for assessing bioavailability owing to its ability to perturb the soil system in the same manner as a plant would by mimicking the rate of removal of an element by plant roots (Lehto et al., 2006; Degryse et al., 2009; Zhang and Davison, 2015). A comprehensive review of the application of DGT in studies of bioavailability can be found in Section 1.9, so the mechanisms by which DGT can mimic root uptake by a plant shall not be discussed here. Most studies relating to DGT and bioavailability are centred on toxic cationic divalent trace metals (Nolan et al., 2005; Perez and Anderson, 2009; Tandy et al., 2011). Only a handful of studies can be found that use DGT to investigate radionuclide bioavailability to plants (Vandenhove et al., 2007; Duquene et al., 2010; Mihalik et al., 2012), and these are confined to U.

No model or assay of bioavailability can be applied to all elements, soil types and plant species. Indeed, the ability of DGT to mimic plant uptake may be limited where uptake of an element is not limited by diffusional supply through the soil (Degryse and Smolders, 2016). Furthermore, DGT treats all taxa across the plant kingdom as identical sinks, yet it is well-recognised that differences in uptake of an element occur right down to the species level, even when an element is of equal availability (White and Broadley, 2003; Watanabe et al.,

2007). In the case of Tc, recent work by Willey et al. (2010) identified a significant phylogenetic signal which mediated the soil-to-plant transfer of Tc for 116 different plant taxa. Plants on the monocot clade were found to take up Tc to a lesser extent than those on the eudicot clade.

The objective of the work presented in this chapter was primarily to assess the ability of DGT to predict plant uptake of Tc across a range of contrasting soils, using perennial ryegrass (*Lolium perenne*) as the test species. For this study, it was decided to focus on Tc since the performance of the mixed binding layer DGT was previously shown to be compromised when measuring Se in alkaline soils (Section 5.2.2.1), with similar results expected for U (Section 3.3.8). Ryegrass is a suitable choice of plant because it germinates easily and grows relatively fast. Although native to southern Europe, North Africa and central Asia, its distribution extends globally to North and South America, Australia, and South Africa (CABI, 2017). Ryegrass is used widely as forage for livestock, and therefore represents an important transfer pathway for Tc from the soil into the food-chain. Uptake of Tc by ryegrass is substantial and was previously found to fit an exponential model of biomass production showing that bioavailability decreased with biomass production as opposed to time (Echevarria et al., 1997).

The ability of DGT to predict ryegrass uptake of Tc in this work was examined by assessing the linearity of the relationship between DGT-measured soil concentrations of Tc and the activity measured in the harvested ryegrass biomass. Typically, in studies investigating the relationship between plant and DGT uptake, the deployment of DGT is made at the end of the growth period immediately after biomass sampling or at the beginning of experiment before growing plants. In this work, it was decided to experiment with deploying DGT in situ within the same container as the ryegrass during the growth phase to determine if this approach was more suitable for predicting plant uptake. At the same time, the ability of DGT to predict

ryegrass uptake was compared to extraction by 0.01 M $CaCl_2$, the conventional approach for assessing plant-available Tc in soil (Echevarria et al., 1997; Tagami and Uchida, 1998).

7.2 Methods

7.2.1 Soil selection and spiking

The eight soils selected to form the basis of this chapter were: BY-W, DY-G, SR-W, TK-G, FD-G, BC-M, WK-A and SR-G (see Appendix A.1 for site description and soil properties). These soils were selected to encompass a range of physico-chemical properties, with particular emphasis on organic carbon (C_{org}), pH and total Al, Fe and Mn oxides. The soils were freshly-sampled from the field and upon return to Lancaster were air-dried in a fume hood before sieving to < 2 mm particle size. Key soil properties were remeasured on the fresh samples to account for localised spatial heterogeneity at sampling sites, the results of which are presented in Appendix A.3. Soil pH was measured in a suspension, comprising soil and deionised (DI) water in a 1:2.5 ratio, after shaking for 30 minutes on an end-over-end shaker to attain equilibrium. The carbon content, taken to represent organic carbon (C_{org}), was determined using a CHNSO elemental analyser. Soils with a pH > 7 were pre-treated to remove inorganic carbon by digesting 2 g of soil in 3 mL of 1 M H_2SO_4-5% $FeSO_4$ (Sparks, 1996). Soil nitrate (NO_3^-) was determined in 2 M KCl soil extracts (1:10 soil:extractant ratio) using a Seal Analytical AA3 segmented flow analyser.

For spiking, 138.82 kBq of ^{99}Tc was added to 2.2 kg (dry weight) of each soil to achieve a spiking concentration of 63.1 kBq kg^{-1} ^{99}Tc (100 µg Tc per kg dry soil). A food blender was used to thoroughly mix and homogenise the spike throughout the soil. The volumetric capacity of the blender meant that each soil was sub-divided by weight into two equal subsamples that were spiked separately. An NH_4TcO_4 stock solution (740 kBq ^{99}Tc mL^{-1}) was diluted in 50 mL of DI water and poured uniformly over the soil within the blender. After an initial blend, DI water

was incrementally added to the soil with intermittent blending until the soil was moist, with a consistency resembling ground coffee. The final moisture content of each soil is listed in Appendix A.3. Each freshly-spiked soil was transferred to four rectangular (22.5 x 11 x 5.5 cm) 800 mL capacity plastic containers (~500 g soil in each), plus a smaller (16.5 x 11 x 6 cm) 600 mL capacity container (~200 g soil) in which the first set of DGT deployments were made. The containers did not have drainage holes to ensure that leaching of Tc could not occur.

7.2.2 Experimental approach and timeframe

The freshly-spiked soils were left to age for 18 days before the ryegrass seeds were sown, such that the decline in availability of Tc during the ryegrass growth phase would be minimised. During this time, each container was periodically given a brief but firm shake and the lid briefly removed to ensure the circulation of air throughout the soil and prevent the onset of anaerobic conditions. Keeping the lids on the containers ensured that moisture loss was kept to a minimum.

After this 18-day period of initial aging, 1.2 g of ryegrass seed was sown on the soil surface of three of the 800 mL containers for each soil type. A seed-free area large enough to accommodate a DGT device was left in the corner of each container. The fourth container acted as a plant-free control. The seeds were gently pressed into the soil and watered with tap water using a trigger spray. Each container was placed in a clear sealed bag for germination and positioned on a well-lit bench under ambient laboratory conditions (Figure 7.1A). Once germinated, the plastic bags were removed and the containers transferred to a growth cabinet in which the samples were randomly distributed. Each time after watering, the samples were randomly redistributed to eliminate any potential heterogeneity in growth conditions within the cabinet that may have influenced growth of the ryegrass. The temperature in the growth cabinet was set to 22°C (85% relative humidity) and the lights operated under a cycle of 16:8

hours light/dark. All samples including the controls received regular input of tap water by aid of a trigger spray to ensure that the soil surface remained moist.

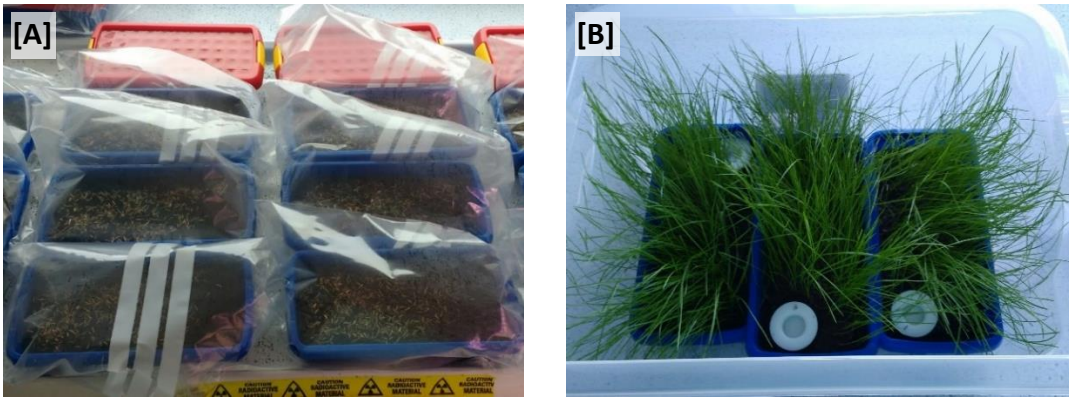

Figure 7.1. *Ryegrass seed containers placed in clear sealed plastic bags for germination* ***[A]****; Single DGT devices deployed on bare soil in the corner of triplicate ryegrass containers* ***[B]****.*

Table 7.1 presents a timeline for the experiment, summarising the procedures at each time point of significance. Three sets of ~24-hour DGT deployments were made: at sowing, during the growth phase (15 days after sowing) and immediately after harvesting (21 days after sowing). The initial set of DGT deployments were made in the control sample (no ryegrass) for each soil. Each container was wetted to saturation and mixed by aid of a spatula before being left overnight to equilibrate. For each soil type, the same volume of water was added to replicates including the control, but the precise volume of water added differed slightly between soil types. Simultaneous triplicate DET deployments were made at sowing and post-harvest to determine the concentration of Tc within the soil solution that can pass through the diffusive gel in DGT. These data were used to calculate R values as described by Equation (1.8) in Section 1.8.

Table 7.1. *Timeline summary of the experimental procedure.*

Time (days)	Summary of procedures
0	Soils are spiked
18	Ryegrass seeds are sown (Figure 7.1A). Control soils are extracted with 0.01 M $CaCl_2$
19	Triplicate DGT and DET deployments
22	Seeds germinate. Bags removed and soils transferred to growth cabinet where they are randomly distributed
33	In situ DGT deployment during growth phase (Figure 7.1B)
39	Ryegrass harvested
40-41	All soils subject to DGT/DET deployments plus 0.01 M $CaCl_2$ extraction

A slightly different $CaCl_2$ extraction method to the one described in Section 2.1.5.3 was used. Here, one gram (dry weight) of soil was extracted with 10 mL of 0.01 M $CaCl_2$ for two hours with constant agitation on a rocker (70 rpm). After the extraction period, 1 mL of the supernatant was obtained after filtration with a syringe filter (0.45 µm pore size).

For the growth phase DGT deployment, no manual mixing of the soil was possible due to the presence of the ryegrass, and the control samples were treated identically. A single DGT device was deployed in situ on the soil surface, which was free of ryegrass (Figure 7.1B). The three containers for each soil type were placed in a large (16 L) clear plastic box which was sealed with a lid to minimise moisture loss from the soil during deployment. Simultaneous triplicate deployments were made within each control soil, which was placed in a clear sealed plastic bag.

Ryegrass plants were grown for a total of 17 days after germination before harvesting, at which point the standing biomass ranged between 10 and 20 cm in height, depending on soil type. A portion of the biomass from each container was harvested and its fresh weight determined. The harvested biomass was subsequently dried in a weighing boat at 75°C in an

oven for ~48 hours, after which the biomass was re-weighed to determine the dry weight. After harvesting, the bulk of the remaining biomass, including the roots, was removed from each container and the soil was saturated with tap water and thoroughly mixed in preparation for the final DGT deployment. Prior to saturation, a small portion (two to three grams) of soil was removed from each container and dried overnight in a weighing boat at 40°C in an oven for the $CaCl_2$ extraction. This drying step ensured that all samples were of a comparable moisture content prior to extraction.

7.2.3 Sample analysis

Oven-dried ryegrass samples were ground using a mortar and pestle prior to digestion. Where possible, 0.1 ± 0.005 g of ground material was weighed into a 13-mL polypropylene digestion tube, followed by 5 mL of concentrated (> 69% w/v) nitric acid (HNO_3). For samples where 0.1 g was unattainable, the maximum possible mass was used and the weight recorded. The tubes were sealed with caps and left in a fume hood for ~24 hours, after which 50 kBq of metastable ^{99}Tc (^{99m}Tc) was added as a yield tracer to each sample to quantify and account for the potential loss of Tc during the digestion process. Technetium-99m is a pure gamma-emitter (E = 142.6 keV), which decays to the ground state of ^{99}Tc with a half-life of 6.03 hours. The unsealed digestion tubes were suspended in water-filled glass beakers and heated to 85 ± 5°C on a hotplate. After one hour of heating, 5 mL of concentrated (> 30% w/v) hydrogen peroxide (H_2O_2) was pipetted into each tube and the heat maintained for a further hour until the solutions had cleared and no solid material was visible. After removal from the hotplate, the samples were allowed to cool for two hours before 1 mL of the digestion solution was pipetted into a 25 mL glass scintillation vial with 20 mL of scintillation cocktail.

Twenty-four hours (four half-lives) after addition of the ^{99m}Tc tracer, the samples were counted using a Perkin Elmer 2480 WIZARD automatic gamma counter. The Tc recovery for

each sample was established by comparing the ^{99m}Tc activity of each sample to the activity of three ^{99m}Tc standards, which were pipetted directly into scintillation vials and not subjected to the digestion procedure. A further five days (~20 half-lives) later, once the ^{99m}Tc activity within each sample had decayed to a negligible level, the ^{99}Tc activity of each sample was determined by liquid scintillation counting. The counting efficiency for the digestion matrix was determined by digesting uncontaminated grass, which was subsequently spiked with 10 Bq of ^{99}Tc. Blank samples to establish the background count rate were also prepared from the blank digestion matrix. Liquid scintillation counting of the three ^{99m}Tc standards enabled the contribution of ^{99}Tc in each sample derived from the decay of ^{99m}Tc to be ascertained and corrected for.

7.3 Results and discussion

7.3.1 Ryegrass ^{99}Tc activities

Table 7.2 and Figure 7.2 present a summary of the ^{99}Tc activity concentrations measured in ryegrass after 21 days growth for each of the eight soil types investigated. At 97 to 122%, the calculated ^{99}Tc recoveries based upon use of the ^{99m}Tc yield tracer were high. Activity concentrations ranged from 414 ± 54 Bq g^{-1} (dry weight) for ryegrass grown on soil BY-W to 3264 ± 445 Bq g^{-1} (dry weight) for soil WK-A. Deviations between triplicate samples grown in separate containers were generally low, the relative error being less than 15% in all cases. Fresh weight activity concentrations were between 9 and 15% of the corresponding activities reported on a dry weight basis, ranging from 40 ± 2 Bg g^{-1} (fresh weight) (BY-W) to 386 ± 63 Bq g^{-1} (fresh weight) (BC-M).

Table 7.2. *Technetium-99 activity concentrations (Bq g^{-1} dry and fresh plant weight) measured in ryegrass after 21 days growth for the eight soils investigated. Reported values for each soil are the mean ± the standard deviation (SD) of triplicate ryegrass samples grown in separate containers.*

Soil	Dry weight		Fresh weight		Soil-to-plant transfer factor
	Bq g^{-1}	± SD	Bq g^{-1}	± SD	
BY-W	414	54.08	40	2.07	7
DY-G	2680	13.57	330	27.07	42
SR-W	2643	331.85	271	47.03	42
WK-A	3264	445.36	308	42.45	52
TK-G	1847	86.37	185	22.37	29
FD-G	2973	191.45	259	33.47	47
BC-M	2640	373.37	386	62.89	42
SR-G	2080	161.65	199	23.02	33

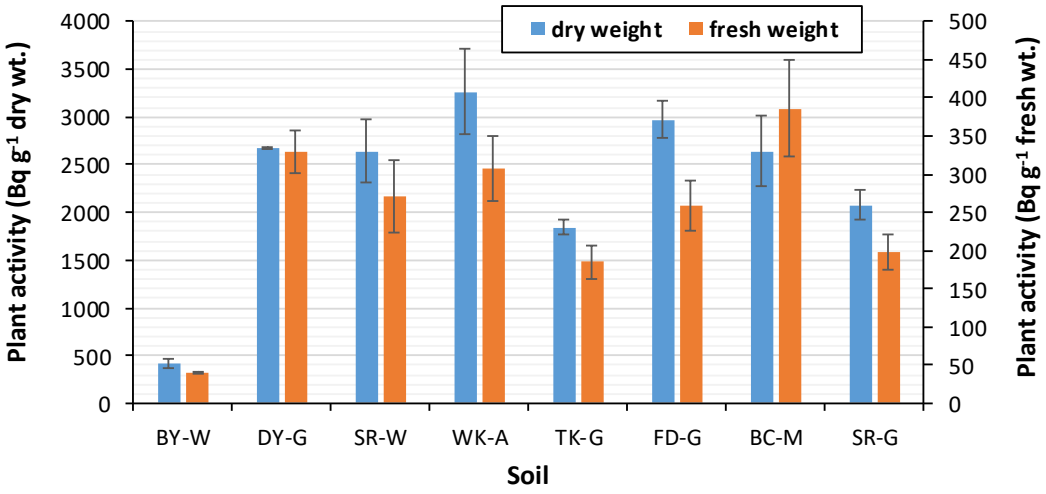

Figure 7.2. *Technetium-99 activity concentrations (Bq g^{-1} dry and fresh plant weight) measured in ryegrass after 21 days growth for the eight soils investigated. Values plotted for each soil are the mean of triplicate ryegrass samples grown in separate containers. Error bars represent one standard deviation of the mean.*

Figure 7.3 reveals that ryegrass uptake of ^{99}Tc would appear to be negatively correlated with the organic carbon (C_{org}) content of the soil. The Spearman's rank correlation coefficient (r_s) is calculated as -0.55. However, the observed negative correlation is highly dependent upon soil BY-W which has a C_{org} content (18.16%) of nearly three times that of soil DY-G with the next

highest C_{org} content (6.77%). In the absence of BY-W, the correlation (r_s) between C_{org} and ryegrass uptake falls to -0.32. Nevertheless, this observation of decreased uptake of Tc by ryegrass in C_{org}-rich soils is also reported for uptake by swiss chard (Sheppard et al., 1983; Ewers and Brown, 2014). In Chapter 4, the interaction between Tc and C_{org} was found to be highly influential in controlling the availability of Tc, so the reduction in ryegrass uptake of Tc with increasing C_{org} would appear to be the result of lower availability of Tc in such soils. Echevarria et al. (2003) reported a significant negative exponential relationship between ryegrass uptake and organic matter (OM) for six soils, but attributed this relationship to the influence that OM exerts on the soil water holding capacity and the subsequent extent of dilution of TcO_4^- in the porewater, coupled in turn to competition with NO_3^- for root uptake.

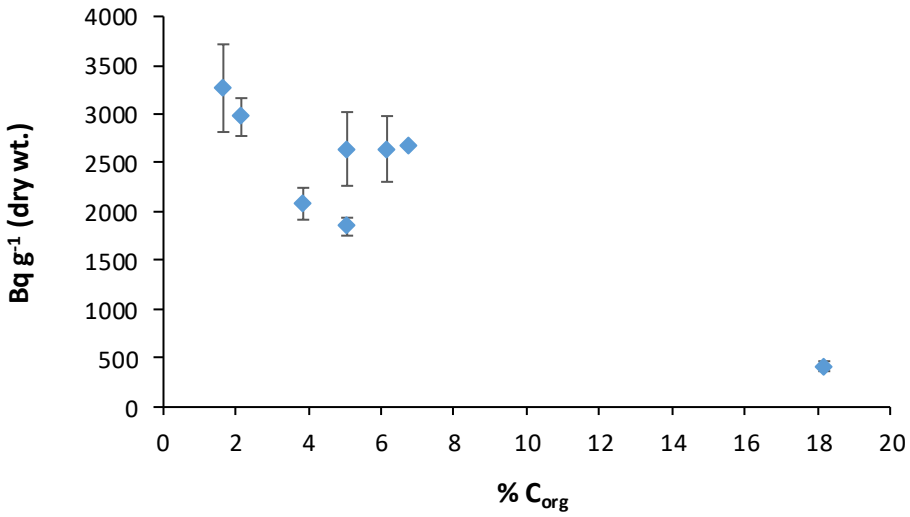

Figure 7.3. *Relationship between ryegrass ^{99}Tc activity (Bq g^{-1} dry weight) and soil organic carbon (C_{org}) content.*

Echevarria et al. (1997), meanwhile, reported uptake of Tc by ryegrass to be a function of biomass production whereby uptake is positively correlated with plant dry matter yield. This observation might suggest that soil fertility or the ryegrass tolerance for the requisite soil is responsible for variation in uptake, given that the rate and magnitude of biomass production will be dictated by the aforementioned factors. Clear differences in biomass production were

observed between the soils in this study, and although no quantitative record of total biomass production at harvest was made, it appeared broadly that soils with lower biomass production exhibited correspondingly lower biomass activities.

Calculated soil-to-plant Tc transfer factors (TFs) in Table 7.2 range from 6.6 (BY-W) to 51.7 (WK-A), with a mean of 36.7. These TFs are comparable to those reported in the scientific literature. For example, for transfer to pasture, the IAEA (2010) list a minimum and maximum of 7.9 and 470, respectively, with a mean of 76. TFs for ryegrass specifically are reported to range from 20 to 370 (Echevarria et al., 2003).

7.3.2 $CaCl_2$ and DGT-measured ^{99}Tc

Table 7.3 and Figure 7.4 present the concentration of Tc extractable by 0.01 M $CaCl_2$ ($Tc_{extractable}$) and the DGT-measured Tc (Tc_{DGT}) within each soil at the time of sowing and post-harvest (ryegrass and control). Between 11 (BY-W) and 72% (SR-W) of the Tc spike was extractable by 0.01 M $CaCl_2$ at sowing (18 days after spiking). On average, across the eight soils, $Tc_{extractable}$ decreased by 34 ± 23% over the ryegrass growth period. Post-harvest, Tc was found to be more extractable in the control soils (no ryegrass) relative to the ryegrass soils by a factor of 1.66 for soil BY-W up to 14.55 for WK-A. Tc_{DGT} was found to decline on average by 75 ± 20% across all eight soils during the ryegrass growth period. This decline ranged from 42% in soil SR-W up to 93% for TK-G. As was the case for $Tc_{extractable}$, Tc_{DGT} post-harvest within the control soils was generally greater than measured in ryegrass soils.

Table 7.3. *Soil concentrations of ^{99}Tc measured by extraction with 0.01 M $CaCl_2$ ($Tc_{extractable}$) and DGT (Tc_{DGT}) at sowing and post-harvest. Values are given as the mean of triplicate samples; σ = standard deviation.*

Soil	Sowing			Post-harvest (ryegrass soil samples)			Post-harvest (control soil samples)			Sowing:post-harvest ratio	
$Tc_{extractable}$	µg kg^{-1}	σ	% error	µg kg^{-1}	σ	% error	µg kg^{-1}	σ	% error	ryegrass	control
BY-W	11.25	0.93	8.23	13.14	1.64	12.45	21.78	1.33	6.10	0.86	0.52
DY-G	19.23	1.03	5.37	—	—	—	—	—	—	—	—
SR-W	71.59	4.85	6.77	24.15	3.55	14.72	90.83	12.07	13.29	2.96	0.79
WK-A	65.42	1.73	2.65	5.65	2.90	51.36	82.22	9.49	11.54	11.57	0.80
TK-G	38.44	1.86	4.83	15.78	4.91	31.11	28.81	3.21	11.13	2.44	1.33
FD-G	64.11	2.97	4.64	10.29	4.99	48.48	79.67	15.52	19.48	6.23	0.80
BC-M	21.06	0.15	0.70	6.51	0.76	11.70	—	—	—	3.23	—
SR-G	68.41	2.75	4.02	27.66	2.08	7.51	—	—	—	2.47	—
Tc_{DGT}	µg L^{-1}	σ	% error	µg L^{-1}	σ	% error	µg L^{-1}	σ	% error	ryegrass	control
BY-W	2.38	0.05	2.17	0.69	0.13	19.38	1.26	0.09	7.40	3.42	1.88
DY-G	7.31	0.42	5.81	0.66	0.17	26.15	0.42	0.01	3.18	11.13	17.58
SR-W	4.61	0.12	2.52	2.67	0.74	27.87	8.82	0.37	4.23	1.73	0.52
WK-A	3.63	0.23	6.26	1.79	0.72	40.49	12.20	0.42	3.47	2.03	0.30
TK-G	13.14	0.12	0.89	0.93	0.24	25.43	1.37	0.06	4.48	14.06	9.62
FD-G	12.81	0.54	4.19	1.77	0.58	32.46	10.80	0.30	2.76	7.22	1.19
BC-M	13.88	0.63	4.54	1.09	0.01	1.18	3.01	0.19	6.26	12.75	4.61
SR-G	12.82	0.24	1.87	3.18	0.43	13.49	7.27	0.20	2.70	4.03	1.76

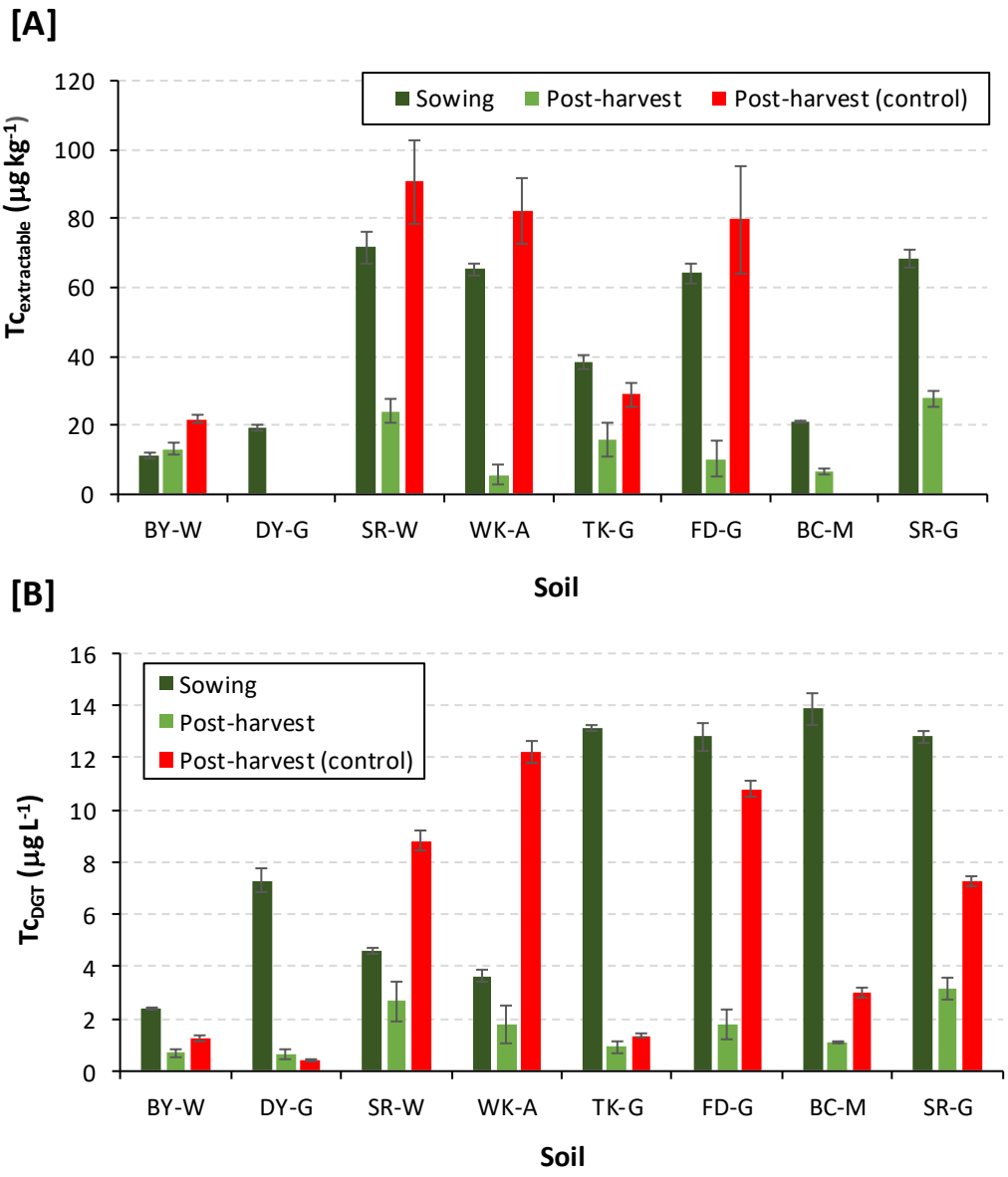

Figure 7.4. *$CaCl_2$-extractable ($Tc_{extractable}$)* ***[A]*** *and DGT-measured concentrations (Tc_{DGT})* ***[B]*** *of ^{99}Tc at sowing and post-harvest (ryegrass and control samples) for the eight soils investigated (minus BY-W in [A]). Plotted values are the mean of triplicate DGT deployments. Error bars represent one standard deviation of the mean. $CaCl_2$ data for BC-M and SR-G are missing in [A].*

The reproducibility between $CaCl_2$ extract replicates for the post-harvest extractions (mean relative error = 25.33%) was found to be significantly poorer than for the extractions made at sowing (mean relative error = 4.65%). The inferior reproducibility in the post-harvest extracts is likely to be explained by the spatial heterogeneity of Tc throughout the soil post-harvest

due to localised depletion by ryegrass roots. Modelling using 2D-DIFS (see Section 1.8 for description of model) has shown that the zone of depletion may extend several millimetres beyond the root surface into the soil (Lehto et al., 2006). As a result, obtaining a small sample for extraction of only a few grams that is representative of the bulk soil throughout the container is challenging, and significant deviation between replicates would be expected.

The reason for the significantly lower availability measured by both DGT and $CaCl_2$ post-harvest within the ryegrass soil samples relative to the control samples is not immediately clear. A crude mass balance suggests that the difference cannot be accounted for by removal of Tc from the soil by ryegrass, since uptake was estimated to be no more than 5% of the spike. The lower values of Tc_{DGT} in the ryegrass soil samples imply that greater reduction of TcO_4^- to insoluble TcO_2 has occurred in these soils. This reduction only occurs under anoxic conditions however, so it could be that a greater extent of reduction has occurred in the ryegrass soil samples, in particular in the presence of reduction hotspots associated with enhanced microbial activity in the rhizosphere. The activity of the plant may also be responsible. For example, plant roots exude an enormous range of organic compounds, which serve a variety of functions (Curl and Truelove, 1986; Walker et al., 2003). Exudate compounds are known to enhance microbial activity by serving as a source of carbon (Kuzyakov et al., 2000), which in turn would lead to the acceleration of Tc complexation with OM thereby reducing its availability. Alternatively, Tc may complex directly with the organic exudates, which depending on their size and stability are likely to be unavailable to DGT.

Figure 7.5 reveals the data acquired from the DGT deployments made in situ during the ryegrass growth phase. Measured values for Tc_{DGT} within both the ryegrass and control soils are within error of each other for half the soils, but in the other four soils Tc_{DGT} measured in situ within the ryegrass soils is between a factor of 1.78 and 2.69 times greater than measured within the control soils. The deviation between DGT triplicates is in general greater for

deployments made within the ryegrass samples (mean relative error = 17.36%) compared to those made in the control soils (mean relative error = 8.25%). The greatest deviation for ryegrass soil deployments was recorded for soil DY-G at 32.34%. The greater variation between DGT triplicates for the in situ deployments within the ryegrass soils is likely to be attributed to heterogeneity in Tc distribution throughout the soil as well as the potential presence of trapped air pockets within the matrix associated with the inability to mix the soils at wetting.

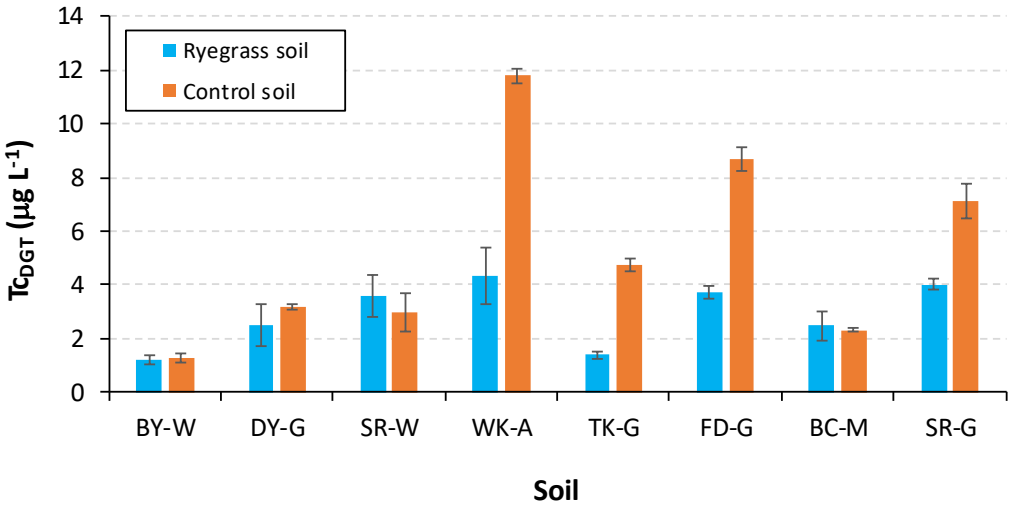

Figure 7.5. *Concentrations of ^{99}Tc measured by DGT (Tc_{DGT}) deployed in situ during the ryegrass growth phase. Concentrations measured simultaneously within control soils (no ryegrass) are also plotted. Values represent the mean of triplicate DGT deployments. Error bars represent one standard deviation of the mean.*

7.3.3 Predicting ryegrass uptake of ^{99}Tc

7.3.3.1 $CaCl_2$

Figure 7.6 presents the relationship across all the soil types between the ^{99}Tc activity measured in the ryegrass (Tc_{plant}) and the concentration of Tc extracted by 0.01 M $CaCl_2$ ($Tc_{extractable}$) at sowing and post-harvest (ryegrass and control soil samples). A weak Spearman's

rank correlation coefficient (r_s = 0.36) is calculated between Tc_{plant} and $Tc_{extractable}$ at sowing and post-harvest (n = 7, r_s = -0.50). Interestingly, the correlation between Tc_{plant} and $Tc_{extractable}$ post-harvest within the control soils appears to be reasonably strong (n = 5, r_s = 0.70); however, given that data points for three soils (DY-G, BC-M and SR-G) are absent from this plot and the relationship is mainly determined by two clusters of data points, this correlation should be treated cautiously.

The inability of $CaCl_2$ to predict uptake of Tc by ryegrass is in contrast to the findings of Echevarria et al. (1997), who reported a correlation coefficient (r) of 0.941 ($p < 0.01$) between the two parameters. However, the study by Echevarria et al. (1997) did not focus on uptake with respect to different soil properties, as only two different soils (both inceptisols) were used. Instead, Echevarria et al. (1997) investigated extractability according to Tc application form (NH_4TcO_4 and Tc bio-incorporated in wheat leaves) and application rates (up to 250 Bq g^{-1}), in addition to incubation times (up to six months). The data presented in this chapter extend the work of Echevarria et al. (1997) by investigating uptake across a range of soil types. No other published data in the literature can be found that attempt to compare plant uptake of Tc with other techniques for assessing availability of Tc to plants in soil.

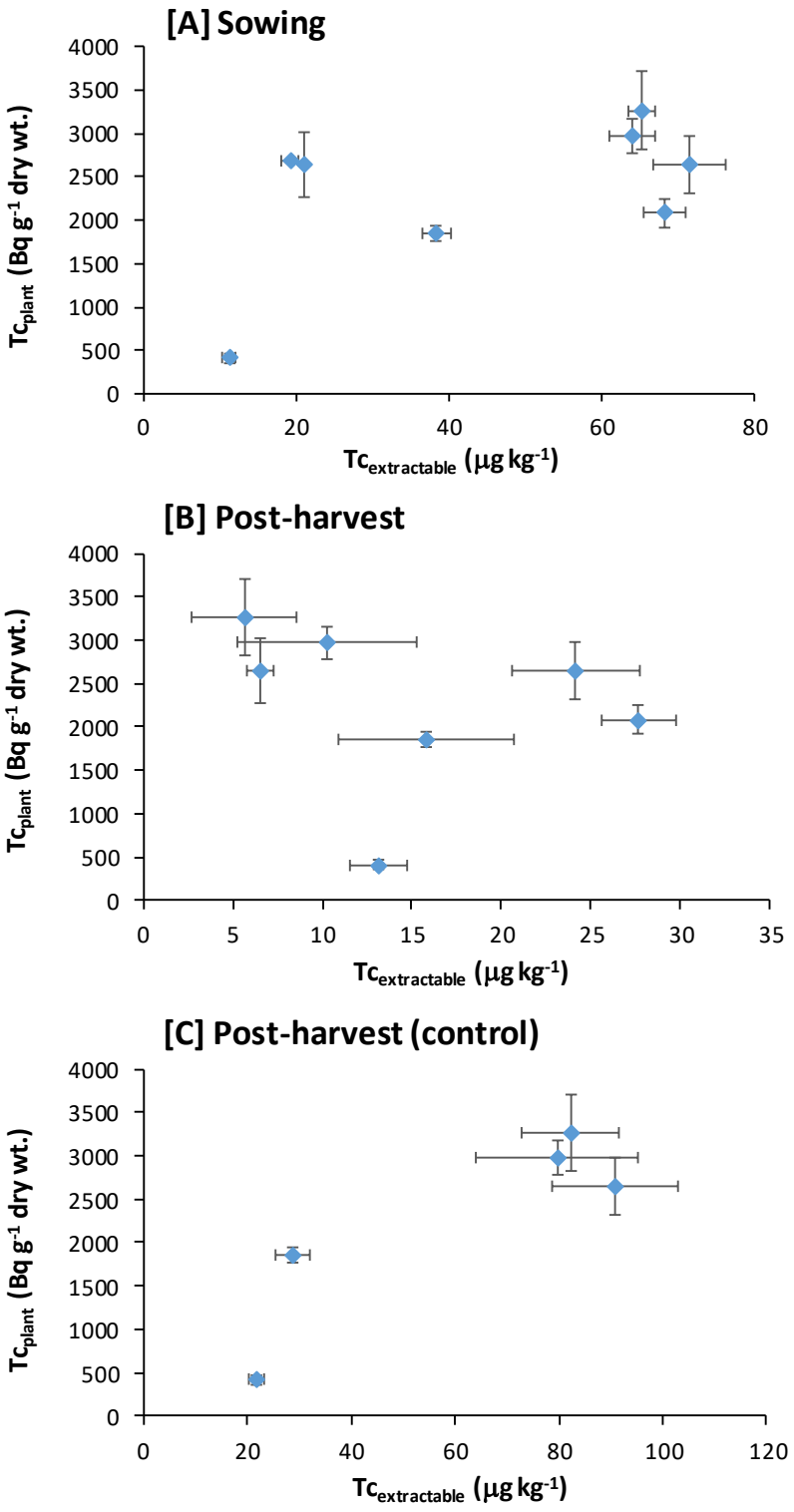

Figure 7.6. *Relationship between ^{99}Tc activities measured in ryegrass plant samples (Bq g^{-1} dry wt.) and $CaCl_2$-extractable Tc within eight different soils at sowing **[A]** and post-harvest for ryegrass **[B]** and control (no ryegrass) **[C]** soils. Plotted values are the mean of triplicate samples. Error bars represent one standard deviation of the mean. No data for soils DY-G [B]; DY-G, BC-M and SR-G [C].*

7.3.3.2 DET

Figure 7.7 presents the relationship between Tc_{plant} and the concentration of Tc species measured in solution by DET (Tc_{DET}) at sowing [A] and post-harvest [B]. DET measures only those species of Tc in solution which are small enough to diffuse through the polyacrylamide diffusive gel layer. Colloidal forms of Tc including solubilised organic complexes of higher molecular weight will therefore be excluded from measurement. Figure 7.7 reveals only a weak to moderate degree of positive correlation between Tc_{DET} and Tc_{plant} at both sowing (r_s = 0.57) and post-harvest (r_s = 0.43), which suggests that the speciation of Tc within the soil solution is of limited significance in governing the uptake of Tc by ryegrass.

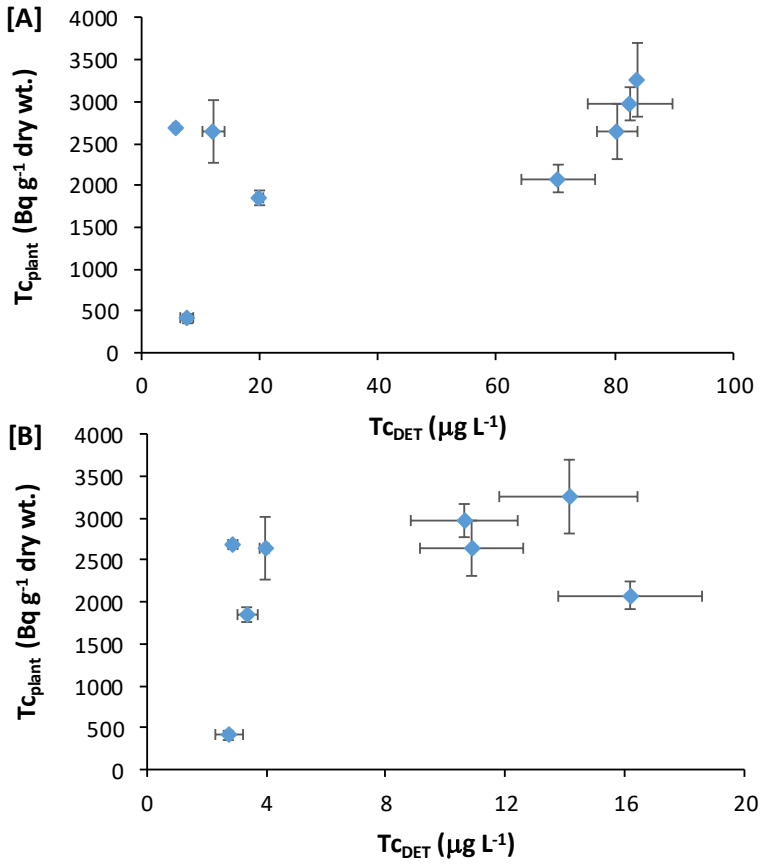

Figure 7.7. *Relationship between ^{99}Tc activities measured in ryegrass plant samples (Bq g^{-1} dry wt.) and the concentration of Tc species measured in the soil solution (µg L^{-1}) of ryegrass soil samples using DET at sowing* ***[A]*** *and post-harvest* ***[B]****. Error bars represent one standard deviation of the mean for triplicate samples.*

7.3.3.3 DGT

Figure 7.8 presents the relationship between Tc_{plant} and Tc_{DGT} after deployments at sowing [A] and post-harvest in both the ryegrass soil samples [B] and control soils (no ryegrass) [C]. No correlation can be found between Tc_{plant} and Tc_{DGT} at sowing (r_s = -0.17) or post-harvest (r_s = 0.24). However, a moderate degree of positive correlation (r_s = 0.62) is calculated between Tc_{plant} and Tc_{DGT} measured within the control soils. This finding that correlation between Tc_{plant} and Tc_{DGT} is stronger in the control soils mirrors that for $Tc_{extractable}$ and Tc_{plant}. Overall, the data presented in Figure 7.6 and Figure 7.8 suggest that DGT does not offer any advantage over a $CaCl_2$ extraction for predicting ryegrass uptake of Tc.

One of the key advantages of using DGT for assessing bioavailability is that it mimics the action of a plant by locally depleting the concentration of labile element and consequently inducing diffusive resupply and release from complexes and the solid phase. As discussed in Section 1.8, this resupply component can be quantified in terms of an R value, an empirical ratio between C_{DGT} and C_{soln}, where higher values indicate a greater extent of resupply. With the exception of soils DY-G, TK-G and BC-M, the R values presented in Figure 7.9 are generally low at both sowing and post-harvest (0.04-0.32, median = 0.20). For the soils in which supply of available Tc from the solid phase is interpreted to be insignificant, DGT would not necessarily be expected to offer any considerable advantage over an equilibrium-based extraction approach for inferring uptake by a plant. Resupply within soils SR-W and WK-A at sowing is inferred to be negligible given that the R values are comparable in magnitude to R_{diff}, the value of R for which no resupply from the solid phase occurs. Omitting these soils from Figure 7.8A yields a marked improvement in the correlation between Tc_{plant} and Tc_{DGT} from r_s = -0.17 to 0.61. At the same time however, a plot of Tc_{plant} versus Tc_{DGT} exclusively for soils in which solid phase resupply is significant (R > 0.5: DY-G, TK-G, BC-M) does not produce a linear relationship.

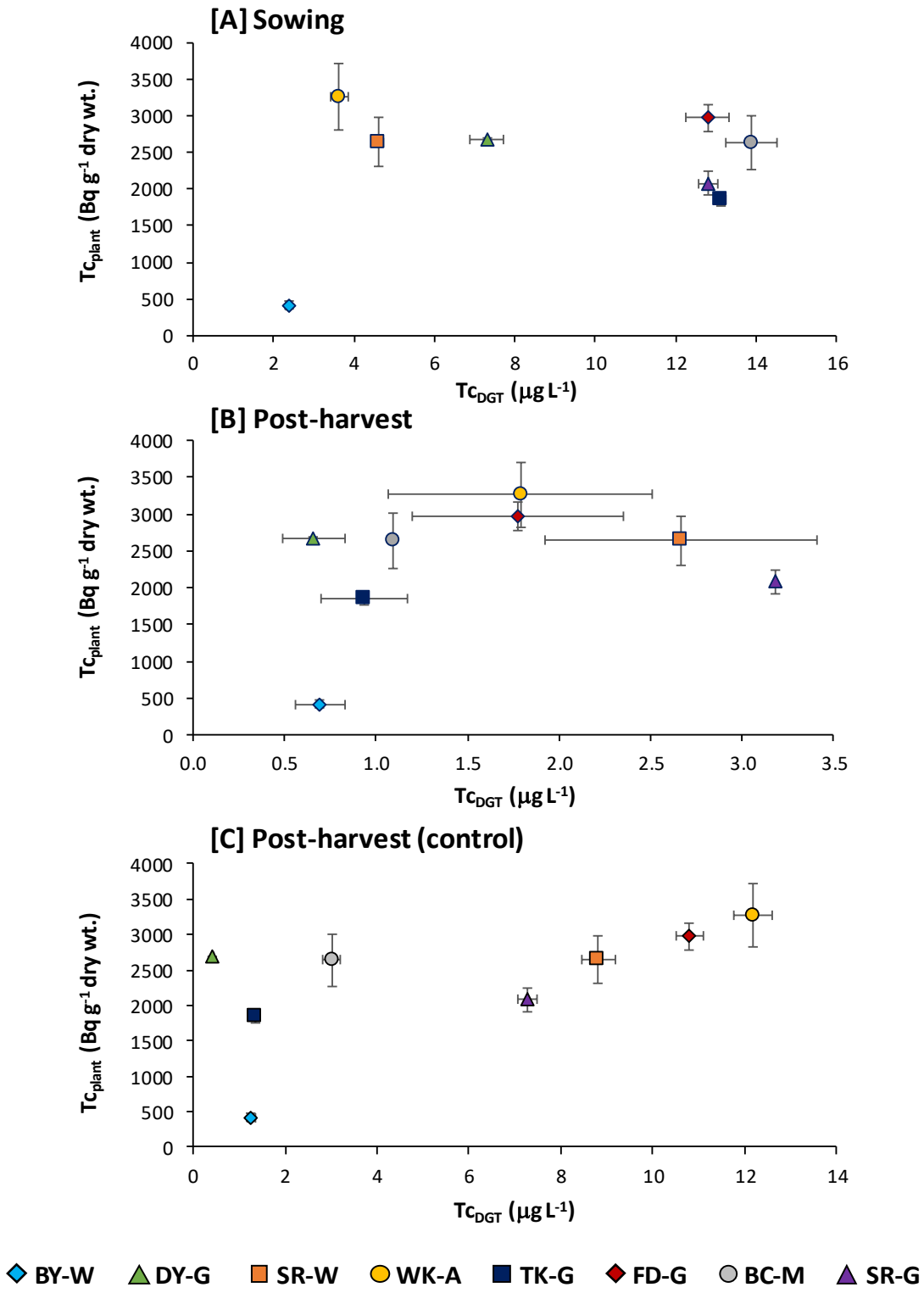

Figure 7.8. *Relationship between ^{99}Tc activities measured in ryegrass plant samples (Bq g^{-1} dry wt.) and DGT uptake (µg L^{-1}) at sowing* ***[A]*** *and post-harvest for ryegrass* ***[B]*** *and control (no ryegrass)* ***[C]*** *soil samples. Plotted values are the mean of triplicate samples. Error bars represent one standard deviation of the mean.*

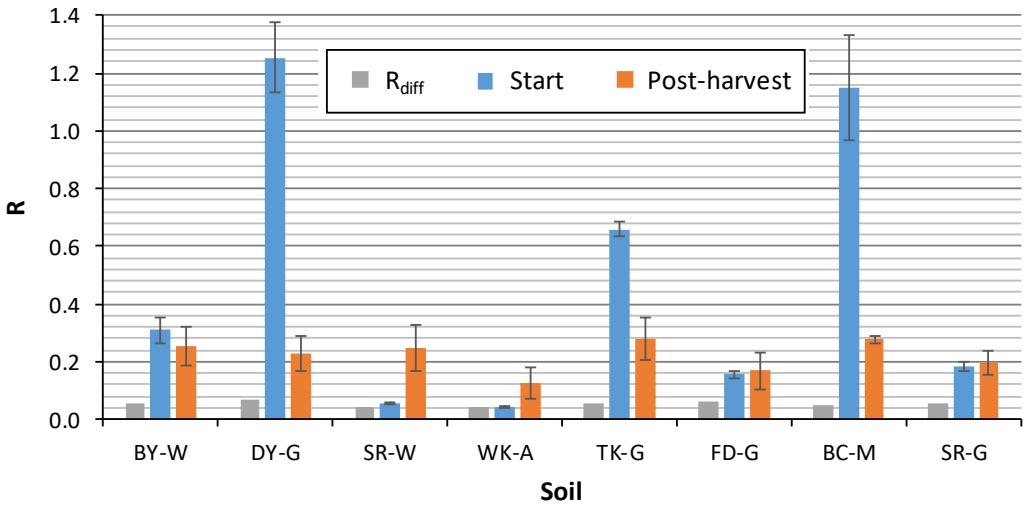

Figure 7.9. *Calculated R_{diff} and R values (C_{DGT}/C_{soln}) for all eight soils at sowing and post-harvest. C_{soln} was measured using DET.*

The limitation of using DGT to predict plant uptake is that it is not designed to account for biological factors, which in some cases may be the limiting factor in uptake. For example, the rate of ryegrass biomass production will be important in determining the extent of uptake of Tc. Although ryegrass can tolerate a broad range of soil types, it is clear that growth rate was highly influenced by soil type since significant variation in the biomass production at harvest is evident. Furthermore, the TEVA DGT is unable to emulate the competitional uptake with NO_3^- that ryegrass is reported to experience (van Loon, 1986; Echevarria et al., 1998; Krijger et al., 2000) since the TEVA resin within the DGT binding layer has no affinity for NO_3^-. Lembrechts et al. (1988), for example, found that ^{99}Tc soil-to-plant transfer diminished substantially with increasing concentrations of NO_3^- in the soil solution, and this relationship prevailed regardless of soil type. In this study however, no correlation was observed between Tc_{plant} and soil NO_3^- concentrations, which suggests that competitive uptake between TcO_4^- and NO_3^-, should it be occurring, cannot explain the variation in Tc_{plant}.

A further point to consider is centred on the evolution of Tc_{DGT} during the ryegrass growth phase, whereby Tc_{DGT} is found to decline by between 42 and 93% (mean = 75%) across the eight soils. Whereas the ryegrass plants have been accumulating Tc from the soil over a 17-day growing period, two singular DGT deployments made at the start and end of this time window will not necessarily reflect the integrated availability of Tc within the soils over this growth period. Ideally, equilibration of Tc within the soil with respect to its availability should be complete before the ryegrass was sown, but data from Figure 4.5 in Section 4.2.2.1 suggest that this would not be possible until at least one year following addition of Tc to the soil. Had a sufficient mass of each soil been available at the conclusion of the primary incubation then these samples would have been used for the experimental work presented in this chapter.

Williams et al. (2011) highlight the importance of organic matter in conjunction with DGT for predicting As release and uptake by rice grain in Bangladesh paddy soils. Individually, no single soil parameter or measure of availability (chemical extractions or DGT) was able to explain the observed variation in As within rice grain. However, a simple regression model which incorporated C_{DGT} and dissolved organic carbon (DOC) could reliably predict plant concentrations ($n = 32$, $R^2 = 0.72$, $p < 0.001$). Williams et al. (2011) concluded that DOC was responsible for solubilising As, of which the resulting complexes would partially contribute to the DGT measurement.

Figure 7.10 reveals that a significant relationship ($n = 8$, $r_s = 0.74$, $\alpha < 0.05$) can be obtained after plotting ryegrass ^{99}Tc activities against Tc_{DGT} measured in situ within the ryegrass soil samples whilst the ryegrass is actively growing. However, the uncertainty associated with this correlation is high due to the considerable variability between DGT triplicates for certain soils, namely BC-M, DY-G, SR-W and WK-A. Furthermore, soil BY-W is found to exert a reasonable degree of influence on the relationship however, since correlation (r_s) calculated after omitting data for this soil falls slightly to 0.61.

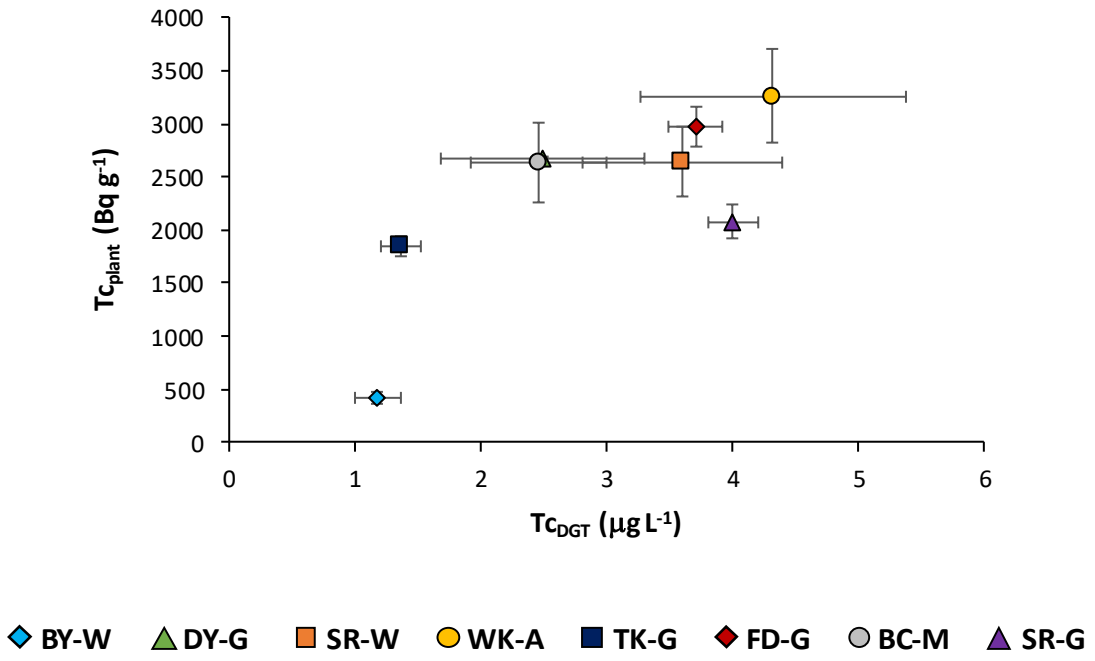

Figure 7.10. *Relationship between ^{99}Tc activities measured in ryegrass plant samples (Tc_{plant}) and the DGT-measured soil concentration of Tc (Tc_{DGT}) through in situ deployment within all eight soils at 11 days after germination. Plotted values are the mean of triplicate samples. Error bars represent one standard deviation of the mean.*

Nevertheless, these data suggest that DGT measurements of Tc availability in situ compared to post-harvest are more promising when it comes to predicting Tc uptake by ryegrass. This may be due to rhizosphere effects on Tc availability, primarily as a result of root exudation of organic compounds as alluded to in Section 7.3.2. Microbial activity is substantially enhanced in the rhizosphere, and this may generate localised oxygen-depleted anaerobic microsites in the soil which promote the reduction of bioavailable TcO_4^- to insoluble TcO_2. Furthermore, the abundance of secreted organic complexing and chelating agents may alter the bioavailability through the formation of Tc(IV)-organic complexes, or even enhance the re-oxidation of insoluble Tc(IV) to more available forms (Gu et al., 2011).

Consideration should be given to the role that soil moisture content plays in determining the availability of Tc measured by DGT and $CaCl_2$ extraction, and similarly the growth and uptake

of Tc by the ryegrass. Initially, the same volume of water was added at each watering event to all samples, but over time more prolific ryegrass growth within certain soil types necessitated a greater input of water than for other soil types. No soil moisture content data are available from this experiment during the ryegrass growth phase as the moisture content was not measured at any point, and no records were kept of how much water was added between soil types at each watering event.

Soil moisture content has an important effect on many biological, physical and chemical processes occurring within soils, and such effects may be responsible for perturbing any relationship that may be present between available Tc measured in the soil and Tc measured in the ryegrass. For example, variations in soil moisture content will affect plant growth and nutrition, the rate of microbial activity, nutrient transformation within the rooting zone and concentrations of dissolved organic carbon (DOC) (Christ and David, 1996). Dissolved organic carbon plays an important role in determining Tc availability within the soil since humic acids act as complexants which will in turn influence Tc solubility. Furthermore, in soils maintained at a relatively high moisture content, more extensive pockets of anoxia may develop which will promote the reduction of TcO_4^- to insoluble species which cannot be taken up by plants.

Ideally, all samples should have been watered to maintain a constant moisture content which was the same across all samples. In the absence of the ryegrass this would have been straightforward as the soil containers could be weighed, with input of water where necessary to ensure a constant weight. However, this direct mass balance approach to maintaining the moisture content is not possible where ryegrass is present due to the increasing weight of the biomass over time with growth, together with the fact that an unknown yet significant volume of water will be stored within the biomass. Instead, soil moisture would need to be monitored in situ within every container using a probe-type sensor or tensiometer. Given the relatively small volume of the containers however, these methods may not have been possible.

7.4 Conclusions

DGT does not exhibit any improvement in performance over a conventional $CaCl_2$ extraction for predicting ryegrass uptake of Tc across a range of soil types when deployments are made at sowing and immediately post-harvest. Similarly, only limited correlation can be found between ryegrass uptake and the concentration of Tc species measured in soil solution by DET, which negates the significance of the molecular weight of solubilised Tc species in influencing uptake. It would appear that biological processes operating within the soil are more significant in controlling the availability of Tc for uptake by ryegrass than diffusion-limited supply of Tc from labile solid phase pools. The insignificant contribution of available Tc from the solid phase is highlighted by the generally low values for R determined at both sowing and post-harvest across the range of soils. DGT is not designed to mimic biological processes occurring within the soil.

An improvement in the predictive capacity of DGT is attained when DGT deployments are made in situ during the ryegrass growth phase. The influence of the rhizosphere on Tc availability, primarily related to root exudation of organic substances and subsequent complexation reactions, as well as enhanced microbial activity promoting anoxia and reduction to insoluble species, is likely to explain the improvement in the predictive capacity of DGT when deployed in situ during active plant growth. Reproducibility between DGT measurements for such deployments can be poor however, so the positive relationship observed between ryegrass uptake and Tc_{DGT} should be treated with caution and investigated further.

If the experimental work presented in this chapter was to be repeated, the approach should be modified in several ways. Firstly, all the biomass to within one centimetre of the soil surface for each sample should be harvested and the weight noted, rather than a fraction of this

biomass. This approach would yield empirical data concerning ryegrass growth rate across the different soil types. Secondly, and perhaps most importantly, the approach to watering the ryegrass samples should be centred on maintaining a constant soil moisture content as opposed to watering 'by eye' as was the approach in the work presented here. As previously discussed, soil moisture content within each sample would likely need to be measured using sensors or tensiometers situated in situ within every sample. The use of such instrumentation would likely necessitate the use of containers with a greater soil depth. Lastly, it would be preferable to use soils with an 'aged' spike for these experiments as opposed to freshly-spiked soil, so as to minimise any potential effect that aging of Tc during the growth phase would have as previously discussed. The research could be extended by investigating plant uptake over multiple and sequential harvests.

Chapter 8: Discussion, reflection and future work

The overarching aim of this thesis was to examine the bioavailability and aging of Tc, Se and U within a range of soil types using DGT. This was achieved through an 18-month controlled laboratory incubation of 20 different spiked soils encompassing a range of properties. The data presented in this thesis are most suited to application in understanding aging of Tc, Se and U in the context of a defined contamination event, for example fallout from a nuclear power plant accident or a nuclear bomb, but also in localised contamination scenarios arising at reprocessing plants. Aerial fallout is likely to span a large area, with deposition to a spectrum of soil types, so knowledge concerning bioavailability is invaluable to help inform the relevant authorities in their post-accident management strategy relating to a handful of key areas. These areas include imposition of restrictions on the movement and consumption of livestock and associated products, in addition to restrictions on the cultivation of land. Both Se and Tc are significant here since they exhibit high soil-to-plant transfer relative to other radionuclides, and so their potential for transfer to the biosphere from soil is greater.

Additionally, the data presented in this thesis will contribute towards research efforts which seek to characterise and evaluate the risk associated with radioactive waste disposal in a geological disposal facility. Since it is accepted that containment of such wastes in the very long-term is likely impossible, information concerning which soil types will immobilise these radionuclides and minimise their transfer to the biosphere may help to inform the location of such a facility.

Chapter 4 elucidated the key role that soil organic carbon (C_{org}) plays in controlling the availability and rate of aging of Tc. In comparison, the Al and Fe oxide content of the soil

coupled with C_{org} was found to be instrumental in determining the availability and rate of aging of Se. Quantitatively, the aging of Tc could be best described by a pseudo-second-order model, yet a natural exponential function provided the best fit for Se.

A convoluted dataset for U is presented in Chapter 6, in which minimal aging of U can be discerned. This was broadly attributed to the effects of multiple wet-dry cycles on soil pH and the concentration of dissolved carbonate ligands. Evidence for aging was found in the secondary incubation for soil samples incubated at a constant moisture content. Despite the apparently limited application of the data for U, the findings are nevertheless significant in that they highlight the resilience of U to aging within a range of soils in a climatic regime characterised by extensive dry periods punctuated by flooding events, such as would be found in continental or equatorial regions. Considering the high levels of U found in phosphate fertilisers, these findings could be significant for agriculture in such geographical regions as the U will remain bioavailable for uptake by crops.

As always with laboratory studies, the question of how applicable or transferrable the acquired data are in understanding what goes on in the environment is pertinent. The controlled laboratory incubations upon which the experimental work in this thesis was centred contain several inherent artificial elements. Cyclical wetting and drying of the soils associated with DGT deployments was shown to affect the dissolution and availability of a number of elements, in particular U (Section 6.2.1.2), as a result of subtle changes in the microbiology and physico-chemical properties of the soils. Wetting and drying is more realistic of what soil experiences in the field however, as opposed to being maintained at a constant moisture content. The controlled nature of the incubation meant that the soils were not exposed to climatic effects which are likely to influence the aging trend, although the incubation temperature (10-15°C) was chose to reflect the mean annual temperature for the UK.

Had a greater mass of each spiked soil been available then it would have been possible to make DGT deployments in subsamples of soil taken from a bulk sample that was incubated at a constant moisture. Firstly, subsampling would have avoided subjecting the soils to multiple wet-dry cycles which were likely responsible for the highly convoluted data yielded for U in Chapter 6. Second, subsampling would have avoided the progressive removal of available element from the soil over time, due primarily to accumulation by DGT. Taking Tc as an example, a mass balance calculation revealed that over the course of the primary incubation, between 2.06 and 26.80% (mean = 15.12%) of the initial Tc spike was cumulatively removed from each soil due to deployment of DGT devices. The mass balance calculation was used to derive a correction factor with which to normalise the measured values of C_{DGT} and C_{soln} (Section 2.3.2.3). However, the depletion of available Tc from the soil system is arguably more representative of what would occur under field conditions since accumulation by plants would have the same effect.

An alternative approach to incubating the soils in a controlled laboratory experiment would have been to scale up to a lysimeter study in which a considerably larger volume of each soil is exposed to the ambient meteorological regime. Each lysimeter could have been spiked through aerial deposition to mimic that of a contamination event. A lysimeter approach would have allowed for plants to be grown in the same soils, and the DGT dataset could be complemented by simultaneous measurements of plant radionuclide activity. In light of the preceding discussion however, the small-scale controlled incubation is a good analogue for evaluating the effect of soil type on the availability and aging of Tc, Se and U, which was ultimately the primary objective of this thesis.

This thesis has demonstrated for the first time the successful application of a Chelex-ferrihydrite mixed binding layer (MBL) DGT for measuring Se and U (Chapter 3). However, certain limitations hinder its performance in soils. Specifically, uptake of Se by ferrihydrite was

shown to be inhibited by the relatively low adsorption affinity at higher pH (> 7) and in the presence of common competing anions such as HCO_3^-. Consequently, suppressed uptake of Se was noted in 14 of the soils from the primary incubation in Chapter 5, and their associated DGT data were later omitted from further quantitative analysis. Peng et al. (2017) proceeded to use ferrihydrite DGT for predicting Se availability to several crops in a study centred on a calcareous soil of pH 7.75. The authors did not recognise any limitation in its performance, although the exceptionally low R values presented are characteristic of impaired uptake by DGT as described in Section 5.2.3. Nevertheless, highly significant correlation was observed between C_{DGT} and Se measured in all the crops tested.

Zirconium (Zr) oxide has recently received increasing attention as a binding agent for oxyanion species including Se because of its superior selectivity for several species over ferrihydrite (Ding et al., 2010; Guan et al., 2015; Ding et al., 2016). When deployed in soil for measuring As, the Zr-oxide binding layer exhibited a greater tolerance to a range of competitive anions compared to ferrihydrite and Metsorb (Sun et al., 2014). Furthermore, Ding et al. (2016) found that Se uptake by Zr oxide was not inhibited when deployed in solution up to pH 8.45. Collectively, these observations suggest that the Zr oxide binding agent may offer an improvement in performance over ferrihydrite for measuring Se in alkaline soils characterised by high concentrations of competing anions.

Uptake of U by the MBL was shown to diminish in the presence of increasing concentrations of HCO_3^- (Section 3.3.8). This was attributed to the formation of anionic uranyl carbonate species which are unable to bind to the Chelex resin. Despite this deficiency of the MBL, the availability of U measured in soils of pH > 7 from the primary incubation in Chapter 6 was in general found to be higher than availability measured in soils with a pH < 7. The effect of competing ions present in the soil solution was not investigated, and this should form the basis of further work. Gregusova and Docekal (2011) reported that DGT incorporating a

Spheron-Oxin resin binding agent was successful in measuring U in waters characterised by high concentrations of HCO_3^- and CO_3^{2-}. Furthermore, U binding was not impaired in the presence of commonly encountered ligands in the soil solution including NO_3^-, SO_4^{2-} and Cl^-. A further line of work would be to assess the feasibility of incorporating the Zr-oxide and Spheron-Oxin resin within the same binding layer to improve the versatility and robustness of DGT for simultaneous measurement of Se and U across a range of soil types.

The overarching implications of the research presented in this thesis can be broadly summarised two-fold. Firstly, the availability and aging of U in contaminated soils is strongly influenced by the prevailing soil conditions, specifically the degree of saturation of the soil, whereas the contribution of the intrinsic soil physico-chemical properties is secondary. In contrast, the soil properties are instrumental in governing availability and aging of Se and Tc, in particular C_{org}. Consequently, remedial efforts to reduce the soil-to-plant radionuclide transfer following a contamination event should look to utilise the complexing capacity of C_{org} in the case of Tc and Se, or prevent the exposure of the soil to wetting/drying events in the case of U. Second, when assessing the radiological risk posed by the soil-to-plant transfer of Tc within contaminated soils, DGT does not appear to be a reliable indicator for such purpose. Where possible, DGT measurements should be made in situ, although in a field setting this is logistically challenging and introduces significant uncertainties to the data. In practice, to reliably ascertain the bioavailability of Tc, it would seem that the best approach is to directly measure the accumulated activity within the plant since there is no observed correlation between DGT-measured soil concentrations and the resultant ryegrass uptake.

Future work should aim to explore the relationship between DGT-measured Se in soil and plant uptake. At the time of writing, Peng et al. (2017) published a study investigating the ability of DGT to predict uptake of Se in several crops (cabbage, broccoli, mustard and wheat) from a calcareous soil. Encouraging results were reported, although this work should be

extended to include a range of soil types, mirroring the approach of Chapter 7. Uptake of Tc and U should be investigated in plants of agricultural significance, including wheat and salad crops, and compared to measurements of DGT availability in soil to validate the robustness of DGT as an indicator of bioavailability. Future work should aim to accommodate DGT deployments made in situ during the growth phase, as these were found to correlate best with ryegrass uptake of Tc (Chapter 7).

The DGT data acquired from the primary incubation could be used to develop a model which describes bioavailability at any given point in time within a soil in relation to key soil properties. This would be most feasible for Tc, given the completeness and clarity of the dataset. The model could be tested or further parameterised by DGT deployments made in soils with historic contamination of Tc, for example from the Chernobyl Exclusion Zone or legacy sites associated with the reprocessing of nuclear waste. Such a model would be of great use in forecasting bioavailability in the wake of a contamination event.

Finally, given the redox-sensitive nature of Tc and Se, DGT could be used to investigate the kinetics of changes in speciation between unavailable and available forms of these elements associated with redox reactions. One approach to explore this would be to saturate the soils to promote anoxic conditions and subsequent reduction to insoluble and unavailable species, before restoring the soils to an aerobic state. A time series of DGT deployments could then be made to monitor the extent of re-oxidation to more available forms of higher redox state.

REFERENCES

Aarkrog, A. (1996) Inventory of nuclear releases in the world. In: F. Luykx and M. Frissel (ed.) *Radioecology and the Restoration of Radioactive-contaminated Sites*. Dordrecht, The Netherlands: Kluwer Academic Publishers. NATO ASI Series.

Abdelouas, A. and B. Grambow (2012) Aquatic chemistry of long-lived mobile fission and activation products in the context of deep geological disposal. In: C. Poinssot and H. Geckeis (ed.) *Radionuclide Behaviour in the Natural Environment: Science, Implications and Lessons for the Nuclear Industry*. Cambridge, UK: Woodhead Publishing.

Abdelouas, A., B. Grambow, M. Fattahi, Y. Andres and E. Leclerc-Cessac (2005) "Microbial reduction of Tc-99 in organic matter-rich soils." *Science of the Total Environment*, 336, 255-268.

Adriano, D., M. Delaney, G. Hoyt and D. Paine (1977) "Availability to plants and soil extraction of Am-241 as influenced by chelating agent, lime and soil type." *Environmental and Experimental Botany*, 17, 69-77.

Agbenin, J. and G. Welp (2012) "Bioavailability of copper, cadmium, zinc and lead in tropical Savanna soils assessed by diffusive gradients in thin films (DGT) and ion exchange resin membranes." *Environmental Monitoring and Assessment*, 184, 2275-2284.

Al-Attar, L. and A. Dyer (2002) "Sorption behaviour of uranium on birnessite, a layered manganese oxide." *Journal of Materials Chemistry*, 12, 1381-1386.

Alef, K. and P. E. Nannipieri (1995) Methods in Applied Soil Microbiology and Biochemistry. San Diego, USA: Academic Press.

Alliance for Nuclear Accountability (2011) *Oak Ridge Reservation* [Online] Available at: http://www.ananuclear.org/Portals/0/documents/Water%20Report/waterreportoakridge.pdf Accessed: 21 March, 2017.

Almas, A., P. Lombnaes, T. Sogn and J. Mulder (2006) "Speciation of Cd and Zn in contaminated soils assessed by DGT-DIFS and WHAM/Model VI in relation to uptake by spinach and ryegrass." *Chemosphere*, 62, 1647-1655.

Andrews, J. E. (2003) An Introduction to Environmental Chemistry, 2nd ed. Oxford, UK: Blackwell Science.

Ansoborlo, E. and C. Adam-Guillermin (2012) Radionuclide transfer processes in the biosphere. In: C. Poinssot and H. Geckeis (ed.) *Radionuclide Behaviour in the Natural Environment: Science, Implications and Lessons for the Nuclear Industry*. Cambridge: Woodhead Publishing**,** pp. 484-513.

Arai, Y. and D. Sparks (2002) "Residence time effects on arsenate surface speciation at the aluminum oxide-water interface." *Soil Science*, 167, 303-314.

Ashworth, D. and G. Shaw (2005) "Soil migration and plant uptake of technetium from a fluctuating water table." *Journal of Environmental Radioactivity*, 81, 155-171.

ATSDR. (2010) K-25 and S-50 uranium and fluoride releases, Oak Ridge Reservation (USDoE). Oak Ridge, Roane County, Tennessee., Atlanta, Georgia, USA: Agency for Toxic Substances and Disease Registry.

Axe, L. and P. Trivedi (2002) "Intraparticle surface diffusion of metal contaminants and their attenuation in microporous amorphous Al, Fe, and Mn oxides." *Journal of Colloid and Interface Science*, 247, 259-265.

Balistrieri, L. and T. Chao (1987) "Selenium adsorption by goethite." *Soil Science Society of America Journal*, 51, 1145-1151.

Balistrieri, L. and T. Chao (1990) "Adsorption of selenium by amorphous iron oxyhydroxide and manganese-dioxide." *Geochimica Et Cosmochimica Acta*, 54, 739-751.

Balogh, J. and D. Grigal (1980) "Soil chromatographic movement of Tc-99 through selected Minnesota soils." *Soil Science*, 130, 278-282.

Balonov, M. (2007) "The Chernobyl Forum: major findings and recommendations." *Journal of Environmental Radioactivity*, 96, 6-12.

Bamforth, P., G. Baston, J. Berry, F. Glasser, T. Heath, C. Jackson, D. Savage and S. Swanton. (2012) Cement materials for use as backfill, sealing and structural materials in geological disposal concepts. A Review of Current Status. Serco.

Banning, A., T. Demmel, T. Rüde and M. Wrobel (2013) "Groundwater uranium origin and fate control in a river valley aquifer." *Environmental Science & Technology*, 47, 13,941-913,948.

Bar-Yosef, B. and D. Meek (1987) "Selenium sorption by kaolinite and montmorillonite " *Soil Science*, 144, 11-19.

Barber, S. A. (1995) Soil Nutrient Bioavailability: A Mechanistic Approach, 2nd ed. New York: Wiley.

Bartlett, R. and B. James (1980) "Studying dried, stored soil samples - some pitfalls." *Soil Science Society of America Journal*, 44, 721-724.

Basso, M., E. Cerrella and A. Cukierman (2002) "Activated carbons developed from a rapidly renewable biosource for removal of cadmium(II) and nickel(II) ions from dilute aqueous solutions." *Industrial & Engineering Chemistry Research*, 41, 180-189.

BBC (2012) "Chernobyl sheep controls lifted in Wales and Cumbria." [Online] British Broadcasting Corporation, 22 March 2012. Available at: http://www.bbc.co.uk/news/uk-wales-17472698

Beckett, P. (1964) "Studies on soil potassium. 2. Immediate Q/I relations of labile potassium in soil." *Journal of Soil Science*, 15, 9-23.

Bednar, A., V. Medina, D. Ulmer-Scholle, B. Frey, B. Johnson, W. Brostoff and S. Larson (2007) "Effects of organic matter on the distribution of uranium in soil and plant matrices." *Chemosphere*, 70, 237-247.

Belli, M., F. Tikhomirov, A. Kliashtorin, A. Shcheglov, B. Rafferty, G. Shaw, E. Wirth, L. Kammerer, W. Ruehm, M. Steiner, B. Delvaux, E. Maes, N. Kruyts, K. Bunzl, A. Dvornik and N.

Kuchma. (1996) Dynamics of radionuclides in forest ecosystems. Report EUR 16544 EN. In: *The radiological consequences of the Chernobyl accident*, A. Karaoglou, G. Desmet, G. Kelly and H. Menzel (eds.). Luxembourg: Commission of the European Communities.

Bennett, R. and N. Willey (2003) "Soil availability, plant uptake and soil to plant transfer of Tc-99 - a review." *Journal of Environmental Radioactivity*, 65, 215-231.

Berkelaar, E. and B. Hale (2003) "Cadmium accumulation by durum wheat roots in ligand-buffered hydroponic culture: uptake of Cd-ligand complexes or enhanced diffusion?" *Canadian Journal of Botany-Revue Canadienne de Botanique*, 81, 755-763.

Berns, A., H. Philipp, H. Narres, P. Burauel, H. Vereecken and W. Tappe (2008) "Effect of gamma-sterilization and autoclaving on soil organic matter structure as studied by solid state NMR, UV and fluorescence spectroscopy." *European Journal of Soil Science*, 59, 540-550.

Bettencourt, A., M. Teixeira, M. Elias and M. Faisca (1988) "Soil-to-plant transfer of Ra-226." *Journal of Environmental Radioactivity*, 6, 49-60.

Bienvenu, P., P. Cassette, G. Andreoletti, M. Be, J. Comte and M. Lepy (2007) "A new determination of Se-79 half-life." *Applied Radiation and Isotopes*, 65, 355-364.

Bio-Rad (2017) *Chelex-100 and Chelex-20 chelating ion-exchange resin instruction manual* [Online] Bio-Rad. Available at: http://www.bio-rad.com/webroot/web/pdf/lsr/literature/LIT200.pdf Accessed: 5 June, 2017.

Bitterli, C., G. Banuelos and R. Schulin (2010) "Use of transfer factors to characterize uptake of selenium by plants." *Journal of Geochemical Exploration*, 107, 206-216.

Black, A., R. McLaren, S. Reichman, T. Speir and L. Condron (2011) "Evaluation of soil metal bioavailability estimates using two plant species (L. *perenne* and T. *aestivum*) grown in a range of agricultural soils treated with biosolids and metal salts." *Environmental Pollution*, 159, 1523-1535.

Boggs, M., M. Islam, W. Dong and N. Wall (2013) "Complexation of Tc(IV) with EDTA at varying ionic strength of NaCl." *Radiochimica Acta*, 101, 13-18.

Boggs, M., T. Minton, W. Dong, S. Lomasney, M. Islam, B. Gu and N. Wall (2011) "Interactions of Tc(IV) with humic substances." *Environmental Science & Technology*, 45, 2718-2724.

Boileau, L., E. Nieboer and D. Richardson (1985) "Uranium accumulation in the lichen *Cladonia rangiferina*. 1. Uptake of cationic, neutral and anionic forms of the uranyl ion." *Canadian Journal of Botany - Revue Canadienne de Botanique*, 63, 384-389.

Braney, M., A. Haworth, N. Jefferies and A. Smith (1993) "A study of the effects of an alkaline plume from a cementitious repository on geological materials." *Journal of Contaminant Hydrology*, 13, 379-402.

Bravin, M., A. Michaud, B. Larabi and P. Hinsinger (2010) "RHIZOtest: a plant-based biotest to account for rhizosphere processes when assessing copper bioavailability." *Environmental Pollution*, 158, 3330-3337.

Brendler, V., G. Geipel, G. Bernhard and H. Nitsche (1995) "Possible impacts of phosphate influx on the uranium speciation and migration in seepage waters." In: *International Conference Workshop on Uranium Mining and Hydrogeology*. Freiberg, Verlag Sven v. Loga, Köln, p. 61.

Bruggeman, C., A. Maes and J. Vancluysen (2007) "The interaction of dissolved Boom Clay and Gorleben humic substances with selenium oxyanions (selenite and selenate)." *Applied Geochemistry*, 22, 1371-1379.

Brun, L., J. Maillet, P. Hinsinger and M. Pepin (2001) "Evaluation of copper availability to plants in copper-contaminated vineyard soils." *Environmental Pollution*, 111, 293-302.

Buffle, J. and M. Tercier-Waeber (2000) In situ voltammetry: concepts and practise for trace metal analysis and speciation. In: J. Buffle and G. Horvai (ed.) *In Situ Monitoring of Aquatic Systems: Chemical Analysis and Speciation*. Chichester: Wiley & Sons**,** pp. 279-405.

Butherus, M. C., J. Brodeur, D. Varhus and C. Ruud (1995) "Hanford tank farms vadose zone monitoring and characterization project." In: *Symposium on Environmental Restoration 95, August 13-17*. Denver, Colorado, USA: U.S. Department of Energy Office of Environmental Restoration.

CABI (2017) *Lolium perenne. Invasive Species Compendium.* [Online] CAB International. Available at: https://plants.usda.gov/factsheet/pdf/fs_lope.pdf Accessed: 17 March, 2017.

Cai, Y. (2000) "Speciation and analysis of mercury, arsenic, and selenium by atomic fluorescence spectrometry." *Trac-Trends in Analytical Chemistry*, 19, 62-66.

Campbell, P. (1995) Interactions between trace metals and aquatic organisms: a critique of the free ion activity model. In: A. Tessier and D. Turner (ed.) *Metal Speciation and Bioavailability in Aquatic Systems*. Chichester: John Wiley & Sons**,** pp. 45-102.

Cataldo, D., R. Wildung and T. Garland (1983) "Root absorption and transport behavior of technetium in soybean." *Plant Physiology*, 73, 849-852.

Cataldo, D. A., T. R. Garland and R. E. Wildung (1984) Plant root absorption and metabolic fate of technetium in plants. In: G. Desmet and C. Myttenaera (ed.) *Technetium in the Environment*. London, UK: Elsevier**,** pp. 265-280.

Cavallaro, N. and M. McBride (1978) "Copper and cadmium adsorption characteristics of selected acid and calcareous soils." *Soil Science Society of America Journal*, 42, 550-556.

CEC. (1990) The radiological exposure of the population of the European Community from radioactivity in northeastern European marine waters - project MARINA. Report by a group of experts convened by the Commission of the European Communities (CEC). Radiation Protection 47, EUR 12483 EN. Luxembourg: CEC.

CEC. (1992) Evaluation of data on the transfer of radionuclides in the food chain. Post Chernobyl Action. CEC, EUR 12550EN, G. Desmet and J. Sinnaeve. Luxembourg: Commission of European Communities.

Chang, L., W. Davison, H. Zhang and M. Kelly (1998) "Performance characteristics for the measurement of Cs and Sr by diffusive gradients in thin films (DGT)." *Analytica Chimica Acta*, 368, 243-253.

Chen, C., H. Zhang and K. Jones (2012) "A novel passive water sampler for in situ sampling of antibiotics." *Journal of Environmental Monitoring*, 14, 1523-1530.

Cheng, H. (2016) "Investigation of diffusion and binding properties for extending applications of the DGT technique." PhD Thesis. Lancaster Environment Centre, Lancaster University, Lancaster, UK.

Chien, S. and W. Clayton (1980) "Application of Elovich equation to the kinetics of phosphate release and sorption in soils." *Soil Science Society of America Journal*, 44, 265-268.

Chomchoei, R., J. Shiowatana and P. Pongsakul (2002) "Continuous-flow system for reduction of metal readsorption during sequential extraction of soil." *Analytica Chimica Acta*, 472, 147-159.

Choppin, G. (2003) "Actinide speciation in the environment." *Radiochimica Acta*, 91, 645-649.

Christ, M. and M. David (1996) "Temperature and moisture effects on the production of dissolved organic carbon in a Spodosol." *Soil Biology & Biochemistry*, 28, 1191-1199.

Clark, S., W. Johnson, M. Malek, S. Serkiz and T. Hinton (1996) "A comparison of sequential extraction techniques to estimate geochemical controls on the mobility of fission product, actinide, and heavy metal contaminants in soils." *Radiochimica Acta*, 74, 173-179.

Cooper, J., K. Randle and R. Sokhi (2003) Radioactive Releases in the Environment: Impact and Assessment. Chichester, West Sussex, UK: Wiley.

Coppin, F., C. Chabroullet and A. Martin-Garin (2009) "Selenite interactions with some particulate organic and mineral fractions isolated from a natural grassland soil." *European Journal of Soil Science*, 60, 369-376.

Coughtrey, P., J. Kirton, N. Mitchell and C. Morris (1989) "Transfer of radioactive caesium from soil to vegetation and comparison with potassium in upland grasslands." *Environmental Pollution*, 62, 281-315.

Courchesne, F. and G. Gobran (1997) "Mineralogical variations of bulk and rhizosphere soils from a Norway spruce stand." *Soil Science Society of America Journal*, 61, 1245-1249.

Cremers, A., A. Elsen, P. Depreter and A. Maes (1988) "Quantitative analysis of radiocaesium retention in soils." *Nature*, 335, 247-249.

Cremers, A., A. Elsen, E. Valcke, J. Wauters, F. J. Sandfalls and G. S.L (1990) "The sensitivity of upland soils to radiocaesium contamination." In: *CEC workshop on the transfer of radionuclides in natural and semi-natural environments*. Udine, Italy: Elsevier Applied Science, pp. 238-248.

Crick, M. and G. Linsley (1984) "An assessment of the radiological impact of the Windscale Reactor fire, October 1957." *International Journal of Radiation Biology*, 46, 479-506.

Curl, E. and B. Truelove (1986) The Rhizosphere, 1st ed., Advanced Series in Agricultural Sciences, Vol. 15. Springer.

Cusnir, R., P. Steinmann, F. Bochud and P. Froidevaux (2014) "A DGT technique for plutonium bioavailability measurements." *Environmental Science & Technology*, 48, 10829-10834.

Dahlqvist, R., H. Zhang, J. Ingri and W. Davison (2002) "Performance of the diffusive gradients in thin films technique for measuring Ca and Mg in freshwater." *Analytica Chimica Acta*, 460, 247-256.

Darcheville, O., L. Fevrier, F. Haichar, O. Berge, A. Martin-Garin and P. Renault (2008) "Aqueous, solid and gaseous partitioning of selenium in an oxic sandy soil under different microbiological states." *Journal of Environmental Radioactivity*, 99, 981-992.

Das, S., M. Hendry and J. Essilfie-Dughan (2011) "Transformation of two-line ferrihydrite to goethite and hematite as a function of pH and temperature." *Environmental Science & Technology*, 45, 268-275.

Davison, W. and H. Zhang (1994) "In situ speciation measurements of trace components in natural waters using thin-film gels." *Nature*, 367, 546-548.

Davison, W. and H. Zhang (2012) "Progress in understanding the use of diffusive gradients in thin films (DGT) – back to basics." *Environmental Chemistry*, 9, 1-13.

DECC. (2014) Implementing Geological Disposal. Department of Energy & Climate Change.

Degryse, F. and E. Smolders (2016) DGT and bioavailability. In: W. Davison (ed.) *Diffusive Gradients in Thin Films for Environmental Measurements*. Cambridge, UK: Cambridge University Press**,** pp. 174-215.

Degryse, F., E. Smolders, I. Oliver and H. Zhang (2003) "Relating soil solution Zn concentration to diffusive gradients in thin films measurements in contaminated soils." *Environmental Science & Technology*, 37, 3958-3965.

Degryse, F., E. Smolders, H. Zhang and W. Davison (2009) "Predicting availability of mineral elements to plants with the DGT technique: a review of experimental data and interpretation by modelling." *Environmental Chemistry*, 6, 198-218.

Dementeyev, V. and N. Syromyatnikov (1968) "Conditions of formation of a sorption barrier to migration of uranium in an oxidising environment." *Geochemistry International*, 5, 394-400.

Denef, K., J. Six, H. Bossuyt, S. Frey, E. Elliott, R. Merckx and K. Paustian (2001) "Influence of dry-wet cycles on the interrelationship between aggregate, particulate organic matter, and microbial community dynamics." *Soil Biology & Biochemistry*, 33, 1599-1611.

Denney, S., J. Sherwood and J. Leyden (1999) "In situ measurements of labile Cu, Cd and Mn in river waters using DGT." *Science of the Total Environment*, 239, 71-80.

Desmet, G., L. van Loon and B. Howard (1991) "Chemical speciation and bioavailability of elements in the environment and their relevance to radioecology." *Science of the Total Environment*, 100, 105-124.

DGT Research (2017) *Commercial Online Shop* [Online] Available at: http://www.dgtresearch.com/product-category/commercial/ Accessed: January 3, 2017.

Dhillon, K., S. Dhillon and R. Dogra (2010) "Selenium accumulation by forage and grain crops and volatilization from seleniferous soils amended with different organic materials." *Chemosphere*, 78, 548-556.

Di Tullo, P., F. Pannier, Y. Thiry, I. Le Hecho and M. Bueno (2016) "Field study of time-dependent selenium partitioning in soils using isotopically enriched stable selenite tracer." *Science of the Total Environment*, 562, 280-288.

Ding, S., D. Xu, Q. Sun, H. Yin and C. Zhang (2010) "Measurement of dissolved reactive phosphorus using the diffusive gradients in thin films technique with a high-capacity binding phase." *Environmental Science & Technology*, 44, 8169-8174.

Ding, S., D. Xu, Y. Wang, Y. Wang, Y. Li, M. Gong and C. Zhang (2016) "Simultaneous measurements of eight oxyanions using high-capacity diffusive gradients in thin films (Zr-oxide DGT) with a high-efficiency elution procedure." *Environmental Science & Technology*, 50, 7572-7580.

Dowding, C., M. Borda, M. Fey and D. Sparks (2005) "A new method for gaining insight into the chemistry of drying mineral surfaces using ATR-FTIR." *Journal of Colloid and Interface Science*, 292, 148-151.

Drever, J. (1997) The geochemistry of natural waters, 3rd. Upper Saddle River, NJ: Prentice Hall, 193.

Drozdzak, J., M. Leermakers, Y. Gao, V. Phrommavanh and M. Descostes (2015) "Evaluation and application of Diffusive Gradients in Thin Films (DGT) technique using Chelex (R)-100, Metsorb (TM) and Diphonix (R) binding phases in uranium mining environments." *Analytica Chimica Acta*, 889, 71-81.

Drozdzak, J., M. Leermakers, Y. Gao, V. Phrommavanh and M. Descostes (2016) "Novel speciation method based on Diffusive Gradients in Thin Films for in situ measurement of uranium in the vicinity of the former uranium mining sites." *Environmental Pollution*, 214, 114-123.

Dublet, G., J. Pacheco, J. Bargar, S. Fendorf, N. Kumar, G. Lowry and G. Brown Jr (2017) "Partitioning of uranyl between ferrihydrite and humic substances at acidic and circum-neutral pH." *Geochimica Et Cosmochimica Acta*, 215, 122-140.

Duc, M., G. Lefevre, M. Fedoroff, J. Jeanjean, J. Rouchaud, F. Monteil-Rivera, J. Dumonceau and S. Milonjic (2003) "Sorption of selenium anionic species on apatites and iron oxides from aqueous solutions." *Journal of Environmental Radioactivity*, 70, 61-72.

Duff, M., J. Coughlin and D. Hunter (2002) "Uranium co-precipitation with iron oxide minerals." *Geochimica et Cosmochimica Acta*, 66, 3533-3547.

Duquene, L., H. Vandenhove, F. Tack, M. Van Hees and J. Wannijn (2010) "Diffusive gradient in thin films (DGT) compared with soil solution and labile uranium fraction for predicting uranium bioavailability to ryegrass." *Journal of Environmental Radioactivity*, 101, 140-147.

Echevarria, G., J. Morel, J. Fardeau and E. Leclerc-Cessac (1998) "Assessment of phytoavailability of nickel in soils " *Journal of Environmental Quality* 27, 1064-1070.

Echevarria, G., J. Morel, L. Florentin and E. Leclerc-Cessac (2003) "Influence of climatic conditions and soil type on $^{99}TcO_4^-$ uptake by ryegrass." *Journal of Environmental Radioactivity*, 70, 85-97.

Echevarria, G., M. Sheppard and J. Morel (2001) "Effect of pH on the sorption of uranium in soils." *Journal of Environmental Radioactivity*, 53, 257-264.

Echevarria, G., P. Vong, E. LeclercCessac and J. Morel (1997) "Bioavailability of technetium-99 as affected by plant species and growth, application form, and soil incubation." *Journal of Environmental Quality*, 26, 947-956.

Echevarria, G., P. Vong and J. Morel (1998) "Effect of NO_3^- on the fate of (TcO_4^-)-Tc-99 system in the soil-plant system." *Journal of Environmental Radioactivity*, 38, 163-171.

Ehlken, S. and G. Kirchner (2002) "Environmental processes affecting plant root uptake of radioactive trace elements and variability of transfer factor data: a review." *Journal of Environmental Radioactivity*, 58, 97-112.

Eisenbud, M. and T. Gesell (1997) Environmental Radioactivity: from Natural, Industrial and Military Sources, 4th ed. San Diego, California, USA: Academic Press.

Eisenbud, M. and T. F. Gesell (1997) Environmental radioactivity : from natural, industrial, and military sources, 4th ed. San Diego, [Calif.] ; London: Academic Press.

Elrashidi, M., D. Adriano, S. Workman and W. Lindsay (1987) "Chemical-equilibria of selenium in soils - a theoretical development." *Soil Science*, 144, 141-152.

Elzinga, E. and R. Reeder (2002) "X-ray absorption spectroscopy study of Cu^{2+} and Zn^{2+} adsorption complexes at the calcite surface: implications for site-specific metal incorporation preferences during calcite crystal growth." *Geochimica et Cosmochimica Acta*, 66, 3943-3954.

Erich, M. and B. Hoskins (2011) "Effects of soil drying on soil pH and nutrient extractability." *Communications in Soil Science and Plant Analysis*, 42, 1167-1176.

Ernstberger, H., W. Davison, H. Zhang, A. Tye and S. Young (2002) "Measurement and dynamic modeling of trace metal mobilization in soils using DGT and DIFS." *Environmental Science & Technology*, 36, 349-354.

Ernstberger, H., H. Zhang, A. Tye, S. Young and W. Davison (2005) "Desorption kinetics of Cd, Zn and Ni measured in soils by DGT." *Environmental Science & Technology*, 39, 1591-1597.

Evans, D., J. Alberts and R. Clark (1983) "Reversible ion-exchange fixation of cesium-137 leading to mobilization from reservoir sediments." *Geochimica et Cosmochimica Acta*, 47, 1041-1049.

Ewers, L. and J. Brown. (2014) Experimental studies on the uptake of technetium-99 to terrestrial crops. Chilton, Oxfordshire: Public Health England.

Ewers, L., A. Eslava-Gomez and J. Brown. (2011) Review of the transfer of technetium to terrestrial crops and animal products. Chilton, Oxfordshire: Public Health England.

Fernald Citizen's Task Force. (1995) Recommendations on remediation levels, waste disposition, priorities and future use. Ross, Ohio:

Fernandez-Martinez, A. and L. Charlet (2009) "Selenium environmental cycling and bioavailability: a structural chemist point of view." *Reviews in Environmental Science and Biotechnology*, 8, 81-110.

Ferri, T. and P. Sangiorgio (1999) "Voltammetric study of the interaction between Se(IV) and dissolved organic matter in environmental aqueous matrices." *Analytica Chimica Acta*, 385, 337-343.

Fitch, A. and P. Helmke (1989) "Donnan equilibrium graphite-furnace atomic-absorption estimates of soil extract complexation capacities." *Analytical Chemistry*, 61, 1295-1298.

Fordyce, F. (2005) Selenium deficiency and toxicity in the environment. In: O. Selinus (ed.) *Essentials of Medical Geology, 1st ed.* Uppsala, Sweden: Elsevier.

Francis, A. (1982) Environmental migration of long-lived radionuclides. IAEA-SM-257/72. Vienna: International Atomic Energy Agency.

Francis, A. (1990) "Microbial dissolution and stabilization of toxic metals and radionuclides in mixed wastes." *Experientia*, 46, 840-851.

Francis, A., J. Duxbury and M. Alexande (1974) "Evolution of dimethylselenide from soils." *Applied Microbiology*, 28, 248-250.

Fredrickson, J., J. Zachara, D. Kennedy, M. Duff, Y. Gorby, S. Li and K. Krupka (2000) "Reduction of U(VI) in goethite (alpha-FeOOH) suspensions by a dissimilatory metal-reducing bacterium." *Geochimica et Cosmochimica Acta*, 64, 3085-3098.

French, M., H. Zhang, J. Pates, S. Bryan and R. Wilson (2005) "Development and performance of the diffusive gradients in thin-films technique for the measurement of technetium-99 in seawater." *Analytical Chemistry*, 77, 135-139.

Froideval, A., M. del Nero, C. Gaillard, R. Barillon, I. Rossini and J. Hazemann (2006) "Uranyl sorption species at low coverage on Al-hydroxide: TRLFS and XAFS studies." *Geochimica et Cosmochimica Acta*, 70, 5270-5284.

Gabler, H., A. Bahr, A. Heidkamp and J. Utermann (2006) "Enriched stable isotopes for determining the isotopically exchangeable element content in soils." *European Journal of Soil Science*, 58, 746-757.

Gao, S., K. Tanji, D. Peters and M. Herbel (2000) "Water selenium speciation and sediment fractionation in a California flow-through wetland system." *Journal of Environmental Quality*, 29, 1275-1283.

Garmo, O., O. Royset, E. Steinnes and T. Flaten (2003) "Performance study of diffusive gradients in thin films for 55 elements." *Analytical Chemistry*, 75, 3573-3580.

Garten, C., F. Hoffman and E. Bondiette (1984) "Field and greenhouse experiments on the fate of technetium in plants and soil." *Health Physics*, 46, 647-656.

Gavrilescu, M., L. Pavel and I. Cretescu (2009) "Characterization and remediation of soils contaminated with uranium." *Journal of Hazardous Materials*, 163, 475-510.

Geraedts, K., C. Bruggeman, A. Maes, L. van Loon, A. Rossberg and T. Reich (2002) "Evidence for the existence of Tc(IV)-humic substance species by X-ray absorption near-edge spectroscopy." *Radiochimica Acta*, 90, 879-884.

Giblin, A., B. Batts and D. Swaine (1981) "Laboratory simulation studies of uranium mobility in natural waters." *Geochimica Et Cosmochimica Acta*, 45, 699-709.

Gibney, E. (2015) "Why Finland now leads the world in nuclear waste storage." [Online] Nature, 2nd December 2015. Available at: http://www.nature.com/news/why-finland-now-leads-the-world-in-nuclear-waste-storage-1.18903

Gleyzes, C., S. Tellier and M. Astruc (2002) "Fractionation studies of trace elements in contaminated soils and sediments: a review of sequential extraction procedures." *Trends in Analytical Chemistry*, 21, 451-467.

Goh, K. and T. Lim (2004) "Geochemistry of inorganic arsenic and selenium in a tropical soil: effect of reaction time, pH and competitive anions on arsenic and selenium adsorption." *Chemosphere*, 55, 849-859.

Graham, E. and C. Silva (1979) "Labile pools and distribution coefficients for soil calcium, magnesium and potassium determined with exchange equilibria and radioisotopes." *Soil Science*, 128, 17-22.

Grambow, B. (2008) "Mobile fission and activation products in nuclear waste disposal." *Journal of Contaminant Hydrology*, 102, 180-186.

Greenland, D. and M. Hayes (1981) The Chemistry of Soil Processes. New York, USA: Wiley-Interscience.

Gregusova, M. and B. Docekal (2011) "New resin gel for uranium determination by diffusive gradients in thin films technique." *Analytica Chimica Acta*, 684, 142-146.

Grogan, H., N. Mitchell, M. Minski and J. Bell (1986) Pathways of radionuclides from soils to wheat. In: P. Coughtrey, M. Martin and M. Unsworth (ed.) *Pollutant Transport and Fate in Ecosystems*. Oxford, UK: Blackwell Scientific Publications.

Gu, B., W. Dong, L. Liang and N. Wall (2011) "Dissolution of technetium(IV) oxide by natural and synthetic organic ligands under both reducing and oxidizing conditions." *Environmental Science & Technology*, 45, 4771-4777.

Gu, B. and C. Ruan (2007) "Determination of technetium and its speciation by surface-enhanced Raman spectroscopy." *Analytical Chemistry*, 79, 2341-2345.

Guan, D., P. Williams, J. Luo, J. Zheng, H. Xu, C. Cai and L. Ma (2015) "Novel precipitated zirconia-based DGT technique for high-resolution imaging of oxyanions in waters and sediments." *Environmental Science & Technology*, 49, 3653-3661.

Gunther, A., G. Bernhard, G. Geipel, T. Reich, A. Rossberg and H. Nitsche (2003) "Uranium speciation in plants." *Radiochimica Acta*, 91, 319-328.

Guo, G., T. Yuan, W. Wang, D. Li and J. Wang (2011) "Effect of aging on bioavailability of copper on the fluvo aquic soil." *International Journal of Environmental Science and Technology*, 8, 715-722.

Gupta, S. and C. Aten (1993) "Comparison and evaluation of extraction media and their suitability in a simple model to predict the biological relevance of heavy metal concentrations in contaminated soils." *International Journal of Environmental Analytical Chemistry*, 51, 25-46.

Gustafsson, J. and L. Johnsson (1994) "The association between selenium and humic substances in forested ecosystems - laboratory evidence " *Applied Organometallic Chemistry*, 8, 141-147.

Guzman, E., E. Regil, L. Gutierrez, M. Alberich and A. Hernandez (2006) "Contamination of corn growing areas due to intensive fertilization in the high plane of Mexico." *Water, Air, & Soil Pollution*, 175, 77-98.

Hammer, D. and C. Keller (2002) "Changes in the rhizosphere of metal-accumulating plants evidenced by chemical extractants." *Journal of Environmental Quality*, 31, 1561-1569.

Hamon, R., I. Bertrand and M. McLaughlin (2002) "Use and abuse of isotopic exchange data in soil chemistry." *Australian Journal of Soil Research*, 40, 1731-1381.

Hamon, R., J. Wundke, M. McLaughlin and R. Naidu (1997) "Availability of zinc and cadmium to different plant species." *Australian Journal of Soil Research*, 35, 1267-1277.

Han, R., W. Zou, Y. Wang and L. Zhu (2007) "Removal of uranium(VI) from aqueous solution by manganese oxide coated zeolite: discussion of adsorption isotherms and pH effect." *Journal of Environmental Radioactivity*, 93, 127-143.

Haq, A., T. Bates and Y. Soon (1980) "Comparison of extractants for plant-available zinc, cadmium, nickel and copper in contaminated soils." *Soil Science Society of America Journal*, 44, 772-777.

Harper, M., W. Davison and W. Tych (2000) "DIFS - a modelling and simulation tool for DGT-induced trace metal remobilisation in sediments and soils." *Environmental Modelling & Software*, 15, 55-66.

Harper, M., W. Davison, H. Zhang and W. Tych (1998) "Kinetics of metal exchange between solids and solutions in sediments and soils interpreted from DGT-measured fluxes." *Geochimica et Cosmochimica Acta*, 62, 2757-2770.

Haudin, C., E. Quillerou, G. Wang, S. Staunton and A. Martin-Garin (2011) "Dynamics of Tc immobilisation in soils under flooded conditions and extent of reoxidation following aeration." *Geomicrobiology Journal*, 28, 410-417.

Haynes, R. and R. Swift (1991) "Concentrations of extractable Cu, Zn, Fe and Mn in a group of soils as influenced by air-drying and oven-drying and re-wetting." *Geoderma*, 49, 319-333.

Haynes, W. and D. Lide (2011) CRC Handbook of Chemistry and Physics: A Ready-Reference Book of Chemical and Physical Data, 92nd ed. London, UK: CRC Press.

Hedley, M., R. White and P. Nye (1982) "Plant-induced changes in the rhizosphere of rape (Brassica napus var. Emerald) seedlings. III. Changes in L value, soil phosphate fractions and phosphatase activity." *New Phytologist*, 91, 41-56.

Henrot, J. (1989) "Bioaccumulation and chemical modification of Tc by soil bacteria." *Health Physics*, 57, 239-245.

Hird, A., D. Rimmer and F. Livens (1995) "Total caesium-fixing potentials of acid organic soils." *Journal of Environmental Radioactivity*, 26, 103-118.

Hird, A., D. Rimmer and F. Livens (1996) "Factors affecting the sorption and fixation of caesium in acid organic soil." *European Journal of Soil Science*, 47, 97-104.

Ho, C. and N. Miller (1986) "Adsorption of uranyl species from bicarbonate solution onto hematite particles." *Journal of Colloid and Interface Science*, 110, 165-171.

Ho, Y. (1995) "Adsorption of heavy metals from waste streams by peat." PhD Thesis. University of Birmingham, Birmingham, UK.

Ho, Y. (2006) "Review of second-order models for adsorption systems." *Journal of Hazardous Materials*, 136, 681-689.

Ho, Y., W. Chiu, C. Hsu and C. Huang (2004) "Sorption of lead ions from aqueous solution using tree fern as a sorbent." *Hydrometallurgy*, 73, 55-61.

Ho, Y. and G. McKay (1999) "Pseudo-second-order model for sorption processes." *Process Biochemistry*, 34, 451-465.

Hockin, S. and G. Gadd (2003) "Linked redox precipitation of sulfur and selenium under anaerobic conditions by sulfate-reducing bacterial biofilms." *Applied and Environmental Microbiology*, 69, 7063-7072.

Hoffman, F., C. Garten, D. Lucas and J. Huckabee (1982) "Environmental behavior of technetium in soil and vegetation - implications for radiological assessments." *Environmental Science & Technology*, 16, 214-217.

Holm, P., T. Christensen, J. Tjell and S. McGrath (1995) "Speciation of cadmium and zinc with application to soil solutions." *Journal of Environmental Quality*, 24, 183-190.

Hooda, P., H. Zhang, W. Davison and A. Edwards (1999) "Measuring bioavailable trace metals by diffusive gradients in thin films (DGT): soil moisture effects on its performance in soils." *European Journal of Soil Science*, 50, 285-294.

Horovitz, L. (2015) "Beyond pessimism: why the treaty on the Non-Proliferation of Nuclear Weapons will not collapse." *Journal of Strategic Studies*, 38.

Hosse, M. and K. Wilkinson (2001) "Determination of electrophoretic mobilities and hydrodynamic radii of three humic substances as a function of pH and ionic strength." *Environmental Science & Technology*, 41, 4305-4310.

Houba, V., E. Temminghoff, G. Gaikhorst and W. van Vark (2000) "Soil analysis procedures using 0.01 M calcium chloride as extraction reagent." *Communications in Soil Science and Plant Analysis*, 31, 1299-1396.

Hough, R., A. Tye, N. Crout, S. McGrath, H. Zhang and S. Young (2005) "Evaluating a 'Free Ion Activity Model' applied to metal uptake by *Lolium perenne* L. grown in contaminated soils." *Plant and Soil*, 270, 1-12.

Hsi, C. and D. Langmuir (1985) "Adsorption of uranyl onto ferric oxyhydroxides - application of the surface complexation site-binding model." *Geochimica et Cosmochimica Acta*, 49, 1931-1941.

Hutchins, C., J. Panther, P. Teasdale, F. Wang, R. Stewart, W. Bennett and H. Zhao (2012) "Evaluation of a titanium dioxide-based DGT technique for measuring inorganic uranium species in fresh and marine waters." *Talanta*, 97, 550-556.

Huynh, T., H. Zhang and B. Noller (2012) "Evaluation and application of the diffusive gradients in thin films technique using a mixed-binding gel layer for measuring inorganic arsenic and metals in mining impacted water and soil." *Analytical Chemistry*, 84, 9988-9995.

IAEA (1994) Handbook of parameter values for the prediction of radionuclide transfer in temperate environments. International Atomic Energy Agency Technical Report no. 364. Vienna, Austria, International Atomic Energy Agency,.

IAEA. (1998) The radiological accident in the reprocessing plant at Tomsk. Vienna, Austria: International Atomic Energy Agency.

IAEA. (2005) Management of high enriched uranium for peaceful purposes: status and trends. IAEA-TECDOC-1452. Vienna, Austria: International Atomic Energy Agency.

IAEA. (2006) Environmental Consequences of the Chernobyl Accident and their Remediation: Twenty Years of Experience. Report of the UN Chernobyl Forum Expert Group., Vienna, Austria:

IAEA. (2010) Handbook of parameter values for the prediction of radionuclide transfer in terrestrial and freshwater environments. Technical Reports Series no. 472. Vienna, Austria: International Atomic Energy Agency.

IAEA. (2015) The Fukushima Daiichi accident. Vienna, Austria: International Atomic Energy Agency.

IAEA (2017) *International Atomic Energy Agency Power Reactor Information System Database* [Online] Available at: https://www.iaea.org/PRIS/home.aspx Accessed: February 22, 2017.

Icenhower, J., N. Qafoku, J. Zachara and W. Martin (2010) "The biogeochemistry of technetium: a review of the behaviour of an artificial element in the natural environment." *American Journal of Science*, 310, 721-752.

Jang, J., B. Dempsey and W. Burgos (2007) "A model-based evaluation of sorptive reactivities of hydrous ferric oxide and hematite for U(VI)." *Environmental Science & Technology*, 41, 4305-4310.

Janke, R. C., R. J. Janke, M. J. Davis and L. J. Habegger (1992) "RI/FS work plan for development for the process area at the U.S. DoE Fernald Site." *Health Physics*, 62 (Suppl.6), S36-S37.

Jannasch, H., B. Honeyman, L. Balistrieri and J. Murray (1988) "Kinetics of trace element uptake by marine particles." *Geochimica Et Cosmochimica Acta*, 52, 567-577.

Jenkinson, S., D. McCubbin, P. Kennedy, A. Dewar, R. Bonfield and K. Leonard (2014) "An estimate of the inventory of technetium-99 in the sub-tidal sediments of the Irish Sea." *Journal of Environmental Radioactivity*, 133, 40-47.

Johnson, T. and T. Bullen (2003) "Selenium isotope fractionation during reduction by Fe(II)-Fe(III) hydroxide-sulfate (green rust)." *Geochimica et Cosmochimica Acta*, 67, 413-419.

Johnsson, L. (1991) "Selenium uptake by plants as a function of soil type, organic matter content and pH." *Plant and Soil*, 133, 57-64.

Jordan, N., N. Marmier, C. Lomenech, E. Giffaut and J. Ehrhardt (2009) "Competition between selenium (IV) and silicic acid on the hematite surface." *Chemosphere*, 75, 129-134.

Jorg, G., R. Buhnemann, S. Hollas, N. Kivel, K. Kossert, S. van Winckel and C. Gostomski (2010) "Preparation of radiochemically pure Se-79 and highly precise determination of its half-life." *Applied Radiation and Isotopes*, 68, 2339-2351.

Juhasz, A., E. Smith, J. Weber, R. Naidu, M. Rees, A. Rofe, T. Kuchel and L. Sansom (2008) "Effect of soil ageing on in vivo arsenic bioavailability in two dissimilar soils." *Chemosphere*, 71, 2180-2186.

Kaiser, K., M. Kaupenjohann and W. Zech (2001) "Sorption of dissolved organic carbon in soils: effects of soil sample storage, soil-to-solution ratio and temperature." *Geoderma*, 99, 317-328.

Kang, Y., H. Yamada, K. Kyuma and T. Hattori (1993) "Speciation of selenium in soil." *Soil Science and Plant Nutrition*, 39, 331-337.

Kang, Y., H. Yamada, K. Kyuma, T. Hattori and S. Kigasawa (1991) "Selenium in soil humic acid." *Soil Science and Plant Nutrition*, 37, 241-248.

Kaplan, D. (2003) "Influence of surface charge of an Fe-oxide and an organic matter-dominated soil on iodide and pertechnetate sorption." *Radiochimica Acta*, 91, 173-178.

Kashiwa, M., S. Nishimoto, K. Takahashi, M. Ike and M. Fujita (2000) "Factors affecting soluble selenium removal by a selenate-reducing bacterium Bacillus sp SF-1." *Journal of Bioscience and Bioengineering*, 89, 528-533.

Kennedy, V., A. Sanchez, D. Oughton and A. Rowland (1997) "Use of single and sequential chemical extractants to assess radionuclide and heavy metal availability from soils for root uptake." *Analyst*, 122, R89-R100.

Kieft, T., E. Soroker and M. Firestone (1987) "Microbial biomass response to a rapid increase in water potential when dry soil is wetted." *Soil Biology & Biochemistry*, 19, 119-126.

Kikkert, J., B. Hale and E. Berkelaar (2013) "Selenium accumulation in durum wheat and spring canola as a function of amending soils with selenite, selenate and/or sulphate." *Plant and Soil*, 372, 629-641.

Klitzke, S. and F. Lang (2007) "Hydrophobicity of soil colloids and heavy metal mobilization: effects of drying." *Journal of Environmental Quality*, 36, 1187-1193.

Koch-Steindl, H. and G. Prohl (2001) "Considerations on the behaviour of long-lived radionuclides in the soil." *Radiation and Environmental Biophysics*, 40, 93-104.

Koopmans, G. and J. Groenenberg (2011) "Effects of soil oven-drying on concentrations and speciation of trace metals and dissolved organic matter in soil solution extracts of sandy soils." *Geoderma*, 161, 147-158.

Koster, M., L. Reijnders, N. van Oost and W. Peijnenburg (2005) "Comparison of the method of diffusive gels in thin films with conventional extraction techniques for evaluating zinc accumulation in plants and isopods." *Environmental Pollution*, 133, 103-116.

Kottler, B., J. White and J. Kelsey (2001) "Influence of soil moisture on the sequestration of organic compounds in soil." *Chemosphere*, 42, 893-898.

Krijger, G., C. Kolloffel and H. Wolterbeek (2000) "Effect of nitrate on uptake of pertechnetate by tomato plants." *Journal of Environmental Quality*, 29, 866-870.

Krouglov, S., A. Filipas, R. Alexakhin and N. Arkhipov (1997) "Long-term study on the transfer of Cs-137 and Sr-90 from Chernobyl-contaminated soils to grain crops." *Journal of Environmental Radioactivity*, 34, 267-286.

Krupka, K. and R. Serne. (2002) Geochemical factors affecting the behaviour of antimony, cobalt, europium, technetium and uranium in vadose sediments. Richland, Washington: P. N. N. Laboratory.

Kuzyakov, Y., J. Friedel and K. Stahr (2000) "Review of mechanisms and quantification of priming effects." *Soil Biology & Biochemistry*, 32, 1485-1498.

Lakanen, E. and R. Ervio (1971) "A comparison of eight extractants for the determination of plant available micronutrients in soils." *Acta Agric. Fennica*, 123, 223-232.

Langmuir, D. (1978) "Uranium solution-mineral equilibria at low-temperatures with applications to sedimentary ore-deposits." *Geochimica et Cosmochimica Acta*, 42, 547-569.

Larsen, S. (1952) "The use of P-32 in studies on the uptake of phosphorus by plants." *Plant and Soil*, 4, 1-10.

Leermakers, M., Y. Gao, J. Navez, A. Poffijn, K. Croes and W. Baeyens (2009) "Radium analysis by sector field ICP-MS in combination with the Diffusive Gradients in Thin Films (DGT) technique." *Journal of Analytical Atomic Spectrometry*, 24, 1115-1117.

Lehto, J. and X. Hou (2011) Chemistry and Analysis of Radionuclides: Laboratory Techniques and Methodology. Weinheim, Germany: Wiley-VCH.

Lehto, N., W. Davison, H. Zhang and W. Tych (2006) "Analysis of micro-nutrient behaviour in the rhizosphere using a DGT-parameterised dynamic plant uptake model." *Plant and Soil*, 282, 227-238.

Lehto, N., W. Davison, H. Zhang and W. Tych (2006) "Theoretical comparison of how soil processes affect uptake of metals by diffusive gradients in thin films and plants." *Journal of Environmental Quality*, 35, 1903-1913.

Lehto, N., L. Sochaczewski, W. Davison, W. Tych and H. Zhang (2008) "Quantitative assessment of soil parameter (K_D and T_c) estimation using DGT measurements and the 2D DIFS model." *Chemosphere*, 71, 795-801.

Lembrechts, J., L. van Loon, J. van Ginkel and G. Desmet (1988) Interpretation of soil-to-plant transfer on the basis of soil solution chemical composition. In: (ed.) *Impact of Nuclear Accidents on the Environment*. Vol. 1**,** pp. 169-179.

Lenhart, J. and B. Honeyman (1999) "Uranium(VI) sorption to hematite in the presence of humic acid." *Geochimica et Cosmochimica Acta*, 63, 2891-2901.

Leonard, K., D. McCubbin, J. Brown, R. Bonfield and T. Brooks (1997) "Distribution of technetium-99 in UK coastal waters." *Marine Pollution Bulletin*, 34, 628-636.

Li, H., E. Lombi, J. Stroud, S. McGrath and F. Zhao (2010) "Selenium speciation in soil and rice: influence of water management and Se fertilization." *Journal of Agricultural and Food Chemistry*, 58, 11837-11843.

Li, J., Q. Peng, D. Liang, S. Liang, J. Chen, H. Sun, S. Li and P. Lei (2016) "Effects of aging on the fraction distribution and bioavailability of selenium in three different soils." *Chemosphere*, 144, 2351-2359.

Li, W., C. Li, J. Zhao and R. Cornett (2007) "Diffusive gradients in thin films technique for uranium measurements in river water." *Analytica Chimica Acta*, 592, 106-113.

Li, W., J. Zhao, C. Li, S. Kiser and R. Cornett (2006) "Speciation measurements of uranium in alkaline waters using diffusive gradients in thin films technique." *Analytica Chimica Acta*, 575, 274-280.

Li, Z., D. Liang, Q. Peng, Z. Cui, J. Huang and Z. Lin (2017) "Interaction between selenium and soil organic matter and its impact on soil selenium bioavailability: A review." *Geoderma*, 295, 69-79.

Li, Z., L. Wu, H. Zhang, Y. Luo and P. Christie (2015) "Effects of soil drying and wetting-drying cycles on the availability of heavy metals and their relationship to dissolved organic matter." *Journal of Soils and Sediments*, 15, 1510-1519.

Libert, M., O. Bildstein, L. Esnault and R. Sellier (2011) "Molecular hydrogen: an abundant energy source for bacterial activity in nuclear waste repositories." *Physics and Chemistry of the Earth*, 36, 1616-1623.

Liu, J., X. Feng, G. Qiu, C. Anderson and H. Yao (2012) "Prediction of methyl mercury uptake by rice plants (*Oryza sativa* L.) using the diffusive gradients in thin films technique." *Environmental Science & Technology*, 46, 11013-11020.

Liu, X., Z. Zhao, B. Duan, C. Hu, X. Zhao and Z. Guo (2015) "Effect of applied sulphur on the uptake by wheat of selenium applied as selenite." *Plant and Soil*, 386, 35-45.

Lloyd, J. and L. Macaskie (1996) "A novel PhosphorImager-based technique for monitoring the microbial reduction of technetium." *Applied and Environmental Microbiology*, 62, 578-582.

Lloyd, J., H. Nolting, V. Sole and K. Bosecker (1998) "Technetium reduction and precipitation by sulfate-reducing bacteria." *Geomicrobiology Journal*, 15, 45-58.

Lloyd, J., V. Sole, C. Van Praagh and D. Lovley (2000) "Direct and Fe(II)-mediated reduction of technetium by Fe(III)-reducing bacteria." *Applied and Environmental Microbiology*, 66, 3743-3749.

Lombi, E., R. Hamon, S. McGrath and M. McLaughlin (2003) "Lability of Cd, Cu and Zn in polluted soils treated with lime, beringite, and red mud and identification of a non-labile colloidal fraction of metals using isotopic techniques." *Environmental Science & Technology*, 37, 979-984.

Lopez, P. and E. Graham (1972) "Labile pool and plant uptake of micronutrients: 1. Determination of labile pool of Mn, Fe, Zn, Co and Cu in deficient soils by isotopic exchange " *Soil Science*, 114, 295-299.

Losi, M. and W. Frakenberger (1998) "Microbial oxidation and solubilization of precipitated elemental selenium in soil." *Journal of Environmental Quality*, 27, 836-843.

Luo, J., F. Weber, O. Cirpka, W. Wu, J. Nyman, J. Carley, P. Jardine, C. Criddle and P. Kitanidis (2007) "Modeling in-situ uranium(VI) bioreduction by sulfate-reducing bacteria." *Journal of Contaminant Hydrology*, 92, 129-148.

Luo, J., H. Zhang, J. Santner and W. Davison (2010) "Performance characteristics of diffusive gradients in thin films equipped with a binding gel layer containing precipitated ferrihydrite for measuring arsenic(V), selenium(VI), vanadium(V) and antimony(V)." *Analytical Chemistry*, 82, 8903-8909.

Luo, J., H. Zhang, F. Zhao and W. Davison (2010) "Distinguishing diffusional and plant control of Cd and Ni uptake by hyperaccumulator and non-hyperaccumulator plants." *Environmental Science & Technology*, 44, 6636-6641.

Ma, Y., E. Lombi, I. Oliver, A. Nolan and M. McLaughlin (2006) "Long-term aging of copper added to soils." *Environmental Science & Technology*, 40, 6310-6317.

Ma, Y. and N. Uren (1997) "The effects of temperature, time and cycles of drying and rewetting on the extractability of zinc added to a calcareous soil." *Geoderma*, 75, 89-97.

Maes, A., K. Geraedts, C. Bruggeman, J. Vancluysen, A. Rossberg and C. Hennig (2004) "Evidence for the interaction of technetium colloids with humic substances by X-ray absorption spectroscopy." *Environmental Science & Technology*, 38, 2044-2051.

Makeyeva, V. (1989) "Effect of wetting and drying on the soil structure." *Soviet Soil Science*, 21, 81-89.

Manceau, A., L. Charlet, M. Boisset, B. Didier and L. Spadini (1992) "Sorption and speciation of heavy metals on hydrous Fe and Mn oxides. From microscopic to macroscopic." In: *Clays and hydrosilicate gels in applied nuclear fields. In: Proceedings of Symposium B on clays and hydrosilicate gels in nuclear fields of the 1991 E-MRS fall conference*. Strasbourg, France: North-Holland.

Marschner, H. (1995) Mineral Nutrition of Higher Plants, 2nd ed. London, UK: Academic Press.

Mason, C., W. Turney, B. Thomson, N. Lu, P. Longmire and C. Chisholm-Brause (1997) "Carbonate leaching of uranium from contaminated soils." *Environmental Science & Technology*, 31, 2707-2711.

Mason, S., R. Hamon, A. Nolan, H. Zhang and W. Davison (2005) "Performance of a mixed binding layer for measuring anions and cations in a single assay using the diffusive gradients in thin films technique." *Analytical Chemistry*, 77, 6339-6346.

Mason, S., A. McNeill, M. McLaughlin and H. Zhang (2010) "Prediction of wheat response to an application of phosphorus under field conditions using diffusive gradients in thin-films (DGT) and extraction methods." *Plant and Soil*, 337, 243-258.

Mathers, A., S. Young, S. McGrath, F. Zhao, N. Crout and E. Bailey (2017) "Determining the fate of selenium in wheat biofortification: an isotopically labelled field trial study." *Plant and Soil*, 420, 61-77.

McAuliffe, C. D., N. S. Hall, L. A. Dean and S. B. Hendricks (1947) "Exchange reactions between phosphates and soils: hydoxylic surfaces of soil minerals." *Soil Science Society of America, Proceedings*, 12, 119-123.

McBeath, T., M. McLaughlin, R. Armstrong, M. Bell, M. Bolland, M. Conyers, R. Holloway and S. Mason (2007) "Predicting the response of wheat (*Triticum aestivum* L.) to liquid and granular phosphorus fertilisers in Australian soils." *Australian Journal of Soil Research*, 45, 448-458.

McLaren, R. and D. Crawford (1973) "Studies on soil copper. 2. Specific adsorption of copper by soils." *Journal of Soil Science*, 24, 443-452.

McLaughlin, M. (2002) Bioavailability of metals to terrestrial plants. In: H. Allen (ed.) *Bioavailability in Terrestrial Ecosystems: Importance of Partitioning for Bioavailability to Invertebrates, Microbes and Plants*. Pensacola, Florida, USA: Society of Environmental Toxicology and Chemistry.

McLaughlin, M., S. Andrew, M. Smart and E. Smolders (1998) "Effects of sulfate on cadmium uptake by Swiss chard: I. Effects of complexation and calcium competition in nutrient solutions." *Plant and Soil*, 202, 211-216.

McLaughlin, M., E. Smolders and R. Merckx. (1998) Soil-root interface: physicochemical processes. In:. Soil Chemistry and Ecosystem Health; Special Publication no. 52, Madison, Wisconsin: Soil Science Society of America.

McLaughlin, M., B. Zarcinas, D. Stevens and N. Cook (2000) "Soil testing for heavy metals." *Communications in Soil Science and Plant Analysis*, 31, 1661-1700.

Meers, E., G. Du Laing, V. Unamuno, E. Lesage, F. Tack and M. Verloo (2006) "Water extractability of trace metals from soils: some pitfalls." *Water, Air and Soil Pollution*, 176, 21-35.

Meers, E., R. Samson, F. Tack, A. Ruttens, M. Vandegehuchte, J. Vangronsveld and M. Verloo (2007) "Phytoavailability assessment of heavy metals in soils by single extractions and accumulation by *Phaseolus vulgaris*." *Environmental and Experimental Botany*, 60, 385-396.

Menzies, N., B. Kusumo and P. Moody (2005) "Assessment of P availability in heavily fertilized soils using the diffusive gradient in thin films (DGT) technique." *Plant and Soil*, 269, 1-9.

Mihalik, J., P. Henner, S. Frelon, V. Camilleri and L. Fevrier (2012) "Citrate-assisted phytoextraction of uranium by sunflowers: study of fluxes in soils and plants and resulting intra-planta distribution of Fe and U." *Environmental and Experimental Botany*, 77, 249-258.

Miller, W. (1994) Natural Analogue Studies in the Geological Disposal of Radioactive Wastes. Amsterdam, The Netherlands: Elsevier.

Mitchell, N., D. Perez-Sanchez and M. Thorne (2013) "A review of the behaviour of U-238 series radionuclides in soils and plants." *Journal of Radiological Protection*, 33, R17-R48.

Mortvedt, J. (1994) "Plant and soil relationships of uranium and thorium decay series radionuclides - a review." *Journal of Environmental Quality*, 23, 643-650.

Mousny, J. and C. Myttenaere (1982) "Transfer of technetium from soil to plant as a function of the type of soil, mode of contamination and vegetative cover." In: *Proceedings of an International Symposium on Migration in the Terrestrial Environment of Long-lived Radionuclides from the Nuclear Fuel Cycle*. Knoxville, USA.

Muhammad, I., M. Puschenreiter and W. Wenzel (2012) "Cadmium and Zn availability as affected by pH manipulation and its assessment by soil extraction, DGT and indicator plants." *Science of the Total Environment*, 416, 490-500.

Munier-Lamy, C., S. Deneux-Mustin, C. Mustin, D. Merlet, J. Berthelin and C. Leyval (2007) "Selenium bioavailability and uptake as affected by four different plants in a loamy clay soil with particular attention to mycorrhizae inoculated ryegrass." *Journal of Environmental Radioactivity*, 97, 148-158.

Naidu, R. and R. Harter (1998) "Effect of different organic ligands on cadmium sorption by and extractability from soils." *Soil Science Society of America Journal*, 62, 644-650.

Nakamaru, Y. and J. Altansuvd (2014) "Speciation and bioavailability of selenium and antimony in non-flooded and wetland soils: a review." *Chemosphere*, 111, 366-371.

Nancharaiah, Y. and P. Lens (2015) "Ecology and biotechnology of selenium-respiring bacteria." *Microbiology and Molecular Biology Reviews*, 79, 61-80.

NDA RWMD. (2010) Geological disposal: generic post-closure safety assessment. NDA Report no. NDA/RWMD/030. Nuclear Decommissioning Authority (NDA) & Radioactive Waste Management Directorate (RWMD).

NEA. (2016) Nuclear Energy Data. NEA no. 3700. Nuclear Energy Agency (NEA) & Organization for Economic Co-operation and Development (OECD).

NEA & OECD. (2008) Moving forward with geological disposal – a collective statement by the NEA Radioactive Waste Management Committee. Nuclear Energy Agency (NEA) & Organization for Economic Co-operation and Development (OECD).

Neal, R. (1995) Selenium. In: B. Alloway (ed.) *Heavy Metals in Soils*. London: Blackie Academic and Professional**,** 260-283.

Neal, R., G. Sposito, K. Holtzclaw and S. Traina (1987) "Selenite adsorption on alluvial soils. 1. Soil composition and pH effects." *Soil Science Society of America Journal*, 51, 1161-1165.

Nirel, P. and F. Morel (1990) "Pitfalls of sequential extrations." *Water Research*, 24, 1055-1056.

Nisbet, A. and S. Shaw (1994) "Summary of a 5-year lysimeter study on the time-dependent transfer of Cs-137, Sr-90, Pu-239, Pu-240 and Am-241 to crops from 3 contrasting soil types: 1. Transfer to the edible portion." *Journal of Environmental Radioactivity*, 23, 1-17.

Nisbet, A. and R. Woodman (2000) "Soil-to-plant transfer factors for radiocesium and radiostrontium in agricultural systems." *Health Physics*, 78, 279-288.

NNDC (2017) *Chart of Nuclides* [Online] National Nuclear Data Center. Available at: http://www.nndc.bnl.gov/chart/reCenter.jsp?z=68&n=91 Accessed: 17 April, 2017.

Nolan, A., E. Lombi and M. McLaughlin (2003) "Metal bioaccumulation and toxicity in soils - why bother with speciation?" *Australian Journal of Chemistry*, 56, 77-91.

Nolan, A., Y. Ma, E. Lombi and M. McLaughlin (2004) "Measurement of labile Cu in soil using stable isotope dilution and isotope ratio analysis by ICP-MS." *Analytical and Bioanalytical Chemistry*, 380, 789-797.

Nolan, A., H. Zhang and M. McLaughlin (2005) "Prediction of zinc, cadmium, lead and copper availability to wheat in contaminated soils using chemical speciation, diffusive gradients in thin films, extraction and isotopic dilution techniques." *Journal of Environmental Quality*, 34, 496-507.

Nolan, A., H. Zhang and M. McLaughlin (2005) "Prediction of zinc, cadmium, lead, and copper availability to wheat in contaminated soils using chemical speciation, diffusive gradients in thin films, extraction, and isotopic dilution techniques." *Journal of Environmental Quality*, 34, 496-507.

Noordijk, H., K. Vanbergeijk, J. Lembrechts and M. Frissel (1992) "Impact of aging and weather conditions on soil-to-plant transfer of radiocesium and radiostrontium." *Journal of Environmental Radioactivity*, 15, 277-286.

Norvell, W. (1984) "Comparison of chelating agents as extractants for metals in diverse soil materials." *Soil Science Society of America Journal*, 48, 1285-1292.

Novozamsky, I., T. Lexmond and V. Houba (1993) "A single extraction procedure of soil for evaluation of uptake of some heavy metals by plants." *International Journal of Environmental Analytical Chemistry*, 51, 47-58.

Nowack, B., S. Koehler and R. Schulin (2004) "Use of diffusive gradients in thin films (DGT) in undisturbed field soils." *Environmental Science & Technology*, 38, 1133-1138.

Oliver, I., Y. Ma, E. Lombi, A. Nolan and M. McLaughlin (2006) "Stable isotope techniques for assessing labile Cu in soils: development of an L-value procedure, its application, and reconciliation with E values." *Environmental Science & Technology*, 40, 3342-3348.

Olyslaegers, G., T. Zeevaert, P. Pinedo, I. Simon, G. Prohl, R. Kowe, Q. Chen, S. Mobbs, U. Bergstrom, B. Hallberg, T. Katona, K. Eged and B. Kanyar (2005) "A comparative radiological assessment of five European biosphere systems in the context of potential contamination of well water from the hypothetical disposal of radioactive waste." *Journal of Radiological Protection*, 25, 375-391.

Oporto, C., E. Smolders, F. Degryse, L. Verheyen and C. Vandecasteele (2009) "DGT-measured fluxes explain the chloride-enhanced cadmium uptake by plants at low but not at high Cd supply." *Plant and Soil*, 318, 127-135.

Oughton, D., B. Salbu, G. Riise, H. Lien, G. Ostby and A. Noren (1992) "Radionuclide mobility and bioavailability in Norwegian and Soviet soils." *Analyst*, 117, 481-486.

Pabalan, R., F. Bertetti, J. Prikryl and D. Turner (1996) "Uranium(VI) sorption onto selected mineral surfaces: key geochemical parameters." *Abstracts of Papers of the American Chemical Society*, 211, 55-GEOC.

Palmer, D. and R. Meyer (1981) "Adsorption of technetium on selected inorganic ion-exchange materials and on a range of naturally-occurring minerals under oxic conditions." *Journal of Inorganic & Nuclear Chemistry*, 43, 2979-2984.

Panther, J., W. Bennett, D. Welsh and P. Teasdale (2014) "Simultaneous measurement of trace metal and oxyanion concentrations in water using diffusive gradients in thin films with a Chelex-Metsorb mixed binding layer." *Analytical Chemistry*, 86, 427-434.

Parida, K., B. Gorai, N. Das and S. Rao (1997) "Studies on ferric oxide hydroxides .3. Adsorption of selenite (SeO32-) on different forms of iron oxyhydroxides." *Journal of Colloid and Interface Science*, 185, 355-362.

Parker, D., R. Chaney and W. Norvell (1995) Chemical equilibrium models: applications to plant nutrition research. In: R. Loeppert, A. Schwab and S. Goldberg (ed.) *Chemical Equilibrium and Reaction Models. Special Publication 42*. Madison, Wisconsin, USA: Soil Science Society of America**,** pp. 163-200.

Parker, D., J. Fedler, Z. Ahnstrom and M. Resketo (2001) "Reevaluating the free-ion activity model of trace metal toxicity toward higher plants: experimental evidence with copper and zinc." *Environmental Toxicology and Chemistry*, 20, 899-906.

Parkin, T. (1987) "Soil microsites as a source of denitrification variability." *Soil Science Society of America Journal*, 51, 1194-1199.

Paulson, A. (1986) "Effects of flow-rate and pretreatment on the extraction of trace-metals from estuarine and coastal seawater by Chelex-100." *Analytical Chemistry*, 58, 183-187.

Payne, T., J. Davis and T. Waite (1996) "Uranium adsorption on ferrihydrite - effects of phosphate and humic acid." *Radiochimica Acta*, 74, 239-243.

Peijnenburg, W. (2004) Fate of contaminants in soil. In: P. Doelman and H. J. P. Eijsackers (ed.) *Vital Soil. Function, Values and Properties. Developments in Soil Science.* Amsterdam, The Netherlands: Elsevier**,** pp. 245-280.

Peltovuori, T. and H. Soinne (2005) "Phosphorus solubility and sorption in frozen, air-dried and field-moist soil." *European Journal of Soil Science*, 56, 821-826.

Peng, Q., M. Wang, Z. Cui, J. Huang, C. Chen, L. Guo and D. Liang (2017) "Assessment of bioavailability of selenium in different plant-soil systems by diffusive gradients in thin-films (DGT)." *Environmental Pollution*, 225, 637-643.

Perez, A. and K. Anderson (2009) "DGT estimates cadmium accumulation in wheat and potato from phosphate fertilizer applications." *Science of the Total Environment*, 407, 5096-5103.

Poinssot, C. and H. Geckeis (2012) Radionuclide Behaviour in the Natural Environment: Science, Implications and Lessons for the Nuclear Industry. Cambridge, UK: Woodhead Publishing Limited.

Ponnamperuma, F., M. Cayton and R. Lantin (1981) "Dilute hydrochloric acid as an extractant for available zinc, copper and boron in rice soils." *Plant and Soil*, 61, 297-310.

Price, H., P. Teasdale and D. Jolley (2013) "An evaluation of ferrihydrite- and Metsorb (TM)-DGT techniques for measuring oxyanion species (As, Se, V, P): effective capacity, competition and diffusion coefficients." *Analytica Chimica Acta*, 803, 56-65.

Punshon, T., K. Gaines, P. Bertsch and J. Burger (2003) "Bioavailability of uranium and nickel to vegetation in a contaminated riparian ecosystem." *Environmental Toxicology and Chemistry*, 22, 1146-1154.

Puschenreiter, M., A. Schnepf, I. Millan, W. Fitz, O. Horak, J. Klepp, T. Schrefl, E. Lombi and W. Wenzel (2005) "Changes of Ni biogeochemistry in the rhizosphere of the hyperaccumulator Thlaspi goesingense." *Plant and Soil*, 271, 205-218.

Puschenreiter, M., F. Wittstock, W. Friesl-Hanl and W. Wenzel (2013) "Predictability of the Zn and Cd phytoextraction efficiency of a *Salix smithiana* clone by DGT and conventional bioavailability assays." *Plant and Soil*, 369, 531-541.

Qin, H., J. Zhu and H. Su (2012) "Selenium fractions in organic matter from Se-rich soils and weathered stone coal in selenosis areas of China." *Chemosphere*, 86, 626-633.

Rajan, S. (1979) "Adsorption of selenite, phosphate and sulfate on hydrous alumina." *Journal of Soil Science*, 30, 709-718.

Ramaswami, A., P. Carr and M. Burkhardt (2001) "Plant-Uptake of Uranium: Hydroponic and Soil System Studies." *International Journal of Phytoremediation*, 3, 189-201.

Ramsey, P. (1989) "Critical values for Spearman's rank order correlation " *Journal of Educational Statistics*, 14, 245-253.

Rashid, M., Y. Kang and K. Sakurai (2002) "Selenium in amorphous iron (hydr)oxide-applied soil as affected by air-drying and pH." *Soil Science and Plant Nutrition*, 48, 243-250.

Reamer, D. and W. Zoller (1980) "Selenium biomethylation products from soil and sewage-sludge." *Science*, 208, 500-502.

Reeder, R., M. Nugent, G. Lamble, C. Tait and D. Morris (2000) "Uranyl incorporation into calcite and aragonite: XAFS and luminescence studies." *Environmental Science & Technology*, 34, 638-644.

Regenspurg, S., C. Margot-Roquier, M. Harfouche, P. Froidevaux, P. Steinmann, P. Junier and R. Bernier-Latmani (2010) "Speciation of naturally-accumulated uranium in an organic-rich soil of an alpine region (Switzerland)." *Geochimica Et Cosmochimica Acta*, 74, 2082-2098.

Rieuwerts, J., I. Thornton, M. Farago and M. Ashmore (1998) "Quantifying the influence of soil properties on the solubility of metals by predictive modelling of secondary data." *Chemical Speciation and Bioavailability*, 10, 83-94.

Rigol, A., M. Roig, M. Vidal and G. Rauret (1999) "Sequential extractions for the study of radiocesium and radiostrontium dynamics in mineral and organic soils from Western Europe and Chernobyl areas." *Environmental Science & Technology*, 33, 887-895.

Roig, M., M. Vidal, G. Rauret and A. Rigol (2007) "Prediction of radionuclide aging in soils from the Chernobyl and Mediterranean areas." *Journal of Environmental Quality*, 36, 943-952.

Rosa, E. and D. Clark (1999) "Historical routes to technological gridlock: nuclear technology as prototypical vehicle." *Research in Social Problems and Public Policy*, 7, 21-57.

Rossler, D., K. Franke, R. Suss, E. Becker and H. Kupsch (2000) "Synthesis and chromatographic characterization of [Tc-99m]technetium-humic acid species." *Radiochimica Acta*, 88, 95-100.

Rout, S., A. Kumar, P. Ravi and R. Tripathi (2016) "Understanding the solid phase chemical fractionation of uranium in soil and effect of ageing." *Journal of Hazardous Materials*, 317, 457-465.

Rowell, D. (1994) Soil Science, Methods & Applications. Essex, UK: Longman Scientific & Technical, 350.

Russell, E. and E. Russell (1973) Soil Conditions and Plant Growth, 10th ed. London, UK: Longman.

Saeki, K., S. Matsumoto and R. Tatsukawa (1995) "Selenite adsorption by manganese oxides." *Soil Science*, 160, 265-272.

Sarathchandra, S. and J. Watkinson (1981) "Oxidation of elemental selenium to selenite by *Bacillus megaterium*." *Science*, 211, 600-601.

Sauve, S., N. Cook, W. Hendershot and M. McBride (1996) "Linking plant tissue concentrations and soil copper pools in urban contaminated soils." *Environmental Pollution*, 94, 153-157.

Sauve, S., A. Dumestre, M. McBride and W. Hendershot (1998) "Derivation of soil quality criteria using predicted chemical speciation of Pb^{2+} and Cu^{2+}." *Environmental Toxicology and Chemistry*, 17, 1481-1489.

Scally, S., W. Davison and H. Zhang (2003) "In situ measurements of dissociation kinetics and labilities of metal complexes in solution using DGT." *Environmental Science & Technology*, 37, 1379-1384.

Schosseler, P., B. Wehrli and A. Schweiger (1999) "Uptake of Cu^{2+} by the calcium carbonates vaterite and calcite as studied by continuous wave (CW) and pulse electron paramagnetic resonance." *Geochimica et Cosmochimica Acta*, 63, 1955-1967.

Schulte, E. and P. Scoppa (1987) "Sources and behaviour of technetium in the environment." *Science of the Total Environment*, 64, 163-179.

Schultz, M., W. Burnett and K. Inn (1998) "Evaluation of a sequential extraction method for determining actinide fractionation in soils and sediments." *Journal of Environmental Radioactivity*, 40, 155-174.

Schwertmann, U. and H. Fechter (1982) "The point of zero charge of natural and synthetic ferrihydrites and its relation to adsorbed silicate." *Clay Minerals*, 17, 471-476.

Schwochau, K. (2000) Technetium: Chemistry and Radiopharmaceutical Applications. Weinheim, Germany: Wiley-VCH.

Seby, F., M. Gautier, G. Lespes and M. Astruc (1997) "Selenium speciation in soils after alkaline extraction." *Science of the Total Environment*, 207, 81-90.

Semple, K., K. Doick, K. Jones, P. Burauel, A. Craven and H. Harms (2004) "Defining bioavailability and bioaccessibility of contaminated soil and sediment is complicated." *Environmental Science & Technology*, 38, 228A-231A.

Shahandeh, H. and L. Hossner (2002) "Enhancement of uranium phytoaccumulation from contaminated soils." *Soil Science*, 167, 269-280.

Shahandeh, H. and L. Hossner (2002) "Role of soil properties in phytoaccumulation of uranium." *Water Air and Soil Pollution*, 141, 165-180.

Shan, X., Z. Wang, W. Wang, S. Zhang and B. Wen (2003) "Labile rhizosphere soil solution fraction for prediction of bioavailability of heavy metals and rare earth elements to plants." *Analytical and Bioanalytical Chemistry*, 375, 400-407.

Shelton, D. and T. Parkin (1991) "Effect of moisture on sorption and biodegradation of carbofuran in soil." *Journal of Agricultural and Food Chemistry*, 39, 2063-2068.

Shelton, D., A. Sadeghi, J. Karns and C. Hapeman (1995) "Effect of wetting and drying of soil on sorption and biodegradation of atrazine." *Weed Science*, 43, 298-305.

Sheppard, M. and D. Thibault (1990) "Default soil solid/liquid partition coefficients, KDs, for 4 major soil types - a compendium." *Health Physics*, 59, 471-482.

Sheppard, M., T. Van der Graaf, D. Thibault and J. Reid (1983) "Technetium and uranium - sorption by and plant uptake from peat and sand." *Health Physics*, 44, 635-643.

Sheppard, S. and W. Evenden (1988) "Critical compilation and review of plant-soil concentration ratios for uranium, thorium and lead." *Journal of Environmental Radioactivity*, 8, 255-285.

Sheppard, S. and W. Evenden (1991) "Heavy-metals in the environment - can aquatic macrophytes mobilize technetium by oxidizing their rhizosphere?" *Journal of Environmental Quality*, 20, 738-744.

Sheppard, S. and W. Evenden (1992) "Bioavailability indexes for uranium - effect of concentration in 11 soils." *Archives of Environmental Contamination and Toxicology*, 23, 117-124.

Sheppard, S., M. Sheppard and W. Evenden (1990) "A novel method used to examine variation in Tc sorption among 34 soils, aerated and anoxic." *Journal of Environmental Radioactivity*, 11, 215-233.

Sheppard, S., G. Sohlenius, L.-G. Omberg, M. Borgiel, S. Grolander and S. Norden. (2011) Soil/liquid partition coefficients (Kd) and plant/soil concentration ratios (CR) for selected soils, tills and sediments at Forsmark. Stockholm, Sweden: Swedish Nuclear Fuel and Waste Management Company.

Sinaj, S., A. Dubois and E. Frossard (2004) "Soil isotopically exchangeable zinc: a comparison between E and L values." *Plant and Soil*, 261, 17-28.

Six, L., P. Pypers, F. Degryse, E. Smolders and R. Merckx (2012) "The performance of DGT versus conventional soil phosphorus tests in tropical soils - an isotope dilution study." *Plant and Soil*, 359, 267-279.

Six, L., E. Smolders and R. Merckx (2013) "The performance of DGT versus conventional soil phosphorus tests in tropical soils - maize and rice responses to P application." *Plant and Soil*, 366, 49-66.

Smolders, E., K. Brans, A. Foldi and R. Merckx (1999) "Cadmium fixation in soils measured by isotopic dilution." *Soil Science Society of America Journal*, 63, 78-85.

Smolders, E., J. Buekers, I. Oliver and M. McLaughlin (2004) "Soil properties affecting toxicity of zinc to soil microbial properties in laboratory-spiked and field-contaminated soils." *Environmental Toxicology and Chemistry*, 23, 2633-2640.

Smolders, E. and M. McLaughlin (1996) "Chloride increases cadmium uptake in Swiss chard in a resin-buffered nutrient solution." *Soil Science Society of America Journal*, 60, 1443-1447.

Smolders, E., K. VandenBrande and R. Merckx (1997) "Concentrations of Cs-137 and K in soil solution predict the plant availability of Cs-137 in soils." *Environmental Science & Technology*, 31, 3432-3438.

Sochaczewski, L., W. Tych, B. Davison and H. Zhang (2007) "2D-DGT induced fluxes in sediments and soils (2D-DIFS)." *Environmental Modelling & Software*, 22, 14-23.

Sogn, T., S. Eich-Greatorex, O. Royset, A. Ogaard and A. Almas (2008) "Use of diffusive gradients in thin films to predict potentially bioavailable selenium in soil." *Communications in Soil Science and Plant Analysis*, 39, 587-602.

Song, J., F. Zhao, Y. Luo, S. McGrath and H. Zhang (2004) "Copper uptake by *Elsholtzia splendens* and *Silene vulgaris* and assessment of copper phytoavailability in contaminated soils." *Environmental Pollution*, 128, 307-315.

Sorensen, L. (1974) "Rate of decomposition of organic matter in soil as influenced by repeated air drying-rewetting and repeated additions of organic material." *Soil Biology & Biochemistry*, 6, 287-292.

Sors, T., D. Ellis and D. Salt (2005) "Selenium uptake, translocation, assimilation and metabolic fate in plants." *Photosynthesis Research*, 86, 373-389.

Soulides, D. and F. Allison (1961) "Effect of drying and freezing soils on carbon dioxide production, available mineral nutrients, aggregation and bacterial population." *Soil Science*, 91, 291-298.

Sparks, D. (1996) Methods of Soil Analysis Part 3: Chemical Methods, Soil Science Society of America Book Series (Book 5). University of Michigan: Soil Science Society of America.

Sparks, D. (2003) Environmental Soil Chemistry, 2nd. San Diego, USA: Academic Press.

Squire, H. and L. Middletone (1966) "Behaviour of ^{137}Cs in soils and pastures - a long term experiment." *Radiation Botany*, 6, 413-423.

Stalmans, M., A. Maes and A. Cremers (1982) Role of organic matter as a geochemical sink for technetium in soils and sediments. In: G. Desmet and C. Myttenaere (ed.) *Technetium in the Environment*. London, UK: Elsevier**,** pp. 91-114.

Stanhope, K., S. Young, J. Hutchinson and R. Kamath (2000) "Use of isotopic dilution techniques to assess the mobilization of nonlabile Cd by chelating agents in phytoremediation." *Environmental Science & Technology*, 34, 4123-4127.

Stockdale, A., W. Davison and H. Zhang (2010) "2D simultaneous measurement of the oxyanions of P, V, As, Mo, Sb, W and U." *Journal of Environmental Monitoring*, 12, 981-984.

Stojanovic, M., S. Blagojevic, D. Stevanovic and L. Martinovic (2006) "Effects of long-term application of phosphorus fertilizers on uranium content of some Serbian soils." *Agrochimica*, 50, 177-186.

Stolz, J. and R. Oremland (1999) "Bacterial respiration of arsenic and selenium." *Fems Microbiology Reviews*, 23, 615-627.

Sun, Q., J. Chen, H. Zhang, S. Ding, Z. Li, P. Williams, H. Cheng, C. Han, L. Wu and C. Zhang (2014) "Improved diffusive gradients in thin films (DGT) measurement of total dissolved inorganic arsenic in waters and soils using a hydrous zirconium oxide binding layer." *Analytical Chemistry*, 86, 3060-3067.

Sun, Q., L. Zhang, S. Ding, C. Li, J. Yang, J. Chen and P. Wang (2015) "Evaluation of the diffusive gradients in thin films technique using a mixed binding gel for measuring iron, phosphorus and arsenic in the environment." *Environmental Science - Processes & Impacts*, 17, 570-577.

Supriatin, S., C. Terrones, W. Bussink and L. Weng (2015) "Drying effects on selenium and copper in 0.01 M calcium chloride soil extractions." *Geoderma*, 255, 104-114.

Surman, J. (2014) "The development of tools for the determination of strontium-90 and technetium-99 in contaminated terrestrial waters." PhD Thesis. Lancaster Environment Centre, Lancaster University, Lancaster.

Sylwester, E., E. Hudson and P. Allen (2000) "The structure of uranium (VI) sorption complexes on silica, alumina and montmorillonite." *Geochimica et Cosmochimica Acta*, 64, 2431-2438.

Taboada-Castro, T., A. Dieguez, B. Lopez and A. Paz-Gonzalez (2000) "Comparison of conventional water testing methods with ion-selective electrodes technique for NO_3^-, Cl^-, Ca^{2+}, K^+ and Na^+." *Communications in Soil Science and Plant Analysis*, 31, 1993-2005.

Tack, F., N. Dezillie and M. Verloo (2002) "Metal concentrations in soil paste extracts as affected by extraction ratio." *The Scientific World Journal*, 2, 966-971.

Tagami, K. and S. Uchida (1996) "Microbial role in immobilization of technetium in soil under waterlogged conditions." *Chemosphere*, 33, 217-225.

Tagami, K. and S. Uchida (1998) "Aging effect on bioavailability of Mn, Co, Zn and Tc in Japanese agricultural soils under waterlogged conditions." *Geoderma*, 84, 3-13.

Tagami, K. and S. Uchida (1999) "Chemical transformation of technetium in soil during the change of soil water conditions." *Chemosphere*, 38, 963-971.

Takeda, A., H. Tsukada, Y. Takaku, S. Hisamatsu and M. Nanzyo (2006) "Accumulation of uranium derived from long-term fertilizer applications in a cultivated Andisol." *Science of the Total Environment*, 367, 924-931.

Tamponnet, C., A. Martin-Garin, M. Gonze, N. Parekh, R. Vallejo, T. Sauras-Yera, J. Casadesus, C. Plassard, S. Staunton, M. Norden, R. Avila and G. Shaw (2008) "An overview of BORIS: Bioavailability of Radionuclides in Soils." *Journal of Environmental Radioactivity*, 99, 820-830.

Tan, K. (1998) Principles of Soil Chemistry, 3rd ed. New York, USA: Marcel Dekker.

Tandy, S., S. Mundus, J. Yngvesson, T. de Bang, E. Lombi, J. Schjoerring and S. Husted (2011) "The use of DGT for prediction of plant-available copper, zinc and phosphorus in agricultural soils." *Plant and Soil*, 346, 167-180.

Templeton, D., F. Ariese, R. Cornelis, L. Danielsson, H. Muntau, H. van Leeuwen and R. Lobinski (2000) "Guidelines for terms related to chemical speciation and fractionation of elements. Definitions, structural aspects, and methodological approaches (IUPAC Recommendations 2000)." *Pure and Applied Chemistry*, 72, 1453-1470.

Tessier, A., P. Campbell and M. Bisson (1979) "Sequential extraction procedure for the speciation of particulate trace-metals." *Analytical Chemistry*, 51, 844-851.

Thibault, D. H., M. I. Sheppard and P. A. Smith. (1990) A critical compilation and review of default soil solid/liquid partition coefficients, K_d, for use in environmental assessments. AECL-10125. Pinawa, Manitoba, Canada: Atomic Energy of Canada Ltd.

Thornton, I. (1995) Metals in the Global Environment: Facts and Misconceptions. Ottawa, Ontario, Canada: International Council on Metals and the Environment.

Till, J. (1984) Source terms for technetium-99 from nuclear fuel cycle facilities. In: G. Desmet and Myttenaere (ed.) *Technetium in the Environment*. London, UK: Elsevier**,** pp. 1-20.

Tolu, J., P. di Tullo, I. Le Hecho, Y. Thiry, F. Pannier, M. Potin-Gautier and M. Bueno (2014) "A new methodology involving stable isotope tracer to compare simultaneously short- and long-term selenium mobility in soils." *Analytical and Bioanalytical Chemistry*, 406, 1221-1231.

Toulhoat, P. (2002) "Confinement and migration of radionuclides in a nuclear waste deep repository." *Comptes Rendus Physique*, 3, 975-986.

Trevors, J. (1996) "Sterilization and inhibition of microbial activity in soil." *Journal of Microbiological Methods*, 26, 53-59.

Trivedi, P. and L. Axe (1999) "A comparison of strontium sorption to hydrous aluminum, iron, and manganese oxides." *Journal of Colloid and Interface Science*, 218, 554-563.

Turner, G., G. Mills, P. Teasdale, J. Burnett, S. Amos and G. Fones (2012) "Evaluation of DGT techniques for measuring inorganic uranium species in natural waters: interferences, deployment time and speciation." *Analytica Chimica Acta*, 739, 37-46.

Tyler, G. and T. Olsson (2001) "Plant uptake of major and minor mineral elements as influenced by soil acidity and liming." *Plant and Soil*, 230, 307-321.

UKSO *NSI Topsoil Uranium* [Online] UK Soil Observatory (hosted by British Geological Survey). Available at: http://www.ukso.org/nsi/Uranium.html Accessed: 25 January, 2017.

UNSCEAR. (1993) Sources and effects of ionizing radiation. UNSCEAR 1993 report to the General Assembly, with scientific annexes. New York, USA: United Nations Scientific Committee on the Effects of Atomic Radiation.

UNSCEAR. (2000) UNSCEAR 2000 report to the General Assembly, with scientific annexes. Volume 1: Sources and effects of ionizing radiation. New York, USA: United Nations Scientific Committee on the Effects of Atomic Radiation.

UNSCEAR. (2011) UNSCEAR 2008 report. Volume 2: (Effects) Scientific annexes C, D and E. New York, USA: United Nations Scientific Committee on the Effects of Atomic Radiation.

US DOE. (1995) Closing the circle on the splitting of the atom - the environmental legacy of nuclear weapons production in the United States and what the Department of Energy is doing about it. Washington D.C, USA: United States Department of Energy Office of Environmental Management.

Utomo, W. and A. Dexter (1982) "Changes in soil aggregate water stability induced by wetting and drying cycles in non-saturated soil." *Journal of Soil Science*, 33, 623-637.

Valcke, E. and A. Cremers (1994) "Sorption-desorption dynamics of radiocesium in organic-matter soils." *Science of the Total Environment*, 157, 275-283.

van der Pligt, J. (1992) Nuclear Energy and the Public. Oxford, UK: Blackwell.

van Dorst, S. and P. Peterson (1984) "Selenium speciation in the soil solution and its relevance to plant uptake." *Journal of the Science of Food and Agriculture*, 35, 601-605.

van Erp, P., V. Houba and M. van Beusichem (2001) "Effect of drying temperature on amount of nutrient elements extracted with 0.01 M $CaCl_2$ soil extraction procedure." *Communications in Soil Science and Plant Analysis*, 32, 33-48.

van Leeuwen, H., R. Town, J. Buffle, R. Cleven, W. Davison, J. Puy, W. van Riemsdijk and L. Sigg (2005) "Dynamic speciation analysis and bioavailability of metals in aquatic systems." *Environmental Science & Technology*, 39, 8545-8556.

van Loon, L. (1986) "Kinetic aspects of the soil-to-plant transfer of technetium." PhD Thesis. Catholic University Leuven, Belgium.

Vandecasteele, C., J. Dehut, S. Vanlaer, D. Deprins and C. Myttenaere (1989) "Long-term availability of Tc deposited on soil after accidental releases." *Health Physics*, 57, 247-254.

Vandenhove, H., K. Antunes, J. Wannijn, L. Duquene and M. van Hees (2007) "Method of diffusive gradients in thin films (DGT) compared with other soil testing methods to predict uranium phytoavailability." *Science of the Total Environment*, 373, 542-555.

Vandenhove, H., G. Olyslaegers, N. Sanzharova, O. Shubina, E. Reed, Z. Shang and H. Velasco (2009) "Proposal for new best estimates of the soil-to-plant transfer factor of U, Th, Ra, Pb and Po." *Journal of Environmental Radioactivity*, 100, 721-732.

Vandenhove, H., M. van Hees, J. Wannijn, K. Wouters and L. Wang (2007) "Can we predict uranium bioavailability based on soil parameters? Part 2: soil solution uranium concentration is not a good bioavailability index." *Environmental Pollution*, 145, 577-586.

Vandenhove, H., M. van Hees, K. Wouters and J. Wannijn (2007) "Can we predict uranium bioavailability based on soil parameters? Part 1: effect of soil parameters on soil solution uranium concentration." *Environmental Pollution*, 145, 587-595.

Viehweger, K. and G. Geipel (2010) "Uranium accumulation and tolerance in *Arabidopsis halleri* under native versus hydroponic conditions." *Environmental and Experimental Botany*, 69, 39-46.

Vulkan, R., F. Zhao, V. Barbosa-Jefferson, S. Preston, G. Paton, E. Tipping and S. McGrath (2000) "Copper speciation and impacts on bacterial biosensors in the pore water of copper-contaminated soils." *Environmental Science & Technology*, 34, 5115-5121.

Waite, T., J. Davis, T. Payne, G. Waychunas and N. Xu (1994) "Uranium(VI) adsorption to ferrihydrite: Application of a surface complexation model." *Geochimica Et Cosmochimica Acta*, 58, 5465-5478.

Walker, T., H. Bais, E. Grotewold and J. Vivanco (2003) "Root exudation and rhizosphere biology." *Plant Physiology*, 132, 44-51.

Wall, J. and L. Krumholz (2006) "Uranium reduction." *Annual Review of Microbiology*, 60, 149-166.

Wang, J., L. Bai, X. Zeng, S. Su, Y. Wang and C. Wu (2014) "Assessment of arsenic availability in soils using the diffusive gradients in thin films (DGT) technique - a comparison study of DGT and classic extraction methods." *Environmental Science - Processes & Impacts*, 16, 2355-2361.

Wang, S., D. Liang, D. Wang, W. Wei, D. Fu and Z. Lin (2012) "Selenium fractionation and speciation in agriculture soils and accumulation in corn (*Zea mays L.*) under field conditions in Shaanxi Province, China." *Science of the Total Environment*, 427, 159-164.

Wang, Y., X. Zeng, Y. Lu, S. Su, L. Bai, L. Li and C. Wu (2015) "Effect of aging on the bioavailability and fractionation of arsenic in soils derived from five parent materials in a red soil region of Southern China." *Environmental Pollution*, 207, 79-87.

Wang, Z., Y. Xu and A. Peng (1996) "Influences of fulvic acid on bioavailability and toxicity." *Biological Trace Element Research*, 55, 147-162.

Warnken, K., H. Zhang and W. Davison (2006) "Accuracy of the diffusive gradients in thin-films technique: diffusive boundary layer and effective sampling area considerations." *Analytical Chemistry*, 78, 3780-3787.

Watanabe, T., M. Broadley, S. Jansen, P. White, J. Takada, K. Satake, T. Takamatsu, S. Tuah and M. Osaki (2007) "Evolutionary control of leaf element composition in plants." *New Phytologist*, 174, 516-523.

Weng, L., F. Vega, S. Supriatin, W. Bussink and W. van Riemsdijk (2011) "Speciation of Se and DOC in soil solution and their relation to Se bioavailability." *Environmental Science & Technology*, 45, 262-267.

White, J., A. Quinones-Rivera and M. Alexander (1998) "Effect of wetting and drying on the bioavailability of organic compounds sequestered in soil." *Environmental Toxicology and Chemistry*, 17, 2378-2382.

White, P., H. Bowen, P. Parmaguru, M. Fritz, W. Spracklen, R. Spiby, M. Meacham, A. Mead, M. Harriman, L. Trueman, B. Smith, B. Thomas and M. Broadley (2004) "Interactions between selenium and sulphur nutrition in *Arabidopsis thaliana*." *Journal of Experimental Botany*, 55, 1927-1937.

White, P. and M. Broadley (2003) "Calcium in plants." *Annals of Botany*, 92, 487-511.

WHO (2016) *Radon and health factsheet* [Online] World Health Organization. Available at: Accessed: August 18, 2018.

Wildung, R., T. Garland, K. McFadden and C. Cowan (1986) Technetium sorption in surface soils. In: G. Desmet and C. Myttenaere (ed.) *Technetium in the Environment*. London: Elsevier Applied Science Publishers**,** 115-129.

Wildung, R., T. Garland, K. McFadden and C. Cowan (1995) Technetium sorption in surface soils. In: G. Desmet and C. Myttenaere (ed.) *Technetium in the Environment*. London, UK: Elsevier**,** pp. 115-129.

Willet, I. and W. Bond (1995) "Sorption of manganese, uranium and radium by highly-weathered soils." *Journal of Environmental Quality*, 24, 834-845.

Willey, N., S. Tang, A. McEwen and S. Hicks (2010) "The effects of plant traits and phylogeny on soil-to-plant transfer of Tc-99." *Journal of Environmental Radioactivity*, 101, 757-766.

Williams, P., H. Zhang, W. Davison, A. Meharg, M. Hossain, G. Norton, H. Brammer and M. Islam (2011) "Organic matter-solid phase interactions are critical for predicting arsenic release and plant uptake in Bangladesh paddy soils." *Environmental Science & Technology*, 45, 6080-6087.

Williams, P., H. Zhang, W. Davison, S. Zhao, Y. Lu, F. Dong, L. Zhang and Q. Pan (2012) "Evaluation of in situ DGT measurements for predicting the concentration of Cd in Chinese field-cultivated rice: impact of soil Cd:Zn ratios." *Environmental Science & Technology*, 46, 8009-8016.

World Nuclear Association *World Uranium Mining Production* [Online] World Nuclear Association. Available at: http://www.world-nuclear.org/information-library/nuclear-fuel-cycle/mining-of-uranium/world-uranium-mining-production.aspx Accessed: July 13, 2018.

Yamada, H., Y. Kang, T. Aso, H. Uesugi, T. Fujimura and K. Yonebayashi (1998) "Chemical forms and stability of selenium in soil." *Soil Science and Plant Nutrition*, 44, 385-391.

Yanagisawa, K. and Y. Muramatsu (1995) "Transfer of technetium from soil to paddy and upland rice " *Journal of Radiation Research*, 36, 171-178.

Young, S., H. Zhang, A. Tye, A. Maxted, C. Thums and I. Thornton (2005) "Characterizing the availability of metals in contaminated soils. I. The solid phase: sequential extraction and isotopic dilution." *Soil Use and Management*, 21, 450-458.

Yu, T. (1997) Chemistry of Variable Charge Soils. New York, USA: Oxford University Press.

Zachara, J. and J. McKinley (1993) "Influence of hydrolysis on the sorption of metal-cations by smectites - importance of edge coordination reactions." *Aquatic Sciences*, 55, 250-261.

Zavodska, L., E. Kosorınova, L. Scerbakova and J. Lesny. (2008) Environmental chemistry of uranium. HEJ Manuscript no.: ENV-081221-A. HU ISSN 1418-7108,

Zawislanski, P. and M. Zavarin (1996) "Nature and rates of selenium transformations: a laboratory study of Kesterson Reservoir soils." *Soil Science Society of America Journal*, 60, 791-800.

Zeldowitsch, J. (1934) "Über den mechanismus der katalytischen oxydation von CO an MnO_2." *Acta Physiochim*, 1, 364-449.

Zhang, H. and W. Davison (1995) "Performance characteristics of diffusion gradients in thin-films for the in situ measurement of trace metals in aqueous solution." *Analytical Chemistry*, 67, 3391-3400.

Zhang, H. and W. Davison (1999) "Diffusional characteristics of hydrogels used in DGT and DET techniques." *Analytica Chimica Acta*, 398, 329-340.

Zhang, H. and W. Davison (2000) "Direct in situ measurements of labile inorganic and organically-bound metal species in synthetic solutions and natural waters using diffusive gradients in thin films." *Analytical Chemistry*, 72, 4447-4457.

Zhang, H. and W. Davison (2006) Predicting metal uptake by plants using the DGT technique. In: I. Twardowska, H. Allen, M. Haggblom and S. Stefaniak (ed.) *Viable Methods of Soil and*

Water Pollution Monitoring, Protection and Remediation. Dordrecht, The Netherlands: Springer**,** pp. 187-198.

Zhang, H. and W. Davison (2015) "Use of diffusive gradients in thin-films for studies of chemical speciation and bioavailability." *Environmental Chemistry*, 12, 85-101.

Zhang, H., W. Davison, R. Gadi and T. Kobayashi (1998) "In situ measurement of dissolved phosphorus in natural waters using DGT." *Analytica Chimica Acta*, 370, 29-38.

Zhang, H., W. Davison, B. Knight and S. McGrath (1998) "In situ measurements of solution concentrations and fluxes of trace metals in soils using DGT." *Environmental Science & Technology*, 32, 704-710.

Zhang, H., E. Lombi, E. Smolders and S. McGrath (2004) "Kinetics of Zn release in soils and prediction of Zn concentration in plants using diffusive gradients in thin films." *Environmental Science & Technology*, 38, 3608-3613.

Zhang, H., F. Zhao, B. Sun, W. Davison and S. McGrath (2001) "A new method to measure effective soil solution concentration predicts copper availability to plants." *Environmental Science & Technology*, 35, 2602-2607.

Zhang, P. and D. Sparks (1990) "Kinetics of selenate and selenite adsorption-desorption at the goethite-water interface." *Environmental Science & Technology*, 24, 1848-1856.

Zhang, Y. and W. Frankenberger (2003) "Determination of selenium fractionation and speciation in wetland sediments by parallel extraction." *International Journal of Environmental Analytical Chemistry*, 83, 315-326.

Zhang, Y. and J. Moore (1997) "Changes in selenium speciation in wetland sediments induced by laboratory testing." *Communications in Soil Science and Plant Analysis*, 28, 341-350.

Zheng, Z., T. Tokunaga and J. Wan (2003) "Influence of calcium carbonate on U(VI) sorption to soils." *Environmental Science & Technology*, 37, 5603-5608.

Zsolnay, A., E. Baigar, M. Jimenez, B. Steinweg and F. Saccomandi (1999) "Differentiating with fluorescence spectroscopy the sources of dissolved organic matter in soils subjected to drying." *Chemosphere*, 38, 45-50.

APPENDICES

Appendix A: Soil properties

Appendix A.1. *Measured physico-chemical properties for all 20 incubated soils.*

Soil	Texture	pH	Alkalinity (mg L^{-1})	organic C (%)	Total oxides (mg kg^{-1}) Al	Mn	Fe
M1-T	sand	6.41	51	0.2	3839	217	1959
M2-T	sand	5.12	—	1.4	10219	103	9746
F1-T	sand	3.32	—	0.7	2211	19	421
F3-T	sand	4.52	—	1.2	6509	410	3667
BC-M	sand	4.18	—	5.5	21124	77	16124
BH-G	clay	7.36	183	6.2	27237	4451	30438
BH-W	clay	7.47	275	7.5	23500	2724	25395
BY-W	clay	3.41	—	10.6	30226	141	22966
CO-A	loam	6.37	18	2.3	26707	508	20965
DY-G	loam	3.90	—	11.4	15841	43	6925
FD-G	clay	6.19	67	5.7	57058	1053	52789
IH-W	sand	3.88	—	9.5	27554	185	18013
NP-A	clay	6.76	61	1.7	15873	501	17725
SB-G	sand	6.02	49	5.0	22103	460	13775
SR-A	loam	7.77	177	3.8	23207	682	22515
SR-G	loam	7.04	165	5.7	36862	874	50808
SR-W	loam	8.00	256	5.2	28029	694	25431
TK-G	loam	5.32	—	6.3	40942	303	25256
WK-A	sand	5.31	—	2.4	19815	645	29614
WS-A	clay	7.71	122	2.6	42149	1037	33255

Appendix A.2. *Primary incubation further soil properties.*

Soil	Soil moisture content at spiking (%)	Soil particle concentration [P_c] (kg L^{-1})	Soil porosity [Φ_s]
F1-T	11	2.19	0.55
WS-A	14	1.74	0.60
IH-W	20	1.36	0.66
M1-T	3	3.85	0.41
NP-A	9	2.57	0.51
SR-W	13	2.29	0.54
SB-G	15	1.71	0.61
TK-G	20	1.44	0.65
CO-A	9	2.36	0.53
FD-G	24	1.39	0.66
BH-W	16	1.54	0.63
DY-G	31	1.02	0.72
SR-A	9	2.00	0.57
M2-T	6	3.41	0.44
BH-G	20	1.56	0.63
WK-A	13	2.15	0.55
SR-G	22	1.54	0.63
F3-T	5	3.08	0.46
BC-M	15	1.85	0.59
BY-W	21	1.45	0.65

Appendix A.3. *Physico-chemical properties determined for freshly-sampled soils used in Chapter 7.*

Soil	Texture	pH	C_{org} (%)	NO_3^- (mg/kg)	moisture content at spiking (%)
BY-W	clay	3.73	18.19	31.28	18
DY-G	loam	5.31	6.77	3.25	11
SR-W	loam	7.82	6.17	108.15	7
WK-A	sand	7.34	1.68	25.08	9
TK-G	loam	5.27	5.04	95.09	9
FD-G	clay	7.79	2.14	44.53	9
BC-M	sand	4.33	5.05	5.61	7
SR-G	loam	7.62	3.86	23.16	14

Appendix B: Technetium

***Appendix B.1**. Primary incubation compiled DGT dataset for all 20 soils. Concentrations (µg L^{-1}) represent the mean (± standard deviation) of triplicate DGT deployments.*

Soil	Day 3	Day 23	Day 46	Day 72	Day 100	Day 143	Day 192
F1-T	6.70 ± 0.46	4.11 ± 0.08	3.64 ± 0.34	3.40 ± 0.09	2.98 ± 0.11	2.95 ± 0.66	3.07 ± 0.11
WS-A	19.04 ± 1.08	13.68 ± 0.67	13.72 ± 1.00	9.95 ± 0.57	7.99 ± 0.34	6.11 ± 0.64	5.38 ± 0.37
IH-W	5.71 ± 0.07	3.25 ± 0.45	2.53 ± 0.09	1.86 ± 0.11	1.54 ± 0.02	1.16 ± 0.05	1.42 ± 0.02
M1-T	30.75 ± 0.30	18.98 ± 2.37	15.75 ± 1.28	11.47 ± 1.20	9.83 ± 0.15	6.57 ± 0.58	7.36 ± 0.32
NP-A	22.22 ± 0.97	14.59 ± 0.73	13.07 ± 1.10	11.09 ± 1.51	7.93 ± 0.25	5.65 ± 0.73	6.95 ± 0.51
SR-W	13.68 ± 0.78	10.22 ± 0.54	8.87 ± 0.33	8.00 ± 0.90	6.12 ± 0.51	3.84 ± 0.13	4.98 ± 0.19
SB-G	11.87 ± 0.51	7.63 ± 0.75	5.47 ± 0.12	3.97 ± 0.15	3.36 ± 0.48	1.91 ± 0.16	2.58 ± 0.13
TK-G	7.45 ± 0.23	1.95 ± 0.18	1.01 ± 0.08	0.72 ± 0.04	0.48 ± 0.01	0.29 ± 0.03	0.37 ± 0.02
CO-A	16.09 ± 0.19	12.25 ± 0.30	10.43 ± 0.88	8.28 ± 1.96	6.81 ± 0.91	7.09 ± 1.01	6.45 ± 0.15
FD-G	5.44 ± 0.23	4.22 ± 2.95	2.77 ± 0.88	2.54 ± 0.15	1.12 ± 0.30	1.35 ± 0.27	0.92 ± 0.02
BH-W	11.41 ± 0.52	9.38 ± 0.44	8.07 ± 0.73	6.83 ± 1.83	6.70 ± 0.08	5.11 ± 0.14	5.28 ± 0.74
DY-G	3.52 ± 0.14	1.12 ± 0.16	0.61 ± 0.03	0.37 ± 0.10	0.50 ± 0.04	0.34 ± 0.02	0.41 ± 0.01
SR-A	14.93 ± 1.13	12.54 ± 1.08	10.91 ± 0.38	9.71 ± 0.29	7.75 ± 0.19	5.15 ± 0.31	6.50 ± 0.46
M2-T	20.50 ± 0.51	17.18 ± 0.96	13.11 ± 0.20	9.72 ± 2.17	9.32 ± 0.36	6.99 ± 0.84	6.44 ± 0.54
BH-G	11.15 ± 0.39	9.20 ± 1.17	5.51 ± 2.79	6.21 ± 0.42	6.02 ± 0.35	5.13 ± 0.45	5.52 ± 0.51
WK-A	14.16 ± 1.11	14.49 ± 2.10	11.28 ± 0.78	9.57 ± 0.24	7.75 ± 0.93	7.15 ± 0.75	7.78 ± 0.09
SR-G	10.06 ± 0.31	7.93 ± 0.31	6.44 ± 0.92	7.47 ± 0.52	5.14 ± 0.16	5.36 ± 0.05	4.68 ± 0.50
F3-T	17.42 ± 0.17	14.02 ± 1.18	11.51 ± 0.27	9.40 ± 0.31	7.12 ± 0.51	6.97 ± 0.16	5.79 ± 0.48
BC-M	4.42 ± 0.32	2.71 ± 0.56	2.02 ± 0.27	1.93 ± 0.71	1.70 ± 0.21	1.68 ± 0.08	1.55 ± 0.14
BY-W	3.86 ± 0.17	2.35 ± 0.40	2.09 ± 0.03	1.70 ± 0.09	1.68 ± 0.13	1.69 ± 0.03	1.71 ± 0.06

continued…

Day 262	Day 346	Day 549
2.98 ± 0.17	2.10 ± 0.11	1.96 ± 0.10
4.19 ± 0.25	2.19 ± 0.19	2.14 ± 0.07
1.04 ± 0.06	0.53 ± 0.02	0.47 ± 0.01
4.44 ± 0.37	2.32 ± 0.62	2.45 ± 0.37
4.49 ± 0.17	2.77 ± 0.10	2.51 ± 0.35
3.22 ± 0.09	1.48 ± 0.22	1.50 ± 0.09
1.72 ± 0.02	1.07 ± 0.03	1.26 ± 0.21
0.19 ± 0.02	0.17 ± 0.02	0.18 ± 0.02
4.73 ± 0.15	2.84 ± 0.25	2.44 ± 0.15
0.67 ± 0.04	0.34 ± 0.04	0.29 ± 0.01
2.99 ± 0.04	2.37 ± 0.04	1.71 ± 0.21
0.32 ± 0.00	0.21 ± 0.00	0.22 ± 0.02
4.53 ± 0.56	3.23 ± 0.15	2.53 ± 0.23
4.51 ± 0.29	3.06 ± 0.17	2.55 ± 0.09
2.86 ± 0.19	2.53 ± 0.09	2.09 ± 0.22
6.24 ± 0.28	3.78 ± 0.26	3.96 ± 0.32
2.78 ± 0.12	2.28 ± 0.08	1.95 ± 0.28
4.50 ± 0.21	3.05 ± 0.25	2.64 ± 0.17
1.18 ± 0.10	0.82 ± 0.04	0.81 ± 0.12
1.23 ± 0.04	0.99 ± 0.02	0.95 ± 0.09

Appendix B.2. *Correction factors used to normalise C_{DGT} and C_{soln} values by accounting for cumulative depletion from the soil with incubation time.*

	Days after spiking									
Soil	**3**	**23**	**46**	**72**	**100**	**143**	**192**	**262**	**346**	**549**
F1-T	1.00	0.98	0.97	0.96	0.94	0.91	0.89	0.88	0.87	0.86
WS-A	1.00	0.93	0.88	0.84	0.80	0.77	0.75	0.72	0.70	0.69
IH-W	1.00	0.98	0.97	0.96	0.95	0.95	0.94	0.93	0.93	0.93
M1-T	1.00	0.93	0.87	0.82	0.78	0.77	0.74	0.71	0.70	0.69
NP-A	1.00	0.93	0.88	0.84	0.80	0.77	0.75	0.72	0.70	0.69
SR-W	1.00	0.96	0.92	0.89	0.86	0.84	0.82	0.80	0.79	0.78
SB-G	1.00	0.96	0.93	0.91	0.90	0.88	0.87	0.86	0.86	0.85
TK-G	1.00	0.97	0.97	0.96	0.96	0.96	0.96	0.95	0.95	0.95
CO-A	1.00	0.95	0.90	0.87	0.84	0.82	0.79	0.76	0.75	0.74
FD-G	1.00	0.97	0.95	0.94	0.93	0.92	0.92	0.91	0.91	0.91
BH-W	1.00	0.96	0.92	0.89	0.86	0.84	0.82	0.79	0.78	0.77
DY-G	1.00	0.98	0.98	0.97	0.97	0.97	0.97	0.97	0.96	0.96
SR-A	1.00	0.94	0.90	0.86	0.83	0.80	0.78	0.75	0.73	0.72
M2-T	1.00	0.92	0.86	0.82	0.79	0.75	0.73	0.70	0.68	0.67
BH-G	1.00	0.95	0.91	0.89	0.87	0.84	0.82	0.80	0.79	0.77
WK-A	1.00	0.94	0.89	0.85	0.81	0.78	0.75	0.72	0.70	0.68
SR-G	1.00	0.95	0.92	0.89	0.86	0.84	0.81	0.79	0.78	0.76
F3-T	1.00	0.93	0.89	0.85	0.82	0.79	0.76	0.74	0.73	0.71
BC-M	1.00	0.98	0.97	0.96	0.96	0.95	0.95	0.94	0.93	0.93
BY-W	1.00	0.98	0.97	0.96	0.96	0.95	0.94	0.94	0.93	0.93

Appendix B.3. *Primary incubation compiled C_{soln} dataset for all 20 soils. Concentrations are expressed per litre of soil solution as measured (µg L^{-1}).*

	Days after spiking									
Soil	**3**	**23**	**46**	**72**	**100**	**143**	**192**	**262**	**346**	**549**
F1-T	50.66	40.98	35.83	31.15	30.70	28.09	31.70	28.90	30.79	29.38
WS-A	279.53	172.89	124.41	108.36	79.96	61.87	57.53	49.47	40.09	29.51
IH-W	45.72	26.71	18.10	16.54	15.11	11.56	13.32	10.42	7.46	6.83
M1-T	0.00	452.85	298.30	240.12	170.89	133.04	129.50	99.07	79.76	61.34
NP-A	432.31	272.54	183.92	160.59	104.79	90.08	96.91	66.24	58.02	49.74
SR-W	189.86	134.62	111.43	105.95	67.93	57.31	60.57	45.88	28.75	19.52
SB-G	151.03	92.26	54.83	45.21	33.65	23.61	24.50	20.80	19.28	20.11
TK-G	52.81	17.20	8.53	5.39	4.59	4.82	5.17	5.50	5.41	5.98
CO-A	295.40	196.26	143.00	117.86	78.05	71.41	72.05	56.54	57.17	44.40
FD-G	152.17	64.73	32.78	22.79	11.62	13.48	10.34	9.64	7.05	5.06
BH-W	122.96	107.41	78.70	74.36	58.96	48.26	46.49	43.19	35.60	28.71
DY-G	30.53	10.89	7.04	6.44	5.41	4.65	5.43	5.45	4.74	4.89
SR-A	217.30	171.41	132.16	111.61	83.15	92.07	75.18	66.80	51.09	36.50
M2-T	476.06	343.52	241.24	186.57	148.25	139.23	114.80	97.79	73.15	59.41
BH-G	138.10	107.22	75.01	71.07	56.59	50.59	47.53	43.57	35.02	29.55
WK-A	218.01	171.03	131.38	130.63	95.97	90.85	95.54	81.14	68.59	60.44
SR-G	129.49	104.71	82.46	75.80	58.12	51.71	49.40	40.00	31.02	22.32
F3-T	415.78	291.64	175.93	169.24	124.97	108.03	95.99	84.13	74.03	63.59
BC-M	51.54	25.04	14.17	20.73	15.96	15.34	18.07	14.65	15.35	15.30
BY-W	39.92	23.37	14.67	14.12	11.81	11.65	12.45	11.17	11.15	11.64

Appendix B.4. *Primary incubation compiled C_{soln} dataset for all in 20 soils, where concentrations are expressed per mass of soil (µg kg^{-1}) and corrected for cumulative depletion from the soil with incubation time.*

	Days after spiking									
Soil	**3**	**23**	**46**	**72**	**100**	**143**	**192**	**262**	**346**	**549**
F1-T	23.09	19.07	16.90	14.86	14.84	14.14	16.16	14.95	16.11	15.52
WS-A	160.58	106.82	81.05	73.95	57.19	46.10	44.36	39.44	32.69	24.43
IH-W	33.66	20.08	13.78	12.69	11.68	9.00	10.43	8.22	5.91	5.43
M1-T	—	126.30	88.84	76.11	56.93	45.09	45.35	36.11	29.70	23.14
NP-A	168.38	113.80	81.35	74.75	50.90	45.44	50.40	35.87	32.14	28.05
SR-W	82.95	61.34	52.82	51.96	34.48	29.92	32.25	25.09	15.96	10.92
SB-G	88.32	56.34	34.48	29.04	21.96	15.64	16.39	14.10	13.17	13.82
TK-G	36.55	12.23	6.11	3.88	3.31	3.48	3.74	3.99	3.93	4.35
CO-A	125.26	88.03	67.04	57.49	39.20	36.98	38.58	31.34	32.39	25.59
FD-G	109.68	48.04	24.80	17.47	9.01	10.51	8.12	7.61	5.58	4.01
BH-W	79.65	72.71	55.26	54.10	44.16	37.31	36.92	35.36	29.64	24.27
DY-G	30.06	10.91	7.08	6.51	5.48	4.72	5.52	5.56	4.84	5.00
SR-A	108.72	90.87	73.33	64.82	50.25	57.54	48.35	44.57	34.92	25.41
M2-T	139.72	109.39	81.96	66.98	55.21	54.15	46.37	40.95	31.40	25.98
BH-G	88.65	72.71	52.84	51.02	41.81	38.47	37.02	35.04	28.60	24.50
WK-A	101.30	84.70	68.62	71.50	54.74	53.87	58.95	52.46	45.78	41.34
SR-G	84.17	71.69	58.56	55.48	43.92	40.12	39.54	32.96	25.96	18.97
F3-T	134.73	101.69	64.39	64.67	49.64	44.28	40.73	36.82	33.07	28.86
BC-M	27.90	13.82	7.90	11.63	9.02	8.72	10.35	8.45	8.89	8.90
BY-W	27.49	16.40	10.38	10.08	8.48	8.43	9.08	8.21	8.24	8.64

Appendix B.5. *2D-DIFS input parameters and associated values.*

Soil	D_s	Time (hrs)	C_{soln} (µg L^{-1})	M (mol cm^{-2})	F (mol cm^{-2} s^{-1})	R	C_{sorbed} (µg kg^{-1})	K_d (L kg^{-1})
F1-T	3.08E-06	23.35	11.88	1.20E-10	1.43E-15	0.19	16.93	1.42
WS-A	3.38E-06	23.30	13.13	1.31E-10	1.56E-15	0.23	22.67	1.73
IH-W	3.71E-06	23.24	3.49	2.86E-11	3.42E-16	0.15	6.94	1.99
M1-T	2.43E-06	23.38	24.78	1.51E-10	1.79E-15	0.14	10.74	0.43
NP-A	2.88E-06	23.20	19.46	1.53E-10	1.83E-15	0.19	11.41	0.59
SR-W	3.02E-06	23.50	9.35	9.25E-11	1.09E-15	0.21	10.82	1.16
SB-G	3.40E-06	23.55	8.48	7.77E-11	9.16E-16	0.17	12.29	1.45
TK-G	3.63E-06	23.52	2.49	1.14E-11	1.34E-16	0.08	5.27	2.11
CO-A	2.98E-06	23.43	20.14	1.50E-10	1.78E-15	0.16	7.45	0.37
FD-G	3.68E-06	23.61	2.32	1.77E-11	2.08E-16	0.14	4.78	2.06
BH-W	3.54E-06	22.70	11.99	1.02E-10	1.25E-15	0.19	14.94	1.25
DY-G	4.11E-06	22.67	2.24	1.30E-11	1.60E-16	0.10	5.21	2.33
SR-A	3.19E-06	21.65	17.50	1.44E-10	1.85E-15	0.20	15.71	0.90
M2-T	2.56E-06	21.60	21.35	1.45E-10	1.86E-15	0.18	15.85	0.74
BH-G	3.53E-06	21.83	11.02	1.20E-10	1.52E-15	0.25	20.34	1.85
WK-A	3.10E-06	21.40	25.93	2.22E-10	2.89E-15	0.22	15.70	0.61
SR-G	3.54E-06	21.63	10.29	1.11E-10	1.42E-15	0.25	17.68	1.72
F3-T	2.67E-06	21.55	24.50	1.50E-10	1.93E-15	0.15	8.76	0.36
BC-M	3.30E-06	21.82	5.86	4.65E-11	5.93E-16	0.15	8.41	1.43
BY-W	3.62E-06	21.50	5.43	5.35E-11	6.91E-16	0.19	12.10	2.23

Δg (cm) = 0.092

D_d (cm^2 s^{-1}) =6.78E-06

Key:

D_s = soil diffusion coefficient

C_{soln} = dissolved concentration

M = mass in resin layer

F = DGT flux

C_{sorbed} = sorbed concentration

K_d = distribution ratio

***Appendix B.6**. Secondary incubation compiled C_{DGT} (µg L^{-1}) dataset. Concentrations represent the mean (± standard deviation) of triplicate DGT deployments.*

		Days after spiking			
Soil	**Moisture regime**	**Day 2**	**Day 23**	**Day 44**	**Day 112**
BH-G	Sterilised/constant moisture	4.40 ± 0.14	5.20 ± 0.12	6.44 ± 0.24	4.20 ± 1.19
	Sterilised/wet-dry cycles	4.33 ± 0.35	3.49 ± 0.17	4.27 ± 0.09	0.57 ± 0.47
	Microbes/constant moisture	5.33 ± 0.48	6.66 ± 0.27	7.32 ± 0.10	3.79 ± 0.45
BY-W	Sterilised/constant moisture	4.27 ± 0.27	2.40 ± 0.08	2.18 ± 0.10	1.57 ± 0.08
	Sterilised/wet-dry cycles	4.14 ± 0.58	2.00 ± 0.03	2.02 ± 0.13	1.00 ± 0.13
	Microbes/constant moisture	4.11 ± 0.19	2.24 ± 0.05	1.90 ± 0.16	1.38 ± 0.09
SR-W	Sterilised/constant moisture	5.02 ± 0.34	2.61 ± 0.08	3.03 ± 0.04	2.49 ± 0.17
	Sterilised/wet-dry cycles	5.54 ± 0.83	1.78 ± 0.04	1.91 ± 0.25	0.71 ± 0.05
	Microbes/constant moisture	5.94 ± 0.24	3.27 ± 0.09	3.76 ± 0.06	2.49 ± 0.04
WK-A	Sterilised/constant moisture	6.65 ± 0.25	0.26 ± 0.03	1.15 ± 0.51	2.97 ± 0.17
	Sterilised/wet-dry cycles	6.84 ± 0.09	2.41 ± 0.28	2.58 ± 0.20	1.46 ± 0.04
	Microbes/constant moisture	6.05 ± 0.45	8.17 ± 0.23	7.42 ± 0.54	3.82 ± 0.24

		Day 3	**Day 23**	**Day 46**	**Day 72**	**Day 100**
BH-G	Microbes/wet-dry cycles	7.40 ± 1.17	6.10 ± 0.39	3.66 ± 2.79	4.12 ± 0.42	4.00 ± 0.35
BY-W	Microbes/wet-dry cycles	9.40 ± 0.40	9.61 ± 0.17	7.48 ± 0.03	6.35 ± 0.09	5.14 ± 0.13
SR-W	Microbes/wet-dry cycles	6.67 ± 0.54	5.27 ± 0.78	4.27 ± 0.33	4.96 ± 0.90	3.41 ± 0.51
WK-A	Microbes/wet-dry cycles	11.56 ± 2.10	9.31 ± 1.11	7.64 ± 0.78	6.24 ± 0.24	4.73 ± 0.93

Appendix B.7. *Secondary incubation compiled C_{soln} ($\mu g\ L^{-1}$) dataset.*

Soil	Moisture regime	Days after spiking			
		2	**23**	**44**	**112**
BH-G	Sterilised/constant moisture	98.12	71.41	56.94	59.21
	Sterilised/wet-dry cycles	104.70	48.10	39.43	49.58
	Microbes/constant moisture	107.50	79.61	65.54	66.46
BY-W	Sterilised/constant moisture	74.13	26.59	19.57	19.95
	Sterilised/wet-dry cycles	73.24	21.02	18.38	25.03
	Microbes/constant moisture	69.24	24.00	15.79	19.01
SR-W	Sterilised/constant moisture	95.75	31.10	28.83	35.15
	Sterilised/wet-dry cycles	99.27	21.05	19.54	20.97
	Microbes/constant moisture	109.90	37.72	35.48	34.53
WK-A	Sterilised/constant moisture	147.00	6.00	16.65	54.30
	Sterilised/wet-dry cycles	152.30	30.05	25.81	36.40
	Microbes/constant moisture	147.50	109.40	79.99	82.00

Soil	Moisture regime	Days after spiking				
		3	**23**	**46**	**72**	**100**
BH-G	Microbes/wet-dry cycles	138.10	107.22	75.01	71.07	56.59
BY-W	Microbes/wet-dry cycles	39.92	23.37	14.67	14.12	11.81
SR-W	Microbes/wet-dry cycles	189.86	134.62	111.43	105.95	67.93
WK-A	Microbes/wet-dry cycles	218.01	171.03	131.38	130.63	95.97

Appendix C: Selenium

Appendix C.1. *Primary incubation compiled DGT dataset for all 20 soils. Concentrations (µg L^{-1}) represent the mean (± standard deviation) of triplicate DGT deployments.*

	Days after spiking																					
Soil	**3**			**23**			**46**			**72**			**100**			**143**			**192**		
F1-T	7.17	±	0.51	7.26	±	1.10	5.29	±	0.13	5.56	±	0.33	8.11	±	0.52	3.48	±	0.24	2.97	±	0.15
WS-A	3.16	±	0.29	2.50	±	0.21	2.01	±	0.39	1.99	±	0.16	1.21	±	0.10	0.80	±	0.05	1.07	±	0.11
IH-W	3.47	±	0.20	2.73	±	0.11	3.09	±	0.13	2.84	±	0.23	1.87	±	0.14	1.28	±	0.07	1.77	±	0.14
M1-T	19.59	±	2.42	14.08	±	2.11	10.14	±	0.02	12.54	±	1.24	3.62	±	0.21	5.56	±	0.49	6.63	±	0.20
NP-A	8.50	±	1.02	4.06	±	0.54	4.21	±	0.23	3.57	±	0.86	1.94	±	0.16	1.43	±	0.19	1.54	±	0.22
SR-W	2.22	±	0.19	1.11	±	0.26	1.18	±	0.08	1.17	±	0.05	0.68	±	0.02	0.29	±	0.04	0.52	±	0.04
SB-G	4.45	±	0.15	2.17	±	0.41	2.37	±	0.19	3.03	±	0.58	1.08	±	0.03	0.51	±	0.03	0.73	±	0.10
TK-G	4.32	±	0.20	2.27	±	0.17	1.59	±	0.14	2.12	±	0.09	1.13	±	0.03	0.61	±	0.02	0.81	±	0.15
CO-A	4.49	±	0.15	4.05	±	0.38	3.69	±	0.20	4.09	±	0.15	2.66	±	0.17	2.10	±	0.09	2.17	±	0.10
FD-G	3.24	±	0.31	2.86	±	0.30	0.86	±	0.05	0.36	±	0.02	0.00	±	0.00	0.00	±	0.00	0.05	±	0.01
BH-W	1.83	±	0.06	1.56	±	0.05	1.09	±	0.03	0.99	±	0.08	0.46	±	0.01	0.25	±	0.06	0.41	±	0.04
DY-G	6.24	±	0.50	4.02	±	0.29	2.78	±	0.22	2.73	±	0.09	1.42	±	0.07	0.66	±	0.04	0.77	±	0.03
SR-A	2.47	±	0.20	1.31	±	0.03	0.92	±	0.04	1.08	±	0.06	0.63	±	0.03	0.32	±	0.02	0.49	±	0.02
M2-T	11.65	±	1.04	8.33	±	0.09	6.41	±	0.63	8.43	±	0.39	6.77	±	0.12	3.47	±	0.43	6.00	±	0.46
BH-G	2.06	±	0.14	1.87	±	0.03	1.46	±	0.12	1.23	±	0.02	0.86	±	0.08	0.61	±	0.08	0.61	±	0.13
WK-A	3.12	±	0.17	2.47	±	0.12	2.68	±	0.42	5.10	±	0.54	2.12	±	0.38	1.60	±	0.18	1.61	±	0.13
SR-G	1.54	±	0.21	1.11	±	0.11	1.15	±	0.12	1.47	±	0.04	0.84	±	0.07	0.33	±	0.05	0.59	±	0.07
F3-T	7.61	±	0.25	5.95	±	0.28	7.22	±	0.08	11.03	±	1.20	6.32	±	1.18	3.50	±	0.11	6.05	±	0.48
BC-M	2.61	±	0.58	1.92	±	0.75	2.10	±	0.17	4.05	±	0.30	2.33	±	0.15	1.51	±	0.04	2.99	±	0.18
BY-W	1.35	±	0.03	0.95	±	0.15	0.87	±	0.07	2.30	±	0.21	1.22	±	0.04	0.62	±	0.05	1.48	±	0.24

continued…

262			346			549		
2.23	±	0.29	1.52	±	0.09	1.49	±	0.10
0.72	±	0.06	0.72	±	0.10	0.59	±	0.08
1.18	±	0.06	1.04	±	0.09	0.77	±	0.10
4.62	±	0.62	4.44	±	0.48	1.51	±	0.04
0.80	±	0.08	0.54	±	0.08	0.35	±	0.01
0.30	±	0.02	0.45	±	0.08	0.29	±	0.02
0.38	±	0.04	0.37	±	0.01	0.31	±	0.02
0.37	±	0.03	0.45	±	0.01	0.25	±	0.00
1.35	±	0.20	1.28	±	0.02	1.03	±	0.04
0.02	±	0.00	0.09	±	0.01	0.05	±	0.01
0.23	±	0.03	0.27	±	0.01	0.24	±	0.02
0.50	±	0.05	0.46	±	0.07	0.37	±	0.04
0.30	±	0.04	0.47	±	0.03	0.44	±	0.10
3.59	±	0.38	2.67	±	0.51	2.52	±	0.28
0.45	±	0.02	0.51	±	0.08	0.38	±	0.02
1.24	±	0.04	1.07	±	0.11	1.16	±	0.07
0.32	±	0.02	0.41	±	0.03	0.35	±	0.02
4.35	±	0.13	4.62	±	0.20	3.25	±	0.06
1.98	±	0.13	1.80	±	0.11	1.86	±	0.12
1.10	±	0.08	1.00	±	0.10	1.29	±	0.06

Appendix C.2. *Correction factors used to normalise C_{DGT} and C_{soln} values by accounting for cumulative depletion from the soil with incubation time.*

	Days after spiking									
Soil	**3**	**23**	**46**	**72**	**100**	**143**	**192**	**262**	**346**	**549**
F1-T	1.00	0.98	0.95	0.94	0.92	0.90	0.89	0.88	0.87	0.86
WS-A	1.00	0.98	0.96	0.95	0.93	0.93	0.92	0.92	0.91	0.91
IH-W	1.00	0.99	0.98	0.97	0.96	0.95	0.95	0.94	0.93	0.93
M1-T	1.00	0.97	0.93	0.91	0.88	0.87	0.85	0.84	0.83	0.82
NP-A	1.00	0.97	0.95	0.93	0.92	0.91	0.90	0.90	0.89	0.89
SR-W	1.00	0.99	0.98	0.97	0.96	0.96	0.96	0.96	0.95	0.95
SB-G	1.00	0.98	0.97	0.96	0.95	0.95	0.95	0.94	0.94	0.94
TK-G	1.00	0.98	0.97	0.97	0.96	0.96	0.95	0.95	0.95	0.95
CO-A	1.00	0.98	0.96	0.94	0.92	0.91	0.90	0.89	0.88	0.88
FD-G	1.00	0.98	0.96	0.96	0.96	0.96	0.96	0.96	0.96	0.96
BH-W	1.00	0.99	0.97	0.96	0.96	0.96	0.95	0.95	0.95	0.95
DY-G	1.00	0.97	0.95	0.94	0.92	0.92	0.91	0.91	0.90	0.90
SR-A	1.00	0.99	0.98	0.97	0.97	0.96	0.96	0.96	0.96	0.95
M2-T	1.00	0.97	0.95	0.93	0.91	0.89	0.88	0.87	0.86	0.85
BH-G	1.00	0.98	0.97	0.96	0.95	0.94	0.94	0.94	0.93	0.93
WK-A	1.00	0.98	0.97	0.95	0.93	0.92	0.91	0.90	0.90	0.89
SR-G	1.00	0.99	0.97	0.97	0.96	0.95	0.95	0.94	0.94	0.94
F3-T	1.00	0.98	0.96	0.95	0.93	0.91	0.90	0.89	0.88	0.87
BC-M	1.00	0.99	0.99	0.98	0.97	0.97	0.96	0.95	0.95	0.94
BY-W	1.00	1.00	0.99	0.99	0.98	0.98	0.97	0.97	0.96	0.96

Appendix C.3. *Primary incubation compiled C_{soln} dataset for all 20 soils. Concentrations are expressed per litre of soil solution as measured (µg L^{-1}).*

	Days after spiking									
Soil	**3**	**23**	**46**	**72**	**100**	**143**	**192**	**262**	**346**	**549**
F1-T	222.24	180.13	189.68	157.51	120.86	103.82	68.44	60.01	53.48	40.75
WS-A	327.05	234.16	183.37	142.14	79.91	69.03	45.39	42.47	33.37	24.14
IH-W	61.50	55.29	52.91	52.80	44.68	40.70	33.35	33.20	31.45	26.56
M1-T	—	382.45	321.95	293.45	204.94	160.85	115.80	90.23	71.83	54.63
NP-A	482.43	289.20	296.33	218.05	147.67	115.63	73.41	47.99	27.88	17.60
SR-W	245.01	165.86	139.49	99.87	59.21	47.96	32.89	27.77	20.32	16.49
SB-G	187.25	108.98	74.58	62.45	51.46	40.47	30.01	23.04	18.49	14.85
TK-G	102.50	61.18	34.08	51.00	19.82	22.43	15.27	13.74	8.06	6.11
CO-A	432.73	345.80	303.27	261.70	169.58	153.39	106.96	88.01	84.14	61.43
FD-G	233.21	87.88	42.70	5.03	0.55	0.63	1.33	0.65	1.61	1.55
BH-W	185.45	143.93	108.99	62.23	38.51	30.81	18.81	18.14	13.35	11.21
DY-G	110.69	80.05	73.70	54.80	38.00	30.36	22.25	19.86	16.66	12.62
SR-A	215.98	132.38	103.52	84.05	55.30	54.16	30.90	30.39	24.11	19.93
M2-T	328.67	253.16	252.28	190.93	156.20	146.94	90.61	81.76	66.07	56.03
BH-G	199.86	152.84	108.48	101.50	62.98	57.70	35.85	32.52	26.54	19.91
WK-A	303.82	251.03	227.94	197.90	161.76	150.47	106.81	94.77	78.64	66.32
SR-G	166.02	134.16	105.09	88.10	67.40	52.89	37.61	30.49	25.52	20.78
F3-T	236.44	178.53	160.13	165.86	123.11	111.01	79.61	75.15	68.44	59.72
BC-M	40.88	32.00	32.42	38.33	34.56	35.58	30.75	29.17	29.57	28.16
BY-W	25.51	22.68	25.80	25.07	23.39	28.31	25.70	27.14	27.57	26.71

Appendix C.4. *Primary incubation compiled C_{soln} dataset for all in 20 soils, where concentrations are expressed per mass of soil (µg kg^{-1}) and corrected for cumulative depletion from the soil with incubation time.*

	Days after spiking									
Soil	**3**	**23**	**46**	**72**	**100**	**143**	**192**	**262**	**346**	**549**
F1-T	101.30	82.11	86.46	71.80	55.09	47.32	31.20	27.36	24.38	18.58
WS-A	187.88	134.51	105.34	81.66	45.91	39.65	26.08	24.40	19.17	13.87
IH-W	45.28	40.71	38.95	38.88	32.90	29.97	24.56	24.45	23.15	19.55
M1-T	—	99.38	83.66	76.25	53.25	41.80	30.09	23.45	18.66	14.20
NP-A	187.90	112.64	115.41	84.92	57.51	45.04	28.59	18.69	10.86	6.86
SR-W	107.04	72.46	60.94	43.63	25.87	20.95	14.37	12.13	8.88	7.20
SB-G	109.50	63.73	43.61	36.52	30.09	23.67	17.55	13.47	10.81	8.68
TK-G	70.94	42.35	23.58	35.30	13.72	15.53	10.57	9.51	5.58	4.23
CO-A	183.50	146.63	128.60	110.97	71.91	65.04	45.36	37.32	35.68	26.05
FD-G	168.09	63.34	30.78	3.63	0.39	0.46	0.96	0.47	1.16	1.12
BH-W	120.14	93.24	70.61	40.31	24.95	19.96	12.18	11.75	8.65	7.26
DY-G	109.00	78.82	72.58	53.97	37.42	29.89	21.91	19.56	16.41	12.43
SR-A	108.06	66.23	51.79	42.05	27.67	27.10	15.46	15.21	12.06	9.97
M2-T	96.46	74.30	74.04	56.04	45.84	43.13	26.59	24.00	19.39	16.44
BH-G	128.30	98.11	69.64	65.16	40.43	37.04	23.01	20.87	17.03	12.78
WK-A	141.18	116.64	105.92	91.96	75.17	69.92	49.63	44.04	36.54	30.82
SR-G	107.91	87.20	68.31	57.26	43.81	34.38	24.45	19.82	16.59	13.51
F3-T	76.62	57.85	51.89	53.75	39.89	35.97	25.80	24.35	22.18	19.35
BC-M	22.13	17.32	17.55	20.75	18.71	19.26	16.64	15.79	16.00	15.24
BY-W	17.57	15.62	17.77	17.26	16.10	19.49	17.70	18.69	18.98	18.39

Appendix C.5. *2D-DIFS input parameters and associated values.*

Soil	D_s	Time (hrs)	C_{soln} (µg L^{-1})	M (mol cm^{-2})	F (mol cm^{-2} s^{-1})	R	C_{sorbed} (µg kg^{-1})	K_d (L kg^{-1})
F1-T	3.08E-06	23.33	16.52	6.69E-14	7.97E-19	0.11	0.87	0.05
IH-W	3.71E-06	23.22	11.78	3.48E-14	4.16E-19	0.07	7.20	0.61
M1-T	2.43E-06	23.33	19.94	6.81E-14	8.10E-19	0.10	1.84	0.09
NP-A	2.88E-06	23.18	7.40	1.56E-14	1.87E-19	0.06	2.52	0.34
SB-G	3.40E-06	23.53	7.34	1.39E-14	1.64E-19	0.05	3.56	0.48
TK-G	3.63E-06	23.48	3.26	7.50E-15	8.86E-20	0.08	4.90	1.50
CO-A	2.98E-06	23.35	26.79	4.64E-14	5.52E-19	0.05	1.80	0.07
FD-G	3.68E-06	23.58	0.65	2.42E-15	2.85E-20	0.09	0.00	0.00
DY-G	4.11E-06	22.63	5.77	1.61E-14	1.97E-19	0.07	1.51	0.26
M2-T	2.56E-06	21.57	19.76	1.05E-13	1.35E-18	0.17	5.70	0.29
WK-A	3.10E-06	21.37	28.26	4.81E-14	6.25E-19	0.05	2.74	0.10
F3-T	2.67E-06	21.53	21.94	1.35E-13	1.74E-18	0.18	9.13	0.42
BC-M	3.30E-06	21.61	11.90	7.77E-14	9.98E-19	0.17	14.46	1.22
BY-W	3.62E-06	21.47	12.80	5.37E-14	6.95E-19	0.11	23.35	1.82

Δg (cm) = 0.092

D_d (cm^2 s^{-1}) = 3.98E-06

Key:

D_s = soil diffusion coefficient

C_{soln} = dissolved concentration

M = mass in resin layer

F = DGT flux

C_{sorbed} = sorbed concentration

K_d = distribution ratio

Appendix C.6. *Secondary incubation compiled C_{DGT} (µg L^{-1}) dataset. Concentrations represent the mean (± standard deviation) of triplicate DGT deployments.*

		Days after spiking								
Soil	**Moisture regime**	**Day 2**			**Day 23**			**Day 44**			**Day 112**		
BH-G	Sterilised/constant moisture	3.38	±	0.32	2.05	±	0.10	2.26	±	0.31	0.91	±	0.24
	Sterilised/wet-dry cycles	3.44	±	0.32	1.82	±	0.12	1.68	±	0.05	1.46	±	0.10
	Microbes/constant moisture	3.49	±	0.15	1.94	±	0.11	2.23	±	0.31	0.57	±	0.02
BY-W	Sterilised/constant moisture	5.63	±	0.47	2.00	±	0.29	3.03	±	0.33	2.49	±	0.07
	Sterilised/wet-dry cycles	5.02	±	0.46	0.66	±	0.04	0.78	±	0.06	0.76	±	0.08
	Microbes/constant moisture	5.85	±	0.59	4.83	±	0.69	5.64	±	0.48	3.83	±	0.05
SR-W	Sterilised/constant moisture	2.80	±	0.40	1.57	±	0.06	1.19	±	0.06	0.41	±	0.03
	Sterilised/wet-dry cycles	2.57	±	0.35	0.48	±	0.02	0.58	±	0.03	0.49	±	0.02
	Microbes/constant moisture	2.86	±	0.27	1.43	±	0.17	1.60	±	0.22	0.43	±	0.02
WK-A	Sterilised/constant moisture	3.00	±	0.41	0.66	±	0.17	0.75	±	0.05	0.57	±	0.02
	Sterilised/wet-dry cycles	3.14	±	0.21	1.34	±	0.09	1.07	±	0.08	0.90	±	0.01
	Microbes/constant moisture	2.95	±	0.54	4.49	±	0.71	4.37	±	0.73	2.20	±	0.49

		Day 3			**Day 23**			**Day 46**			**Day 72**			**Day 100**		
BH-G	Microbes/wet-dry cycles	27.76	±	0.14	25.16	±	0.03	19.63	±	0.12	16.60	±	0.02	11.59	±	0.08
BY-W	Microbes/wet-dry cycles	41.97	±	0.03	33.21	±	0.15	36.04	±	0.07	68.60	±	0.21	28.58	±	0.04
SR-W	Microbes/wet-dry cycles	20.70	±	0.19	14.95	±	0.26	15.47	±	0.08	19.83	±	0.05	11.28	±	0.02
WK-A	Microbes/wet-dry cycles	102.36	±	0.17	80.10	±	0.12	97.16	±	0.42	148.33	±	0.54	85.08	±	0.38

Appendix C.7. *Secondary incubation compiled C_{soln} (µg L^{-1}) dataset.*

Soil	Moisture regime	Days after spiking			
		2	**23**	**44**	**112**
BH-G	Sterilised/constant moisture	146.1	107	69.4	34.62
	Sterilised/wet-dry cycles	159.4	94.47	68.25	91.15
	Microbes/constant moisture	146.6	92.45	60.55	20.23
BY-W	Sterilised/constant moisture	115.20	66.17	51.11	35.02
	Sterilised/wet-dry cycles	114.90	23.48	17.88	21.36
	Microbes/constant moisture	118.80	76.47	51.67	51.31
SR-W	Sterilised/constant moisture	171.00	74.41	44.43	21.20
	Sterilised/wet-dry cycles	173.10	18.70	13.87	16.11
	Microbes/constant moisture	169.00	72.26	48.25	22.89
WK-A	Sterilised/constant moisture	205.90	16.96	10.91	11.46
	Sterilised/wet-dry cycles	211.80	25.51	18.67	22.49
	Microbes/constant moisture	202.60	147.00	100.90	93.92

Soil	Moisture regime	Days after spiking				
		3	**23**	**46**	**72**	**100**
BH-G	Microbes/wet-dry cycles	199.86	152.84	108.48	101.50	62.98
BY-W	Microbes/wet-dry cycles	25.51	22.68	25.80	25.07	23.39
SR-W	Microbes/wet-dry cycles	245.01	165.86	139.49	99.87	59.21
WK-A	Microbes/wet-dry cycles	303.82	251.03	227.94	197.90	161.76

Appendix D: Uranium

Appendix D.1. *Primary incubation compiled DGT dataset for all 20 soils. Concentrations (µg L^{-1}) represent the mean (± standard deviation) of triplicate DGT deployments.*

	Days after spiking																							
Soil	**3**			**23**			**46**			**72**			**100**			**143**			**192**					
F1-T	4.28	±	0.38	2.59	±	0.43	1.88	±	0.30	2.53	±	0.14	2.71	±	0.22	2.28	±	0.05	2.81	±	0.08			
WS-A	5.65	±	0.74	4.63	±	1.13	1.69	±	0.68	3.84	±	0.59	2.58	±	0.32	4.18	±	0.50	3.77	±	0.14			
IH-W	2.42	±	0.46	1.12	±	0.06	0.85	±	0.04	1.45	±	0.26	0.94	±	0.04	1.15	±	0.02	1.72	±	0.07			
M1-T	12.77	±	1.68	3.46	±	0.62	2.36	±	0.40	2.68	±	0.34	2.40	±	0.29	2.41	±	0.03	2.92	±	0.76			
NP-A	0.49	±	0.04	0.53	±	0.15	0.45	±	0.09	0.53	±	0.03	0.41	±	0.05	0.80	±	0.22	1.37	±	0.30			
SR-W	19.24	±	1.63	5.75	±	1.45	5.11	±	0.48	13.89	±	0.15	13.11	±	0.45	12.43	±	0.78	8.83	±	0.31			
SB-G	0.90	±	0.11	0.42	±	0.03	0.26	±	0.02	0.26	±	0.04	0.47	±	0.05	0.52	±	0.02	1.13	±	0.07			
TK-G	1.20	±	0.20	0.50	±	0.09	0.34	±	0.17	0.54	±	0.15	0.22	±	0.01	0.54	±	0.01	1.12	±	0.15			
CO-A	0.84	±	0.06	0.63	±	0.04	0.63	±	0.02	0.64	±	0.02	0.61	±	0.06	0.65	±	0.03	1.31	±	0.08			
FD-G	0.59	±	0.14	0.73	±	0.63	0.14	±	0.00	0.20	±	0.04	0.21	±	0.01	0.27	±	0.02	0.88	±	0.04			
BH-W	4.92	±	0.39	0.73	±	0.15	0.40	±	0.05	0.42	±	0.11	1.38	±	0.26	7.22	±	1.61	6.75	±	0.42			
DY-G	0.79	±	0.09	0.57	±	0.04	0.58	±	0.04	0.62	±	0.04	0.87	±	0.26	0.76	±	0.04	1.53	±	0.03			
SR-A	21.39	±	0.17	16.29	±	1.02	10.73	±	0.81	13.70	±	1.71	11.51	±	0.24	12.19	±	1.05	10.50	±	0.82			
M2-T	9.49	±	1.21	5.73	±	0.17	3.84	±	0.08	3.63	±	0.50	3.44	±	0.50	2.84	±	0.27	3.03	±	0.20			
BH-G	3.71	±	0.27	0.41	±	0.04	0.19	±	0.12	6.64	±	0.46	1.31	±	0.25	3.93	±	0.33	3.21	±	0.07			
WK-A	0.60	±	0.08	0.44	±	0.10	0.18	±	0.05	0.26	±	0.03	0.35	±	0.05	0.27	±	0.04	0.96	±	0.00			
SR-G	8.26	±	0.30	2.89	±	1.13	1.23	±	0.46	6.54	±	0.73	4.80	±	0.04	5.27	±	0.58	6.63	±	0.43			
F3-T	19.31	±	1.64	12.69	±	0.96	9.06	±	1.26	8.90	±	0.54	11.19	±	0.84	9.67	±	0.42	8.77	±	0.32			
BC-M	3.45	±	0.28	1.97	±	0.23	1.19	±	0.26	1.50	±	0.14	1.36	±	0.45	1.37	±	0.27	1.95	±	0.20			
BY-W	3.48	±	0.21	2.20	±	0.20	2.16	±	0.17	2.00	±	0.09	2.25	±	0.22	2.39	±	0.03	2.20	±	0.31			

continued…

262			346			549		
2.61	±	0.05	3.64	±	0.10	3.88	±	0.18
4.68	±	0.42	4.43	±	0.50	14.25	±	2.34
1.93	±	0.07	2.81	±	0.05	2.83	±	0.20
3.15	±	0.25	4.11	±	0.85	2.67	±	0.66
1.44	±	0.14	1.81	±	0.08	0.97	±	0.12
7.56	±	0.03	10.77	±	0.74	19.16	±	0.31
1.14	±	0.07	1.45	±	0.05	0.91	±	0.27
1.23	±	0.12	1.40	±	0.01	0.54	±	0.00
1.31	±	0.10	1.72	±	0.06	0.79	±	0.05
0.89	±	0.02	1.32	±	0.05	0.42	±	0.01
6.47	±	0.34	5.62	±	0.34	11.38	±	0.64
1.65	±	0.02	2.91	±	0.07	2.17	±	0.12
9.69	±	0.21	12.04	±	0.95	25.36	±	1.80
3.06	±	0.41	4.73	±	0.44	5.13	±	1.03
2.71	±	0.77	4.42	±	0.73	10.15	±	0.84
1.20	±	0.15	1.32	±	0.08	0.70	±	0.14
5.67	±	0.34	5.35	±	0.33	11.41	±	0.77
9.27	±	1.08	8.19	±	0.41	12.51	±	0.27
1.84	±	0.11	2.22	±	0.12	2.81	±	0.14
2.69	±	0.08	3.22	±	0.09	4.34	±	0.35

Appendix D.2. *Primary incubation compiled C_{soln} dataset for all 20 soils. Concentrations are expressed per litre of soil solution as measured (µg L^{-1}).*

	Days after spiking									
Soil	**3**	**23**	**46**	**72**	**100**	**143**	**192**	**262**	**346**	**549**
F1-T	19.33	17.93	15.39	15.98	16.61	19.66	24.32	26.31	34.18	40.86
WS-A	242.17	134.85	72.41	135.10	87.55	120.18	94.45	156.00	166.90	212.60
IH-W	9.01	8.01	7.38	6.73	7.20	10.07	14.88	16.69	22.94	25.74
M1-T	—	14.21	13.84	14.23	16.69	19.36	24.55	22.20	24.41	24.58
NP-A	5.33	8.78	8.63	7.55	12.06	14.70	11.02	13.08	13.48	10.83
SR-W	431.77	100.83	72.23	130.18	249.82	168.74	130.80	131.00	139.40	184.20
SB-G	14.27	12.57	1.75	2.40	11.23	8.72	9.90	10.93	12.69	16.91
TK-G	7.31	4.00	1.14	5.82	2.32	8.63	9.50	9.91	6.23	11.30
CO-A	3.65	4.35	4.86	4.93	5.21	5.68	8.66	8.32	9.19	9.63
FD-G	4.37	1.74	2.45	2.26	2.77	2.57	4.76	4.94	5.35	4.86
BH-W	124.80	20.77	13.50	9.01	62.71	154.51	129.50	98.17	136.60	196.30
DY-G	21.17	12.01	9.43	11.90	16.88	14.89	20.04	22.14	25.02	27.53
SR-A	272.56	162.82	111.46	125.46	155.04	188.05	140.50	130.80	147.50	182.00
M2-T	32.35	22.27	15.39	17.13	16.42	16.55	21.96	21.82	27.01	34.54
BH-G	76.64	8.31	7.55	85.52	56.40	62.27	85.88	52.20	96.94	179.90
WK-A	4.04	2.10	1.65	1.78	1.82	2.12	5.65	5.88	5.67	9.55
SR-G	142.17	41.79	24.41	89.13	112.19	95.13	113.80	81.77	137.10	128.00
F3-T	105.52	83.07	64.16	67.11	76.90	79.09	90.04	92.51	102.10	112.30
BC-M	5.87	8.66	10.38	5.82	6.46	7.70	12.26	13.44	16.61	17.91
BY-W	14.25	10.94	9.15	9.96	13.00	14.94	19.28	19.42	21.44	23.62

Appendix D.3. *2D-DIFS input parameters and associated values.*

Soil	D_s	Time (hrs)	C_{soln} (µg L^{-1})	M (mol cm^{-2})	F (mol cm^{-2} s^{-1})	R	C_{sorbed} (µg kg^{-1})	K_d (L kg^{-1})
F1-T	1.72E-06	23.33	19.21	5.53E-11	6.59E-16	0.20	0.19	0.010
WS-A	1.89E-06	23.27	99.23	2.03E-10	2.42E-15	0.14	0.09	0.001
IH-W	2.08E-06	23.22	14.42	4.02E-11	4.81E-16	0.20	0.15	0.011
M1-T	1.36E-06	23.34	16.34	3.81E-11	4.53E-16	0.16	0.07	0.004
NP-A	1.61E-06	23.18	7.62	1.37E-11	1.64E-16	0.13	0.00	0.000
SR-W	1.69E-06	23.48	93.42	2.75E-10	3.25E-15	0.21	0.26	0.003
SB-G	1.90E-06	23.53	5.97	1.31E-11	1.55E-16	0.15	0.00	0.000
TK-G	2.03E-06	23.50	3.90	7.73E-12	9.13E-17	0.14	0.05	0.013
CO-A	1.67E-06	23.35	6.34	1.13E-11	1.35E-16	0.13	0.00	0.000
FD-G	2.06E-06	23.59	3.37	6.09E-12	7.17E-17	0.13	0.00	0.000
BH-W	1.98E-06	22.68	71.26	1.58E-10	1.93E-15	0.16	0.00	0.000
DY-G	2.30E-06	22.64	14.43	3.00E-11	3.68E-16	0.15	0.11	0.008
SR-A	1.79E-06	21.63	95.35	3.35E-10	4.31E-15	0.27	0.29	0.003
M2-T	1.43E-06	21.57	18.84	6.76E-11	8.71E-16	0.27	0.28	0.015
BH-G	1.97E-06	21.80	62.89	1.35E-10	1.72E-15	0.16	0.00	0.000
WK-A	1.73E-06	21.79	4.16	9.18E-12	1.19E-16	0.17	0.05	0.012
SR-G	1.98E-06	21.58	55.39	1.51E-10	1.94E-15	0.21	0.09	0.002
F3-T	1.49E-06	21.53	48.65	1.65E-10	2.13E-15	0.26	0.52	0.011
BC-M	1.85E-06	21.60	9.30	3.71E-11	4.77E-16	0.30	0.20	0.022
BY-W	2.03E-06	21.47	15.79	5.70E-11	7.38E-16	0.28	0.32	0.020

Δg (cm) = 0.092

D_d (cm^2 s^{-1}) =3.80E-06

Key:

D_s = soil diffusion coefficient

C_{soln} = dissolved concentration

M = mass in resin layer

F = DGT flux

C_{sorbed} = sorbed concentration

K_d = distribution ratio

Appendix D.4. *Secondary incubation compiled C_{DGT} (µg L^{-1}) dataset. Concentrations represent the mean (± standard deviation) of triplicate DGT deployments.*

		Days after spiking								
Soil	**Moisture regime**	**Day 2**			**Day 23**			**Day 44**			**Day 112**		
BH-G	Sterilised/constant moisture	11.85	±	0.95	1.68	±	0.08	0.25	±	0.02	0.36	±	0.26
	Sterilised/wet-dry cycles	16.52	±	1.68	17.15	±	3.00	18.64	±	1.24	15.44	±	1.70
	Microbes/constant moisture	6.02	±	0.30	1.56	±	0.17	0.39	±	0.13	0.76	±	0.32
BY-W	Sterilised/constant moisture	1.59	±	0.28	1.93	±	0.07	0.73	±	0.10	0.56	±	0.05
	Sterilised/wet-dry cycles	1.43	±	0.06	2.62	±	0.09	1.65	±	0.04	1.96	±	0.66
	Microbes/constant moisture	1.43	±	0.25	1.60	±	0.07	0.55	±	0.15	0.32	±	0.15
SR-W	Sterilised/constant moisture	12.85	±	2.35	4.25	±	0.40	2.28	±	0.15	2.30	±	0.03
	Sterilised/wet-dry cycles	15.11	±	4.19	7.34	±	0.52	10.28	±	0.60	12.79	±	0.90
	Microbes/constant moisture	12.88	±	0.62	3.53	±	0.34	2.29	±	0.04	2.74	±	0.08
WK-A	Sterilised/constant moisture	4.64	±	0.88	2.46	±	0.44	0.95	±	0.28	0.26	±	0.04
	Sterilised/wet-dry cycles	3.81	±	0.75	2.10	±	0.03	1.30	±	0.19	0.92	±	0.08
	Microbes/constant moisture	2.53	±	0.33	2.06	±	0.03	0.42	±	0.07	0.35	±	0.27

		Day 3			**Day 23**			**Day 46**			**Day 72**			**Day 100**		
BH-G	Microbes/wet-dry cycles	3.71	±	0.27	0.41	±	0.04	0.19	±	0.12	3.35	±	0.46	1.31	±	0.25
BY-W	Microbes/wet-dry cycles	3.48	±	0.21	2.20	±	0.20	2.16	±	0.17	8.67	±	0.09	2.25	±	0.22
SR-W	Microbes/wet-dry cycles	19.24	±	1.63	5.75	±	1.45	5.11	±	0.48	0.63	±	0.15	13.11	±	0.45
WK-A	Microbes/wet-dry cycles	0.60	±	0.08	0.44	±	0.10	0.18	±	0.05	0.24	±	0.03	0.35	±	0.05

Appendix D.5. *Secondary incubation compiled C_{soln} ($\mu g\ L^{-1}$) dataset.*

Soil	Moisture regime	Days after spiking			
		3	**23**	**44**	**112**
BH-G	Sterilised/constant moisture	104.4	17.14	6.94	5.19
	Sterilised/wet-dry cycles	96.28	225.6	182.5	222.3
	Microbes/constant moisture	71.39	12.03	9.41	10.57
BY-W	Sterilised/constant moisture	11.93	11.87	9.61	3.16
	Sterilised/wet-dry cycles	11.18	14.74	15.75	18.21
	Microbes/constant moisture	12.09	7.42	6.87	2.82
SR-W	Sterilised/constant moisture	88.05	29.51	9.95	13.73
	Sterilised/wet-dry cycles	87.11	74.74	67.23	138.4
	Microbes/constant moisture	104.6	18.11	12.7	17.96
WK-A	Sterilised/constant moisture	17.63	14.65	11.51	4.74
	Sterilised/wet-dry cycles	15.29	17.11	13.92	14.88
	Microbes/constant moisture	9.86	8.25	7.91	4.1

Soil	Moisture regime	Days after spiking				
		3	**23**	**46**	**72**	**100**
BH-G	Microbes/wet-dry cycles	76.64	8.31	7.55	85.52	56.40
BY-W	Microbes/wet-dry cycles	14.25	10.94	9.15	9.96	13.00
SR-W	Microbes/wet-dry cycles	431.77	100.83	72.23	130.18	249.82
WK-A	Microbes/wet-dry cycles	4.04	2.10	1.65	1.78	1.82